Topological Invariants of Graphs

By

Imran Nadeem

CIIT/FA13-PMATH-003/LHR

PhD Thesis

In

Mathematics

COMSATS University Islamabad
Lahore Campus - Pakistan

Fall, 2018

COMSATS University Islamabad

Topological Invariants of Graphs

A Thesis Presented to

COMSATS University Islamabad, Lahore Campus

In partial fulfillment

of the requirement for the degree of

PhD (Mathematics)

By

Imran Nadeem

CIIT/FA13-PMATH-003/LHR

Fall, 2018

Topological Invariants of Graphs

A Post Graduate Thesis submitted to the department of Mathematics as partial fulfillment of the requirement for the award of Degree of PhD in Mathematics.

Name	Registration Number
Imran Nadeem	CIIT/FA13-PMATH-003/LHR

Supervisor

Dr. Hani Shaker

Associate Professor Department of Mathematics

COMSATS University Islamabad, Lahore Campus.

Certificate of Approval

This is to certify that the research work presented in this thesis entitled "Topological Invariants of Graphs" was conducted by Mr. Imran Nadeem,CIIT/ FA13-PMATH-003/LHR, under the supervision of Dr. Hani Shaker. No part of this thesis has been submitted anywhere else for any other degree. This thesis is submitted to the Department of Mathematics, COMSATS University Islamabad, Lahore Campus, in partial fulfillment of the requirements for the degree of Doctor of Philosophy in the field of Mathematics.

Student Name: Imran Nadeem Signature:__________

External Committee:

Signature: __________

Prof. Dr. Akhlaq Ahmad Bhatti
Professor
Department of Sciences and Humanities
NUCES (FAST), Lahore.

Signature:__________

Dr. Imran Javaid
Associate Professor
CASPAM
BZU, Multan.

Signature: __________

Dr. Hani Shaker

Supervisor,
Department of Mathematics,
CUI, Lahore Campus.

Signature: __________

Dr. Sarfraz Ahmad

HOD,
Department of Mathematics,
CUI, Lahore Campus.

Signature: __________

Prof. Dr. Shamsul Qamar
Chairperson,
Department of Mathematics,
CUI.

Author's Declaration

I Imran Nadeem, CIIT/FA13-PMATH-003/LHR, hereby state that my PhD thesis titled "Topological Invariants of Graphs" is my own work and has not been submitted previously by me for taking any degree from this University "COMSATS University Islamabad, Lahore Campus" or anywhere else in the country/world.

At any time if my statement is found to be incorrect even after my Graduate the university has the right to withdraw my PhD degree.

Date: 27-05-2019 Signature: Imran.

Imran Nadeem

CIIT/FA13-PMATH-003/LHR

Plagiarism Undertaking

I solemnly declare that research work presented in the thesis titled "Topological Invariants of Graphs" is solely my research work with no significant contribution from any other person small contribution/help wherever taken has been duly acknowledge and that complete thesis has been written by me.

I understand the zero-tolerance policy of HEC and COMSATS University Islamabad, Lahore Campus towards plagiarism. Therefore, I as an author of the above titled thesis declare that no portion of my thesis has been plagiarized and material used as reference is properly referred/cited.

I undertake that if I am found guilty of any formal plagiarism in the above titled thesis even after award of PhD degree, the University reserves the right to withdraw/revoke my PhD degree and that HEC and the University has the right to publish my name on the HEC/University website on which names of students are placed who submitted plagiarized thesis.

Date: 27-05-2019

Signature: Imran

Imran Nadeem

CIIT/FA13-PMATH-003/LHR

Certificate

It is certified that Imran Nadeem with registration number CIIT/FA13-PMATH-003/LHR has carried out all the work related to this thesis under my supervision at the Department of Mathematics, COMSATS University Islamabad, Lahore Campus and the work fulfills the requirement for award of PhD degree.

Date: 27-05-2019

Supervisor:

Dr. Hani Shaker
Associate Professor,
Department of Mathematics,
CUI, Lahore Campus

Head of Department:

Dr. Sarfraz Ahmad
Associate Professor,
Department of Mathematics,
CUI, Lahore Campus

DEDICATION

To My Parents and Brothers

Acknowledgements

All praises to ALLAH Almighty who created the universe and knows whatever is in it hidden or evident, who bestowed upon me the intellectual ability and wisdom to search for it's secret and whose blessings flourished my thoughts and thrived my ambitions and enabled me to contribute sincerely to the sacred wealth of knowledge. Special praise and regards to his last messenger Muhammad (PBUH) who is a tower of guidance and knowledge for humanity.

I feel much pleasure in expressing my hearties gratitude to my ever-affectionate supervisor Dr. Hani Shaker for his dynamic and friendly supervision. Whose indispensable guidance, deep consideration, constructive comments and active cooperation enable me to complete my work successfully. All the words I know are insufficient to pay my tribute to him.

I would like to thank to Dr. Sarfraz Ahmed, Head of Department, Dr. Kashif Ali, Associate Head of Department, Dr. Muhammad Hussain, PhD Coordinator and all my teachers for their suggestions, guidance and constant support.

I would like to thank all my friends, class fellows and colleagues for their suggestions, sympathetic attitude and work discussion during my studies.

Of course, at this stage I cannot forget my whole family especially my respectable parents and my brothers for their prayers, continuing support and love. Their prayers have lightened up my spirit to finish this thesis.

COMSATS University Islamabad, Lahore Campus.

Imran Nadeem

CIIT/FA13-PMATH-003/LHR

ABSTRACT

Topological Invariants of Graphs

Chemical graph theory provides useful tools such as molecular descriptors to develop strong intrinsic relationship between the physicochemical features of chemical compounds and their molecular graphs. The study of molecular descriptors provides a theoretical basis for the fabrication of chemical materials and is helpful in making up for the lack of chemical experiments. There are two prominent types of molecular descriptors; the topological indices and counting polynomials. Further, topological indices can be categorized in two major classes: one class is based on degree and the other class is based on distance. In this thesis, we present the study of certain topological indices belonging to degree- and distance-based classes and counting polynomials for some well-known nanostructures. We also present a comparative study between different topological indices belonging to degree- and distance-based classes for general graphs. In addition, we study the para-line transformation of graphs and obtain the general expressions of certain topological indices for this transformation. We achieve the lower and upper bounds of certain distance-based topological indices for the para-line transformation of graphs.

List of Publications from Thesis

[1] Nadeem, I., & Shaker, H. (2016) "On eccentric connectivity index of TiO_2 nanotubes", *Acta Chim. Slov.* **63**, 363–368.

[2] Nadeem, I., & Shaker, H. (2016) "On topological indices of tri-hexagonal boron nanotubes", *J. Optoelectron. Adv. Mater.*, **18(9-10)**, 893–898.

[3] Shaker, H., Nadeem, I., Hussain, M., & Naseem, A. (2017) "Valency based topological indices of tri-hexagonal boron nanotori", *MAGNT Research Report*, **4**, 153–159.

[4] Nadeem, I., & Shaker, H. (2018) "Inequalities between degree- and distance-based graph invariants", *J. Inequal. Appl.* 2018:39.

[5] Liu, J-. B., Shaker, H., Nadeem, I., & Hussain, M. (2018) "Topological aspects of boron nanotubes", *Adv. Mater. Sci. Eng.* 5729291.

[6] Liu, J-. B., Shaker, H., & Nadeem, I., Farhani, M. R. "On eccentric connectivity index of t-polyacenic nanotubes", *Adv. Mater. Sci. Eng.* 9062535.

[7] Nadeem, I., Shaker, H., Hussain, M., & Naseem, A. "Topological indices of para-line graphs of certain V-phenylenic nanostructures", *Open Math.* **17(1)**, 260–266.

[8] Shaker, H., Nadeem, I., & Imran, M. "Omega and related counting polynomials of TiO_2 nanostructures", accepted in *Utilitas Mathematica*.

Further Submitted Work from Thesis

[1] Nadeem, I., Shaker, H., & Imran, M. "Eccentricity-based topological indices of three-layer TiO_2 nanotubes".

[2] Shaker, H., Nadeem, I. "Topological descriptors of iterated para-line graphs of molecular graphs".

[3] Nadeem, I., & Shaker, H. "General expressions of graph invariants for para-line transformation of graphs".

[4] Nadeem, I., Shaker, H. "Bounds for distance-based topological indices of para-line transformed graph".

[5] Nadeem, I., & Shaker, H. "Topological indices of graphs under para-line transformation of graphs".

Table of Contents

List of Figures

Chapter 1

Introduction

Graph theory is a branch of mathematics which took birth in eighteenth century. In 1736, Euler solved a problem, recognized as the Königsberg bridges problem. The question had been raised up in this problem whether it was feasible to visit all the seven bridges covering the river Pregel in Königsberg not more than once without returning one's footsteps. Euler transformed this problem to a graph theoretical problem and found a splendid solution. This solution pointed out that the introduction of a new field of mathematics is called the graph theory. Thereafter, the idea of graph was individually presented by Gustav Robert Kirchhoff during his working on electrical circuits and Arthur Cayley who was investigating on the quantification of organic isomers at that time.

Graph theory has found several remarkable applications in operational research, physics, computer science, chemistry, architecture, economics, sociology, anthropology and psychology. In the current study, we are interested in the area of graph theory which has considerable applications in chemistry, called the chemical graph theory.

In 1874, one of the outstanding pioneers of chemical graph theory, Alexander Crum Brown predicted that "chemistry will become a branch of applied mathematics; but it will not cease to be an experimental science. Mathematics may enable us retrospectively to justify results obtained by experiment, may point out useful lines of research and even sometimes predict entirely novel discoveries. We do not know when the change will take place, or whether it will be gradual or sudden". This prediction was immediately to be executed when Arthur Cayley presented the article "On the Mathematical Theory of Isomers", which expresses the first remarkable chemical application of graph theory. Arthur Cayley was motivated in counting the possible isomers of an alkane and due to this intention he presented a new concept to depict the structure of alkane in the form of a diagram, called the molecular graph that was made of points (vertices) labelled by atoms and links (edges) corresponded to the chemical bonding between atoms.

Molecular descriptors, being numerical functions of molecular graph, are the graph invariants and play a crucial role in chemical graph theory. These descriptors are used in quantitative structure-activity relationship (QSAR) and structure-property relationship (QSPR) studies to relate biological or chemical properties of chemical compounds to specific molecular descriptors, thus enabling prediction of properties of chemical compounds based on their corresponding molecular graph only and without their synthesization. Molecular descriptors are of two types: one is topological indices and the other is counting polynomials. Topological indices represent an important type of molecular descriptors and encode information on atom adjacency and branching within a chemical compound. In recent years, topological indices have obtained significant popularity and various novel topological indices have been presented and studied in the chemical graph theory literature. On the other hand, counting polynomials are the important tools that are recently used to study and characterize the molecular graphs.

The contents of this thesis are divided as follows:

In Chapter 2, basic graph-theoretic notions concerning the thesis are defined together with the notations that are needed in the subsequent chapters.

In chapter 3 is devoted to the study of chemical graph theory which includes the discussion on topological indices and counting polynomials.

In chapter 4, some fundamental results of graph theory and some connections between topological indices are presented.

Boron containing nanostructures are high-interest materials due to the presence of multicenter bonds and have novel electronic properties. These materials have some important issues in nanodevice applications like mechanical and thermal stability. Therefore, they require theoretical studies on the other properties. In chapter 5, different degree-based topological indices have been studied such as ABC, the fourth ABC (ABC_4), GA, and the fifth GA (GA_5) indices for the molecular graphs of several boron containing nanostructures by using the edge-partition technique.

The eccentric connectivity index (ECI) belongs to the distance-based descriptors that was recently applied for the modeling of biological activities having diverse nature. The ECI has been proved to provide a high degree of predictability compared to Wiener index with regard to diuretic activity and anti-inflammatory activity. The prediction accuracy rate of ECI is better than the Zagreb indices in case of anticonvulsant activity. Titania nanotubular materials are of high interest metal oxide substances due to their widespread technological applications. Polyacene chemical materials also received much attention due to their interesting optical, thermodynamic, electronic, ferromagnetic and photoconductive properties. The numerous studies on the use of these materials also require theoretical studies on the other properties of such materials. In chapter 6, the *ECI* has been studied for three- and six-layer titania nanotube and whole class of polyacene nanotubes. In this chapter, we also studied certain variants of *ECI* for three-layer titania nanotube and counting polynomials for six-layer titania nanotube.

In chapter 7, inequalities between certain degree- and distance-based topological indices have been derived which provide a way to study topological indices belonging to different classes relatively.

In chapter 8, general expressions for certain topological indices of para-line transformed graph have been derived which is useful to increase the applicability of the concerned topological indices. In addition, we formulate some topological indices/coindices for the iterated para-line transformed graphs of any graph. In this chapter, we also achieved the bounds for different topological indices belonging to distance-based class for the para-line transformed graph.

In chapter 9, conclusion is presented and some open problems are proposed.

Chapter 2

Basic Concepts

2.1 Introduction

This chapter covers the fundamental concepts about graph theory. These concepts are essential to provide substantial and strong basis for the current study.

2.2 Graph Theoretical Terminology

In this section we provide a formal definition of graph and its components related terminology.

Definition 2.2.1. A graph $G = (V_G, E_G)$ comprises two sets: V_G, the vertex set and E_G, the edge set which consist of elements called vertices and edges respectively such that an unordered pair of vertices (υ_a, υ_b) is assigned to each edge e_{ab} in E_G written as $e_{ab} \leftrightarrow (\upsilon_a, \upsilon_b)$, where υ_a and υ_b are termed the end vertices of e_{ab}.

Definition 2.2.2. If $e_{ab} \leftrightarrow (\upsilon_a, \upsilon_b)$, then the pair of vertices (υ_a, υ_b) are termed adjacent and e_{ab} is termed incident with these vertices.

Definition 2.2.3. Two distinct edges $e_{ab} \leftrightarrow (\upsilon_a, \upsilon_b)$ and $e_{cd} \leftrightarrow (\upsilon_c, \upsilon_d)$ are termed adjacent edges if any one of its end vertices are identical i.e. either $\upsilon_a \equiv \upsilon_c$ or $\upsilon_b \equiv \upsilon_d$ and are represented by $e_{ab} \sim e_{cd}$.

Definition 2.2.4. Edges having have the same end vertices are termed parallel or multiple. A loop is an edge that has identical end vertices. A graph having parallel edges or loops is termed a multigraph.

Definition 2.2.5. A graph independent from parallel edges and loops is termed a simple graph.

A graph is represented by several ways. However, commonly a graph represents diagrammatically such that a dot corresponds to a vertex and a line segment corresponds to an edge.

Example 2.2.1. *A multigraph $G = (V_G, E_G)$ is shown in Figure 2.1 (a) where*

$$V_G = \{\upsilon_1, \upsilon_2, \upsilon_3, \upsilon_4, \upsilon_5, \upsilon_6\}$$

and

$$E_G = \{e_{12}, e_{23}, e'_{23}, e''_{23}, e_{13}, e_{24}, e'_{24}, e_{14}, e_{25}, e_{34}, e_{45}, e_{55}\}.$$

The edges with their end vertices are given by:

$$\begin{aligned}
&e_{12} \leftrightarrow (\upsilon_1, \upsilon_2),\ \ e_{23} \leftrightarrow (\upsilon_2, \upsilon_3),\ \ e'_{23} \leftrightarrow (\upsilon_2, \upsilon_3),\\
&e''_{23} \leftrightarrow (\upsilon_2, \upsilon_3),\ \ e_{13} \leftrightarrow (\upsilon_1, \upsilon_3),\ \ e_{24} \leftrightarrow (\upsilon_2, \upsilon_4),\\
&e'_{24} \leftrightarrow (\upsilon_2, \upsilon_4),\ \ e_{14} \leftrightarrow (\upsilon_1, \upsilon_4),\ \ e_{25} \leftrightarrow (\upsilon_2, \upsilon_5),\\
&e_{34} \leftrightarrow (\upsilon_3, \upsilon_4),\ \ e_{45} \leftrightarrow (\upsilon_4, \upsilon_5),\ \ e_{55} \leftrightarrow (\upsilon_5, \upsilon_5).
\end{aligned}$$

A simple graph $H = (V_H, E_H)$ is shown in Figure 2.1 (b) where

$$\begin{aligned}
V_H &= \{\upsilon_1, \upsilon_2, \upsilon_3, \upsilon_4, \upsilon_5, \upsilon_6\} \text{ and}\\
E_H &= \{e_{12}, e_{23}, e_{13}, e_{24}, e_{14}, e_{25}, e_{34}, e_{45}\}.
\end{aligned}$$

The edges with their end vertices are presented as:

$$\begin{aligned}
&e_{12} \leftrightarrow (\upsilon_1, \upsilon_2),\ \ e_{23} \leftrightarrow (\upsilon_2, \upsilon_3),\ \ e_{13} \leftrightarrow (\upsilon_1, \upsilon_3),\ \ e_{24} \leftrightarrow (\upsilon_2, \upsilon_4),\\
&e_{14} \leftrightarrow (\upsilon_1, \upsilon_4),\ \ e_{25} \leftrightarrow (\upsilon_2, \upsilon_5),\ \ e_{34} \leftrightarrow (\upsilon_3, \upsilon_4),\ \ e_{45} \leftrightarrow (\upsilon_4, \upsilon_5).
\end{aligned}$$

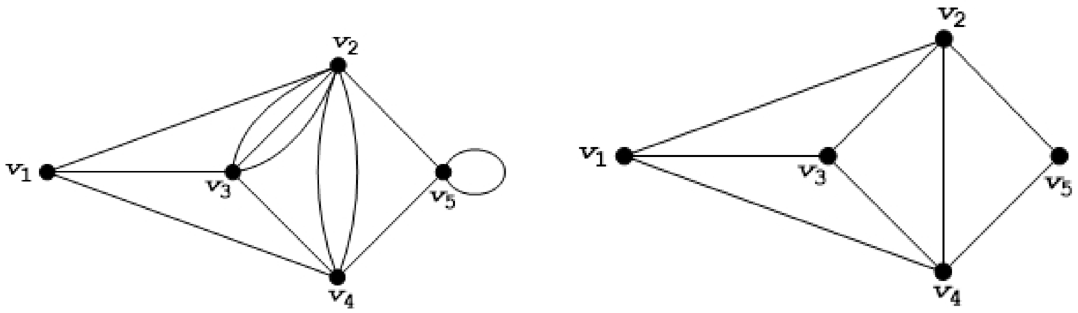

(a) (b)

Figure 2.1: (a) A multigraph G. (b) A simple graph H.

Definition 2.2.6. The numerical quantities associated to graph G, obtained by counting its vertices and edges respectively, are termed order and size of G. A graph having order n and size m is often termed a (n,m)-graph. A $(1,0)$-graph is called the trivial graph.

Example 2.2.2. *In Figure 2.1, the graphs G and H are* $(5,12)$*-graph and* $(5,8)$*-graph respectively.*

Definition 2.2.7. If every pair of distinct vertices of G are adjacent, then G is termed a complete graph. A complete graph having order n is represented by K_n.

Example 2.2.3. *For* $1 \leq n \leq 5$*, the complete graphs* K_n *are presented as*

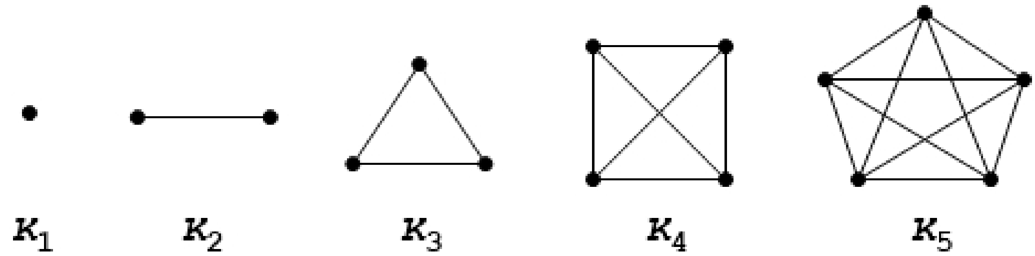

Figure 2.2: A list of complete graphs $K_n for$ $1 \leq n \leq 5$.

Remark 2.2.1. A complete graph K_n is $\left(n, \frac{n(n-1)}{2}\right)$-graph.

Definition 2.2.8. Let $H = (V_H, E_H)$ be a (n,m)-graph, then its complement is represented by $\overline{H} = (V_{\overline{H}}, E_{\overline{H}})$ and having the vertex set $V_{\overline{H}} = V_H$ in which two vertices $\upsilon_a, \upsilon_b \in V_{\overline{H}}$ are adjacent by the edge e_{ab} iff $e_{ab} \notin E_H$. And the size of $\overline{H}$ is defined as $|E_{\overline{H}}| = \binom{n}{2} - m$.

Example 2.2.4. *Let* $H = (V_H, E_H)$ *be a* $(5,6)$*-graph where*

$$V_H = \{\upsilon_1, \upsilon_2, \upsilon_3, \upsilon_4, \upsilon_5\}, \;\; E_H = \{e_{12}, e_{15}, e_{25}, e_{23}, e_{45}, e_{34}\},$$

and edges with their end vertices are presented as:

$$e_{12} \leftrightarrow (\upsilon_1, \upsilon_2), \;\; e_{15} \leftrightarrow (\upsilon_1, \upsilon_5), \;\; e_{23} \leftrightarrow (\upsilon_2, \upsilon_3),$$
$$e_{45} \leftrightarrow (\upsilon_4, \upsilon_5), \;\; e_{25} \leftrightarrow (\upsilon_2, \upsilon_5), \;\; e_{34} \leftrightarrow (\upsilon_3, \upsilon_4).$$

then its compliment $\overline{H}$ *is a* $(5,4)$*-graph with the vertex set* $V_{\overline{H}} = V_H$ *and edges with their end vertices are presented as:*

$$e_{13} \leftrightarrow (\upsilon_1, \upsilon_3), \;\; e_{35} \leftrightarrow (\upsilon_3, \upsilon_5), \;\; e_{24} \leftrightarrow (\upsilon_2, \upsilon_4), \;\; e_{14} \leftrightarrow (\upsilon_1, \upsilon_4).$$

The graphs of H and its complement $\overline{H}$ are shown in Figure 2.3.

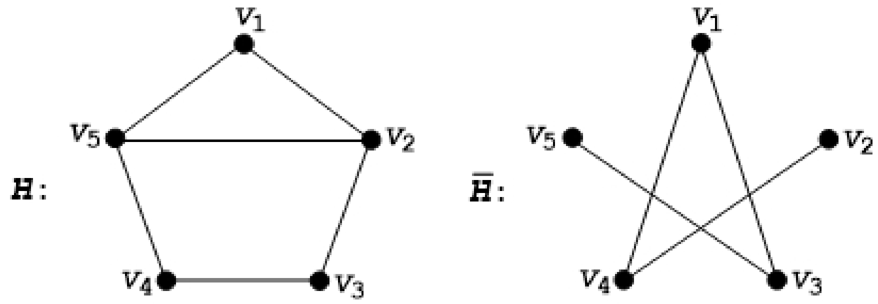

Figure 2.3: The complement $\overline{H}$ of a graph H.

Remark 2.2.2. A (n,m)-graph G and its complement (n,m')-graph $\overline{G}$ define a partition of complete graph K_n.

Definition 2.2.9. A subset of V_K having no pair of adjacent vertices, is termed an independent-vertex set of graph K. The maximum cardinality among all the independent sets of K is termed independence number of K, represented by $\alpha(K)$.

Example 2.2.5. *Consider a graph K as presented in Figure 2.4, then the independent-*

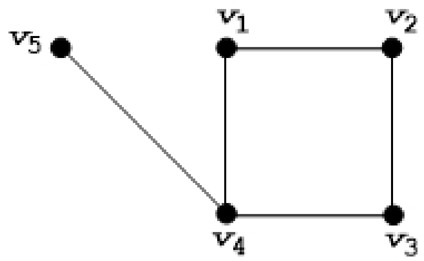

Figure 2.4: A graph K.

vertex sets of K are given by:

The independent-vertex set having no element is ϕ.

The independent-vertex sets having one element are

$\{\upsilon_1\}$, $\{\upsilon_2\}$, $\{\upsilon_3\}$, $\{\upsilon_4\}$, *and* $\{\upsilon_5\}$.

The independent-vertex sets having two elements are

$\{\upsilon_1,\upsilon_3\}$, $\{\upsilon_3,\upsilon_5\}$, $\{\upsilon_2,\upsilon_4\}$, $\{\upsilon_1,\upsilon_5\}$, and $\{\upsilon_2,\upsilon_5\}$.
The independent-vertex set having three elements is $\{\upsilon_1,\upsilon_3,\upsilon_5\}$.
Among all independent sets of graph K, the independent set having maximum cardinality is 3. Therefore $\alpha(K)=3$.

Definition 2.2.10. The degree of a vertex $\upsilon \in V_G$ is a numerical quantity which is obtained by counting the edges which have the same end vertex υ and it is represented by $d_G(\upsilon)$. The minimum and maximum degrees are respectively represented by δ_G and Δ_G.

Definition 2.2.11. A graph having all of its vertices of equal degree, is termed a regular graph.

Definition 2.2.12. The neighborhood set of a vertex $\upsilon \in V_G$ comprises all vertices adjacent to υ and it is represented by $N_G(\upsilon)$. i.e.

$$N_G(\upsilon)=\{w \in V_G \mid w\upsilon \in E_G\}.$$

Definition 2.2.13. The degree sum of a vertex υ is represented by $\delta_G(\upsilon)$ and is formulated by summing the degrees of all vertices adjacent to υ. i.e.

$$\delta_G(\upsilon)=\sum_{w\in N_G(\upsilon)} d_G(w).$$

Likewise, the degree product of υ is symbolized by $M_G(\upsilon)$ and is obtained by multiplying degrees of all vertices adjacent to υ. i.e.

$$M_G(\upsilon)=\prod_{w\in N_G(\upsilon)} d_G(w).$$

Example 2.2.6. *From the graph G, presented in Figure 2.5, we have*

$$d_G(\upsilon_1)=3,\ d_G(\upsilon_2)=d_G(\upsilon_3)=d_G(\upsilon_5)=2,\ d_G(\upsilon_4)=4 \text{ and } d_G(\upsilon_6)=1.$$

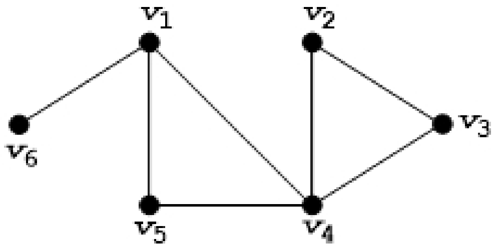

Figure 2.5: A graph G.

The degree sum of each vertex of G is computed as follows:

$$\begin{aligned}
\delta_G(\upsilon_1) &= d_G(\upsilon_4)+d_G(\upsilon_6)+d_G(\upsilon_5)=7,\\
\delta_G(\upsilon_2) &= d_G(\upsilon_3)+d_G(\upsilon_4)=6,\\
\delta_G(\upsilon_3) &= d_G(\upsilon_2)+d_G(\upsilon_4)=6,\\
\delta_G(\upsilon_4) &= d_G(\upsilon_1)+d_G(\upsilon_3)+d_G(\upsilon_5)+d_G(\upsilon_2)=9,\\
\delta_G(\upsilon_5) &= d_G(\upsilon_1)+d_G(\upsilon_4)=7,\\
\delta_G(\upsilon_6) &= d_G(\upsilon_1)=3.
\end{aligned}$$

Also, for each vertex of G, the degree product is calculated as follows:

$$\begin{aligned}
M_G(\upsilon_1) &= d_G(\upsilon_4)\cdot d_G(\upsilon_6)\cdot d_G(\upsilon_5)=8,\\
M_G(\upsilon_2) &= d_G(\upsilon_3)\cdot d_G(\upsilon_4)=8,\\
M_G(\upsilon_3) &= d_G(\upsilon_2)\cdot d_G(\upsilon_4)=8,\\
M_G(\upsilon_4) &= d_G(\upsilon_1)\cdot d_G(\upsilon_3)\cdot d_G(\upsilon_5)\cdot d_G(\upsilon_2)=24,\\
M_G(\upsilon_5) &= d_G(\upsilon_1)\cdot d_G(\upsilon_4)=12,\\
M_G(\upsilon_6) &= d_G(\upsilon_1)=3.
\end{aligned}$$

2.2.1 Subgraphs and Cliques

In this section, we discuss subparts or subcomponents of graphs.

Definition 2.2.14. A graph $H=(V_H,E_H)$ is termed subgraph of a graph $K=(V_K,E_K)$ if $V_H \subseteq V_K$ and $E_H \subseteq E_K$.

Definition 2.2.15. A subgraph graph H of a graph K is termed a spanning subgraph if $V_H = V_K$.

Definition 2.2.16. A subgraph H of a graph K is termed an induced subgraph if whenever $\upsilon_a, \upsilon_b \in V_H$ and $e_{ab} \leftrightarrow (\upsilon_a, \upsilon_b) \in E_K$, then $e_{ab} \in E_H$.

Example 2.2.7. *Consider the graphs K, H_1 and H_2 in Figure 2.6. The vertex and the*

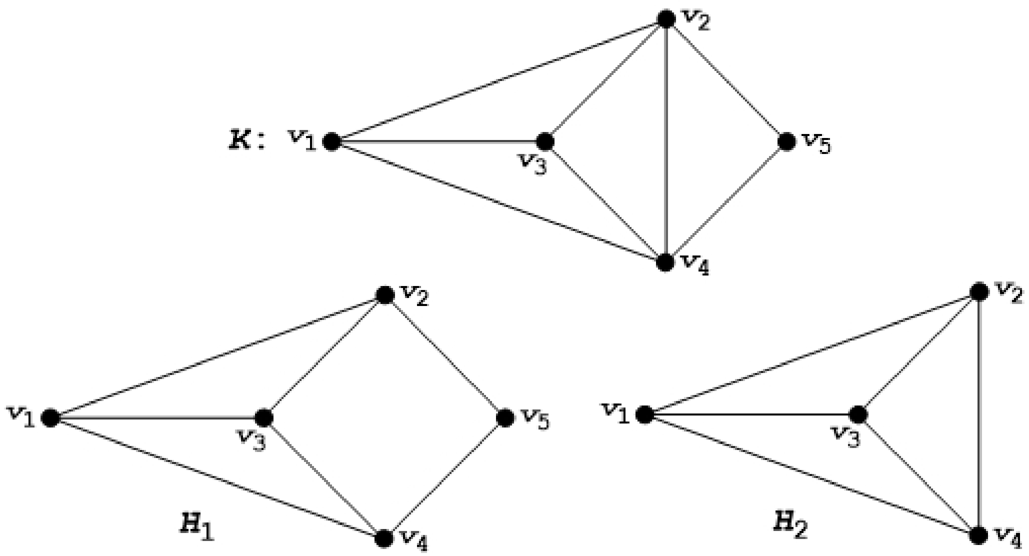

Figure 2.6: A spanning subgraph H_1 and induced subgraph H_2 of graph K.

edge sets of K are respectively given as

$$V_K = \{\upsilon_1, \upsilon_2, \upsilon_3, \upsilon_4, \upsilon_5\} \text{ and } E_K = \{e_{12}, e_{25}, e_{13}, e_{14}, e_{23}, e_{34}, e_{24}, e_{45}\},$$

The graph H_1 is a spanning subgraph of graph K having the vertex and edge sets respectively as

$$V_{H_1} = V_K \text{ and } E_{H_1} = \{e_{12}, e_{25}, e_{13}, e_{14}, e_{23}, e_{34}, e_{45}\} \subset E_K,$$

and the graph H_2 is an induced subgraph of graph K having the vertex and edge sets respectively as

$$V_{H_2} = \{\upsilon_1, \upsilon_2, \upsilon_3, \upsilon_4\} \subset V_K \text{ and } E_{H_2} = \{e_{12}, e_{13}, e_{14}, e_{23}, e_{34}, e_{24}\} \subset E_K.$$

Definition 2.2.17. A subset of vertices $C \subseteq V_G$ is termed a clique if the subgraph induced by C is a complete graph.

Remark 2.2.3. A singleton subset of the vertex set of any graph is always a clique.

Remark 2.2.4. A two ton subset of the vertex set of any graph which consists of adjacent vertices is always a clique.

Example 2.2.8. *A graph G presented in Figure 2.7 having the vertex set* $V_G = \{\upsilon_1, \upsilon_2, \upsilon_3, \upsilon_4, \upsilon_5, \upsilon_6, \upsilon_7, \upsilon_8, \upsilon_9, \upsilon_{10}, \upsilon_{11}, \upsilon_{12}, \upsilon_{13}, \upsilon_{14}, \upsilon_{15}, \upsilon_{16}, \upsilon_{17}\}$

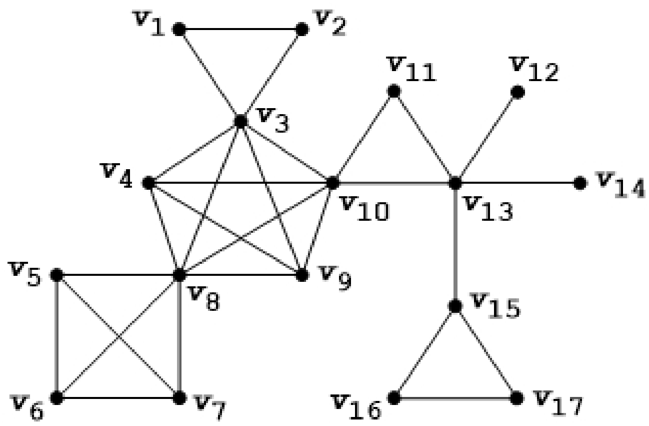

Figure 2.7: A graph G contains certain cliques.

and the subsets of V_G as follows:

$$\begin{aligned} C_1 &= \{\upsilon_1, \upsilon_2, \upsilon_3\} \subset V_G \\ C_2 &= \{\upsilon_{10}, \upsilon_{11}, \upsilon_{13}\} \subset V_G \\ C_3 &= \{\upsilon_{15}, \upsilon_{16}, \upsilon_{17}\} \subset V_G \\ C_4 &= \{\upsilon_5, \upsilon_6, \upsilon_7, \upsilon_8\} \subset V_G \\ C_5 &= \{\upsilon_3, \upsilon_4, \upsilon_8, \upsilon_9, \upsilon_{10}\} \subset V_G. \end{aligned}$$

Then the subgraphs of G induced by each of the subsets C_1, C_2 and C_3 is a complete graph K_3, therefore the sets C_1, C_2 and C_3 are the cliques of graph G having three vertices. The subset C_4 is a clique of G having four vertices because the subgraph *induced by C_4 is complete graph K_4. Also, the subset C_5 is a clique of G having five vertices because the subgraph induced by C_5 is complete graph K_5.*

2.2.2 Paths and Cycles

Definition 2.2.18. In a graph $G = (V_G, E_G)$, a $\upsilon_0 - \upsilon_t$ walk W of length t is a finite sequence

$$W : \upsilon_0 \to e_{01} \to \upsilon_1 \to e_{12} \to \upsilon_2 \to \cdots \to \upsilon_{t-1} \to e_{(t-1)t} \to \upsilon_t$$

having the terms as vertices and edges alternately such that if $\upsilon_i,\ e_{ij},\ \upsilon_j$, then $e_{ij} \leftrightarrow (\upsilon_i, \upsilon_j)$ for $0 \leq i, j \leq t$.

Example 2.2.9. *From the graph G, presented in Figure 2.8,*

$$W : \upsilon_0 \to e_{03} \to \upsilon_3 \to e_{23} \to \upsilon_2 \to e_{24} \to \upsilon_4 \to e_{34} \to \upsilon_3 \to e_{23} \to \upsilon_2 \to e_{12} \to \upsilon_1$$

is a walk of length 6 *in G.*

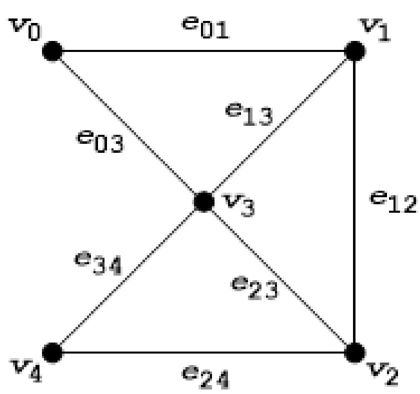

Figure 2.8: The graph G.

Definition 2.2.19. If all edges $e_{01}, e_{12}, \ldots, e_{(t-1)t}$ of the walk

$$W : \upsilon_0 \to e_{01} \to \upsilon_1 \to e_{12} \to \upsilon_2 \to \cdots \to \upsilon_{t-1} \to e_{(t-1)t} \to \upsilon_t$$

having no identical edges, then this walk is termed a trail. i.e. in a trail an edge cannot appear more than once.

Example 2.2.10. *From the graph G, presented in Figure 2.8,*

$$T : \upsilon_0 \to e_{03} \to \upsilon_3 \to e_{23} \to \upsilon_2 \to e_{24} \to \upsilon_4 \to e_{34} \to \upsilon_3 \to e_{13} \to \upsilon_1$$

is a trail having length 5 *in graph G.*

Definition 2.2.20. A $\upsilon_0 - \upsilon_t$ trail $T : \upsilon_0 \to e_{01} \to \upsilon_1 \to e_{12} \to \upsilon_2 \to \cdots \to \upsilon_{t-1} \to e_{(t-1)t} \to \upsilon_t$ is open or closed accordingly as $\upsilon_0 \neq \upsilon_t$ or $\upsilon_0 = \upsilon_t$ respectively.

Definition 2.2.21. A closed trail in a graph G is termed a circuit.

Example 2.2.11. *From the graph G, presented in Figure 2.8,*

$$\upsilon_0 \to e_{03} \to \upsilon_3 \to e_{23} \to \upsilon_2 \to e_{24} \to \upsilon_4 \to e_{34} \to \upsilon_3 \to e_{13} \to \upsilon_1 \to e_{01} \to \upsilon_0$$

is a circuit of length 6 *in graph G.*

Definition 2.2.22. A $\upsilon_0 - \upsilon_t$ path is a trail in which a vertex cannot appear more than once. The path graph having n vertices with length $n-1$ is symbolized by P_n.

Example 2.2.12. *From the graph G, presented in Figure 2.8,*

$$\upsilon_0 \to e_{03} \to \upsilon_3 \to e_{34} \to \upsilon_4 \to e_{24} \to \upsilon_2 \to e_{12} \to \upsilon_1$$

is a path having length 4.

Definition 2.2.23. A circuit is termed a cycle if a vertex cannot appear more than once except for the first and last. A cycle having n edges is termed a n-cycle and is denoted by C_n.

Example 2.2.13. *From the graph G, presented in Figure 2.8,*

$$\upsilon_0 \to e_{01} \to \upsilon_1 \to e_{12} \to \upsilon_2 \to e_{24} \to \upsilon_4 \to e_{34} \to u_3 \to e_{03} \to u_0$$

is a cycle having length 5 *in graph G.*

2.2.3 Connected and Disconnected Graphs

In this part, we define/discuss the connectedness of graphs.

Definition 2.2.24. A pair of vertices (υ_a, υ_b) in a graph H is said to be a connected pair of vertices if there is a path from υ_a to υ_b. Otherwise it is termed a disconnected pair of vertices.

Definition 2.2.25. If each pair of vertices (υ_a, υ_b) in a graph H is a connected pair of vertices, then graph H is termed a connected graph.

Definition 2.2.26. If there is at least one disconnected pair of vertices (υ_a, υ_b) in graph H then H is termed a disconnected graph.

Definition 2.2.27. A maximal connected subgraph of a disconnected graph H is termed its component.

Remark 2.2.5. A connected graph has exactly one connected component.

Example 2.2.14. *Consider a graph H having 12 vertices in Figure 2.9, then H is a disconnected graph comprises three components H_1, H_2 and H_3 since there are several disconnected pairs of vertices. i.e. (υ_1, υ_7) as there is no path which connects the vertices υ_1 and υ_7.*

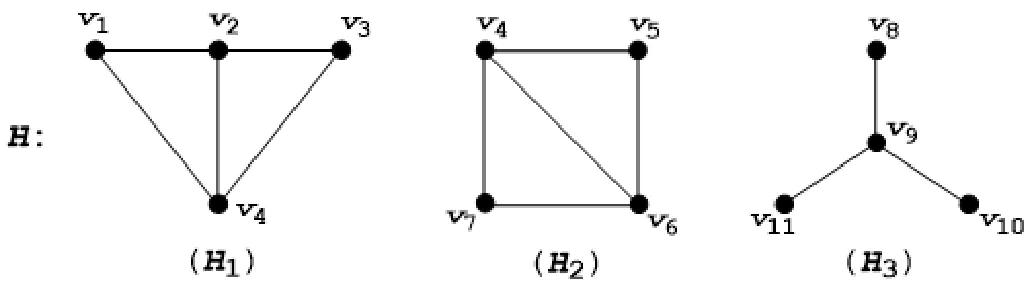

Figure 2.9: A disconnected graph H with three components H_1, H_2 and H_3.

2.2.4 Trees

Definition 2.2.28. A graph having no cycle is termed an acyclic graph.

Definition 2.2.29. A tree is a simple $(n, n-1)$-graph that is connected as well as acyclic.

Example 2.2.15. *A tree T having 22 vertices and 21 edges is presented in Figure 2.10.*

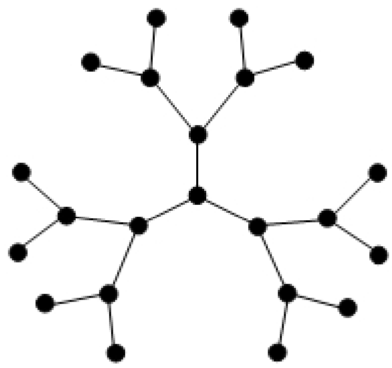

Figure 2.10: A tree T.

Definition 2.2.30. A forest is a simple graph such that each of its component is a tree. Thus any tree is a connected forest.

2.2.5 Distance in Graphs

In this part, we talk about distance or metric related terminology of graphs.

Definition 2.2.31. Let H be a connected graph then the distance between a pair of vertices (υ_a, υ_b) is symbolized by $d(\upsilon_a, \upsilon_b)$ and is obtained by counting the edges lying in the shortest path between them.

Example 2.2.16. *From the connected graph H, presented in Figure 2.11, the pair of*

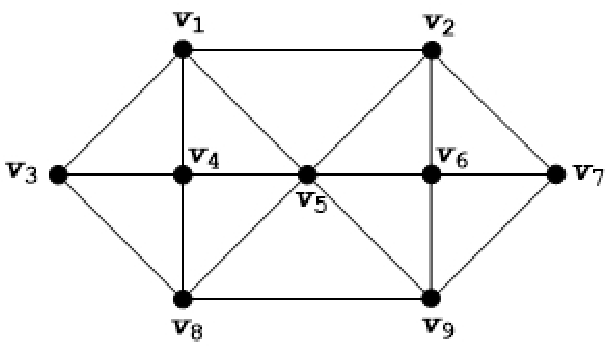

Figure 2.11: A graph H.

vertices (υ_3, υ_7) *is connected by the shortest path* $\upsilon_3 \to e_{13} \to \upsilon_1 \to e_{12} \to \upsilon_2 \to e_{27} \to \upsilon_7$ *or* $\upsilon_3 \to e_{13} \to \upsilon_1 \to e_{12} \to \upsilon_2 \to e_{27} \to \upsilon_7$. *There are three edges lying in this path, so we have*

$$d(\upsilon_3, \upsilon_7) = 3.$$

Definition 2.2.32. For a positive integer k, the k-neighborhood set of a vertex $\upsilon_a \in V_G$ is represented by $N_k(\upsilon_a|G)$ and defined as $N_k(\upsilon_a|G) = \{\upsilon_b \in V_G : d(\upsilon_a, \upsilon_b) = k\}$.

Definition 2.2.33. The k-distance degree of a vertex $\upsilon_a \in V_G$ is symbolized by $d_k(\upsilon_a|G)$ and defined as $d_k(\upsilon_a|G) = |N_k(\upsilon_a|G)|$. Obviously $d_1(\upsilon_a|G) = d_G(\upsilon_a)$ for every $\upsilon_a \in V_G$.

Definition 2.2.34. The distance sum of a vertex $\upsilon_a \in V_H$ is symbolized by $d(\upsilon_a|H)$ and presented as:

$$d(\upsilon_a|H) = \sum_{\upsilon_b \in V_H} d(\upsilon_a, \upsilon_b)$$

Example 2.2.17. *Consider a connected graph H in Figure 2.11 then the distances from the vertex* $\upsilon_1 \in V_H$ *to all other vertices are given by:*

$$\begin{aligned} d(\upsilon_1, \upsilon_2) &= d(\upsilon_1, \upsilon_3) = d(\upsilon_1, \upsilon_4) = d(\upsilon_1, \upsilon_5) = 1 \\ d(\upsilon_1, \upsilon_6) &= d(\upsilon_1, \upsilon_7) = d(\upsilon_1, \upsilon_8) = d(\upsilon_1, \upsilon_9) = 2. \end{aligned}$$

The distance sum of the vertex υ_1 *is calculated as:*

$$\begin{aligned} d(\upsilon_1|H) &= d(\upsilon_1, \upsilon_2) + d(\upsilon_1, \upsilon_3) + d(\upsilon_1, \upsilon_4) + d(\upsilon_1, \upsilon_5) \\ &\quad + d(\upsilon_1, \upsilon_6) + d(\upsilon_1, \upsilon_7) + d(\upsilon_1, \upsilon_8) + d(\upsilon_1, \upsilon_9) \\ &= 12. \end{aligned}$$

Definition 2.2.35. The eccentricity of a given vertex $\upsilon_a \in V_H$ is denoted by $\varepsilon(\upsilon_a)$ and is obtained by computing the maximum distance from υ_a to any other vertex $\upsilon_b \in V_H$. i.e.

$$\varepsilon(\upsilon_a) = \max_{\upsilon_b \in V_H} d(\upsilon_a, \upsilon_b)$$

Example 2.2.18. *From the graph H, presented in Figure 2.12 having vertex set*

$$V_H = \{\upsilon_1, \upsilon_2, \upsilon_3, \upsilon_4, \upsilon_5, \upsilon_6, \upsilon_7, \upsilon_8, \upsilon_9, \upsilon_{10}\}$$

then the eccentricity of each vertex of H is presented as:

$$\varepsilon(\upsilon_1) = \varepsilon(\upsilon_8) = \varepsilon(\upsilon_9) = \varepsilon(\upsilon_{10}) = 4$$
$$\varepsilon(\upsilon_2) = \varepsilon(\upsilon_3) = \varepsilon(\upsilon_4) = \varepsilon(\upsilon_6) = \varepsilon(\upsilon_7) = 3$$
$$\varepsilon(\upsilon_5) = 2.$$

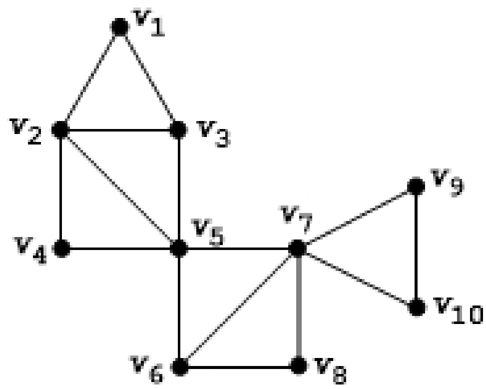

Figure 2.12: A graph H.

Definition 2.2.36. The maximum and minimum eccentricities of a graph H are called respectively the diameter d_H and radius r_H of H. i.e.

$$d_H = \max_{\upsilon_a \in V_H} \varepsilon(\upsilon_a) \text{ and } r_H = \min_{\upsilon_a \in V_H} \varepsilon(\upsilon_a).$$

Example 2.2.19. *The diameter and radius of graph H given in Figure 2.12 are respectively presented as:*

$$d_H = 4 \textit{ and } r_H = 2.$$

Definition 2.2.37. If all the vertices have the same eccentricity then H is termed a self-centered graph and otherwise a non-self-centered graph.

Clearly for a self-centered graph H we have

$$r_H = d_H.$$

Definition 2.2.38. Two edges $e_{ab} = (\upsilon_a, \upsilon_b)$ and $e_{cd} = (\upsilon_c, \upsilon_d)$ of a graph G are termed *codistant*, represented by $e_{ab}\ co\ e_{cd}$ iff for a non-negative integer t,

$$d(\upsilon_a, \upsilon_c) = d(\upsilon_b, \upsilon_d) = t \text{ and } d(\upsilon_a, \upsilon_d) = d(\upsilon_b, \upsilon_c) = t + 1$$

or vice versa.

It can be checked that the relation *co* may not be an equivalence relation, i.e. *co* is reflexive and symmetric but it may not be transitive.

Definition 2.2.39. Let G be a simple graph and $C(e_{ab})$ be the set comprises edges of G that are *codistant* to the edge $e_{ab} \in E(G)$ i.e.

$$C(e_{ab}) = \{e_{cd} \in E(G) : e_{cd}\ co\ e_{ab}\}.$$

If *co* is an equivalence relation on the set $C(e_{ab})$, then this set is termed an orthogonal cut (oc) of G.

Definition 2.2.40. A graph G is termed a *co-graph* iff its edge set E_G can be partitioned into disjoint orthogonal cuts.

Definition 2.2.41. If any two edges of an orthogonal-cut of a graph G are co-distant within the same face of G, this type of orthogonal-cut is termed as quasi-orthogonal cut (qoc).

2.2.6 Graph Isomorphism and Graph Invariant

Definition 2.2.42. A graph $H = (V_H, E_H)$ is termed isomorphic to a graph $K = (V_K, E_K)$ if there is a bijection $\psi : V_H \to V_K$ such that each edge $e_{ab} \leftrightarrow (\upsilon_a, \upsilon_b)$ in H corresponds to an edge $e_{cd} \leftrightarrow (\upsilon_c, \upsilon_d)$ in K in such a way that $\upsilon_a \leftrightarrow \upsilon_c$ and $\upsilon_b \leftrightarrow \upsilon_d$. Such a bijection between the graphs H and K is called a graph isomorphism, symbolically written as $H \cong K$.

Example 2.2.20. *In Figure 2.13, an isomorphism is given between the graphs H and K* *by the following one-to-one correspondences of vertices and edges respectively.*

$$v_1 \leftrightarrow w_1,\ \ v_2 \leftrightarrow w_2,\ \ v_3 \leftrightarrow w_5,\ \ v_4 \leftrightarrow w_6,\ \ v_5 \leftrightarrow w_4,\ \ v_6 \leftrightarrow w_3$$

and

$$(v_1,v_2) \leftrightarrow (w_1,w_2),\ \ (v_2,v_3) \leftrightarrow (w_2,w_5),\ \ (v_3,v_4) \leftrightarrow (w_5,w_6),$$
$$(v_1,v_4) \leftrightarrow (w_1,w_6),\ \ (v_1,v_5) \leftrightarrow (w_1,w_4),\ \ (v_2,v_6) \leftrightarrow (w_2,w_3),$$
$$(v_3,v_5) \leftrightarrow (w_5,w_4),\ \ (v_4,v_6) \leftrightarrow (w_6,w_3),\ \ (v_5,v_6) \leftrightarrow (w_4,w_3).$$

The graph G given in Figure 2.14 is not isomorphic to the graph H (or K) because G

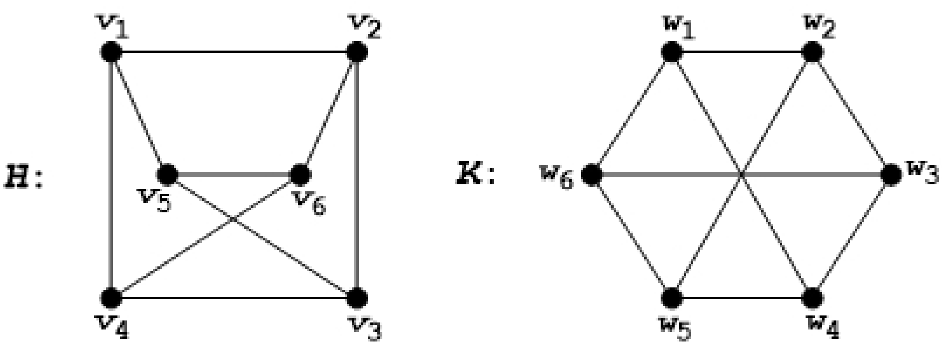

Figure 2.13: Two isomorphic graphs H and K.

contain a cycle of length three and H (or K) does not contain a cycle of length three.

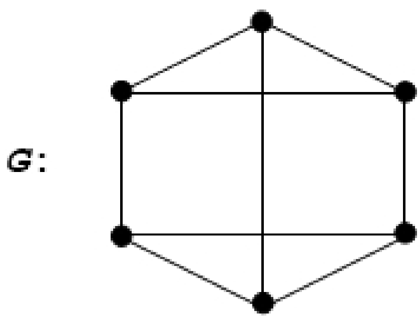

Figure 2.14: A graph G.

Note that If there is a graph isomorphism between two simple graphs H and K then clearly they must have

- $|V_H| = |V_K|$
- $|E_H| = |E_K|$
- The corresponding vertices of both graphs have the same degree
- Both graphs have the same cycles in number
- Both graphs have the same cliques in number
- Both graphs have the same girth
- Both graphs have the same radius
- Both graphs have the same diameter
- The distance between the vertices $\upsilon_a, \upsilon_b \in V_H$ is same as the distance between the corresponding vertices $f(\upsilon_a), f(\upsilon_b) \in V_K$
- Both graphs have the same spanning trees in number
- Both graphs have the same chromatic number
- Both graphs have the same metric dimension
- Both graphs have the same connectedness
- Both graphs have the same incidence and adjacency matrices
- Both graphs have the same independence number

However, the above conditions are not sufficient for two graphs to be isomorphic.

Definition 2.2.43. A graph invariant is defined as a function ϕ from the class of graphs Ω to the class of values $\Re$ such as real numbers or polynomials i.e. $\phi : \Omega \to \Re$ such that $\phi(G) = \phi(H)$ for any two isomorphic graphs $G, H \in \Omega$.

Example 2.2.21. *For a graph G, the numerical quantities associated with G such as order, size, radius and diameter etc are the graph invariants because any other graph H which is isomorphic to G must have the equal order, size, radius and diameter as of G.*

2.2.7 Transformation of Graphs

Definition 2.2.44. Let H be a (n,m)-graph then its subdivision graph is denoted by $S(H)$ and is obtained from H by replacing each of its path of length one by a path of length two.

The order and size of $S(H)$ are respectively given by:

$$|V_{S(H)}| = n+m \quad \text{and} \quad |E_{S(H)}| = 2m.$$

Definition 2.2.45. Let H be a (n,m)-graph then its vertex-semi total graph is symbolized by $R(H)$ and is obtained by adding a vertex υ_c corresponding to each edge $e_{ab} \leftrightarrow (\upsilon_a, \upsilon_b) \in E_H$ such that υ_c adjacent to the vertices υ_a and υ_b.

The order and size of $R(H)$ are respectively presented as:

$$|V_{R(H)}| = n+m \quad \text{and} \quad |E_{R(H)}| = 3m.$$

Definition 2.2.46. Let H be a (n,m)-graph then its edge-semi total graph is denoted by $Q(H)$ and is obtained by adding a new vertex υ_c corresponding to each edge $e_{ab} \leftrightarrow (\upsilon_a, \upsilon_b) \in E_H$ such that a pair of new vertices are adjacent if their corresponding edges share a vertex in H.

The order and size of $Q(H)$ are respectively presented as:

$$|V_{Q(H)}| = n+m \quad \text{and} \quad |E_{Q(H)}| = m + \frac{1}{2} \sum_{\upsilon_a \in V_H} d(\upsilon_a)^2.$$

Definition 2.2.47. Let H be a (n,m)-graph then its total graph is denoted by $T(H)$ and is obtained by taking the vertex set $V_H \cup E_H$ such that a pair of vertices of $T(H)$ being adjacent iff the corresponding elements of H are incident or adjacent.

The order and size of $T(H)$ are respectively presented as:

$$|V_{T(H)}| = n+m \quad \text{and} \quad |E_{T(H)}| = 2m + \frac{1}{2}\sum_{\upsilon_a \in V_H} d(\upsilon_a)^2.$$

Example 2.2.22. *For the cycle C_4, its subdivision graph $S(C_4)$, vertex-semi total graph $R(C_4)$, edge-semi total graph $Q(C_4)$ and total graph $T(C_4)$ are shown in Figure 2.15.*

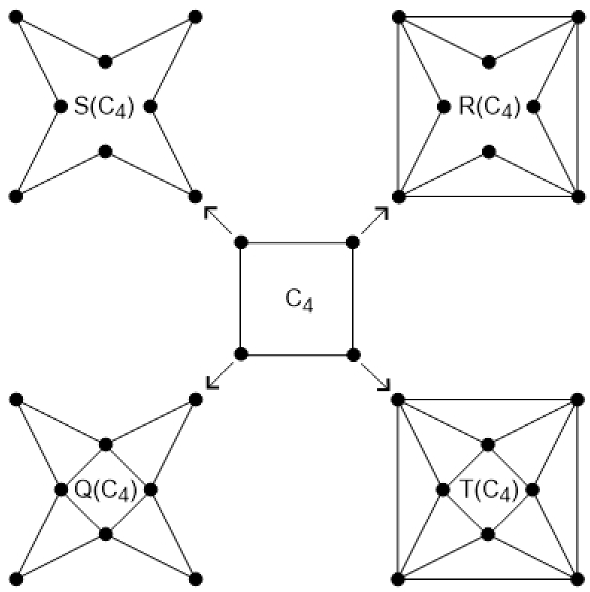

Figure 2.15: The four transformed graphs $S(C_4)$, $R(C_4)$, $Q(C_4)$ and $T(C_4)$ of the cycle C_4.

Definition 2.2.48. Let H be a (n,m)-graph then its line graph is denoted by $L(H)$ and is obtained by taking the vertices corresponding to the edges of H such that two vertices of $L(H)$ being adjacent iff the corresponding edges in H share a vertex.

Definition 2.2.49. The t-th iterated line graphs of a graph H are inductively presented as:

$$L^t(H) = \begin{cases} H, & \text{if } t = 0; \\ L(L^{t-1}(H)), & \text{if } t > 0 \end{cases}$$

Example 2.2.23. *The t-th iterated line graphs of a graph H are presented in Figure 2.16 for $t = 1$ and $t = 2$.*

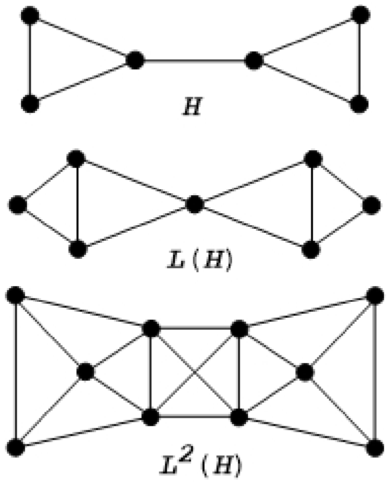

Figure 2.16: The t-th iterated line graphs of the graph H for $t = 1$ and $t = 2$.

Definition 2.2.50. Let H be a (n,m)-graph then its para-line graph is denoted by $PL(H)$ and is obtained from H by finding the line graph of $S(H)$.

Definition 2.2.51. The t-th iterated para-line graphs of a graph H are inductively presented as:

$$PL^t(H) = \begin{cases} H, & \text{if } t = 0; \\ PL(PL^{t-1}(H)), & \text{if } t > 0 \end{cases}$$

Example 2.2.24. *For $t = 1$ and $t = 2$, the t-th para-line graphs of a graph H are shown in Figure 2.17.*

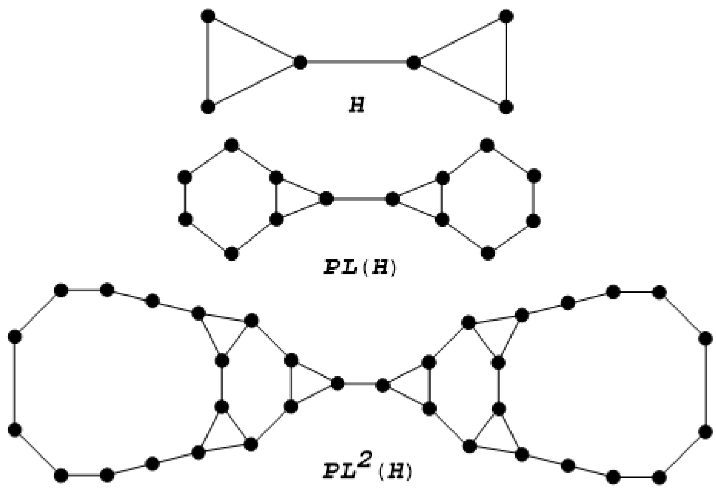

Figure 2.17: The t-th iterated para-line graphs of the graph H for $t = 1$ and $t = 2$.

Chapter 3

Chemical Graph Theory

3.1 Introduction

Graph theory exploited in the study of molecular graphs of chemical compounds which represents a multidisciplinary field, is called the chemical graph theory. By applying the tools of graph theory, it attempts to explore the structural phenomena involved in structure-property and -activity relationships. These tools comprise the topological indices and counting polynomials.

Definition 3.1.1. A molecular graph is a depiction of the structural formula of a chemical compound in which vertices represent atoms and the edges represent the chemical bonds between the atoms.

Example 3.1.1. *For example, the molecular graph of the benzene chemical compound* C_6H_6 *is presented in Figure 3.1.*

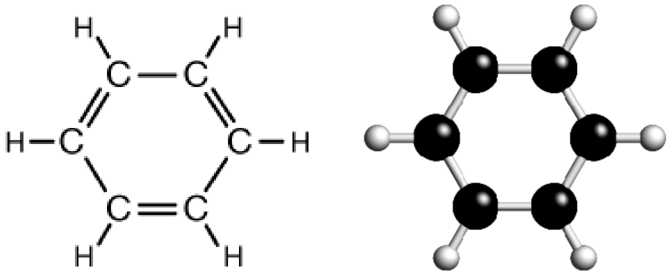

Figure 3.1: Benzene C_6H_6 and its molecular graph.

3.2 Molecular Descriptors

Quantitative structure-activity relationship (QSAR) is the final conclusion of the procedure which begins with an appropriate characterization of molecular graphs and ends with some prediction on the nature of chemical compounds in biological and physico-chemical systems in analysis. QSARs are placed on the hypothesis that the structure of a molecule must hold characteristics responsible for its biological, physical, and chemical properties and on the capability to capture these characteristics into numerical descriptors. The study in which a chemical property or biological activity of a chemical compound is modelled as a response variable, is termed the quantitative structureproperty relationship (QSPR). For physico-chemical properties and biological activities, the

QSAR/QSPR model is generally presented as

$$P = f(x_1, x_2, \ldots, x_n)$$

where P represents the physicochemical property or biological activity, $x_1, x_2, \ldots, x_n$ are n molecular descriptors, and the function f represents the connection between response and descriptors.

The molecular graph of a chemical structure corresponding to a chemical compound is strongly related to its physicochemical properties or biological activities such as strain energy, boiling point, and heat of formation. The molecular descriptor is the numerical function that translates the chemical phenomena encoded within a symbolic representation of a molecule into an effective number [86]. Thus, the study of the molecular descriptors on molecular graph of chemical materials can make up for lack of chemical experiments and can provide a theoretical basis for the manufacturing of chemical materials. The molecular descriptors can be categorized into two significant types: one is topological indices and the other type is counting polynomials.

3.3 Topological Indices

A topological index is the graph invariant which is used to correlate the physical features or chemical reactivities or biological activities of a chemical compound with its molecular graph. In this sense, topological indices are based on the topological architecture of corresponding molecular graph of the chemical compound. The use of the topological indices is particularly important when the use of experimental methods leads to waste of time, financial expenditures in large amounts and theoretical methods have not been successful. In recent years many topological indices have been recorded and used for chemical documentation, isomer discrimination, measure of structural similarity/dissimilarity, complexity, chirality, stability/diversity of chemical databases. These include molecular connectivity indices, Wiener index, eccentric connectivity index, etc. The role of topological indices for exploring biological activity in structure-activity relationship is considered as predominant by topological architecture of chemical structure and the simple connectivity between neighboring atoms without taking the nature of atoms or nature of chemical bonding considered as major determinant of biological activity of the chemical compound.

Generally, topological indices can be categorized in two major classes: one is degree-based indices/coindices and the other is distance-based indices.

3.3.1 Degree-based Topological Indices/Coindices

The general expression for the class of degree-based topological indices can be presented in two ways as

$$DTI_1(G) = \sum_{p\in V_G} f(g(p)) \tag{3.3.1}$$

$$DTI_2(G) = \sum_{pq\in E_G} f(g(p), g(q)) \tag{3.3.2}$$

where the function $g(p)$ represents degree of vertex p or degree sum or degree product of p.

In recent years, various valuable degree-based topological indices have been proposed in order to explore the characteristics of a molecular graph. In Table 3.1, we present the most studied degree-based topological indices in the literature which are formulated by taking the suitable function in (3.3.1)-(3.3.2) where α is any non zero real number.

While considering contribution of non adjacent pair of vertices in determining the weighted Wiener polynomial of certain graphs, Došlić [31] presented the first and second Zagreb coindices correspondingly as follows

$$\overline{M_1}(G) = \sum_{pq\notin E_G} [d_G(p) + d_G(q)]$$

and

$$\overline{M_2}(G) = \sum_{pq\notin E_G} d_G(p)\cdot d_G(q).$$

Furtula et al. [42] introduced the concept of F-coindex which is presented as follows

$$\overline{F}(G) = \sum_{pq\notin E_G} \left[(d_G(p))^2 + (d_G(q))^2\right]$$

Table 3.1: Degree-based topological indices

Degree-based topological index	$f(g(p))$ or $f(g(p),g(q))$
First Zagreb index (M_1) [48]	$(d_G(p))^2$
Second Zagreb index (M_2) [48]	$d_G(p)\cdot d_G(q)$
Randić connectivity index (χ) [75]	$\frac{1}{\sqrt{d_G(p)\cdot d_G(q)}}$
Harmonic index (H) [38]	$\frac{2}{\sqrt{d_G(p)+d_G(q)}}$
General Randić connectivity index (R_α) [12]	$(d_G(p)\cdot d_G(q))^\alpha$
Atom-bond connectivity index (ABC) [36]	$\sqrt{\frac{d_G(p)+d_G(q)-2}{d_G(p)\cdot d_G(q)}}$
First general Zagreb index (M_1^α) [64]	$(d_G(p))^\alpha$
First geometric-arithmetic index (GA) [88]	$\frac{2\sqrt{d_G(p)\cdot d_G(q)}}{d_G(p)+d_G(q)}$
General sum-connectivity index (χ_α) [101]	$(d_G(p)+d_G(q))^\alpha$
Fourth atom-bond connectivity index (ABC_4) [45]	$\sqrt{\frac{\delta_G(p)+\delta_G(q)-2}{\delta_G(p)\cdot\delta_G(q)}}$
Augmented Zagreb index (AZI) [40]	$\left(\frac{d_G(p)\cdot d_G(q)}{d_G(p)+d_G(q)-2}\right)^3$
Symmetric division deg index (SDD) [89]	$\frac{d_G(p)}{d_G(q)}+\frac{d_G(q)}{d_G(p)}$
Inverse sum indeg index (ISI) [89]	$\frac{d_G(p)d_G(q)}{d_G(p)+d_G(q)}$
Fifth geometric-arithmetic index (GA_5) [46]	$\frac{2\sqrt{\delta_G(p)\cdot\delta_G(q)}}{\delta_G(p)+\delta_G(q)}$
Fifth atom-bond connectivity index (ABC_5) [15]	$\sqrt{\frac{M_G(p)+M_G(q)-2}{M_G(p)\cdot M_G(q)}}$
Redefined third Zagreb index (ReZ_3) [76]	$d_G(p)d_G(q)[d_G(p)+d_G(q)]$
Forgotten topological index or F-index (F) [41]	$(d_G(p))^3$

In 2004, Miličević et al. [67] presented the reformulated Zagreb indices by reformulating the Zagreb indices in terms of edge-degrees instead of vertex-degrees. For a graph

G, the first and second reformulated Zagreb indices are represented by $EM_1(G)$ and $EM_2(G)$ respectively and defined as follows:

$$EM_1(G) = \sum_{e \in E_G} d_G(e)^2 \quad \text{and} \quad EM_2(G) = \sum_{\substack{e \sim f \\ e,f \in E_G}} d_G(e) \cdot d_G(f)$$

Recently, Naji et al. [71] introduced distance-degree-based topological indices, formulated by using 2-distance degrees of vertices, called the leap Zagreb indices. For a graph G, the first, second, and third leap Zagreb indices are represented by $LM_1(G)$, $LM_2(G)$, and $LM_3(G)$ respectively and are defined as follows:

$$LM_1(G) = \sum_{p \in V_G} d_2(p/G)^2, \;\; LM_2(G) = \sum_{pq \in E_G} d_2(p/G)\, d_2(q/G)$$

and

$$LM_3(G) = \sum_{p \in V_G} d_G(p) d_2(p/G).$$

3.3.2 Distance-based Topological Indices

The first distance-based index was introduced in 1947 by the chemist Harold Wiener [95] and is called the Wiener index (WI), presented as

$$W(G) = \sum_{\{p,q\} \subseteq V_G} d(p,q).$$

This index has most of the chemical applications for the chemical compounds which have acyclic molecular graphs i.e. trees [30, 49].

The eccentricity related topological indices belong to the class of distance-based indices. The general expressions for these indices, can be defined in the following ways as

$$ETI_1(G) = \sum_{p \in V_G} f(d_G(p), \varepsilon(p)), \tag{3.3.3}$$

$$ETI_2(G) = \sum_{p \in V_G} f(M_G(p), \varepsilon(p)), \tag{3.3.4}$$

$$ETI_3(G) = \sum_{p \in V_G} f(\delta_G(p), \varepsilon(p)), \tag{3.3.5}$$

$$ETI_4(G) = \sum_{pq \in E_G} f(\varepsilon(p), \varepsilon(q)). \tag{3.3.6}$$

By choosing the appropriate function in (3.3.3)-(3.3.6) from the following list of functions, we formulate the corresponding eccentricity-based topological index.

Table 3.2: Eccentricity-based topological indices

Eccentricity-based Topological Index	Function
Eccentric connectivity index (ξ^c) [80]	$f(d_G(p), \varepsilon(p)) = d_G(p) \cdot \varepsilon(p)$
Connective eccentric index (C^{ξ}) [47]	$f(d_G(p), \varepsilon(p)) = d_G(p)/\varepsilon(p)$
Augmented eccentric connectivity index (ξ^{ac}) [33]	$f(M_G(p), \varepsilon(p)) = M_G(p)/\varepsilon(p)$
Modified eccentric connectivity index (ξ_c) [6]	$f(\delta_G(p), \varepsilon(p)) = \delta_G(p) \cdot \varepsilon(p)$
Reverse eccentric connectivity index ($^{RE}\xi^c$) [34]	$f(\delta_G(p), \varepsilon(p)) = \varepsilon(p)/\delta_G(p)$
Third atom-bond connectivity index (ABC_3) [63]	$f(\varepsilon(p), \varepsilon(q)) = \sqrt{\frac{\varepsilon(p)+\varepsilon(q)-2}{\varepsilon(p)\cdot\varepsilon(q)}}$

3.4 Counting Polynomials

Counting polynomials are another important graph invariants which provide a way to explore the characteristics of molecular graphs.
In order to count *qoc* strips in a graph G, Diudea [24] introduced the Omega polynomial which is formulated as follows

$$\Omega(G,x) = \sum_k r(G,k)x^k$$

where $r(G,k)$ represents the number of *qoc* strips of length k and the sum runs up to the maximum length of *qoc* strips in G. It can be check that

$$|E_G| = [d(\Omega(G,x))/dx]_{x=1}.$$

The Omega polynomial found application in the topological description of polyhedral coverings appearing in complex nanostructures. This counting polynomial is also useful in accounts for the spirality, helicity and ring distribution of nanotubular structures [27]. The coefficient of the first power term of this polynomial, called n_p has good ability in predicting the resonance energy in planar benzenoids as well as the stability of small fullerenes [25].

By using the Omega polynomial, a topological index was introduced, called the Cluj-Ilmenau index [93] which is formulated as

$$CI(G) = [\Omega'^2 - \Omega' - \Omega'']_{x=1}.$$

Another counting polynomial was introduced depending upon the *qoc* strips, called the Sadhana polynomial and is presented as

$$Sd(G,x) = \sum_k r(G,k)x^{|E(G)|-k}.$$

From the Sadhana polynomial, a topological index is obtained, called the Sadhana index [55] which is presented as

$$Sd = [d(Sd(G,x))/dx]_{x=1} = \sum_k r(G,k)(|E(G)|-k).$$

In the comparative study of modeling resonance energy and benzene character of polyacenes and helicenes, the Sadhana index was declared the best index compare to other well-known indices such as Wiener, szeged, PI and Randić connectivity indices [56, 57].

By using the *qoc* strips, Diudea [26] presented another counting polynomial, called the Theta polynomial which is formulated as

$$\Theta(G,x) = \sum_k r(G,k)kx^k.$$

From this counting polynomial, Theta index is defined as $[d(\Theta(G,x))/dx]_{x=1}$.

Chapter 4

Some Known Results

4.1 Introduction

In this chapter, we recall some preliminary results and the relations of topological indices with some graph parameters, i.e. the order, size, radius and diameter. We also present some known connections between topological indices of any graph.

4.2 Known Results

In the coming result, a well known relation is presented between the size of a graph and the degrees of its vertices.

Theorem 4.2.1. *[16] For any simple graph G with size m, we have*

$$\sum_{v \in V_G} d_G(v) = 2m. \tag{4.2.1}$$

This relation is known as "handshaking lemma".
The relation of diameter of a connected graph with its radius, is presented in the next result.

Theorem 4.2.2. *[16] Consider a connected graph having radius r_G and diameter d_G, then*

$$r_G \leq d_G \leq 2r_G \tag{4.2.2}$$

and the left equality holds iff G is a self-centered graph.

The bounds for eccentric connectivity index related to radius and diameter respectively, are presented in the coming Theorem.

Theorem 4.2.3. *[101] Consider a connected graph G having size m, radius r_G and diameter d_G, then*

$$2mr_G \leq \xi^c(G) \leq 2md_G \tag{4.2.3}$$

and the equality holds iff G is a self-centered graph.

The bounds for connective eccentric index related to diameter and radius respectively, are presented in the coming result.

Theorem 4.2.4. *[22] Consider a connected graph G having size m, radius r_G and diameter d_G, then*

$$\frac{2m}{d_G} \leq C^{\xi}(G) \leq \frac{2m}{r_G} \tag{4.2.4}$$

and the equality holds iff G is a self-centered graph.

The bounds for augmented eccentric connectivity index related to diameter and radius respectively, are presented in the next result.

Theorem 4.2.5. *[23] Consider a connected graph G having order n, radius r_G, diameter d_G, minimum degree δ and maximum degree Δ, then*

$$\frac{\delta^{\delta}}{d_G} \leq \frac{1}{n}.\xi^{ac}(G) \leq \frac{\Delta^{\Delta}}{r_G} \tag{4.2.5}$$

and the equality holds iff G is a regular self-centered graph.

Theorem 4.2.6. *[63] Consider a connected graph G having size m, radius $r_G \geq 2$ and diameter d_G, then*

$$\frac{\sqrt{2}m}{d_G}\sqrt{d_G - 1} \leq ABC_3(G) \leq \frac{\sqrt{2}m}{r_G}\sqrt{r_G - 1}. \tag{4.2.6}$$

and the equality holds iff G is a self-centered graph.

The inequality between eccentric connectivity index and Wiener index, is presented in the coming result.

Theorem 4.2.7. *[18] Consider a connected graph G having order $n \geq 3$, then*

$$W(G) \leq \frac{2}{3}n\xi^{c}(G) - n + 1 \tag{4.2.7}$$

The relation between Randić connectivity index and diameter, is given in the following result.

Theorem 4.2.8. *[98] Consider a connected graph G having order $n \geq 3$, then*

$$R(G) - \frac{1}{2}d_G \geq \sqrt{2} - 1 \tag{4.2.8}$$

and the equality holds iff $G \cong P_n$.

The relation between ABC index and radius, is given in the next result.

Theorem 4.2.9. *[32] Consider a connected graph G having order $n \geq 2$, then*

$$ABC(G) - r_G \geq \frac{n-1}{\sqrt{2}} - \left\lfloor \frac{n}{2} \right\rfloor \tag{4.2.9}$$

and the equality holds iff $G \cong P_n$ for $n \geq 3$.

The relation between harmonic index and diameter, is given in the coming result.

Theorem 4.2.10. *[65] Consider a connected graph G having order $n \geq 4$ and diameter d_G, then*

$$H(G) - d_G \leq \frac{n}{2} - 1 \tag{4.2.10}$$

and the equality holds iff $G \simeq K_n$.

The relations of GA index with Randić connectivity and harmonic indices are achieved in the next results.

Theorem 4.2.11. *[4] Consider a connected graph G having order $n \geq 3$, then*

$$\sqrt{\frac{4}{3}}R(G) \leq GA(G) \leq (n-1)R(G) \tag{4.2.11}$$

the left and right equalities hold iff $G \cong P_3$ and $G \cong K_n$ respectively.

Theorem 4.2.12. *[4] Consider a connected graph G having order $n \geq 2$, then*

$$H(G) \leq GA(G) \leq (n-1)H(G) \tag{4.2.12}$$

the left and right equalities hold iff $G \cong P_n$ and $G \cong K_n$ respectively.

In the coming result, a general expression for the Wiener index of any tree is presented.

Theorem 4.2.13. *[28] For any $(n, n-1)$-tree T, we have*

$$W(T) = \frac{1}{4}\left[\sum_{v \in V_T} d_T(v) \cdot d(v|T) + n(n-1)\right]. \tag{4.2.13}$$

A connection between of Wiener index (WI) between any tree and its line graph is presented in the coming result.

Theorem 4.2.14. *[14] For any $(n,n-1)$ tree T, we have*

$$W(L(T)) = W(T) - \binom{n}{2}. \tag{4.2.14}$$

By using this connection, one can compute this index for the line graph $L(T)$ by using the WI of parent tree T and its order n without formulating this index directly for the line graph $L(T)$. For this reason, its redundant to formulate WI for the line graph $L(T)$. In the following result, a relation for the Wiener index of a tree with its k-th subdivided tree is presented.

Theorem 4.2.15. *[29] For any $(n,n-1)$-tree T and its k-th subdivided (n_k,n_k-1)-tree $S^k(T)$, we have*

$$W(S^k(T)) = (k+1)^3 \cdot W(T) + \binom{n_k+1}{3} - (k+1)^3 \cdot \binom{n+1}{3} \tag{4.2.15}$$

where $n_k = k(n-1)+n$.

Ashrafi et al. presented the following relation between first Zagreb index of molecular graph and its complement.

Theorem 4.2.16. *[7] Consider a molecular (p,q)-graph G and its complement (p',q')-graph $\overline{G}$, then*

$$M_1(\overline{G}) = M_1(G) + 2(p-1)(q'-q) \tag{4.2.16}$$

where $m' = \binom{p}{2} - q$.

Das et al. presented the following connection between first Zagreb coindex and first Zagreb index.

Theorem 4.2.17. *[19] Consider a molecular (p,q)-graph G, then*

$$\overline{M_1}(G) = 2q(p-1) - M_1(G). \tag{4.2.17}$$

The following is the relations between F-coindex, F-index and first Zagreb index of a molecular graph and of its complement.

Theorem 4.2.18. *[42] Consider a molecular (r,s)-graph G and its complement $\overline{G}$, then*

$$(a)\ \overline{F}(G) = (r-1)M_1(G) - F(G), \tag{4.2.18}$$

$$(b)\ F(\overline{G}) = r(r-1)^3 - 6s(r-1)^2 + 3(r-1)M_1(G) - F(G), \tag{4.2.19}$$

$$(c)\ \overline{F}(\overline{G}) = 2s(r-1)^2 - 2(r-1)M_1(G) + F(G). \tag{4.2.20}$$

For any simple graph, the first general Zagreb index of its para-line transformed graph is given in the coming Theorem.

Theorem 4.2.19. *[74] Consider $PL(G)$ symbolize the para-line transformed graph of a simple graph G, then*

$$M_1^{\alpha}(PL(G)) = \sum_{v \in V_G} [d_G(v)]^{\alpha+1} \tag{4.2.21}$$

where α is any real number.

In the coming result, a connection of general product-connectivity index (R_α) between any graph and its para-line transformed graph is presented.

Theorem 4.2.20. *[74] Consider a para-line transformed graph $PL(G)$ of any simple graph G, then*

$$R_\alpha(PL(G)) = R_\alpha(G) + \frac{1}{2} \sum_{v \in V_G} \left[(d_G(v))^{2\alpha+1} (d_G(v) - 1) \right] \tag{4.2.22}$$

where α is any real number.

By using this connection, one can formulate this index for the para-line transformed graph $PL(G)$ by using the R_α index of the parent graph G and parent graph degrees without formulating this index directly for the para-line transformed graph $PL(G)$. For this reason, its redundant to compute R_α for the para-line transformed graph $PL(G)$.
In the coming result, the bounds of third ABC index are presented depending upon some indices based on degrees.

Theorem 4.2.21. *[63] Consider a para-line transformed graph $PL(G)$ of any simple graph G, then*

$$\frac{1}{\sqrt{n^2m - nM_1(G) + M_2(G)}} \leq ABC_3(G) \leq \frac{1}{\sqrt{2}}\sqrt{2nm^2 - mM_1(G) - 2m^2}. \quad (4.2.23)$$

In the next result, a lower bound of Wiener index is presented in terms of first Zagreb index for the connected graphs which are independent of 3- and 4-cycles.

Theorem 4.2.22. *[100] For any connected (r,s)-graph G with girth greater than for, we have*

$$W(G) \geq \frac{3r(r-1)}{2} - \frac{1}{2}M_1(G) - s. \quad (4.2.24)$$

All the above stated results are used in obtaining certain new results of this Thesis. The results (4.2.2)−(4.2.12) are used in deriving inequality relations between topological indices belonging to degree- and distance-based classes. The results (4.2.14) and (4.2.15) are used in establishing a relation of Wiener index between a tree and its para-line transformed graph. Then, a general expression of the Wiener index for the para-line transformed of any tree are achieved by using the result (4.2.13). To obtain the general expressions of some topological indices/coindices for the iterated para-line transformed graph of any graph, the results (4.2.16)−(4.2.20) are used. Some lower and upper bounds for certain distance-based topological indices are achieved by using the results (4.2.1), (4.2.7) and (4.2.21)−(4.2.24).

Chapter 5

Degree-based Topological Indices of Nanostructures

5.1 Introduction

In this chapter, we formulate different topological indices belonging to degree-based class such as ABC, ABC_4, GA and GA_5 indices of boron triangular nanotube, boron-α nanotube, tri-hexagonal boron nanotube, tri-hexagonal boron nanotorus, and boron-α nanotorus. In addition, we formulate different topological indices belonging to degree-based class for the para-line transformed graphs of V-phenylenic Nanostructures.

5.2 Boron Nanostructures

For the last 20 years, various types of boron-containing nanomaterials such as boron nanoclusters, boron nanowires, boron nanotubes, boron nanobelts, boron nanoribbons, boron nanosheets, and boron fullerenes have been experimentally synthesized and identified. Boron nanomaterials have been considered as excellent materials for enhancing the characteristics of optoelectronic nanodevices because of their broad elastic modulus, high-melting point, excessive conductivity, great emission uniformity, and low turn-on field. These materials can carry excessive emission current, which recommends that they may have great prospective applications in the field emission area [61]. Furthermore, boron nanomaterials also have some better properties compared to carbon nanomaterials such as excessive resistance to oxidation at high temperatures and great chemical stability and are stable broad band-gap semiconductor [8, 68]. Due to these properties, boron nanomaterials may have great applications at high temperatures or in corrosive environments functioning as supercapacitors, solid lubricants, fuel cells, and batteries [17]. Moreover, the extensive range of boron nanomaterials themselves could be the building blocks for combining with other existing nanomaterials to design and create materials with new properties. For this reason, the boron-nitrogen clusters have been developed in [83], and boron-nitrogen cages have been computed in [82]. The boron fullerenes are the cage molecules [72] which can serve as the building blocks for fabrication of new hybrid nanostructures with novel properties. For the stability, mechanical and electronic properties of boron nanostructure materials, we refer to [73].

The boron triangular nanotube was constructed in 2004 [61] and acquired from a car-

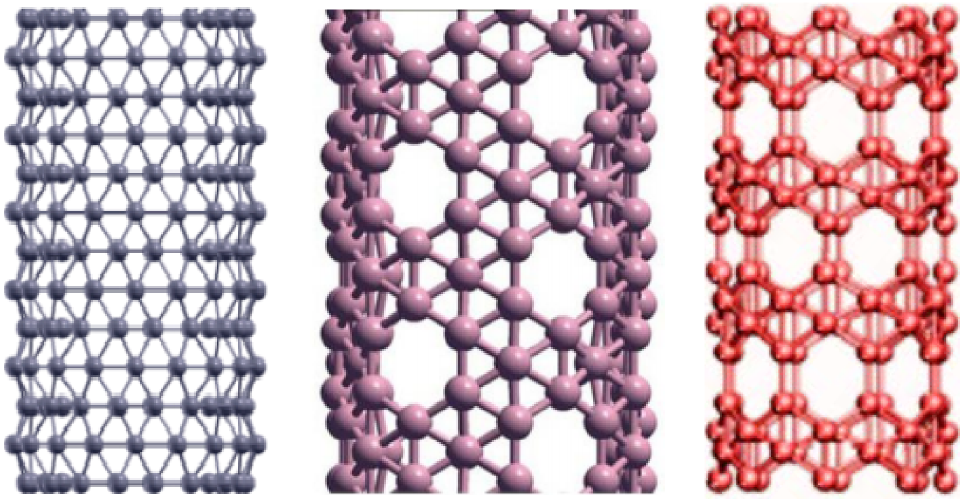

(a) (b) (c)

Figure 5.1: 3D perceptions of (a) boron triangular nanotube, (b) boron-α nanotube and (c) tri-hexagonal boron nanotube.

bon hexagonal nanotube with the condition that the addition of an extra atom to the center of each hexagon. Also, a special boron nanotube, called boron-α nanotube, was constructed from a carbon hexagonal nanotube in 2008, with the condition that the addition of an extra atom to the center of certain hexagon [63, 84]. It is reported in [81, 98] that these nanotubes are significant materials for optical, electronic, chemical, and bio-sensing applications. Wang et al. [92] predicted a new class of boron nanotubes which are are formed by removing some atoms from boron triangular nanotubes and thus constructed from triangles and hexagons, called the Tri-Hexagonal boron nanotubes. These nanotubes are sparser than the other boron nanotubes and after relaxation it remains flat and metallic independent of their chirality. The thermal stability and mechanical properties of boron nanotubes are important issues in nanodevice applications and thus require intensive study. The 3D perceptions of boron triangular, boron-α and tri-hexagonal boron nanotubes are presented in Figure 5.1.

5.3 Degree-based Indices of Boron Triangular Nanotube

In this part, we formulate different degree-based topological indices such as ABC, ABC_4, GA and GA_5 indices of boron triangular nanotube.

We denote the molecular graph of boron triangular nanotubes by $BT[m,n]$, where m

and n symbolize number of rows and columns in a 2D sheet of $BT[m,n]$ respectively as shown in Figure 5.2. The order and size of $BT[m,n]$ are $3mn/2$ and $3n(3m-2)/2$ respectively.

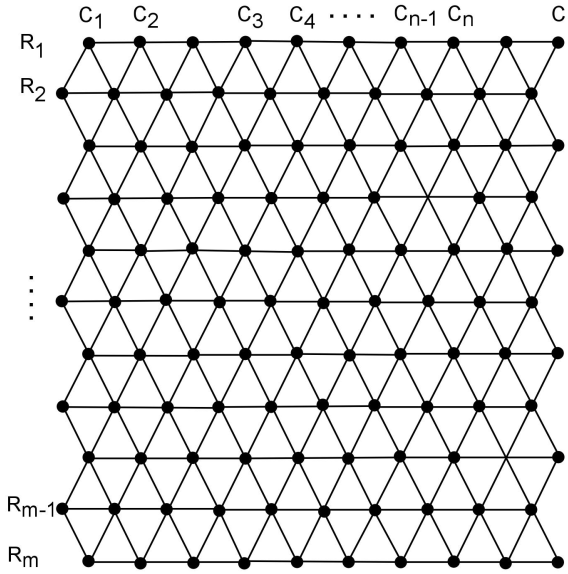

Figure 5.2: A 2D sheet of boron triangular nanotube $BT[m,n]$.

In the coming result, we formulate the "ABC, ABC_4, GA, and GA_5" indices for $BT[m,n]$.

Theorem 5.3.1. *Consider the boron triangular nanotube $BT[m,n]$, where $m \geq 3$ and n even, then*

$$\begin{aligned}
ABC(BT[m,n]) &= \frac{3\sqrt{10}}{4}mn + \frac{3\sqrt{6}}{4}n - 2\sqrt{10}n + 2\sqrt{3}n, \\
GA(BT[m,n]) &= \frac{9}{2}mn + \frac{12\sqrt{6}}{5}n - 9n, \\
ABC_4(BT[m,n]) &= \frac{\sqrt{70}}{8}mn - \frac{7\sqrt{70}}{12}n + \frac{3\sqrt{62}}{32}n + \frac{3\sqrt{38}}{20}n + \frac{\sqrt{33}}{4}n + \frac{3\sqrt{5}}{4}n, \\
GA_5(BT[m,n]) &= \frac{9}{2}mn + \frac{72\sqrt{2}}{17}n + \frac{24\sqrt{10}}{13}n - 15n.
\end{aligned}$$

Proof. Consider the boron triangular nanotube $G = BT[m,n]$. There are three partite subsets of the edge set E_G according to degree of end vertices, presented as

$$\begin{aligned}
E_{4,4} &= \{pq \in E_G \mid d_G(p) = d_G(q) = 4\}, \\
E_{4,6} &= \{pq \in E_G \mid d_G(p) = 4 \text{ and } d_G(q) = 6\},
\end{aligned}$$

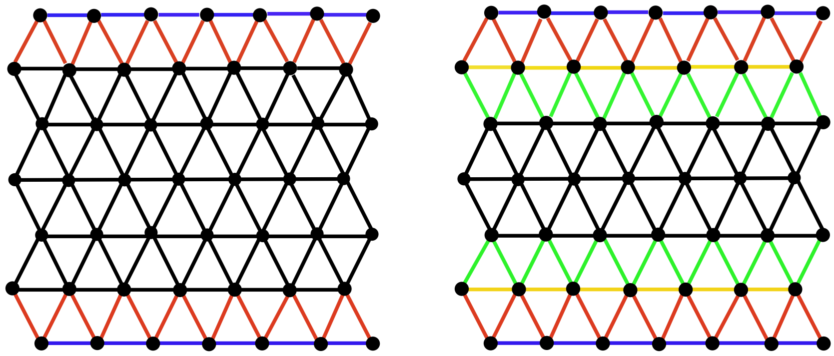

(a) (b)

Figure 5.3: The edge partitions of $BT[7,4]$ nanotube: corresponding to (a) degree of end vertices and (b) degree sum of neighbor vertices.

$$E_{6,6} = \{pq \in E_G \mid d_G(p) = d_G(q) = 6\}.$$

Therefore, we have $|E_{4,4}| = 3n$, $|E_{4,6}| = 6n$ and $|E_{6,6}| = 3n(3m-8)/2$. The representative edges of these partite sets are presented in Figure 5.3 (a) in which blue, red, and black edges correspond to $E_{4,4}$, $E_{4,6}$, and $E_{6,6}$ respectively. The ABC and GA indices of G are formulated as

$$\begin{aligned}
ABC(G) &= \sum_{pq\in E_G} \sqrt{\frac{d_G(p)+d_G(q)-2}{d_G(p)\cdot d_G(q)}} \\
&= \sum_{pq\in E_{4,4}} \sqrt{\frac{d_G(p)+d_G(q)-2}{d_G(p)\cdot d_G(q)}} + \sum_{pq\in E_{4,6}} \sqrt{\frac{d_G(p)+d_G(q)-2}{d_G(p)\cdot d_G(q)}} \\
&\quad + \sum_{pq\in E_{6,6}} \sqrt{\frac{d_G(p)+d_G(q)-2}{d_G(p)\cdot d_G(q)}} \\
&= |E_{4,4}|\cdot\sqrt{\frac{4+4-2}{4\cdot 4}} + |E_{4,6}|\cdot\sqrt{\frac{4+6-2}{4\cdot 6}} + |E_{6,6}|\cdot\sqrt{\frac{6+6-2}{6\cdot 6}} \\
&= \frac{3\sqrt{10}}{4}mn + \frac{3\sqrt{6}}{4}n - 2\sqrt{10}n + 2\sqrt{3}n
\end{aligned}$$

and

$$\begin{aligned}
GA(G) &= \sum_{pq\in E_G} \frac{2\sqrt{d_G(p)\cdot d_G(q)}}{d_G(p)+d_G(q)} \\
&= \sum_{pq\in E_{4,4}} \frac{2\sqrt{d_G(p)\cdot d_G(q)}}{d_G(p)+d_G(q)} + \sum_{pq\in E_{4,6}} \frac{2\sqrt{d_G(p)\cdot d_G(q)}}{d_G(p)+d_G(q)}
\end{aligned}$$

$$
\begin{aligned}
& + \sum_{pq \in E_{6,6}} \frac{2\sqrt{d_G(p) \cdot d_G(q)}}{d_G(p) + d_G(q)} \\
= \; & |E_{4,4}| \cdot \frac{2\sqrt{4 \cdot 4}}{4+4} + |E_{4,6}| \cdot \frac{2\sqrt{4 \cdot 6}}{4+6} + |E_{6,6}| \cdot \frac{2\sqrt{6 \cdot 6}}{6+6} \\
= \; & \frac{9}{2}mn + \frac{12\sqrt{6}}{5}n - 9n.
\end{aligned}
$$

Similarly, the edge partite subsets of E_G according to degree sum of neighboring vertices, expressed as

$$
\begin{aligned}
S_{20,20} &= \{pq \in E_G \mid \delta_G(p) = \delta_G(q) = 20\}, \\
S_{20,32} &= \{pq \in E_G \mid \delta_G(p) = 20 \text{ and } \delta_G(q) = 32\}, \\
S_{32,32} &= \{pq \in E_G \mid \delta_G(p) = \delta_G(q) = 32\}, \\
S_{32,36} &= \{pq \in E_G \mid \delta_G(p) = 32 \text{ and } \delta_G(q) = 36\}, \\
S_{36,36} &= \{pq \in E_G \mid \delta_G(p) = \delta_G(q) = 36\}.
\end{aligned}
$$

Therefore we have $|S_{20,20}| = 3q$, $|S_{20,32}| = 6q$, $|S_{32,32}| = 3q$, $|S_{32,36}| = 6q$, and $|S_{36,36}| = 3q(3p-14)/2$. The representative edges of these partite sets are presented in Figure 5.3 (b) in which blue, red, yellow, green, and black edges belong to $S_{20,20}$, $S_{20,32}$, $S_{32,32}$, $S_{32,36}$, and $S_{36,36}$ respectively. The ABC_4 and GA_5 indices of G are computed as

$$
\begin{aligned}
ABC_4(G) &= \sum_{pq \in E_G} \sqrt{\frac{\delta_G(p) + \delta_G(q) - 2}{\delta_G(p) \cdot \delta_G(q)}} \\
&= \sum_{pq \in S_{20,20}} \sqrt{\frac{\delta_G(p) + \delta_G(q) - 2}{\delta_G(p) \cdot \delta_G(q)}} + \sum_{pq \in S_{20,32}} \sqrt{\frac{\delta_G(p) + \delta_G(q) - 2}{\delta_G(p) \cdot \delta_G(q)}} \\
&\quad + \sum_{pq \in S_{32,32}} \sqrt{\frac{\delta_G(p) + \delta_G(q) - 2}{\delta_G(p) \cdot \delta_G(q)}} + \sum_{pq \in S_{32,36}} \sqrt{\frac{\delta_G(p) + \delta_G(q) - 2}{\delta_G(p) \cdot \delta_G(q)}} \\
&\quad + \sum_{pq \in S_{36,36}} \sqrt{\frac{\delta_G(p) + \delta_G(q) - 2}{\delta_G(p) \cdot \delta_G(q)}} \\
&= |S_{20,20}| \cdot \sqrt{\frac{20+20-2}{20 \cdot 20}} + |S_{20,32}| \cdot \sqrt{\frac{20+20-2}{20 \cdot 32}} + |S_{32,32}| \cdot \sqrt{\frac{32+32-2}{32 \cdot 32}} \\
&\quad + |S_{32,36}| \cdot \sqrt{\frac{32+36-2}{32 \cdot 36}} + |S_{36,36}| \cdot \sqrt{\frac{36+36-2}{36 \cdot 36}}
\end{aligned}
$$

$$= \frac{\sqrt{70}}{8}mn - \frac{7\sqrt{70}}{12}n + \frac{3\sqrt{62}}{32}n + \frac{3\sqrt{38}}{20}n + \frac{\sqrt{33}}{4}n + \frac{3\sqrt{5}}{4}n$$

and

$$\begin{aligned}
GA_5(G) &= \sum_{pq\in E_G} \frac{2\sqrt{\delta_G(p)\cdot\delta_G(q)}}{\delta_G(p)+\delta_G(q)} \\
&= \sum_{pq\in S_{20,20}} \frac{2\sqrt{\delta_G(p)\cdot\delta_G(q)}}{\delta_G(p)+\delta_G(q)} + \sum_{pq\in S_{20,32}} \frac{2\sqrt{\delta_G(p)\cdot\delta_G(q)}}{\delta_G(p)+\delta_G(q)} \\
&\quad + \sum_{pq\in S_{32,32}} \frac{2\sqrt{\delta_G(p)\cdot\delta_G(q)}}{\delta_G(p)+\delta_G(q)} + \sum_{pq\in S_{32,36}} \frac{2\sqrt{\delta_G(p)\cdot\delta_G(q)}}{\delta_G(p)+\delta_G(q)} \\
&\quad + \sum_{pq\in S_{36,36}} \frac{2\sqrt{\delta_G(p)\cdot\delta_G(q)}}{\delta_G(p)+\delta_G(q)} \\
&= |S_{20,20}|\cdot\frac{2\sqrt{20\cdot 20}}{20+20} + |S_{20,32}|\cdot\frac{2\sqrt{20\cdot 32}}{20+32} + |S_{32,32}|\cdot\frac{2\sqrt{32\cdot 32}}{32+32} \\
&\quad + |S_{32,36}|\cdot\frac{2\sqrt{32\cdot 36}}{32+36} + |S_{36,36}|\cdot\frac{2\sqrt{36\cdot 36}}{36+36} \\
&= \frac{9}{2}mn + \frac{72\sqrt{2}}{17}n + \frac{24\sqrt{10}}{13}n - 15n.
\end{aligned}$$

□

5.4 Degree-based Indices of Boron-α Nanotube

In this part, we achieve the expressions for the ABC, ABC_4, GA and GA_5 indices of boron-α nanotubes.

We denote the molecular graph of boron-α nanotube by $BA[m,n]$, where m symbolize number of rows and n symbolize number of columns in a 2D sheet of $BA[m,n]$ as presented in Figure 5.4. We categorize $BA[m,n]$ into two classes according to m. We name these classes as $BA(X)[m,n]$ and $BA(Y)[m,n]$ for $m \equiv 2 \ mod\ 3$ and $m \equiv 0 \ mod\ 3$, respectively. The order and size of $BA(X)[m,n]$ and $BA(Y)[m,n]$ are given in Table 5.1.

Table 5.1: The order and size of boron-α nanotubes.

Boron-α naotube	order	size
$BA(X)[m,n]$	$n(4m+1)/3$	$n(7m-2)/2$
$BA(Y)[m,n]$	$4mn/3$	$n(7m-4)/2$

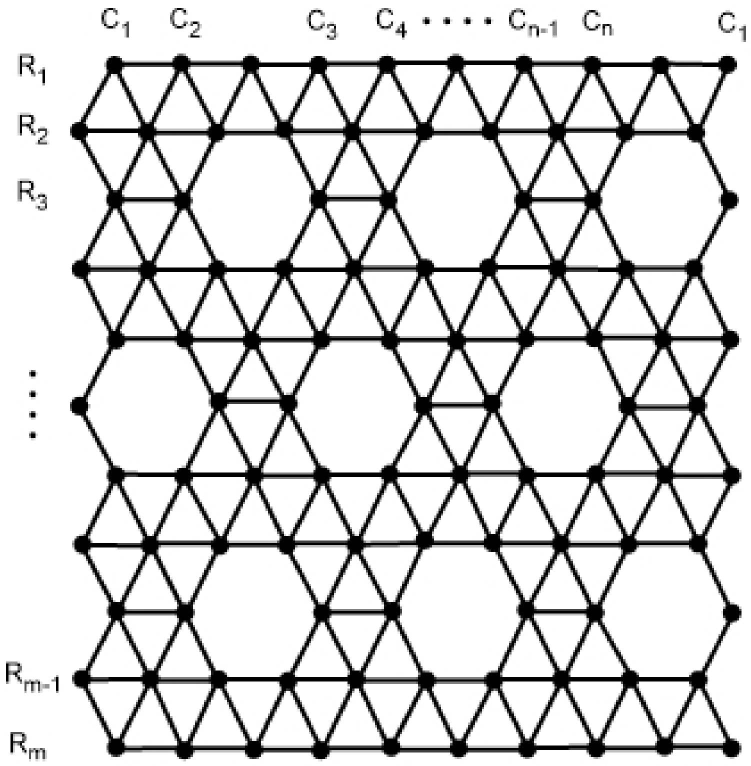

Figure 5.4: A 2D sheet of boron-α nanotube $BA[m,n]$.

In the coming result, we formulate the "ABC, ABC_4, GA, and GA_5" indices for $BA(X)[m,n]$ nanotube.

Theorem 5.4.1. *For the boron-α nanotube $BA(X)[m,n]$, we have*

$$
\begin{aligned}
ABC\left(BA(X)[m,n]\right) &= \frac{3\sqrt{2}}{5}mn+\frac{6}{\sqrt{30}}mn+\frac{3\sqrt{6}}{4}n+\frac{4\sqrt{7}}{\sqrt{20}}n+\frac{2}{\sqrt{3}}n-\frac{8\sqrt{2}}{5}n-\frac{18}{\sqrt{30}}n,\\
GA\left(BA(X)[m,n]\right) &= \frac{4\sqrt{30}}{11}mn+\frac{3}{2}mn+\frac{16\sqrt{5}}{9}n+\frac{8\sqrt{6}}{10}n-\frac{12\sqrt{30}}{11}n-n,\\
ABC_4\left(BA(X)[m,n]\right) &= \frac{\sqrt{13}}{9}mn+\frac{\sqrt{22}}{9}mn+\frac{2\sqrt{35}}{3\sqrt{38}}n+\frac{\sqrt{10}}{3\sqrt{3}}n+\frac{\sqrt{41}}{6}n+\frac{3\sqrt{5}}{\sqrt{133}}n\\
&\quad+\frac{7}{9\sqrt{2}}n+\frac{5}{\sqrt{84}}n+\frac{6}{19}n+\frac{\sqrt{46}}{24}n+\frac{\sqrt{53}}{3\sqrt{21}}n-\frac{14\sqrt{13}}{27}n-\frac{5\sqrt{22}}{9}n,\\
GA_5\left(BA(X)[m,n]\right) &= \frac{36\sqrt{10}}{57}mn+\frac{3}{2}mn+\frac{12\sqrt{38}}{37}n+\frac{8\sqrt{3}}{7}n+\frac{8\sqrt{114}}{43}n+\frac{8\sqrt{133}}{47}n\\
&\quad+\frac{24\sqrt{2}}{17}n+\frac{4\sqrt{42}}{13}n+\frac{24\sqrt{21}}{55}n-\frac{180\sqrt{10}}{57}n-5n.
\end{aligned}
$$

Proof. Consider the boron-α nanotube $H = BA(X)[m,n]$. There are five partite subsets of the edge set E_H according to degree of end vertices, presented as

$$\begin{aligned}
E_{4,4} &= \{pq \in E_H \mid d_H(p) = d_H(q) = 4\},\\
E_{4,5} &= \{pq \in E_H \mid d_H(p) = 4 \text{ and } d_H(q) = 5\},\\
E_{4,6} &= \{pq \in E_H \mid d_H(p) = 4 \text{ and } d_H(q) = 6\},\\
E_{5,5} &= \{pq \in E_H \mid d_H(p) = d_H(q) = 5\},\\
E_{5,6} &= \{pq \in E_H \mid d_H(p) = 5 \text{ and } d_H(q) = 6\}.
\end{aligned}$$

Therefore, we have $|E_{4,4}| = 3n$, $|E_{4,5}| = 4n$, $|E_{4,6}| = 2n$, $|E_{5,5}| = n(3m-8)/2$, and $|E_{5,6}| = 2n(m-3)$. The representative edges of these partite sets are presented in Figure 5.5. The ABC and GA indices of H are formulated as

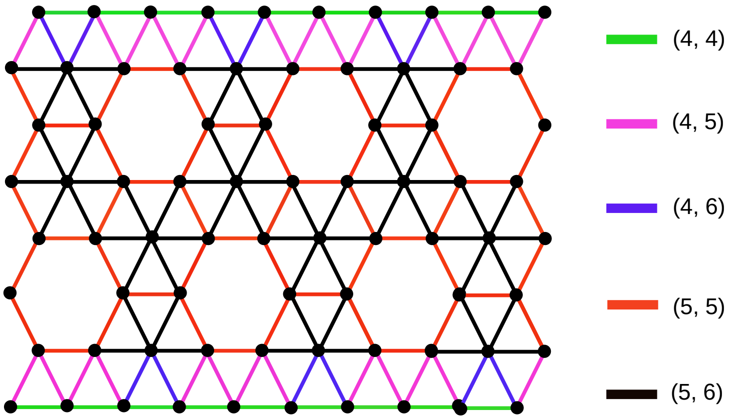

Figure 5.5: The edge partitions of $BA(X)[8,6]$ according to degree of end vertices.

$$\begin{aligned}
ABC(H) &= \sum_{pq\in E_H} \sqrt{\frac{d_H(p)+d_H(q)-2}{d_H(p)\cdot d_H(q)}}\\
&= \sum_{pq\in E_{4,4}} \sqrt{\frac{d_H(p)+d_H(q)-2}{d_H(p)\cdot d_H(q)}} + \sum_{pq\in E_{4,5}} \sqrt{\frac{d_H(p)+d_H(q)-2}{d_H(p)\cdot d_H(q)}}\\
&\quad + \sum_{pq\in E_{4,6}} \sqrt{\frac{d_H(p)+d_H(q)-2}{d_H(p)\cdot d_H(q)}} + \sum_{pq\in E_{5,5}} \sqrt{\frac{d_H(p)+d_H(q)-2}{d_H(p)\cdot d_H(q)}}\\
&\quad + \sum_{pq\in E_{5,6}} \sqrt{\frac{d_H(p)+d_H(q)-2}{d_H(p)\cdot d_H(q)}}
\end{aligned}$$

$$\begin{aligned}
&= |E_{4,4}|\cdot\sqrt{\frac{4+4-2}{4\cdot 4}}+|E_{4,5}|\cdot\sqrt{\frac{4+5-2}{4\cdot 5}}+|E_{4,6}|\cdot\sqrt{\frac{4+6-2}{4\cdot 6}}\\
&\quad+|E_{5,5}|\cdot\sqrt{\frac{5+5-2}{5\cdot 5}}+|E_{5,6}|\cdot\sqrt{\frac{5+6-2}{5\cdot 6}}\\
&= \frac{3\sqrt{2}}{5}mn+\frac{6}{\sqrt{30}}mn+\frac{3\sqrt{6}}{4}n+\frac{4\sqrt{7}}{\sqrt{20}}n+\frac{2}{\sqrt{3}}n-\frac{8\sqrt{2}}{5}n-\frac{18}{\sqrt{30}}n
\end{aligned}$$

and

$$\begin{aligned}
GA(H) &= \sum_{pq\in E_H}\frac{2\sqrt{d_H(p)\cdot d_H(q)}}{d_H(p)+d_H(q)}\\
&= \sum_{pq\in E_{4,4}}\frac{2\sqrt{d_H(p)\cdot d_H(q)}}{d_H(p)+d_H(q)}+\sum_{pq\in E_{4,5}}\frac{2\sqrt{d_H(p)\cdot d_H(q)}}{d_H(p)+d_H(q)}\\
&\quad+\sum_{pq\in E_{4,6}}\frac{2\sqrt{d_H(p)\cdot d_H(q)}}{d_H(p)+d_H(q)}+\sum_{pq\in E_{5,5}}\frac{2\sqrt{d_H(p)\cdot d_H(q)}}{d_H(p)+d_H(q)}\\
&\quad+\sum_{pq\in E_{5,6}}\frac{2\sqrt{d_H(p)\cdot d_H(q)}}{d_H(p)+d_H(q)}\\
&= |E_{4,4}|\cdot\frac{2\sqrt{4\cdot 4}}{4+4}+|E_{4,5}|\cdot\frac{2\sqrt{4\cdot 5}}{4+5}+|E_{4,6}|\cdot\frac{2\sqrt{4\cdot 6}}{4+6}\\
&\quad+|E_{5,5}|\cdot\frac{2\sqrt{5\cdot 5}}{5+5}+|E_{5,6}|\cdot\frac{2\sqrt{5\cdot 6}}{5+6}\\
&= \frac{4\sqrt{30}}{11}mn+\frac{3}{2}mn+\frac{16\sqrt{5}}{9}n+\frac{8\sqrt{6}}{10}n-\frac{12\sqrt{30}}{11}n-n.
\end{aligned}$$

Also, there are eleven edge partite subsets of E_G according to degree sum of neighboring vertices, expressed as

$$\begin{aligned}
S_{18,19} &= \{pq\in E_H \mid \delta_H(p)=18 \text{ and } \delta_H(q)=19\},\\
S_{18,24} &= \{pq\in E_H \mid \delta_H(p)=18 \text{ and } \delta_H(q)=24\},\\
S_{19,19} &= \{pq\in E_H \mid \delta_H(p)=\delta_H(q)=19\},\\
S_{19,24} &= \{pq\in E_H \mid \delta_H(p)=19 \text{ and } \delta_H(q)=24\},\\
S_{19,28} &= \{pq\in E_H \mid \delta_H(p)=19 \text{ and } \delta_H(q)=28\},\\
S_{24,24} &= \{pq\in E_H \mid \delta_H(p)=\delta_H(q)=24\},\\
S_{24,27} &= \{pq\in E_H \mid \delta_H(p)=24 \text{ and } \delta_H(q)=27\},\\
S_{24,28} &= \{pq\in E_H \mid \delta_H(p)=24 \text{ and } \delta_H(q)=28\},
\end{aligned}$$

$$
\begin{aligned}
S_{27,27} &= \{pq \in E_H \mid \delta_H(p) = \delta_H(q) = 27\}, \\
S_{27,28} &= \{pq \in E_H \mid \delta_H(p) = 27 \text{ and } \delta_H(q) = 28\}, \\
S_{27,30} &= \{pq \in E_H \mid \delta_H(p) = 27 \text{ and } \delta_H(q) = 30\}.
\end{aligned}
$$

Therefore we have $|S_{18,19}| = 2n$, $|S_{18,24}| = 2n$, $|S_{19,19}| = n$, $|S_{19,24}| = 2n$, $|S_{19,28}| = 2n$, $|S_{24,24}| = n$, $|S_{24,27}| = 2n$, $|S_{24,28}| = 2n$, $|S_{27,27}| = n(3m-14)/2$, $|S_{27,28}| = 2n$ and $|S_{27,30}| = 2n(m-5)$. The representative edges of these partite sets are presented in Figure 5.6. The ABC_4 and GA_5 indices of H are computed as

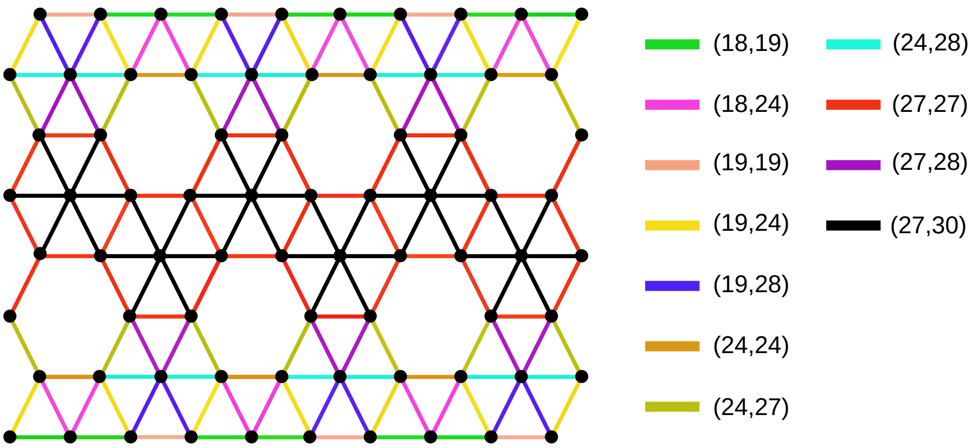

Figure 5.6: The edge partitions of $BA(X)[8,6]$ according to degree sum of neighboring vertices.

$$
\begin{aligned}
ABC_4(H) &= \sum_{pq \in E_H} \sqrt{\frac{\delta_H(p)+\delta_H(q)-2}{\delta_H(p)\cdot\delta_H(q)}} \\
&= \sum_{pq \in S_{18,19}} \sqrt{\frac{\delta_H(p)+\delta_H(q)-2}{\delta_H(p)\cdot\delta_H(q)}} + \sum_{pq \in S_{18,24}} \sqrt{\frac{\delta_H(p)+\delta_H(q)-2}{\delta_H(p)\cdot\delta_H(q)}} \\
&\quad + \sum_{pq \in S_{19,19}} \sqrt{\frac{\delta_H(p)+\delta_H(q)-2}{\delta_H(p)\cdot\delta_H(q)}} + \sum_{pq \in S_{19,24}} \sqrt{\frac{\delta_H(p)+\delta_H(q)-2}{\delta_H(p)\cdot\delta_H(q)}} \\
&\quad + \sum_{pq \in S_{19,28}} \sqrt{\frac{\delta_H(p)+\delta_H(q)-2}{\delta_H(p)\cdot\delta_H(q)}} + \sum_{pq \in S_{24,24}} \sqrt{\frac{\delta_H(p)+\delta_H(q)-2}{\delta_H(p)\cdot\delta_H(q)}} \\
&\quad + \sum_{pq \in S_{24,27}} \sqrt{\frac{\delta_H(p)+\delta_H(q)-2}{\delta_H(p)\cdot\delta_H(q)}} + \sum_{pq \in S_{24,28}} \sqrt{\frac{\delta_H(p)+\delta_H(q)-2}{\delta_H(p)\cdot\delta_H(q)}}
\end{aligned}
$$

$$
\begin{aligned}
& + \sum_{pq \in S_{27,27}} \sqrt{\frac{\delta_H(p)+\delta_H(q)-2}{\delta_H(p)\cdot\delta_H(q)}} + \sum_{pq \in S_{27,28}} \sqrt{\frac{\delta_H(p)+\delta_H(q)-2}{\delta_H(p)\cdot\delta_H(q)}} \\
& + \sum_{pq \in S_{27,30}} \sqrt{\frac{\delta_H(p)+\delta_H(q)-2}{\delta_H(p)\cdot\delta_H(q)}} \\
= \; & |S_{18,19}|\cdot\sqrt{\frac{18+19-2}{18\cdot 19}} + |S_{18,24}|\cdot\sqrt{\frac{18+24-2}{18\cdot 24}} + |S_{19,19}|\cdot\sqrt{\frac{19+19-2}{19\cdot 19}} \\
& + |S_{19,24}|\cdot\sqrt{\frac{19+24-2}{19\cdot 24}} + |S_{19,28}|\cdot\sqrt{\frac{19+28-2}{19\cdot 28}} + |S_{24,24}|\cdot\sqrt{\frac{24+24-2}{24\cdot 24}} \\
& + |S_{24,27}|\cdot\sqrt{\frac{24+27-2}{24\cdot 27}} + |S_{24,28}|\cdot\sqrt{\frac{24+28-2}{24\cdot 28}} + |S_{27,27}|\cdot\sqrt{\frac{27+27-2}{27\cdot 27}}, \\
& + |S_{27,28}|\cdot\sqrt{\frac{27+28-2}{27\cdot 28}} + |S_{27,30}|\cdot\sqrt{\frac{27+30-2}{27\cdot 30}} \\
= \; & \frac{\sqrt{13}}{9}mn + \frac{\sqrt{22}}{9}mn + \frac{2\sqrt{35}}{3\sqrt{38}}n + \frac{\sqrt{10}}{3\sqrt{3}}n + \frac{\sqrt{41}}{6}n + \frac{3\sqrt{5}}{\sqrt{133}}n + \frac{7}{9\sqrt{2}}n + \frac{5}{\sqrt{84}}n \\
& + \frac{6}{19}n + \frac{\sqrt{46}}{24}n + \frac{\sqrt{53}}{3\sqrt{21}}n - \frac{14\sqrt{13}}{27}n - \frac{5\sqrt{22}}{9}n
\end{aligned}
$$

and

$$
\begin{aligned}
GA_5(H) \; = \; & \sum_{pq \in E_H} \frac{2\sqrt{\delta_H(p)\cdot\delta_H(q)}}{\delta_H(p)+\delta_H(q)} \\
= \; & \sum_{pq \in S_{18,19}} \frac{2\sqrt{\delta_H(p)\cdot\delta_H(q)}}{\delta_H(p)+\delta_H(q)} + \sum_{pq \in S_{18,24}} \frac{2\sqrt{\delta_H(p)\cdot\delta_H(q)}}{\delta_H(p)+\delta_H(q)} \\
& + \sum_{pq \in S_{19,19}} \frac{2\sqrt{\delta_H(p)\cdot\delta_H(q)}}{\delta_H(p)+\delta_H(q)} + \sum_{pq \in S_{19,24}} \frac{2\sqrt{\delta_H(p)\cdot\delta_H(q)}}{\delta_H(p)+\delta_H(q)} \\
& + \sum_{pq \in S_{19,28}} \frac{2\sqrt{\delta_H(p)\cdot\delta_H(q)}}{\delta_H(p)+\delta_H(q)} + \sum_{pq \in S_{24,24}} \frac{2\sqrt{\delta_H(p)\cdot\delta_H(q)}}{\delta_H(p)+\delta_H(q)} \\
& + \sum_{pq \in S_{24,27}} \frac{2\sqrt{\delta_H(p)\cdot\delta_H(q)}}{\delta_H(p)+\delta_H(q)} + \sum_{pq \in S_{24,28}} \frac{2\sqrt{\delta_H(p)\cdot\delta_H(q)}}{\delta_H(p)+\delta_H(q)} \\
& + \sum_{pq \in S_{27,27}} \frac{2\sqrt{\delta_H(p)\cdot\delta_H(q)}}{\delta_H(p)+\delta_H(q)} + \sum_{pq \in S_{27,28}} \frac{2\sqrt{\delta_H(p)\cdot\delta_H(q)}}{\delta_H(p)+\delta_H(q)} \\
& + \sum_{pq \in S_{27,30}} \frac{2\sqrt{\delta_H(p)\cdot\delta_H(q)}}{\delta_H(p)+\delta_H(q)} \\
= \; & |S_{18,19}|\cdot\frac{2\sqrt{18\cdot 19}}{18+19} + |S_{18,24}|\cdot\frac{2\sqrt{18\cdot 24}}{18+24} + |S_{19,19}|\cdot\frac{2\sqrt{19\cdot 19}}{19+19} \\
& + |S_{19,24}|\cdot\frac{2\sqrt{19\cdot 24}}{19+24} + |S_{19,28}|\cdot\frac{2\sqrt{19\cdot 28}}{19+28} + |S_{24,24}|\cdot\frac{2\sqrt{24\cdot 24}}{24+24}
\end{aligned}
$$

$$
\begin{aligned}
& +|S_{24,27}|\cdot\frac{2\sqrt{24\cdot 27}}{24+27}+|S_{24,28}|\cdot\frac{2\sqrt{24\cdot 28}}{24+28}+|S_{27,27}|\cdot\frac{2\sqrt{27\cdot 27}}{27+27}\\
& +|S_{27,28}|\cdot\frac{2\sqrt{27\cdot 28}}{27+28}+|S_{27,30}|\cdot\frac{2\sqrt{27\cdot 30}}{27+30}\\
= & \frac{36\sqrt{10}}{57}mn+\frac{3}{2}mn+\frac{12\sqrt{38}}{37}n+\frac{8\sqrt{3}}{7}n+\frac{8\sqrt{114}}{43}n+\frac{8\sqrt{133}}{47}n\\
& +\frac{24\sqrt{2}}{17}n+\frac{4\sqrt{42}}{13}n+\frac{24\sqrt{21}}{55}n-\frac{180\sqrt{10}}{57}n-5n.
\end{aligned}
$$

□

For $BA(Y)[m,n]$ nanotube, ABC, ABC_4, GA and GA_5 indices are formulated in Theorem 5.4.2.

Theorem 5.4.2. *Consider the boron-α nanotube $BA(Y)[m,n]$, then*

$$
\begin{aligned}
ABC\,(BA(Y)[m,n]) &= \frac{6}{\sqrt{50}}mn+\frac{\sqrt{30}}{5}mn+\frac{3\sqrt{6}}{8}n+\sqrt{\frac{2}{5}}n+\frac{\sqrt{7}}{3\sqrt{2}}n+\frac{\sqrt{7}}{\sqrt{5}}n+\frac{1}{\sqrt{3}}n\\
&\quad +\frac{1}{3}n-\frac{8\sqrt{2}}{5}n-\frac{\sqrt{30}}{2}n,\\
GA\,(BA(Y)[m,n]) &= \frac{4\sqrt{30}}{11}mn+\frac{3}{2}mn+\frac{\sqrt{15}}{4}n+\frac{2\sqrt{2}}{3}n+\frac{8\sqrt{5}}{9}n+\frac{2\sqrt{6}}{5}n\\
&\quad -\frac{10\sqrt{30}}{11}n-2n,\\
ABC_4\,(BA(Y)[m,n]) &= \frac{\sqrt{13}}{9}mn+\frac{2\sqrt{5}}{9}mn+\frac{\sqrt{26}}{28}n+\frac{\sqrt{37}}{5\sqrt{14}}n+\frac{\sqrt{38}}{2\sqrt{91}}n+\frac{\sqrt{35}}{3\sqrt{38}}n\\
&\quad +\frac{\sqrt{10}}{6\sqrt{3}}n+\frac{3}{19}n+\frac{\sqrt{41}}{2\sqrt{114}}n+\frac{3\sqrt{5}}{2\sqrt{133}}n+\frac{\sqrt{46}}{48}n+\frac{7}{18\sqrt{2}}n\\
&\quad +\frac{5}{4\sqrt{21}}n+\frac{2\sqrt{3}}{25}n+\frac{7}{5\sqrt{26}}n+\frac{\sqrt{2}}{3\sqrt{3}}n+\frac{\sqrt{53}}{5\sqrt{30}}n+\frac{\sqrt{17}}{3\sqrt{26}}n\\
&\quad +\frac{\sqrt{53}}{6\sqrt{21}}n-\frac{14\sqrt{13}}{27}n-\frac{10\sqrt{5}}{9}n\\
GA_5\,(BA(Y)[m,n]) &= \frac{12\sqrt{10}}{19}mn+\frac{3}{2}mn+\frac{10\sqrt{14}}{39}n+\frac{\sqrt{91}}{10}n+\frac{6\sqrt{38}}{37}n+\frac{4\sqrt{3}}{7}n,\\
&\quad +\frac{4\sqrt{114}}{43}n+\frac{4\sqrt{133}}{47}n+\frac{12\sqrt{2}}{17}n+\frac{2\sqrt{42}}{13}n+\frac{10\sqrt{26}}{51}n\\
&\quad +\frac{15\sqrt{3}}{26}n+\frac{2\sqrt{30}}{11}n+\frac{6\sqrt{78}}{53}n+\frac{12\sqrt{21}}{55}n-\frac{60\sqrt{10}}{19}n-5n.
\end{aligned}
$$

Proof. Consider the boron-α nanotube $K=BA(Y)[m,n]$. From Figure 5.7, we can see that there are eight partite subsets of E_K according to degree of end vertices, presented

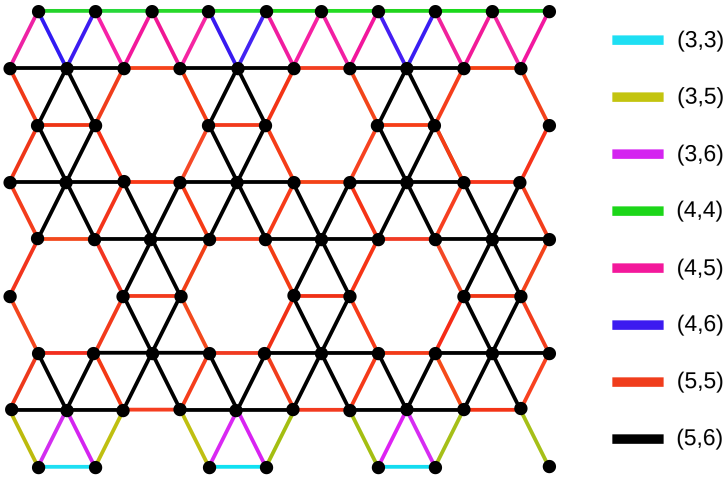

Figure 5.7: The edge partitions of $BA(Y)[9,6]$ according to degree of end vertices.

as

$$\begin{aligned}
E_{3,3} &= \{pq \in E_K \mid d_K(p) = d_K(q) = 3\}, \\
E_{3,5} &= \{pq \in E_K \mid d_K(p) = 3 \text{ and } d_K(q) = 5\}, \\
E_{3,6} &= \{pq \in E_K \mid d_K(p) = 3 \text{ and } d_K(q) = 6\}, \\
E_{4,4} &= \{pq \in E_K \mid d_K(p) = d_K(q) = 4\}, \\
E_{4,5} &= \{pq \in E_K \mid d_K(p) = 4 \text{ and } d_K(q) = 5\}, \\
E_{4,6} &= \{pq \in E_K \mid d_K(p) = 4 \text{ and } d_K(q) = 6\}, \\
E_{5,5} &= \{pq \in E_K \mid d_K(p) = d_K(q) = 5\}, \\
E_{5,6} &= \{pq \in E_K \mid d_K(p) = 5 \text{ and } d_K(q) = 6\}.
\end{aligned}$$

Therefore, we have $|E_{3,3}| = n/2$, $|E_{3,5}| = n$, $|E_{3,6}| = n$, $|E_{4,4}| = 3n/2$, $|E_{4,5}| = 2n$, $|E_{4,6}| = n$, $|E_{5,5}| = n(3m-8)/2$, and $|E_{5,6}| = n(2m-5)$. The ABC and GA indices of K are computed as

$$\begin{aligned}
ABC(K) &= \sum_{pq \in E_K} \sqrt{\frac{d_K(p)+d_K(q)-2}{d_K(p) \cdot d_K(q)}} \\
&= \sum_{pq \in E_{3,3}} \sqrt{\frac{d_K(p)+d_K(q)-2}{d_K(p) \cdot d_K(q)}} + \sum_{pq \in E_{3,5}} \sqrt{\frac{d_K(p)+d_K(q)-2}{d_K(p) \cdot d_K(q)}}
\end{aligned}$$

$$
\begin{aligned}
& + \sum_{pq \in E_{3,6}} \sqrt{\frac{d_K(p)+d_K(q)-2}{d_K(p)\cdot d_K(q)}} + \sum_{pq \in E_{4,4}} \sqrt{\frac{d_K(p)+d_K(q)-2}{d_K(p)\cdot d_K(q)}} \\
& + \sum_{pq \in E_{4,5}} \sqrt{\frac{d_K(p)+d_K(q)-2}{d_K(p)\cdot d_K(q)}} + \sum_{pq \in E_{4,6}} \sqrt{\frac{d_K(p)+d_K(q)-2}{d_K(p)\cdot d_K(q)}} \\
= \; & |E_{3,3}| \cdot \sqrt{\frac{3+3-2}{3\cdot 3}} + |E_{3,5}| \sqrt{\frac{3+5-2}{3\cdot 5}} + |E_{3,6}| \cdot \sqrt{\frac{3+6-2}{3\cdot 6}} \\
& + |E_{4,4}| \cdot \sqrt{\frac{4+4-2}{4\cdot 4}} + |E_{4,5}| \cdot \sqrt{\frac{4+5-2}{4\cdot 5}} + |E_{4,6}| \cdot \sqrt{\frac{4+6-2}{4\cdot 6}} \\
& + |E_{5,5}| \cdot \sqrt{\frac{5+5-2}{5\cdot 5}} + \sum_{pq \in E_{5,6}} \sqrt{\frac{5+6-2}{5\cdot 6}} \\
= \; & \frac{6}{\sqrt{50}} mn + \frac{\sqrt{30}}{5} mn + \frac{3\sqrt{6}}{8} n + \sqrt{\frac{2}{5}} n + \frac{\sqrt{7}}{3\sqrt{2}} n + \frac{\sqrt{7}}{\sqrt{5}} n + \frac{1}{\sqrt{3}} n + \frac{1}{3} n \\
& - \frac{8\sqrt{2}}{5} n - \frac{\sqrt{30}}{2} n
\end{aligned}
$$

and

$$
\begin{aligned}
GA(K) = \; & \sum_{pq \in E_K} \frac{2\sqrt{d_K(p)\cdot d_K(q)}}{d_K(p)+d_K(q)} \\
= \; & \sum_{pq \in E_{3,3}} \frac{2\sqrt{d_K(p)\cdot d_K(q)}}{d_K(p)+d_K(q)} + \sum_{pq \in E_{3,5}} \frac{2\sqrt{d_K(p)\cdot d_K(q)}}{d_K(p)+d_K(q)} \\
& + \sum_{pq \in E_{3,6}} \frac{2\sqrt{d_K(p)\cdot d_K(q)}}{d_K(p)+d_K(q)} + \sum_{pq \in E_{4,4}} \frac{2\sqrt{d_K(p)\cdot d_K(q)}}{d_K(p)+d_K(q)} \\
& + \sum_{pq \in E_{4,5}} \frac{2\sqrt{d_K(p)\cdot d_K(q)}}{d_K(p)+d_K(q)} + \sum_{pq \in E_{4,6}} \frac{2\sqrt{d_K(p)\cdot d_K(q)}}{d_K(p)+d_K(q)} \\
& + \sum_{pq \in E_{5,5}} \frac{2\sqrt{d_K(p)\cdot d_K(q)}}{d_K(p)+d_K(q)} + \sum_{pq \in E_{5,6}} \frac{2\sqrt{d_K(p)\cdot d_K(q)}}{d_K(p)+d_K(q)} \\
= \; & |E_{3,3}| \cdot \frac{2\sqrt{3\cdot 3}}{3+3} + |E_{3,5}| \cdot \frac{2\sqrt{3\cdot 5}}{3+5} + |E_{3,6}| \cdot \frac{2\sqrt{3\cdot 6}}{3+6} + |E_{4,4}| \cdot \frac{2\sqrt{4\cdot 4}}{4+4} \\
& + |E_{4,5}| \cdot \frac{2\sqrt{4\cdot 5}}{4+5} + |E_{4,6}| \cdot \frac{2\sqrt{4\cdot 6}}{4+6} + |E_{5,5}| \cdot \frac{2\sqrt{5\cdot 5}}{5+5} + |E_{5,6}| \cdot \frac{2\sqrt{5\cdot 6}}{5+6} \\
= \; & \frac{4\sqrt{30}}{11} mn + \frac{3}{2} mn + \frac{\sqrt{15}}{4} n + \frac{2\sqrt{2}}{3} n + \frac{8\sqrt{5}}{9} n + \frac{2\sqrt{6}}{5} n - \frac{10\sqrt{30}}{11} n - 2n.
\end{aligned}
$$

Similarly, there are nineteen edge partite subsets of E_K according to degree sum of neighboring vertices, expressed as

$$\begin{aligned}
S_{14,14} &= \{pq \in E_K \mid \delta_K(p) = \delta_K(q) = 14\},\\
S_{14,25} &= \{pq \in E_K \mid \delta_K(p) = 14 \text{ and } \delta_K(q) = 25\},\\
S_{14,26} &= \{pq \in E_K \mid \delta_K(p) = 14 \text{ and } \delta_K(q) = 26\},\\
S_{18,19} &= \{pq \in E_K \mid \delta_K(p) = 18 \text{ and } \delta_K(q) = 19\},\\
S_{18,24} &= \{pq \in E_K \mid \delta_K(p) = 18 \text{ and } \delta_K(q) = 24\},\\
S_{19,19} &= \{pq \in E_K \mid \delta_K(p) = \delta_K(q) = 19\},\\
S_{19,24} &= \{pq \in E_K \mid \delta_K(p) = 19 \text{ and } \delta_K(q) = 24\},\\
S_{19,28} &= \{pq \in E_K \mid \delta_K(p) = 19 \text{ and } \delta_K(q) = 28\},\\
S_{24,24} &= \{pq \in E_K \mid \delta_K(p) = \delta_K(q) = 24\},\\
S_{24,27} &= \{pq \in E_K \mid \delta_K(p) = 24 \text{ and } \delta_K(q) = 27\},\\
S_{24,28} &= \{pq \in E_K \mid \delta_K(p) = 24 \text{ and } \delta_K(q) = 28\},\\
S_{25,25} &= \{pq \in E_K \mid \delta_K(p) = \delta_K(q) = 25\},\\
S_{25,26} &= \{pq \in E_K \mid \delta_K(p) = 25 \text{ and } \delta_K(q) = 26\},\\
S_{25,27} &= \{pq \in E_K \mid \delta_K(p) = 25 \text{ and } \delta_K(q) = 27\},\\
S_{25,30} &= \{pq \in E_K \mid \delta_K(p) = 25 \text{ and } \delta_K(q) = 30\},\\
S_{26,27} &= \{pq \in E_K \mid \delta_K(p) = 26 \text{ and } \delta_K(q) = 27\},\\
S_{27,27} &= \{pq \in E_K \mid \delta_K(p) = \delta_K(q) = 27\},\\
S_{27,28} &= \{pq \in E_K \mid \delta_K(p) = 27 \text{ and } \delta_K(q) = 28\},\\
S_{27,30} &= \{pq \in E_K \mid \delta_K(p) = 27 \text{ and } \delta_K(q) = 30\}.
\end{aligned}$$

Therefore, we have $|S_{14,14}| = n/2$, $|S_{14,25}| = n$, $|S_{14,26}| = n$, $|S_{18,19}| = n$, $|S_{18,24}| = n$, $|S_{19,19}| = n/2$, $|S_{19,24}| = n$, $|S_{19,28}| = n$, $|S_{24,24}| = n/2$, $|S_{24,27}| = n$ and $|S_{24,28}| = n$, $|S_{25,25}| = n/2$, $|S_{25,26}| = n$, $|S_{25,27}| = n$, $|S_{25,30}| = n$, $|S_{26,27}| = n$, $|S_{27,27}| = n(3m-14)/2$, $|S_{27,28}| = n$ and $|S_{27,30}| = 2n(m-5)$. The representative edges of these partite sets corresponding to certain colors are presented in Figure 5.8. The ABC_4 and GA_5 indices of K are computed as

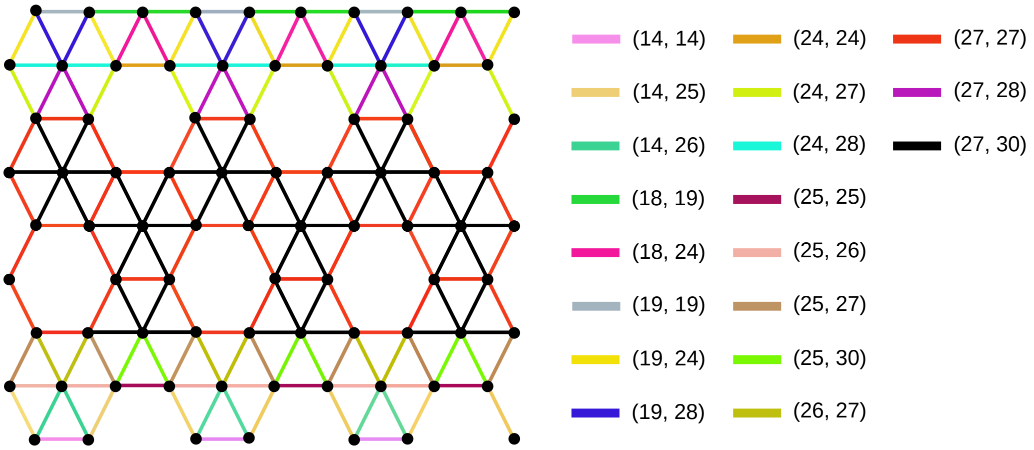

Figure 5.8: The edge partitions of $BA(X)[9,6]$ according to degree sum of neighboring vertices.

$$\begin{aligned}
ABC_4(K) &= \sum_{pq\in E_K}\sqrt{\frac{\delta_K(p)+\delta_K(q)-2}{\delta_K(p)\cdot\delta_K(q)}}\\
&= \sum_{pq\in S_{14,14}}\sqrt{\frac{\delta_K(p)+\delta_K(q)-2}{\delta_K(p)\cdot\delta_K(q)}}+\sum_{pq\in S_{14,25}}\sqrt{\frac{\delta_K(p)+\delta_K(q)-2}{\delta_K(p)\cdot\delta_K(q)}}\\
&\quad+\sum_{pq\in S_{14,26}}\sqrt{\frac{\delta_K(p)+\delta_K(q)-2}{\delta_K(p)\cdot\delta_K(q)}}+\sum_{pq\in S_{18,19}}\sqrt{\frac{\delta_K(p)+\delta_K(q)-2}{\delta_K(p)\cdot\delta_K(q)}}\\
&\quad+\sum_{pq\in S_{18,24}}\sqrt{\frac{\delta_K(p)+\delta_K(q)-2}{\delta_K(p)\cdot\delta_K(q)}}+\sum_{pq\in S_{19,19}}\sqrt{\frac{\delta_K(p)+\delta_K(q)-2}{\delta_K(p)\cdot\delta_K(q)}}\\
&\quad+\sum_{pq\in S_{19,24}}\sqrt{\frac{\delta_K(p)+\delta_K(q)-2}{\delta_K(p)\cdot\delta_K(q)}}+\sum_{pq\in S_{19,28}}\sqrt{\frac{\delta_K(p)+\delta_K(q)-2}{\delta_K(p)\cdot\delta_K(q)}}\\
&\quad+\sum_{pq\in S_{24,24}}\sqrt{\frac{\delta_K(p)+\delta_K(q)-2}{\delta_K(p)\cdot\delta_K(q)}}+\sum_{pq\in S_{24,27}}\sqrt{\frac{\delta_K(p)+\delta_K(q)-2}{\delta_K(p)\cdot\delta_K(q)}}\\
&\quad+\sum_{pq\in S_{24,28}}\sqrt{\frac{\delta_K(p)+\delta_K(q)-2}{\delta_K(p)\cdot\delta_K(q)}}+\sum_{pq\in S_{25,25}}\sqrt{\frac{\delta_K(p)+\delta_K(q)-2}{\delta_K(p)\cdot\delta_K(q)}}\\
&\quad+\sum_{pq\in S_{25,26}}\sqrt{\frac{\delta_K(p)+\delta_K(q)-2}{\delta_K(p)\cdot\delta_K(q)}}+\sum_{pq\in S_{25,27}}\sqrt{\frac{\delta_K(p)+\delta_K(q)-2}{\delta_K(p)\cdot\delta_K(q)}}\\
&\quad+\sum_{pq\in S_{25,30}}\sqrt{\frac{\delta_K(p)+\delta_K(q)-2}{\delta_K(p)\cdot\delta_K(q)}}+\sum_{pq\in S_{26,27}}\sqrt{\frac{\delta_K(p)+\delta_K(q)-2}{\delta_K(p)\cdot\delta_K(q)}}\\
&\quad+\sum_{pq\in S_{27,27}}\sqrt{\frac{\delta_K(p)+\delta_K(q)-2}{\delta_K(p)\cdot\delta_K(q)}}+\sum_{pq\in S_{27,28}}\sqrt{\frac{\delta_K(p)+\delta_K(q)-2}{\delta_K(p)\cdot\delta_K(q)}}
\end{aligned}$$

$$
\begin{aligned}
& + \sum_{pq \in S_{27,30}} \sqrt{\frac{\delta_K(p)+\delta_K(q)-2}{\delta_K(p)\cdot\delta_K(q)}} \\
= \;& |S_{14,14}|\sqrt{\frac{14+14-2}{14\cdot 14}} + |S_{14,25}|\sqrt{\frac{14+25-2}{14\cdot 25}} + |S_{14,26}|\sqrt{\frac{14+26-2}{14\cdot 26}} \\
& +|S_{18,19}|\sqrt{\frac{18+19-2}{18\cdot 19}} + |S_{18,24}|\sqrt{\frac{18+24-2}{18\cdot 24}} + |S_{19,19}|\sqrt{\frac{19+19-2}{19\cdot 19}} \\
& +|S_{19,24}|\sqrt{\frac{19+24-2}{19\cdot 24}} + |S_{19,28}|\sqrt{\frac{19+28-2}{19\cdot 28}} + |S_{24,24}|\sqrt{\frac{24+24-2}{24\cdot 24}} \\
& +|S_{24,27}|\sqrt{\frac{24+27-2}{24\cdot 27}} + |S_{24,28}|\sqrt{\frac{24+28-2}{24\cdot 28}} + |S_{25,25}|\sqrt{\frac{25+25-2}{25\cdot 25}} \\
& +|S_{25,26}|\sqrt{\frac{25+26-2}{25\cdot 26}} + |S_{25,27}|\sqrt{\frac{25+27-2}{25\cdot 27}} + |S_{25,30}|\sqrt{\frac{25+30-2}{25\cdot 30}} \\
& +|S_{26,27}|\sqrt{\frac{26+27-2}{26\cdot 27}} + |S_{27,27}|\sqrt{\frac{27+27-2}{27\cdot 27}} + |S_{27,28}|\sqrt{\frac{27+28-2}{27\cdot 28}} \\
& +|S_{27,30}|\sqrt{\frac{27+30-2}{27\cdot 30}} \\
= \;& \frac{\sqrt{13}}{9}mn + \frac{2\sqrt{5}}{9}mn + \frac{\sqrt{26}}{28}n + \frac{\sqrt{37}}{5\sqrt{14}}n + \frac{\sqrt{38}}{2\sqrt{91}}n + \frac{\sqrt{35}}{3\sqrt{38}}n + \frac{\sqrt{10}}{6\sqrt{3}}n + \frac{3}{19}n \\
& + \frac{\sqrt{41}}{2\sqrt{114}}n + \frac{3\sqrt{5}}{2\sqrt{133}}n + \frac{\sqrt{46}}{48}n + \frac{7}{18\sqrt{2}}n + \frac{5}{4\sqrt{21}}n + \frac{2\sqrt{3}}{25}n + \frac{7}{5\sqrt{26}}n \\
& + \frac{\sqrt{2}}{3\sqrt{3}}n + \frac{\sqrt{53}}{5\sqrt{30}}n + \frac{\sqrt{17}}{3\sqrt{26}}n + \frac{\sqrt{53}}{6\sqrt{21}}n - \frac{14\sqrt{13}}{27}n - \frac{10\sqrt{5}}{9}n
\end{aligned}
$$

and

$$
\begin{aligned}
GA_5(K) \;=\;& \sum_{pq \in E_K} \frac{2\sqrt{\delta_K(p)\cdot\delta_K(q)}}{\delta_K(p)+\delta_K(q)} \\
=\;& \sum_{pq \in S_{14,14}} \frac{2\sqrt{\delta_K(p)\cdot\delta_K(q)}}{\delta_K(p)+\delta_K(q)} + \sum_{pq \in S_{14,25}} \frac{2\sqrt{\delta_K(p)\cdot\delta_K(q)}}{\delta_K(p)+\delta_K(q)} \\
& + \sum_{pq \in S_{14,26}} \frac{2\sqrt{\delta_K(p)\cdot\delta_K(q)}}{\delta_K(p)+\delta_K(q)} + \sum_{pq \in S_{18,19}} \frac{2\sqrt{\delta_K(p)\cdot\delta_K(q)}}{\delta_K(p)+\delta_K(q)} \\
& + \sum_{pq \in S_{18,24}} \frac{2\sqrt{\delta_K(p)\cdot\delta_K(q)}}{\delta_K(p)+\delta_K(q)} + \sum_{pq \in S_{19,19}} \frac{2\sqrt{\delta_K(p)\cdot\delta_K(q)}}{\delta_K(p)+\delta_K(q)} \\
& + \sum_{pq \in S_{19,24}} \frac{2\sqrt{\delta_K(p)\cdot\delta_K(q)}}{\delta_K(p)+\delta_K(q)} + \sum_{pq \in S_{19,28}} \frac{2\sqrt{\delta_K(p)\cdot\delta_K(q)}}{\delta_K(p)+\delta_K(q)} \\
& + \sum_{pq \in S_{24,24}} \frac{2\sqrt{\delta_K(p)\cdot\delta_K(q)}}{\delta_K(p)+\delta_K(q)} + \sum_{pq \in S_{24,27}} \frac{2\sqrt{\delta_K(p)\cdot\delta_K(q)}}{\delta_K(p)+\delta_K(q)}
\end{aligned}
$$

$$
\begin{aligned}
& + \sum_{pq\in S_{24,28}} \frac{2\sqrt{\delta_K(p)\cdot\delta_K(q)}}{\delta_K(p)+\delta_K(q)} + \sum_{pq\in S_{25,25}} \frac{2\sqrt{\delta_K(p)\cdot\delta_K(q)}}{\delta_K(p)+\delta_K(q)} \\
& + \sum_{pq\in S_{25,26}} \frac{2\sqrt{\delta_K(p)\cdot\delta_K(q)}}{\delta_K(p)+\delta_K(q)} + \sum_{pq\in S_{25,27}} \frac{2\sqrt{\delta_K(p)\cdot\delta_K(q)}}{\delta_K(p)+\delta_K(q)} \\
& + \sum_{pq\in S_{25,30}} \frac{2\sqrt{\delta_K(p)\cdot\delta_K(q)}}{\delta_K(p)+\delta_K(q)} + \sum_{pq\in S_{26,27}} \frac{2\sqrt{\delta_K(p)\cdot\delta_K(q)}}{\delta_K(p)+\delta_K(q)} \\
& + \sum_{pq\in S_{27,27}} \frac{2\sqrt{\delta_K(p)\cdot\delta_K(q)}}{\delta_K(p)+\delta_K(q)} + \sum_{pq\in S_{27,28}} \frac{2\sqrt{\delta_K(p)\cdot\delta_K(q)}}{\delta_K(p)+\delta_K(q)} \\
& + \sum_{pq\in S_{27,30}} \frac{2\sqrt{\delta_K(p)\cdot\delta_K(q)}}{\delta_K(p)+\delta_K(q)} \\
= \quad & |S_{14,14}|\frac{2\sqrt{14\cdot 14}}{14+14} + |S_{14,25}|\frac{2\sqrt{14\cdot 25}}{14+25} + |S_{14,26}|\frac{2\sqrt{14\cdot 26}}{14+26} \\
& +|S_{18,19}|\frac{2\sqrt{18\cdot 19}}{18+19} + |S_{18,24}|\frac{2\sqrt{18\cdot 24}}{18+24} + |S_{19,19}|\frac{2\sqrt{19\cdot 19}}{19+19} \\
& +|S_{19,24}|\frac{2\sqrt{19\cdot 24}}{19+24} + |S_{19,28}|\frac{2\sqrt{19\cdot 28}}{19+28} + |S_{24,24}|\frac{2\sqrt{24\cdot 24}}{24+24} \\
& +|S_{24,27}|\frac{2\sqrt{24\cdot 27}}{24+27} + |S_{24,28}|\frac{2\sqrt{24\cdot 28}}{24+28} + |S_{25,25}|\frac{2\sqrt{25\cdot 25}}{25+25} \\
& +|S_{25,26}|\frac{2\sqrt{25\cdot 26}}{25+26} + |S_{25,27}|\frac{2\sqrt{25\cdot 27}}{25+27} + |S_{25,30}|\frac{2\sqrt{25\cdot 30}}{25+30} \\
& +|S_{26,27}|\frac{2\sqrt{26\cdot 27}}{26+27} + |S_{27,27}|\frac{2\sqrt{27\cdot 27}}{27+27} + |S_{27,28}|\frac{2\sqrt{27\cdot 28}}{27+28} \\
& +|S_{27,30}|\frac{2\sqrt{27\cdot 30}}{27+30} \\
= \quad & \frac{12\sqrt{10}}{19}mn + \frac{3}{2}mn + \frac{10\sqrt{14}}{39}n + \frac{\sqrt{91}}{10}n + \frac{6\sqrt{38}}{37}n + \frac{4\sqrt{3}}{7}n + \frac{4\sqrt{114}}{43}n \\
& + \frac{4\sqrt{133}}{47}n + \frac{12\sqrt{2}}{17}n + \frac{2\sqrt{42}}{13}n + \frac{10\sqrt{26}}{51}n + \frac{15\sqrt{3}}{26}n + \frac{2\sqrt{30}}{11}n \\
& + \frac{6\sqrt{78}}{53}n + \frac{12\sqrt{21}}{55}n - \frac{60\sqrt{10}}{19}n - 5n.
\end{aligned}
$$

$\square$

5.5 Degree-based Indices of Tri-hexagonal Boron Nanotube

In this part, we formulate ABC, ABC_4, GA and GA_5 indices for the tri-hexagonal boron nanotube.

We represent the molecular graph of tri-hexagonal nanotube by $C_3C_6(H)[p,q]$ where p symbolize number of hexagons in one column and q symbolize number of hexagons in one row in two-dimensional sheet of $C_3C_6(H)[p,q]$ as presented in Figure 5.9. This molecular graph has $8pq$ vertices and $q(18p-1)$ edges. In the coming Theorem, we formulate the "ABC, ABC_4, GA and GA_5" indices of tri-hexagonal boron nanotube.

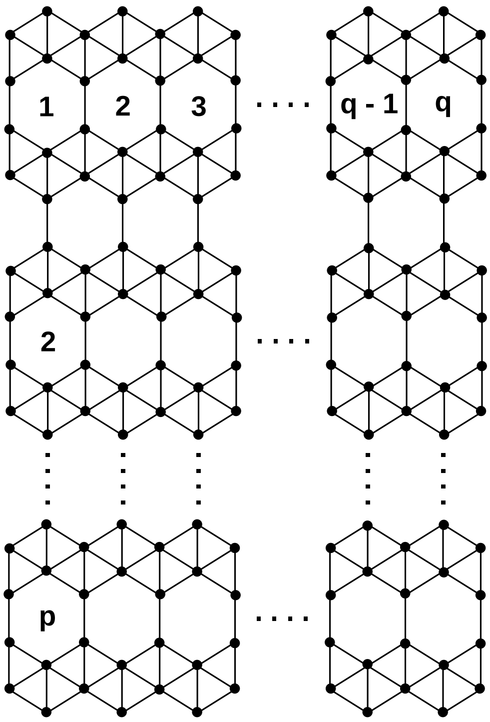

Figure 5.9: A 2D sheet of tri-hexagonal boron nanotube $C_3C_6(H)[p,q]$.

Theorem 5.5.1. *Consider the Tri-Hexagonal boron nanotube $C_3C_6(H)[p,q]$, then*

$$\begin{aligned} ABC\left(C_3C_6(H)[p,q]\right) &= \left(\frac{5\sqrt{30}+60\sqrt{7}+16\sqrt{10}}{10\sqrt{5}}\right)pq+\left(\frac{24\sqrt{2}-\sqrt{30}-12\sqrt{7}}{4\sqrt{5}}\right)q, \\ GA\left(C_3C_6(H)[p,q]\right) &= \left(\frac{16\sqrt{5}+18}{3}\right)pq+\left(\frac{9\sqrt{15}-16\sqrt{5}-6}{6}\right)q, \end{aligned}$$

$$
\begin{aligned}
ABC_4\left(C_3C_6(H)[p,q]\right) &= \left(\frac{12\sqrt{39}}{\sqrt{418}}+\frac{2\sqrt{42}}{11}+\frac{12}{19}\right)pq+\left(\frac{2\sqrt{34}}{3\sqrt{35}}+\frac{2\sqrt{37}}{\sqrt{95}}\right)q \\
&\quad+\left(\frac{2\sqrt{11}}{5}-\frac{12\sqrt{39}}{\sqrt{418}}-\frac{2\sqrt{42}}{11}-\frac{6}{19}+\frac{4\sqrt{38}}{\sqrt{399}}+\frac{2\sqrt{13}}{\sqrt{35}}\right)q, \\
GA_5(C_3C_6(H)[p,q]) &= \left(\frac{24\sqrt{418}}{41}+6\right)pq+\left(\frac{16\sqrt{3}}{7}+\frac{\sqrt{35}}{3}\right)q \\
&\quad+\left(\frac{8\sqrt{95}}{39}+\frac{8\sqrt{399}}{40}+\frac{16\sqrt{105}}{41}-\frac{24\sqrt{418}}{41}-5\right)q.
\end{aligned}
$$

Proof. Consider the Tri-Hexagonal boron nanotube $G = C_3C_6(H)[p,q]$. There are four partitions of edge set according to degree of end vertices, presented as

$$
\begin{aligned}
E_{3,5} &= \{pq \in E_G \mid d_G(p) = 3 \text{ and } d_G(q) = 5\}, \\
E_{4,4} &= \{pq \in E_G \mid d_G(p) = d_G(q) = 4\}, \\
E_{4,5} &= \{pq \in E_G \mid d_G(p) = 4 \text{ and } d_G(q) = 5\}, \\
E_{5,5} &= \{pq \in E_G \mid d_G(p) = d_G(q) = 5\}.
\end{aligned}
$$

The representative edges of these partite sets are presented in Figure 5.10 in which red, green, black, and blue edges belong to $E_{3,5}$, $E_{4,4}$, $E_{4,5}$, and $E_{5,5}$ respectively. Therefore,

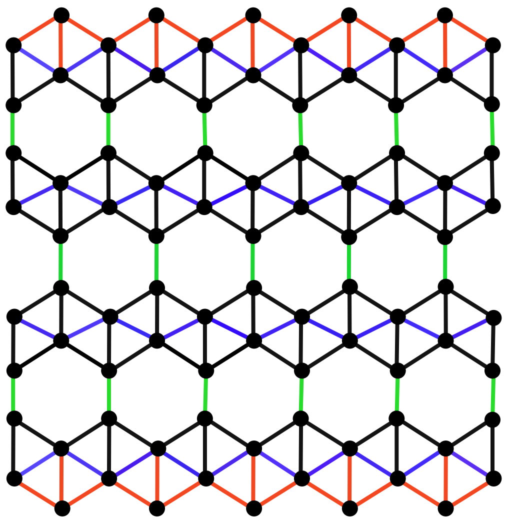

Figure 5.10: The edge partitions of $C_3C_6(H)[p,q]$ according to degree of end vertices.

we have $|E_{3,5}| = 6q$, $|E_{4,4}| = q(2p-1)$, $|E_{4,5}| = 6q(2p-1)$, and $|E_{5,5}| = 4pq$. The ABC

and GA indices of G are formulated as

$$
\begin{aligned}
ABC(G) &= \sum_{pq\in E_G}\sqrt{\frac{d_G(p)+d_G(q)-2}{d_G(p)\cdot d_G(q)}} \\
&= \sum_{pq\in E_{3,5}}\sqrt{\frac{d_G(p)+d_G(q)-2}{d_G(p)\cdot d_G(q)}}+\sum_{pq\in E_{4,4}}\sqrt{\frac{d_G(p)+d_G(q)-2}{d_G(p)\cdot d_G(q)}} \\
&\quad +\sum_{pq\in E_{4,5}}\sqrt{\frac{d_G(p)+d_G(q)-2}{d_G(p)\cdot d_G(q)}}+\sum_{pq\in E_{5,5}}\sqrt{\frac{d_G(p)+d_G(q)-2}{d_G(p)\cdot d_G(q)}} \\
&= |E_{3,5}|\cdot\sqrt{\frac{3+5-2}{3\cdot 5}}+|E_{4,4}|\cdot\sqrt{\frac{4+4-2}{4\cdot 4}}+|E_{4,5}|\cdot\sqrt{\frac{4+5-2}{4\cdot 5}} \\
&\quad +|E_{5,5}|\cdot\sqrt{\frac{5+5-2}{5\cdot 5}} \\
&= \left(\frac{5\sqrt{30}+60\sqrt{7}+16\sqrt{10}}{10\sqrt{5}}\right)pq+\left(\frac{24\sqrt{2}-\sqrt{30}-12\sqrt{7}}{4\sqrt{5}}\right)q
\end{aligned}
$$

and

$$
\begin{aligned}
GA(G) &= \sum_{pq\in E(G)}\frac{2\sqrt{d_G(p)\cdot d_G(q)}}{d_G(p)+d_G(q)} \\
&= \sum_{pq\in E_{3,5}}\frac{2\sqrt{d_G(p)\cdot d_G(q)}}{d_G(p)+d_G(q)}+\sum_{pq\in E_{4,4}}\frac{2\sqrt{d_G(p)\cdot d_G(q)}}{d_G(p)+d_G(q)} \\
&\quad +\sum_{pq\in E_{4,5}}\frac{2\sqrt{d_G(p)\cdot d_G(q)}}{d_G(p)+d_G(q)}+\sum_{pq\in E_{5,5}}\frac{2\sqrt{d_G(p)\cdot d_G(q)}}{d_G(p)+d_G(q)} \\
&= |E_{3,5}|\cdot\frac{2\sqrt{3\cdot 5}}{3+5}+|E_{4,4}|\cdot\frac{2\sqrt{4\cdot 4}}{4+4}+|E_{4,5}|\cdot\frac{2\sqrt{4\cdot 5}}{4+5}+|E_{5,5}|\cdot\frac{2\sqrt{5\cdot 5}}{5+5} \\
&= \left(\frac{16\sqrt{5}+18}{3}\right)pq+\left(\frac{9\sqrt{15}-16\sqrt{5}-6}{6}\right)q.
\end{aligned}
$$

Also, there are eight partitions of the edge set according to degree sum of neighboring vertices, presented as

$$
\begin{aligned}
S_{15,20} &= \{pq\in E_G \mid \delta_G(p)=15 \text{ and } \delta_G(q)=20\}, \\
S_{15,21} &= \{pq\in E_G \mid \delta_G(p)=15 \text{ and } \delta_G(q)=21\}, \\
S_{19,19} &= \{pq\in E(G) \mid \delta_G(p)=\delta_G(q)=19\}, \\
S_{19,20} &= \{pq\in E_G \mid \delta_G(p)=19 \text{ and } \delta_G(q)=20\},
\end{aligned}
$$

$$\begin{aligned}
S_{19,21} &= \{pq \in E_G \mid \delta_G(p) = 19 \text{ and } \delta_G(q) = 21\},\\
S_{19,22} &= \{pq \in E_G \mid \delta_G(p) = 19 \text{ and } \delta_G(q) = 22\},\\
S_{20,21} &= \{pq \in E_G \mid \delta_G(p) = 20 \text{ and } \delta_G(q) = 21\},\\
S_{22,22} &= \{pq \in E_G \mid \delta_G(p) = \delta_G(q) = 22\}.
\end{aligned}$$

The representative edges of these partite sets are presented in Figure 5.11 in which red, sky blue, green, purple, pink, black, yellow, and blue edges belong to $S_{15,20}$, $S_{15,21}$, $S_{19,19}$, $S_{19,20}$, $S_{19,21}$, $S_{19,22}$, $S_{20,21}$, and $S_{22,22}$ respectively.

Therefore, we have $|S_{15,20}| = 4q$, $|S_{15,21}| = 2q$, $|S_{19,19}| = q(2p-1)$, $|S_{19,20}| = 2q$,

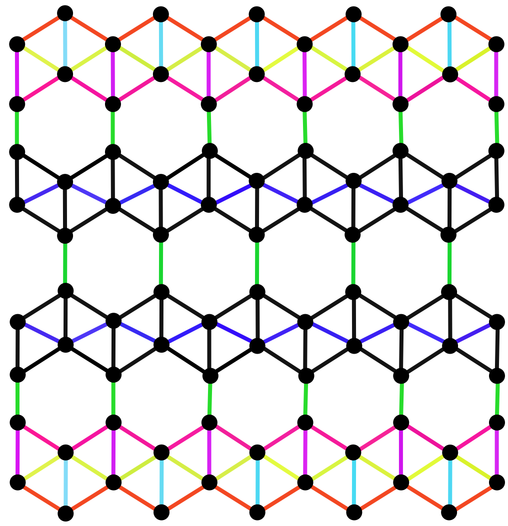

Figure 5.11: The edge partitions of $C_3C_6(H)[p,q]$ according to degree sum of neighbor vertices.

$|S_{19,21}| = 4q$, $|S_{19,22}| = 12q(p-1)$, $|S_{20,21}| = 4q$, and $|S_{22,22}| = 4q(p-1)$. In the following, ABC_4 and GA_5 indices of G are formulated as

$$\begin{aligned}
ABC_4(G) &= \sum_{pq\in E(G)} \sqrt{\frac{\delta_G(p)+\delta_G(q)-2}{\delta_G(p)\cdot\delta_G(q)}}\\
&= \sum_{pq\in S_{15,20}} \sqrt{\frac{\delta_G(p)+\delta_G(q)-2}{\delta_G(p)\delta_G(q)}} + \sum_{pq\in S_{15,21}} \sqrt{\frac{\delta_G(p)+\delta_G(q)-2}{\delta_G(p)\cdot\delta_G(q)}}\\
&\quad + \sum_{pq\in S_{19,19}} \sqrt{\frac{\delta_G(p)+\delta_G(q)-2}{\delta_G(p)\cdot\delta_G(q)}} + \sum_{pq\in S_{19,20}} \sqrt{\frac{\delta_G(p)+\delta_G(q)-2}{\delta_G(p)\cdot\delta_G(q)}}
\end{aligned}$$

$$
\begin{aligned}
&+\sum_{pq\in S_{19,21}}\sqrt{\frac{\delta_G(p)+\delta_G(q)-2}{\delta_G(p)\cdot\delta_G(q)}}+\sum_{pq\in S_{19,22}}\sqrt{\frac{\delta_G(p)+\delta_G(q)-2}{\delta_G(p)\cdot\delta_G(q)}}\\
&+\sum_{pq\in S_{20,21}}\sqrt{\frac{\delta_G(p)+\delta_G(q)-2}{\delta_G(p)\cdot\delta_G(q)}}+\sum_{pq\in S_{22,22}}\sqrt{\frac{\delta_G(p)+\delta_G(q)-2}{\delta_G(p)\cdot\delta_G(q)}}\\
=\;& |S_{15,20}|\sqrt{\frac{15+20-2}{15\times 20}}+|S_{15,21}|\sqrt{\frac{15+21-2}{15\times 21}}+|S_{19,19}|\sqrt{\frac{19+19-2}{19\times 19}}\\
&+|S_{19,20}|\sqrt{\frac{19+20-2}{19\times 20}}+|S_{19,21}|\sqrt{\frac{19+21-2}{19\times 21}}+|S_{19,22}|\sqrt{\frac{19+22-2}{19\times 22}}\\
&+|S_{20,21}|\sqrt{\frac{20+21-2}{20\times 21}}+|S_{22,22}|\sqrt{\frac{22+22-2}{22\times 22}}\\
=\;& \left(\frac{12\sqrt{39}}{\sqrt{418}}+\frac{2\sqrt{42}}{11}+\frac{12}{19}\right)pq+\left(\frac{2\sqrt{34}}{3\sqrt{35}}+\frac{2\sqrt{37}}{\sqrt{95}}\right)q\\
&+\left(\frac{2\sqrt{11}}{5}-\frac{12\sqrt{39}}{\sqrt{418}}-\frac{2\sqrt{42}}{11}-\frac{6}{19}+\frac{4\sqrt{38}}{\sqrt{399}}+\frac{2\sqrt{13}}{\sqrt{35}}\right)q.
\end{aligned}
$$

and

$$
\begin{aligned}
GA_5(G) &= \sum_{pq\in E(G)}\frac{2\sqrt{\delta_G(p)\cdot\delta_G(q)}}{\delta_G(p)+\delta_G(q)}\\
&= \sum_{pq\in S_{15,20}}\frac{2\sqrt{\delta_G(p)\cdot\delta_G(q)}}{\delta_G(p)+\delta_G(q)}+\sum_{pq\in S_{15,21}}\frac{2\sqrt{\delta_G(p)\cdot\delta_G(q)}}{\delta_G(p)+\delta_G(q)}\\
&\quad+\sum_{pq\in S_{19,19}}\frac{2\sqrt{\delta_G(p)\cdot\delta_G(q)}}{\delta_G(p)+\delta_G(q)}+\sum_{pq\in S_{19,20}}\frac{2\sqrt{\delta_G(p)\cdot\delta_G(q)}}{\delta_G(p)+\delta_G(q)}\\
&\quad+\sum_{pq\in S_{19,21}}\frac{2\sqrt{\delta_G(p)\cdot\delta_G(q)}}{\delta_G(p)+\delta_G(q)}+\sum_{pq\in S_{19,22}}\frac{2\sqrt{\delta_G(p)\cdot\delta_G(q)}}{\delta_G(p)+\delta_G(q)}\\
&\quad+\sum_{pq\in S_{21,22}}\frac{2\sqrt{\delta_G(p)\cdot\delta_G(q)}}{\delta_G(p)+\delta_G(q)}+\sum_{pq\in S_{22,22}}\frac{2\sqrt{\delta_G(p)\cdot\delta_G(q)}}{\delta_G(p)+\delta_G(q)}\\
&= |S_{15,20}|\frac{2\sqrt{15\cdot 20}}{15+20}+|S_{15,21}|\frac{2\sqrt{15\cdot 21}}{15+21}+|S_{19,19}|\frac{2\sqrt{19\cdot 19}}{19+19}\\
&\quad+|S_{19,20}|\frac{2\sqrt{19\cdot 20}}{19+20}+|S_{19,21}|\frac{2\sqrt{19\cdot 21}}{19+21}+|S_{19,22}|\frac{2\sqrt{19\cdot 22}}{19+22}\\
&\quad+|S_{20,21}|\frac{2\sqrt{20\cdot 21}}{20+21}+|S_{22,22}|\frac{2\sqrt{22\cdot 22}}{22+22}
\end{aligned}
$$

$$
\begin{aligned}
&= \left(\frac{24\sqrt{418}}{41}+6\right)pq+\left(\frac{16\sqrt{3}}{7}+\frac{\sqrt{35}}{3}\right)q \\
&\quad+\left(\frac{8\sqrt{95}}{39}+\frac{8\sqrt{399}}{40}+\frac{16\sqrt{105}}{41}-\frac{24\sqrt{418}}{41}-5\right)q.
\end{aligned}
$$

□

5.6 Degree-based Indices of Certain Boron Nanotori

The 3D nanostructure materials hold a remarkable morphology compared to 1D or 2D which are thought to produce a vast surface area and to promote the operation of reactants and products comprehensively, so that electrochemical capability can be tremendously enhanced [85]. In this part, we formulate ABC, ABC_4, GA and GA_5 indices for tri-hexagonal boron and boron-α nanotori.

We denote the molecular graph of tri-hexagonal boron nanotorus by $THBC_3C_6[p,q]$, where p and q symbolize number of hexagons in a row and column respectively of the 2D graph of $THBC_3C_6[p,q]$ as presented in Figure 5.12. It is easy to observe that order of $THBC_3C_6[p,q]$ is $8pq$ whereas its size is $18pq$. In the coming Theorem, we obtain

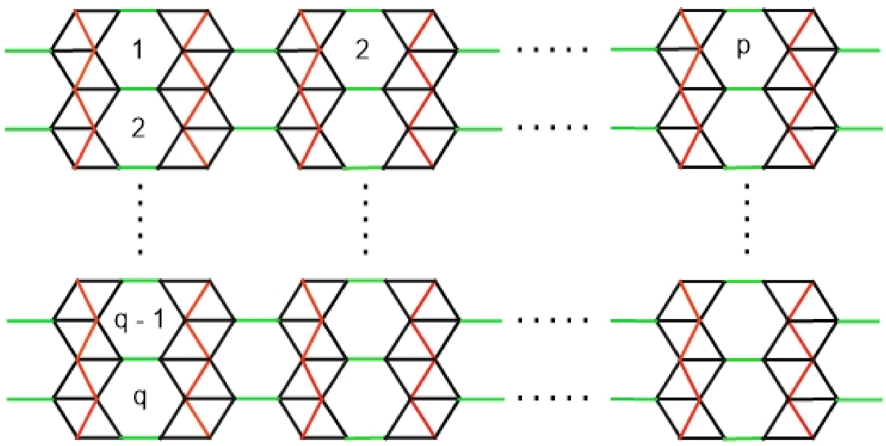

Figure 5.12: A 2D molecular graph of tri-hexagonal boron nanotorus $THBC_3C_6[p,q]$.

the expressions of ABC ABC_4, GA, and GA_5 indices of tri-hexagonal nanotorus.

Theorem 5.6.1. *Consider the Tri-Hexagonal boron nanotorus $THBC_3C_6(S)[p,q]$, then*

$$\begin{aligned}
ABC\left(THBC_3C_6[p,q]\right) &= \left(\frac{\sqrt{6}}{2}+\frac{6\sqrt{7}}{\sqrt{5}}+\frac{8\sqrt{2}}{5}\right)pq,\\
GA\left(THBC_3C_6[p,q]\right) &= \left(6+\frac{16\sqrt{5}}{3}\right)pq,\\
ABC_4\left(THBC_3C_6[p,q]\right) &= \left(\frac{12}{19}+\frac{12\sqrt{39}}{\sqrt{418}}+\frac{2\sqrt{42}}{11}\right)pq,\\
GA_5\left(THBC_3C_6[p,q]\right) &= \left(6+\frac{24\sqrt{418}}{41}\right)pq.
\end{aligned}$$

Proof. Consider the Tri-Hexagonal boron nanotorus $G = THBC_3C_6[p,q]$. There are three partite subsets of edge set E_G according to degree of end vertices, presented as

$$\begin{aligned}
E_{4,4} &= \{pq \in E_G \mid d_G(p) = d_G(q) = 4\},\\
E_{4,5} &= \{pq \in E_G \mid d_G(p) = 4 \text{ and } d_G(q) = 5\},\\
E_{5,5} &= \{pq \in E_G \mid d_G(p) = d_G(q) = 5\}.
\end{aligned}$$

The representative edges of the partite sets $E_{4,4}$, $E_{4,5}$, and $E_{5,5}$ are assigned the colors green, black, and red respectively as shown in Figure 5.12. The cardinality of each partite set is given in Table 5.2. From Table 5.2, the *ABC* and *GA* indices of G are formulated as

Table 5.2: The cardinalities of partite subsets of E_G according to degree of end vertices.

$E_{p,q}$	$\lvert E_{p,q}\rvert$	Color
$E_{4,4}$	$2pq$	Green
$E_{4,5}$	$12pq$	Black
$E_{5,5}$	$4pq$	Red

$$\begin{aligned}
ABC(G) &= \sum_{pq\in E(G)} \sqrt{\frac{d_G(p)+d_G(q)-2}{d_G(p)\cdot d_G(q)}}\\
&= \sum_{pq\in E_{4,4}} \sqrt{\frac{d_G(p)+d_G(q)-2}{d_G(p)\cdot d_G(q)}} + \sum_{pq\in E_{4,5}} \sqrt{\frac{d_G(p)+d_G(q)-2}{d_G(p)\cdot d_G(q)}}
\end{aligned}$$

$$
\begin{aligned}
& + \sum_{pq \in E_{5,5}} \sqrt{\frac{d_G(p)+d_G(q)-2}{d_G(p)\cdot d_G(q)}} \\
= \ & |E_{4,4}|\cdot\sqrt{\frac{4+4-2}{4\cdot 4}} + |E_{4,5}|\cdot\sqrt{\frac{4+5-2}{4\cdot 5}} + |E_{5,5}|\cdot\sqrt{\frac{5+5-2}{5\cdot 5}} \\
= \ & \left(\frac{\sqrt{6}}{2} + \frac{6\sqrt{7}}{\sqrt{5}} + \frac{8\sqrt{2}}{5}\right) pq
\end{aligned}
$$

and

$$
\begin{aligned}
GA(G) &= \sum_{pq\in E_G} \frac{2\sqrt{d_G(p)\cdot d_G(q)}}{d_G(p)+d_G(q)} \\
&= \sum_{pq\in E_{4,4}} \frac{2\sqrt{d_G(p)\cdot d_G(q)}}{d_G(p)+d_G(q)} + \sum_{pq\in E_{4,5}} \frac{2\sqrt{d_G(p)\cdot d_G(q)}}{d_G(p)+d_G(q)} + \sum_{pq\in E_{5,5}} \frac{2\sqrt{d_G(p)\cdot d_G(q)}}{d_G(p)+d_G(q)}
\end{aligned}
$$

$$
\begin{aligned}
&= |E_{4,4}|\cdot\frac{2\sqrt{4\cdot 4}}{4+4} + |E_{4,5}|\cdot\frac{2\sqrt{4\cdot 5}}{4+5} + |E_{5,5}|\cdot\frac{2\sqrt{5\cdot 5}}{5+5} \\
&= \left(6 + \frac{16\sqrt{5}}{3}\right) pq.
\end{aligned}
$$

Also, there are three partite subsets E_G according to degree sum of neighbor vertices, presented as

$$
\begin{aligned}
S_{19,19} &= \{pq \in E(G) \mid \delta_G(p) = \delta_G(q) = 19\}, \\
S_{19,22} &= \{pq \in E(G) \mid \delta_G(p) = 19 \text{ and } \delta_G(q) = 22\}, \\
S_{22,22} &= \{pq \in E(G) \mid \delta_G(p) = \delta_G(q) = 22\}.
\end{aligned}
$$

The representative edges of the partite sets $S_{19,19}$, $S_{19,22}$, and $S_{22,22}$ corresponding to the colors green, black, and red edges respectively are presented in Figure 5.12. The cardinalities of all these partite sets are given in Table 5.3. From this Table, the ABC_4 and GA_5 indices of G are formulated as

$$
ABC_4(G) = \sum_{pq\in E(G)} \sqrt{\frac{\delta_G(p)+\delta_G(q)-2}{\delta_G(p)\cdot\delta_G(q)}}
$$

Table 5.3: The cardinalities of partite subsets of E_G according to degree sum of neighbor vertices.

$S_{p,q}$	$\|S_{p,q}\|$	Color
$S_{19,19}$	$2pq$	Green
$S_{19,22}$	$12pq$	Black
$S_{22,22}$	$4pq$	Red

$$
\begin{aligned}
&= \sum_{pq\in S_{19,19}} \sqrt{\frac{\delta_G(p)+\delta_G(q)-2}{\delta_G(p)\cdot\delta_G(q)}} + \sum_{pq\in S_{19,22}} \sqrt{\frac{\delta_G(p)+\delta_G(q)-2}{\delta_G(p)\cdot\delta_G(q)}} \\
&\quad + \sum_{pq\in S_{22,22}} \sqrt{\frac{\delta_G(p)+\delta_G(q)-2}{\delta_G(p)\cdot\delta_G(q)}} \\
&= |S_{19,19}|\cdot\sqrt{\frac{19+19-2}{19\cdot 19}} + |S_{19,22}|\cdot\sqrt{\frac{19+22-2}{19\cdot 22}} + |S_{22,22}|\cdot\sqrt{\frac{22+22-2}{22\cdot 22}} \\
&= \left(\frac{12}{19}+\frac{12\sqrt{39}}{\sqrt{418}}+\frac{2\sqrt{42}}{11}\right)pq
\end{aligned}
$$

and

$$
\begin{aligned}
GA_5(G) &= \sum_{pq\in E_G} \frac{2\sqrt{\delta_G(p)\cdot\delta_G(q)}}{\delta_G(p)+\delta_G(q)} \\
&= \sum_{pq\in S_{19,19}} \frac{2\sqrt{\delta_G(p)\cdot\delta_G(q)}}{\delta_G(p)+\delta_G(q)} + \sum_{pq\in S_{19,22}} \frac{2\sqrt{\delta_G(p)\cdot\delta_G(q)}}{\delta_G(p)+\delta_G(q)} \\
&\quad + \sum_{pq\in S_{19,22}} \frac{2\sqrt{\delta_G(p)\delta_G(q)}}{\delta_G(p)+\delta_G(q)} \\
&= |S_{19,19}|\cdot\frac{2\sqrt{19\cdot 19}}{19+19} + |S_{19,22}|\cdot\frac{2\sqrt{19\cdot 22}}{19+22} + |S_{22,22}|\cdot\frac{2\sqrt{22\cdot 22}}{22+22} \\
&= \left(6+\frac{24\sqrt{418}}{41}\right)pq.
\end{aligned}
$$

□

We denote the molecular graph of boron-α nanotorus by $THBAC_3C_6[p,q]$, where $p = 6m$ denotes the number of rows and $q = 2n$ denotes the number of columns in the 2D sheet of $THBAC_3C_6[p,q]$ as presented in Figure 5.13. It is easy to observe that the order of $THBAC_3C_6[p,q]$ is $4pq/3$ whereas its size is $7pq/2$. In the coming result, we formulate the"ABC, ABC_4, GA and GA_5"indices of boron-α nanotorus.

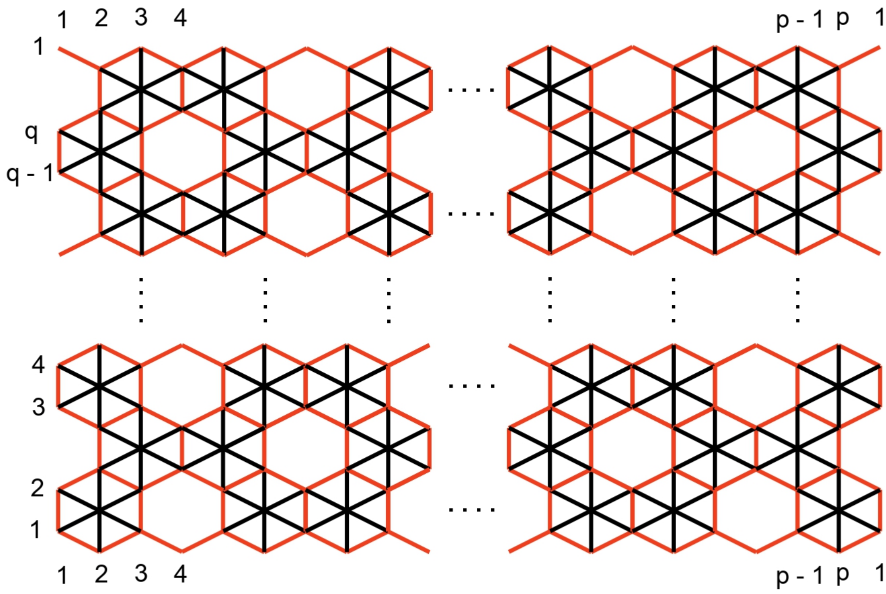

Figure 5.13: A 2D molecular graph of boron-α nanotorus $THBAC_3C_6[p,q]$.

Theorem 5.6.2. *Consider the Tri-Hexagonal boron-α nanotorus $THBAC_3C_6[p,q]$, then*

$$\begin{aligned}
ABC\left(THBAC_3C_6[p,q]\right) &= \left(\frac{3\sqrt{2}+\sqrt{30}}{5}\right)pq,\\
GA\left(THBAC_3C_6[p,q]\right) &= \left(\frac{4\sqrt{30}}{11}+\frac{3}{2}\right)pq,\\
ABC_4\left(THBAC_3C_6[p,q]\right) &= \left(\frac{\sqrt{13}+\sqrt{22}}{9}\right)pq,\\
GA_5\left(THBAC_3C_6[p,q]\right) &= \left(\frac{36\sqrt{10}}{57}+\frac{3}{2}\right)pq.
\end{aligned}$$

Proof. Consider the boron-α nanotorus $K = THBAC_3C_6[p,q]$. There are two disjoint partite subsets of E_K according to degree of end vertices, presented as

$$\begin{aligned}
E_{5,5} &= \{uv \in E_K \mid d_K(u) = d_K(v) = 5\},\\
E_{5,6} &= \{uv \in E_K \mid d_G(u) = 5 \text{ and } d_G(v) = 6\}.
\end{aligned}$$

The representative edges of the partite subsets $E_{5,5}$ and $E_{5,6}$ corresponding to the colors red and black respectively as presented in Figure 5.13. The cardinalities of these partite sets are given in Table 5.4. By using this Table, ABC and GA indices of K are formulated as

Table 5.4: The cardinalities of partite subsets of E_G according to degree of end vertices.

$E_{p,q}$	$\lvert E_{p,q}\rvert$	Color
$E_{5,5}$	$3pq/2$	Red
$E_{5,6}$	$2pq$	Black

$$\begin{aligned}
ABC(K) &= \sum_{pq\in E_K}\sqrt{\frac{d_K(p)+d_K(q)-2}{d_K(p)\cdot d_K(q)}} \\
&= \sum_{pq\in E_{5,5}}\sqrt{\frac{d_K(p)+d_K(q)-2}{d_K(p)\cdot d_K(q)}}+\sum_{pq\in E_{5,6}}\sqrt{\frac{d_K(p)+d_K(q)-2}{d_K(p)\cdot d_K(q)}} \\
&= |E_{5,5}|\cdot\sqrt{\frac{5+5-2}{5\cdot 5}}+|E_{5,6}|\cdot\sqrt{\frac{5+6-2}{5\cdot 6}} \\
&= \left(\frac{3\sqrt{2}+\sqrt{30}}{5}\right)pq
\end{aligned}$$

and

$$\begin{aligned}
GA(K) &= \sum_{pq\in E_K}\frac{2\sqrt{d_K(p)\cdot d_K(q)}}{d_K(p)+d_K(q)} \\
&= \sum_{pq\in E_{5,5}}\frac{2\sqrt{d_K(p)\cdot d_K(q)}}{d_K(p)+d_K(q)}+\sum_{pq\in E_{5,6}}\frac{2\sqrt{d_K(p)\cdot d_K(q)}}{d_K(p)+d_K(q)} \\
&= |E_{5,5}|\cdot\frac{2\sqrt{5\cdot 5}}{5+5}+|E_{5,6}|\cdot\frac{2\sqrt{5\cdot 6}}{5+6} \\
&= \left(\frac{4\sqrt{30}}{11}+\frac{3}{2}\right)pq.
\end{aligned}$$

Also, there are three partite subsets of E_K according to degree sum of neighbor vertices, presented as

$$\begin{aligned}
S_{27,27} &= \{uv\in E_K \mid d_G(u)=d_G(v)=27\}, \\
S_{27,30} &= \{uv\in E_K \mid d_G(u)=27 \text{ and } d_G(v)=30\}.
\end{aligned}$$

The representative edges of the partite subsets $S_{27,27}$ and $S_{27,30}$ corresponding to red and black colors respectively as presented in Figure 5.13. The cardinalities of these partite sets are given in Table 5.5. From this Table, the ABC_4 and GA_5 indices are formulated as

Table 5.5: The cardinalities of partite sets according to degree sum of neighbor vertices.

$S_{p,q}$	$\|S_{p,q}\|$	Color
$S_{27,27}$	$3pq/2$	Red
$S_{27,30}$	$2pq$	Black

$$\begin{aligned}
ABC_4(K) &= \sum_{pq\in E_K}\sqrt{\frac{\delta_G(p)+\delta_G(q)-2}{\delta_G(p)\cdot\delta_G(q)}}\\
&= \sum_{pq\in S_{27,27}}\sqrt{\frac{\delta_G(p)+\delta_G(q)-2}{\delta_G(p)\cdot\delta_G(q)}}+\sum_{pq\in S_{27,30}}\sqrt{\frac{\delta_G(p)+\delta_G(q)-2}{\delta_G(p)\cdot\delta_G(q)}}\\
&= |S_{27,27}|\cdot\sqrt{\frac{27+27-2}{27\cdot 27}}+|S_{27,30}|\cdot\sqrt{\frac{27+30-2}{27\cdot 30}}\\
&= \left(\frac{\sqrt{13}+\sqrt{22}}{9}\right)pq
\end{aligned}$$

and

$$\begin{aligned}
GA_5(K) &= \sum_{pq\in E_K}\frac{2\sqrt{\delta_K(p)\cdot\delta_K(q)}}{\delta_K(p)+\delta_K(q)}\\
&= \sum_{pq\in S_{27,27}}\frac{2\sqrt{\delta_K(p)\cdot\delta_K(q)}}{\delta_K(p)+\delta_K(q)}+\sum_{pq\in S_{27,30}}\frac{2\sqrt{\delta_K(p)\cdot\delta_K(q)}}{\delta_K(p)+\delta_K(q)}\\
&= |S_{27,27}|\cdot\frac{2\sqrt{27\cdot 27}}{27+27}+|S_{27,30}|\cdot\frac{2\sqrt{27\cdot 30}}{27+30}\\
&= \left(\frac{36\sqrt{10}}{57}+\frac{3}{2}\right)pq.
\end{aligned}$$

□

5.7 Degree-based Indices of Para-line Transformed Graphs of V-phenylenic Nanostructures

In this section, we formulate the general Randić connectivity, first general Zagreb, general sum-connectivity, ABC, GA, ABC_4 and GA_5 indices for the para-line transformed graphs of certain V-Phenylenic nanostructures.

Let $TUC_4C_6C_8[m,n]$ represents the V-phenylenic nanostructures where m denotes the number of hexagons in a row and n denotes the number of rows of hexagons in V-Phenylenic $2D$-lattice, V-Phenylenic nanotube and nanotorus as presented respectively in Figure 3 (a), (b) and (c). The order and size of these nanostructures are given in Table 5.6.

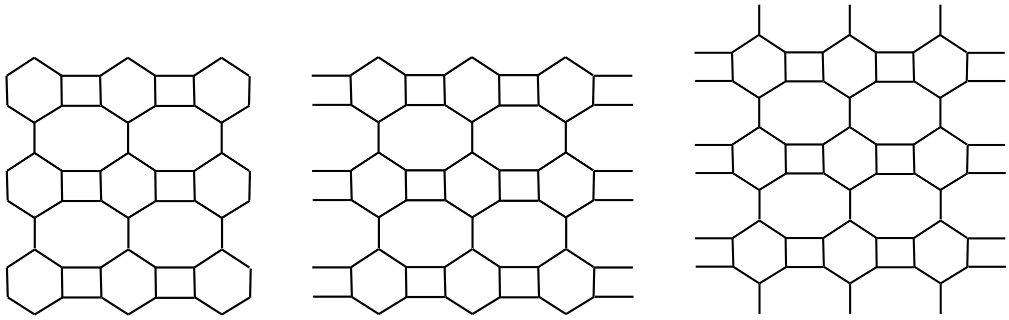

(a) (b) (c)

Figure 5.14: (a) A $2D$-lattice $TUC_4C_6C_8[3,3]$. (b) A $TUC_4C_6C_8[3,3]$ nanotube. (c) A $TUC_4C_6C_8[3,3]$ nanotorus.

Table 5.6: The order and size of V-phenylenic nanostructures.

Graph	Order	Size
$2D$-lattice $TUC_4C_6C_8[m,n]$	$6mn$	$9mn-m-2n$
$TUC_4C_6C_8[m,n]$ nanotube	$6mn$	$9mn-m$
$TUC_4C_6C_8[m,n]$ nanotorus	$6mn$	$9mn$

In the coming Theorem, we present the general Randić, first general Zagreb, general sum-connectivity, *ABC* and *GA* indices for the para-line transformed graph of $2D$-lattice $TUC_4C_6C_8[m,n]$.

Theorem 5.7.1. *Consider the para-line transformed graph G of* $2D$*-lattice* $TUC_4C_6C_8[m,n]$*, then*

$$(a)\quad R_\alpha(G)=2.4^\alpha(m+3n+2)+4.6^\alpha(m+n-2)+9^\alpha(27mn-11m-20n+4),$$

$$(b)\quad M_\alpha(G)=2^{\alpha+2}(m+2n)+2.3^{\alpha+1}(3mn-m-2n),$$

$$(c)\quad \chi_\alpha(G)=2.4^\alpha(m+3n+2)+4.5^\alpha(m+n-2)+6^\alpha(27mn-11m-20n+4),$$

$$(d)\quad ABC(G)=\sqrt{2}(3m+5n-2)+18mn-\frac{22}{3}m-\frac{40}{3}n+\frac{8}{3},$$

$$(e)\quad GA(G)=-9m-14n+8+\frac{8}{5}(m+n-2)\sqrt{6}+27mn.$$

Proof. The subdivided graph of $2D$-lattice $TUC_4C_6C_8[m,n]$ and its para-line transformed graph G are presented in Figure 5.15. It can easily be checked that $|V_G| =$

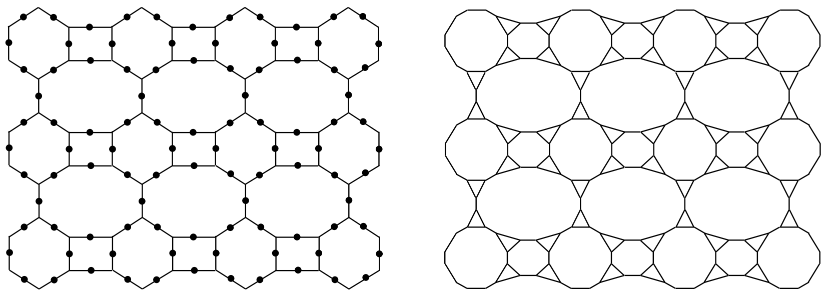

(a) (b)

Figure 5.15: (a) A Subdivided $2D$-lattice $TUC_4C_6C_8$ with $m = 4$ and $n = 3$. (b) The Para-line transformed graph G.

$2(9mn - m - 2n)$. Among them, there are $4(m+2n)$ and $6(3mn - m - 2n)$ vertices of degree 2 and 3 respectively. By using hand shaking lemma (4.2.1), we have

$$4(m+2n)(2) + 6(3mn - m - 2n)(3) = 2|E_G|$$
$$|E_G| = 27mn - 5m - 10n.$$

So, we have the following disjoint edge partite subsets of E_G according to degree of end vertices.

$$\begin{aligned} E_{2,2} &= \{pq \in E_G \mid d_G(p) = d_G(q) = 2\}, \\ E_{2,3} &= \{pq \in E_G \mid d_G(p) = 2 \text{ and } d_G(q) = 3\}, \\ E_{3,3} &= \{pq \in E_G \mid d_G(p) = d_G(q) = 3\}. \end{aligned}$$

We use cardinalities of partite sets given in Table 5.7 and by choosing the corresponding

Table 5.7: The cardinalities of the edge partite subsets of E_G according to degree of end vertices.

$E_{p,q}$	$\lvert E_{p,q}\rvert$
$E_{2,2}$	$2p+6q+4$
$E_{2,3}$	$4p+4q-8$
$E_{3,3}$	$27pq-11p-20q+4$

function $f(d_G(p), d_G(q))$ in the generalized expression given in (3.3.2) to obtain the required results. $\square$

In the coming Theorem, we formulate the ABC_4 and GA_5 indices for the para-line transformed graph of $2D$-lattice $TUC_4C_6C_8[m,n]$.

Theorem 5.7.2. *Consider the para-line transformed graph G of $2D$-lattice $TUC_4C_6C_8[m,n]$, then for $m > 1$ and $n \geq 1$*

$$\begin{aligned}(a)\ ABC_4(G) &= \frac{\sqrt{6}}{2}(n+4)+\frac{2\sqrt{35}}{5}n+\frac{4\sqrt{2}}{5}(m-2)+\frac{\sqrt{110}}{5}(m+n-2)\\ &\quad +\frac{2\sqrt{30}}{3}(m+n-2)+12mn-\frac{76}{9}m-\frac{112}{9}n+\frac{80}{9},\\ (b)\ GA_5(G) &= -17m-26n+\frac{16\sqrt{5}}{9}n+\frac{16\sqrt{10}}{13}(m+n-2)+\frac{96\sqrt{2}}{17}(m+n-2)\\ &\quad +27mn+24.\end{aligned}$$

Proof. For $m > 1$ and $n \geq 1$, it can easily be checked from Figure 4 that in G $|V_4| = 4(n+2)$, $|V_5| = 4(m+n-2)$, $|V_8| = 4(m+n-2)$ and $|V_9| = 2(9mn-5m-8n+4)$. So, we have the following disjoint edge partite subsets of E_G which consists of edges having end vertices labeled by degree sum of adjacent vertices and their cardinalities are given in Table 5.8.

$$\begin{aligned}S_{4,4} &= \{pq \in E_G \mid \delta_G(p) = \delta_G(q) = 4\},\\ S_{4,5} &= \{pq \in E_G \mid \delta_G(p) = 4 \text{ and } \delta_G(q) = 5\},\\ S_{5,5} &= \{pq \in E_G \mid \delta_G(p) = \delta_G(q) = 5\},\\ S_{5,8} &= \{pq \in E_G \mid \delta_G(p) = 5 \text{ and } \delta_G(q) = 8\},\\ S_{8,9} &= \{pq \in E_G \mid \delta_G(p) = 8 \text{ and } \delta_G(q) = 9\},\\ S_{9,9} &= \{pq \in E_G \mid \delta_G(p) = \delta_G(q) = 9\}.\end{aligned}$$

By using Table 5.8 and choosing the corresponding function $f(\delta_G(p), \delta_G(q))$ in the generalized expression given in (3.3.1), we get the required results. $\square$

In the coming Theorem, we present the general Randić, first general Zagreb, general sum-connectivity, ABC and GA indices for the para-line transformed graph of $TUC_4C_6C_8[m,n]$ nanotube.

Table 5.8: The cardinalities of the edge partite subsets of E_G with respect to degree sum of adjacent vertices.

$S_{p,q}$	$\|S_{p,q}\|$
$S_{4,4}$	$2(n+4)$
$S_{4,5}$	$4n$
$S_{5,5}$	$2(m-2)$
$S_{5,8}$	$4(m+n-2)$
$S_{8,9}$	$8(m+n-2)$
$S_{9,9}$	$27mn-19m-28n+20$

Theorem 5.7.3. *Consider the para-line transformed graph H of $TUC_4C_6C_8[m,n]$ nanotube, then*

$$
\begin{aligned}
(a) \quad & R_\alpha(H) = 2.4^\alpha m + 4.6^\alpha m + 9^\alpha(27mn-11m),\\
(b) \quad & M_\alpha(H) = 2^{\alpha+2}m + 2.3^{\alpha+1}(3mn-m),\\
(c) \quad & \chi_\alpha(H) = 2.4^\alpha m + 4.5^\alpha m + 6^\alpha(27mn-11m),\\
(d) \quad & ABC(H) = 3\sqrt{2}m + \frac{\sqrt{7}}{3}(27mn-11m),\\
(e) \quad & GA(H) = -9m + \frac{8\sqrt{6}}{5}m + 27mn.
\end{aligned}
$$

Proof. The subdivided graph of $TUC_4C_6C_8[m,n]$ nanotube and its para-line graph H are presented in Figure 5.16. One can easily verify that $|V_H| = 2(9pq-p)$. Among

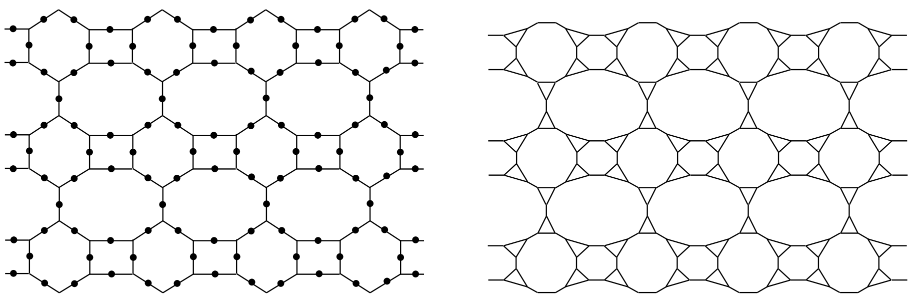

(a) (b)

Figure 5.16: (a) A Subdivided graph of $TUC_4C_6C_8$ nanotube for $m=4$ and $n=3$. (b) The Para-line transformed graph H.

them, there are $4m$ and $6m(3n-1)$ vertices of degree 2 and 3 respectively. By using hand shaking lemma (4.2.1), we have

$$\begin{aligned} 4m(2)+6m(3n-1)(3) &= 2|E_H| \\ |E_H| &= 27mn-5m. \end{aligned}$$

Therefore, we get the following disjoint edge partite subsets of E_H and presented its cardinalities in Table 5.9.

$$\begin{aligned} E_{2,2} &= \{pq \in E_H \mid d_G(p) = d_G(q) = 2\}, \\ E_{2,3} &= \{pq \in E_H \mid d_G(p) = 2 \text{ and } d_G(q) = 3\}, \\ E_{3,3} &= \{pq \in E_H \mid d_G(p) = d_G(p) = 3\}. \end{aligned}$$

We apply generalized formula given in (3.3.2) to the information in Table 5.9 by choos-

Table 5.9: The cardinalities of the edge partite subsets of E_H according to degree of end vertices.

$E_{p,q}$	$\lvert E_{(p,q)}\rvert$
$E_{2,2}$	$2m$
$E_{2,3}$	$4m$
$E_{3,3}$	$27mn-11m$

ing the corresponding functions $f(d_G(p), d_G(q))$ and get the desired results. □

In the coming result, we present the ABC_4 and GA_5 indices for the para-line transformed graph of $TUC_4C_6C_8[m,n]$ nanotube.

Theorem 5.7.4. *Consider the para-line transformed graph H of $TUC_4C_6C_8[m,n]$ nanotube, then*

$$\begin{aligned} (a) \quad & ABC_4(H) = 12mn + \frac{4\sqrt{2}}{5}m + \frac{\sqrt{110}}{5}m + \frac{2\sqrt{30}}{3}m - \frac{76}{9}m, \\ (b) \quad & GA_5(H) = 27mn - 17m + \frac{16\sqrt{10}}{13}m + \frac{96\sqrt{2}}{17}m. \end{aligned}$$

Proof. For $m \geq 1$ and $n \geq 1$, It can easily be checked from Figure 5.16 that in H, $|V_5| = 4m$, $|V_8| = 4m$ and $|V_9| = 2(9mn-5m)$. So, we have the following edge partite subsets of E_H which consists of edges having end vertices labeled by degree sum of adjacent vertices and their cardinalities are given in Table 5.10.

Table 5.10: The cardinalities of the edge partite subsets of E_H with respect to degree sum of adjacent vertices.

$S_{p,q}$	$\|S_{p,q}\|$
$\delta_{(5,5)}$	$2m$
$S_{5,8}$	$4m$
$S_{8,9}$	$8m$
$S_{9,9}$	$27mn-19n$

$$\begin{aligned} S_{5,5} &= \{pq \in E_G \mid \delta_G(p) = \delta_G(q) = 5\}, \\ S_{5,8} &= \{pq \in E_G \mid \delta_G(p) = 5 \text{ and } \delta_G(q) = 8\}, \\ S_{8,9} &= \{pq \in E_G \mid \delta_G(p) = 8 \text{ and } \delta_G(q) = 9\}, \\ S_{9,9} &= \{pq \in E_G \mid \delta_G(p) = \delta_G(q) = 9\}. \end{aligned}$$

We apply generalized formula (3.3.1) to Table 5.10 by taking the corresponding function $f(\delta_G(p), \delta_G(q))$ and get the desired indices. □

In the coming Theorem, we formulate the general Randić, first general Zagreb, general sum-connectivity, ABC and GA indices for the para-line transformed graph of $TUC_4C_6C_8[m,n]$ nanotorus.

Theorem 5.7.5. *Consider the para-line graph K of $TUC_4C_6C_8[p,q]$ nanotorus, then*

$$\begin{aligned} (a) &\quad R_\alpha(G) = 27.9^\alpha mn, \\ (b) &\quad M_\alpha(G) = 18.3^\alpha mn, \\ (c) &\quad \chi_\alpha(G) = 27.6^\alpha mn, \\ (d) &\quad ABC(K) = 18pq, \\ (e) &\quad GA(K) = 27pq. \end{aligned}$$

Proof. The subdivided graph of $TUC_4C_6C_8[m,n]$ nanotorus and its para-line transformed graph K are presented in Figure 5.17 One can easily check that in K, $|V_K| =$

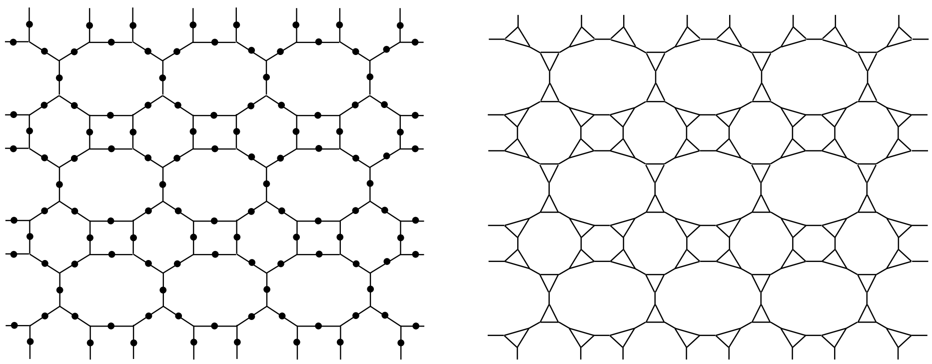

(a) (b)

Figure 5.17: (a) A Subdivided $TUC_4C_6C_8$ nanotorus with $m = 4$ and $n = 3$. (b) The Para-line transformed graph K.

$18mn$ and all these vertices are of degree 3. By using hand shaking lemma (4.2.1), we have $|E_K| = 27mn$. So, we have exactly one edge partition of E_K which is given by

$$E_{3,3} = \{pq \in E_K \mid d_G(p) = d_G(q) = 3\}$$

and clearly $|E_{(3,3)}| = |E_K| = 27mn$.
With this cardinality, we apply the general expression given in (3.3.2) by setting the corresponding function $f(d_G(p), d_G(q))$ and get the desired indices. $\square$

In the coming result, we formulate the ABC_4 and GA_5 indices for the para-line transformed of $TUC_4C_6C_8[p,q]$ nanotorus.

Theorem 5.7.6. *Consider the para-line transformed graph K of $TUC_4C_6C_8[p,q]$ nanotorus, then*

$$\begin{aligned} (a) &\quad ABC_4(K) = 12mn, \\ (b) &\quad GA_5(K) = 27mn. \end{aligned}$$

Proof. It is easy to see from Figure 5.17 that $|V_9| = 18mn$. So, we have exactly one edge partition with respect to end vertices labeled by degree sum of adjacent vertices, given by

$$S_{9,9} = \{pq \in E_K \mid \delta_G(p) = \delta_G(q) = 9\}$$

and clearly $|S_{(9,9)}| = |E_K| = 27mn$.

With this cardinality, we apply the general expression given in (3.3.2) by choosing the corresponding function $f(\delta_G(p), \delta_G(q))$ to obtain the required results. $\square$

Chapter 6

Topological Description of Titania and Polyacene Nanostructures

6.1 Introduction

In this chapter, we present the expressions of eccentric connectivity index (ECI) for the three-layer titania nanotube, six-layer titania nanotube and whole class of polyacenic nanotubes. We also present the expressions of certain variants of ECI such as connective eccentric index, reverse eccentric connectivity index and modified eccentric connectivity index for the three-layer titania nanotube. In addition, we study different counting polynomials of six-layer titania 2D lattice and six-layer titania nanotube.

6.2 Titania Nanotubes

The titanium nanotubular materials, called titania by a generic name, are of high interest metal oxide substances because of their extensive applications in producing catalytic, gas-sensing and corrosionresistance materials [99]. As a widely known semiconductor having many technological applications, Titania (TiO_2) nanotubes are comprehensively used and considered in materials science [9]. The TiO_2 nanotubes were consistently manufactured using various techniques [91] and carefully dealt as anticipated technological materials. Theoretical studies on the stability and electronic characteristics of titania nanostructures have extensively been studied [37, 53, 35]. The numerous studies on the use of titania in technological applications also required theoretical studies on stability and other properties of such structures [87, 90, 103].
In nature, titania nanotubes are categorized in two constructions, one is single-walled titania nanotubes (SW TiO_2 NTs) and other is multi-walled titania nanotubes (MW TiO_2 NTs). From the three mineral constructions of titanium dioxide, anatase is one, the remaining two are rutile and brookite. Titania nanotubes are constructed by rolling up the stoichiometric two- periodic (2D) sheets cut from the energetically stable anatase surface, which involves either six $(O-Ti-O\_O-Ti-O)$ or three $(O-Ti-O)$ layers. The three-layer model of the anatase slab comprise three atomic layers $(O-Ti-O)$, however, its structural optimization results in formation of fluorite-type slab. In Figure 6.1, three-layer hexagonal and three-layer centered rectangular titania sheets are depicted.

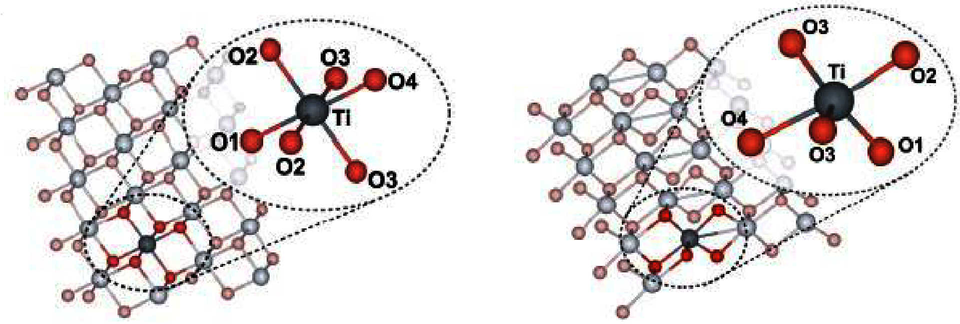

(a) (b)

Figure 6.1: Ti atoms having two types of coordination in: (a) three-layer hexagonal titania sheet (six-fold) and (b) six-layer centered rectangular titania sheet (five-fold).

6.3 Eccentricity-based Indices of Three-layer Titania Nanotube

In this part, we formulate different eccentricity-based connectivity indices such as eccentric connectivity, connective eccentric, reverse eccentric connectivity and modified eccentric connectivity indices for the three-layer titania nanotube.
The molecular graph of three-layer titania nanotube is represented by $TNT_3[m,n]$ and is shown in Figure 6.2, where m and n represent the number of titanium atoms in each row and column respectively. This molecular graph has $2n$ number of rows.

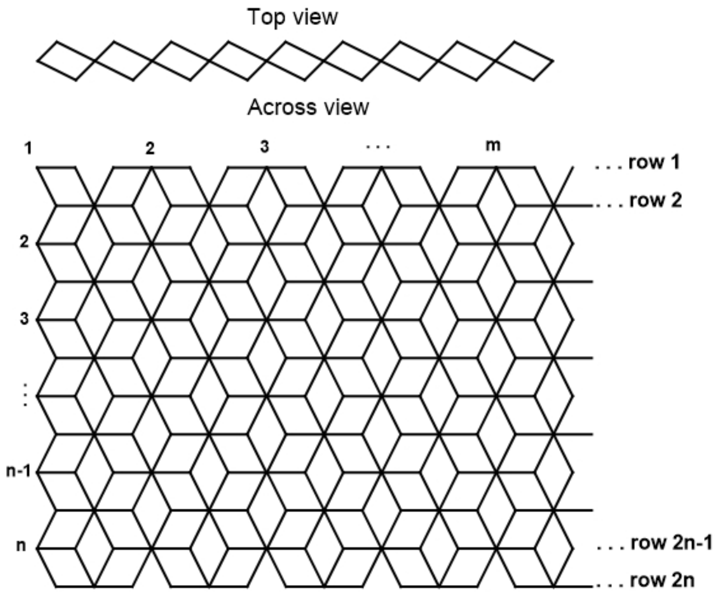

Figure 6.2: The molecular graph of three-layer titania nanotube $TNT_3[m,n]$.

In the molecular graph G of $TNT[m,n]$ nanotubes, we have the vertex partitions $V_{d_G(v)}$ with respect to the degree $d_G(v)$ of its vertices as follows:

$$\begin{aligned} V_2 &= \{p \in V_G | d_G(p) = 2\}, \\ V_3 &= \{p \in V_G | d_G(p) = 3\}, \\ V_4 &= \{p \in V_G | d_G(p) = 4\}, \\ V_6 &= \{p \in V_G | d_G(p) = 6\}. \end{aligned}$$

The cardinalities of these vertex partitions are presented in the Table 6.1.

Table 6.1: Cardinalities of vertex partitions of $TNT[m,n]$.

Vertex partition	Cardinality
V_2	$2mn+4m$
V_3	$2mn$
V_4	$2m$
V_6	$2mn$

Also, we have the vertex partitions of G with respect to degree sum of neighbor vertices as follows:

$$\begin{aligned} S_{10} &= \{p \in V_G | \delta(p) = 10\}, \\ S_{16} &= \{p \in V_G | \delta(p) = 16\}, \\ S_{18} &= \{p \in V_G | \delta(p) = 18\}. \end{aligned}$$

The cardinality of these partite sets are presented in Table 6.2.

Table 6.2: The vertex degree sum partitions of $TNT[m,n]$ along with their cardinalities.

Vertex partition	Cardinality
S_{10}	$6m$
S_{16}	$6m$
S_{18}	$6m(n-2)$

In the next result, we formulate the eccentric connectivity index of $TNT[m,n]$ nanotube.

Theorem 6.3.1. *For the three-layer titania nanotube $TNT_3[m,n]$, we have*

$$\xi^c(TNT[m,n]) = \begin{cases} 24m^2n+36mn^2-28mn-8m^2+8m, & \text{if } m \le n; \\ 12m^3+48mn^2-40mn+4m^2+8m, & \text{if } n < m < 2n-1; \\ 48m^2n-16m^2, & \text{if } m \ge 2n-1. \end{cases}$$

Proof. Consider $G = TNT[m,n]$. According to variation of eccentricity of vertices, we have the following cases.

Case 1. When $m \le n$.

In this case, the eccentricity of a vertex in i^{th} row is the same as the eccentricity of a vertex in $(2n+1-i)^{\text{th}}$ row where $i = 1,2,\ldots,n$. Let v_i be a vertex in i^{th} row, then eccentricity of v_i is given by

$$\varepsilon(v_i) = 2n+m-i \quad \text{where } i = 1,2,\ldots,n.$$

A shortest path having maximal length in $G = TNT[4,6]$ nanotube is shown in Figure 6.3. Hence

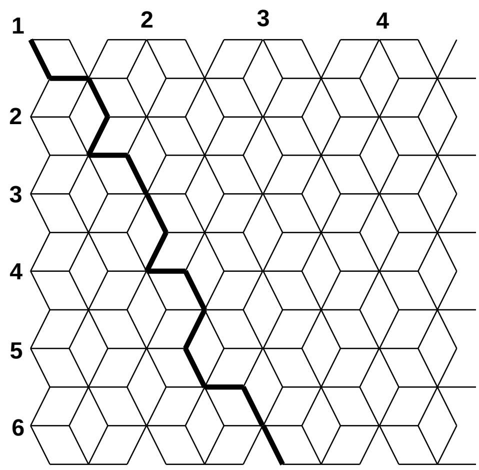

Figure 6.3: A shortest path having maximal length in $G = TNT[4,6]$ nanotube.

$$\begin{aligned}\xi^c(G) &= \sum_{p\in V_G} d_G(p)\cdot\varepsilon(p) \\ &= 2[(2m)(2)(2n+m-1)+(m)(4)(2n+m-1)+(2m)(3)\sum_{i=2}^{n}(2n+m-i) \\ &\quad +(m)(6)\sum_{i=2}^{n}(2n+m-i)]\end{aligned}$$

$$= 24m^2n + 36mn^2 - 28mn - 8m^2 + 8m.$$

Case 2. When $n < m < 2n-1$.

In this case, the eccentricity of a vertex in i^{th} row is the same as the eccentricity of a vertex in $(2n+1-i)^{\text{th}}$ row where $i = 1,2,\ldots,2n-m-1$. Let v_i be a vertex in i^{th} row, then eccentricity of v_i is given by

$$\varepsilon(v_i) = 2n+m-i \quad \text{where } i = 1,2,\ldots,2n-m-1.$$

The eccentricity of each vertex in the remaining $2m-2n+2$ rows is $2m$.

A shortest path having maximal length in $G = TNT[6,4]$ nanotube is shown in Figure 6.4.

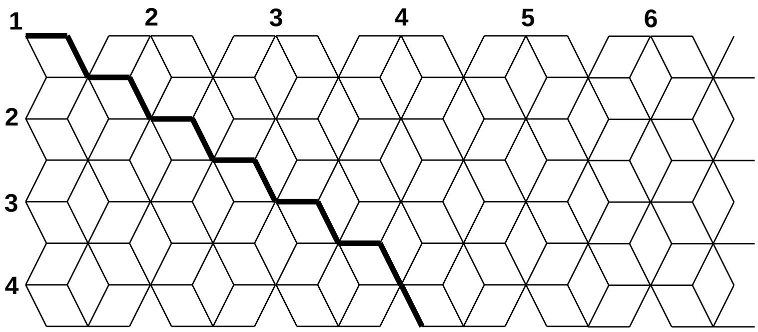

Figure 6.4: A shortest path having maximal length in $G = TNT[6,4]$ nanotube.

Hence

$$\begin{aligned}
\xi^c(G) &= \sum_{v \in V(G)} d_G(p) \cdot \varepsilon(p) \\
&= 2[(2m)(2)(2n+m-1) + (m)(4)(2n+m-1) + (2m)(3)\sum_{i=2}^{2n-m-1}(2n+m-i) \\
&\quad + (m)(6)\sum_{i=2}^{2n-m-1}(2n+m-i)] + (2m-2n+2)(2m)(3)(2m) \\
&\quad + (2m-2n+2)(m)(6)(2m) \\
&= 12m^3 + 48mn^2 - 40mn + 4m^2 + 8m.
\end{aligned}$$

Case 3. When $m \geq 2n-1$.

In this case, the eccentricity of each vertex of graph G is $2m$. Hence

$$
\begin{aligned}
\xi^c(G) &= \sum_{p\in V(G)} d_G(p)\cdot \varepsilon(p) \\
&= 2[(2m)(2)(2m)+(m)(4)(2m)]+(2n-2)(2m)(3)(2m)+(2n-2)(m)(6)(2m) \\
&= 48m^2n-16m^2.
\end{aligned}
$$

□

By going through the computations of Theorem 6.3.1, it is easy to compute the connective eccentric index of $TNT[m,n]$ nanotube. We present it as a corollary and omit its proof.

Corollary 6.3.2. *For the three-layer titania nanotube $TNT[m,n]$, we have*

$$
C^{\xi}(TNT[m,n]) = \begin{cases} \frac{16m}{2n+m-1}+24m\sum_{i=2}^{n}\frac{1}{2n+m-i}, & \text{if } m\leq n; \\ \frac{16m}{2n+m-1}+12(m+n-1)+24m\sum_{i=2}^{2n-m-1}\frac{1}{2n+m-i}, & \text{if } n<m<2n-1; \\ 12n-4, & \text{if } m\geq 2n-1. \end{cases}
$$

In the next result, the reverse eccentric connectivity index of $TNT[m,n]$ nanotube is computed.

Theorem 6.3.3. *For the three-layer titania nanotube $TNT[m,n]$, we have*

$$
{}^{RE}\xi^c(TNT[m,n]) = \begin{cases} \frac{m}{120}(60n^2+40mn+54n+37m-42), & \text{if } m\leq n; \\ \frac{m}{120}(80n^2+20m^2+34n+57m-42), & \text{if } n<m<2n-1; \\ \frac{m^2}{60}(40n+37), & \text{if } m\geq 2n-1. \end{cases}
$$

Proof. Consider $G=TNT[m,n]$. According to variation of eccentricity of vertices, we have the following cases.

Case 1. When $m\leq n$.

For this case, we have already discussed the eccentricity of vertices of G in case 1 of Theorem 6.3.1. By using Table 6.4, the reverse eccentric connectivity index of G is formulated as follows:

$$\begin{aligned}
{}^{RE}\xi^{c}(G) &= \sum_{p\in V(G)} \frac{\varepsilon(p)}{\delta_G(p)} \\
&= \frac{2(3m)(2n+m-1)}{10} + \frac{2(3m)(2n+m-2)}{16} + 2(3m)\sum_{i=3}^{n} \frac{2n+m-i}{18} \\
&= \frac{m}{120}(60n^2+40mn+54n+37m-42).
\end{aligned}$$

Case 2. When $n < m < 2n-1$.

For this case, we have already discussed the eccentricity of vertices of G in case 2 of Theorem 1. From Table 6.4, the reverse eccentric connectivity index of G is formulated as follows:

$$\begin{aligned}
{}^{RE}\xi^{c}(G) &= \sum_{p\in V(G)} \frac{\varepsilon(p)}{\delta_G(p)} \\
&= \frac{2(3m)(2n+m-1)}{10} + \frac{2(3m)(2n+m-2)}{16} + 2(3m)\sum_{i=3}^{2n-m-1} \frac{2n+m-i}{18} \\
&\quad + \frac{(2m-2n+2)(3m)(2m)}{18} \\
&= \frac{m}{120}(80n^2+20m^2+34n+57m-42).
\end{aligned}$$

Case 3. When $m \geq 2n-1$.

In this case, the eccentricity of each vertex of graph G is $2m$. By using Table 6.4, the reverse eccentric connectivity index of G is computed as follows:

$$\begin{aligned}
{}^{RE}\xi^{c}(G) &= \sum_{p\in V(G)} \frac{\varepsilon(p)}{\delta_G(p)} \\
&= \frac{2(3m)(2m)}{10} + \frac{2(3m)(2m)}{16} + \frac{(2n-4)(3m)(2m)}{18} \\
&= \frac{m^2}{60}(40n+37).
\end{aligned}$$

□

By going through the computations of Theorem 6.3.3, it is easy to compute the modified eccentric connectivity index of $TNT[m,n]$ nanotube. We present it as a corollary and omit its proof.

Corollary 6.3.4. *For the three-layer titania nanotube $TNT[m,n]$, we have*

$$\xi_c(TNT[m,n]) = \begin{cases} 108m^2n + 162mn^2 - 174mn - 60m^2 + 72m, & \text{if } m \leq n; \\ 54m^3 + 216mn^2 - 228mn - 6m^2 + 72m, & \text{if } n < m < 2n-1; \\ 216m^2n - 120m^2, & \text{if } m \geq 2n-1. \end{cases}$$

6.4 Eccentric Connectivity Index and Counting Polynomials of Six-layer Titania Nanostructures

We divide this section into two subsections. In the first subsection we formulate the eccentric connectivity index of six-layer titania nanotube. In the second subsection, we formulate different counting polynomials for 2D six-layer titania lattice and the corresponding six-layer titania nanotube.

6.4.1 Eccentric Connectivity Index of Six-layer Titania Nanotube

The molecular graph of six-layer titania nanotube is denoted by $TiO_2[m,n]$ presented in Figure 6.5, where m symbolizes the number of octagons in a row and n symbolizes the number of octagons in a column of the titania nanotube. The molecular graph of $TiO_2[m,n]$ nanotube has $2n+2$ rows and m columns. For each i^{th} row and j^{th} column, we label the vertices of $TiO_2[m,n]$ nanotube by u_{ij}, v_{ij}, x_{ij} and y_{ij} as shown in Figure 6.6.

According to the variation of degrees in graph G of $TiO_2[m,n]$ nanotube, we can observe that $2 \leq d_G(v) \leq 5$ and the vertex partite sets are presented as follows:

$$\begin{aligned} V_2 &= \{p \in V_G | d_G(p) = 2\}, \\ V_3 &= \{p \in V_G | d_G(p) = 3\}, \\ V_4 &= \{p \in V_G | d_G(p) = 4\}, \\ V_5 &= \{p \in V_G | d_G(p) = 5\}. \end{aligned}$$

The cardinalities of all vertex partitions are presented in Table 6.3.

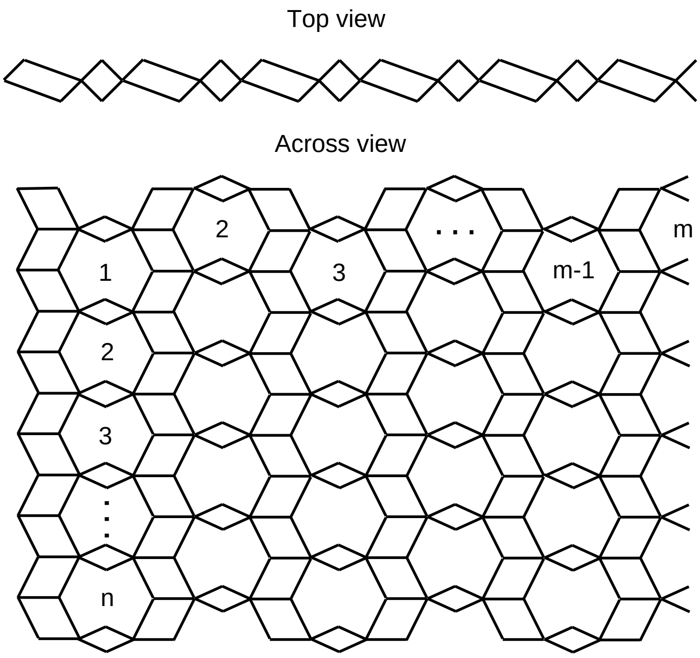

Figure 6.5: The molecular graph of six-layer titania nanotube $TiO_2[m,n]$.

Table 6.3: Cardinalities of the vertex partitions of $TiO_2[m,n]$.

Vertex partition	Cardinality
V_2	$2mn+4m$
V_3	$2mn$
V_4	$2m$
V_5	$2mn$

In the coming results, we formulate the eccentric connectivity index of $TiO_2[m,n]$ nanotubes.

Theorem 6.4.1. *Consider the six-layer titania nanotube $TiO_2[m,n]$, then for $n \leq \lfloor \frac{m-2}{4} \rfloor$ we have*

$$\xi^c(TiO_2[m,n]) = 40m^2n + 32m^2.$$

Proof. Consider $G = TiO_2[m,n]$. When $n \leq \lfloor \frac{m-2}{4} \rfloor$, the eccentricity of every vertex in

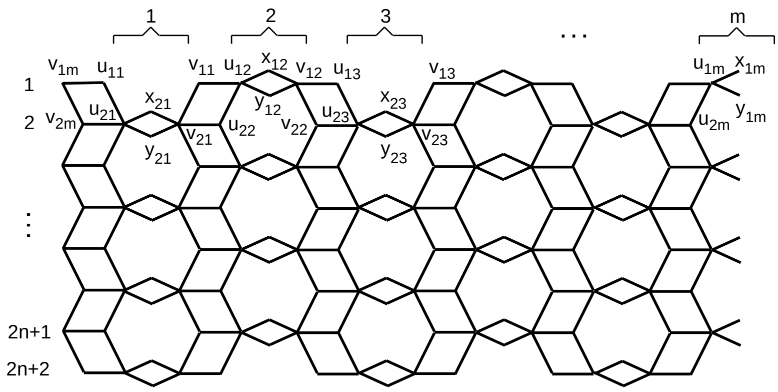

Figure 6.6: The labeled vertices of $TiO_2[m,n]$ nanotube.

every row is $2m$. Hence

$$\begin{aligned}
\xi^c(G) &= \sum_{p\in V_G} d_G(p)\cdot\varepsilon(p) \\
&= (2mn+2m)(2)(2m)+(2m)(2)(2m)+(2mn)(3)(2m)+(2m)(4)(2m) \\
&\quad +(2mn)(5)(2m) \\
&= 40m^2n+32m^2.
\end{aligned}$$

□

Theorem 6.4.2. *Consider $TiO_2[m,n]$ symbolize the six-layer titania nanotube, where $m=2p$, then for p even we have*

$$\xi^c(TiO_2[m,n]) = \begin{cases} 160p^2n+48pn+104p^2+24p, & \text{if } p=2n; \\ 28p^3+48p^2n+112pn^2+128pn+64p^2+24p, & \text{if } \frac{p-2}{2}<n<p-1 \\ & \text{and } p\neq 2n; \\ 120p^2n+68pn^2+112pn+96p^2+52p, & \text{if } n\geq p-1 \text{ and } n \text{ is odd}; \\ 120p^2n+60pn^2+72pn+104p^2+24p, & \text{if } n>p-1 \text{ and } n \text{ is even.} \end{cases}$$

Proof. Consider $G=TiO_2[m,n]$. According to variation of eccentricity of vertices, we have the following cases.

Case 1. When $p=2n$

In this case the eccentricity of the vertices u_{ij}, v_{ij} is $3p+2n+1$ where $i=1,2n+2$. The eccentricity of each vertex in the remaining $2n$ rows is $4p$. Hence

$$\begin{aligned}
\xi^c(G) &= \sum_{p\in V_G} d_G(p)\cdot\varepsilon(p)\\
&= 2(2p)(2)(3p+2n+1)+2(2p)(4)(3p+2n+1)+(2p)(2n)(3)(4p)\\
&\quad +(2p)(2n)(5)(4p)+2p(2n+2)(2)(4p)\\
&= 160p^2n+48pn+104p^2+24p.
\end{aligned}$$

Case 2. when $\frac{p-2}{2}<n<p-1$ and $p\neq 2n$

In this case the eccentricity of the vertices u_{ij}, v_{ij} is the same as the eccentricity of vertices $u_{(2n+3-i)j}$, $v_{(2n+3-i)j}$ where $i=1,2,\ldots,2n-p+1$. The eccentricity of these vertices in i^{th} row is given by

$$\varepsilon(u_{ij})=\varepsilon(v_{ij})=3p+2n+2-i \quad \text{where } i=1,2,\ldots,2n-p+1.$$

The eccentricity of vertices u_{ij}, v_{ij} in remaining $2p-2n$ rows is $4p$.

Also, the eccentricity of the vertices $x_{ij}, y_{ij}, x_{(i+1)j}, y_{(i+1)j}$ is same as the eccentricity of the vertices $x_{(2n+3-i)j}$, $y_{(2n+3-i)j}$, $x_{(2n+2-i)j}$, $y_{(2n+2-i)j}$ where $i=1,2,\ldots,(2n-p)/2$. The eccentricity of these vertices in i^{th} row is given by

$$\varepsilon(x_{ij})=\varepsilon(y_{ij})=3p+2n+2-2i \quad \text{where } i=1,2,\ldots,(2n-p)/2.$$

The eccentricity of the vertices x_{ij}, y_{ij} in the remaining $(2p-2n+2)$ rows is $4p$.

Hence

$$\begin{aligned}
\xi^c(G) &= \sum_{p\in V_G} d_G(p)\cdot\varepsilon(p)\\
&= 2(2p)(2)(3p+2n+1)+2(2p)(4)(3p+2n+1)\\
&\quad +2(2p)(3)\sum_{i=2}^{2n-p+1}(3p+2n+2-i)+2(2p)(5)\sum_{i=2}^{2n-p+1}(3p+2n+2-i)\\
&\quad +(2p)(2p-2n)(3)(4p)+(2p)(2p-2n)(5)(4p)\\
&\quad +4(2p)(2)\sum_{i=1}^{(2n-p)/2}(3p+2n+2-2i)+(2p)(2p-2n+2)(2)(4p)\\
&= 28p^3+48p^2n+112pn^2+128pn+64p^2+24p.
\end{aligned}$$

Case 3. When $n \geq p-1$ and n is odd

In this case the eccentricity of vertices u_{ij}, v_{ij} is same as the eccentricity of vertices $u_{(2n+3-i)j}$, $v_{(2n+3-i)j}$ where $i = 1, 2, \ldots, n+1$. The eccentricity of these vertices in i^{th} row is given by

$$\varepsilon(u_{ij}) = \varepsilon(v_{ij}) = 3p + 2n + 2 - i \quad \text{where } i = 1, 2, \ldots, n+1.$$

Also, the eccentricity of the vertices x_{ij}, y_{ij}, $x_{(i+1)j}$, $y_{(i+1)j}$ is same as the eccentricity of the vertices $x_{(2n+3-i)j}$, $y_{(2n+3-i)j}$, $x_{(2n+2-i)j}$, $y_{(2n+2-i)j}$ where $i = 1, 2, \ldots, (n+1)/2$. The eccentricity of these vertices in i^{th} row is given by

$$\varepsilon(x_{ij}) = \varepsilon(y_{ij}) = 3p + 2n + 2 - 2i \quad \text{where } i = 1, 2, \ldots, (n+1)/2.$$

The shortest paths having maximal length in $TiO_2[8,7]$ nanotube are shown in Figure 6.7. Hence

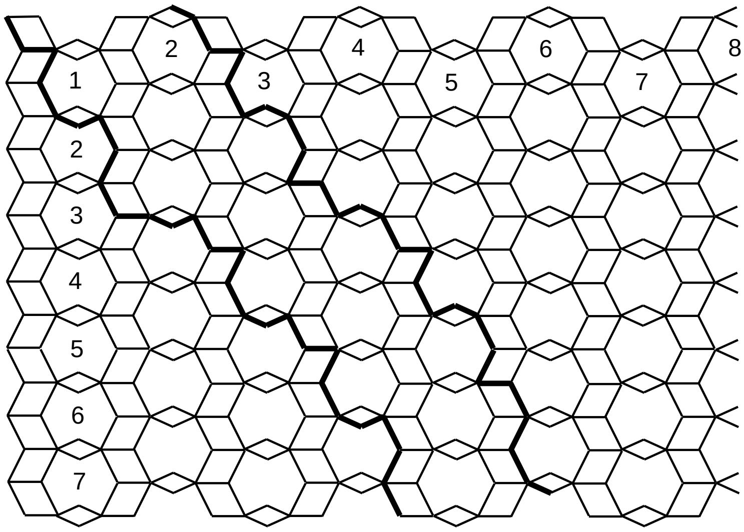

Figure 6.7: The shortest paths having maximal length in $TiO_2[8,7]$ nanotube.

$$\begin{aligned}
\xi^c(G) &= \sum_{p \in V_G} d_G(p) \cdot \varepsilon(p) \\
&= 2(2p)(2)(3p+2n+1) + 2(2p)(4)(3p+2n+1) \\
&\quad +2(2p)(3)\sum_{i=2}^{n+1}(3p+2n+2-i) + 2(2p)(5)\sum_{i=2}^{n+1}(3p+2n+2-i) \\
&\quad +4(2p)(2)\sum_{i=1}^{(n+1)/2}(3p+2n+2-2i) \\
&= 120p^2n + 68pn^2 + 112pn + 96p^2 + 52p.
\end{aligned}$$

Case 4. When $n > p-1$ and n is even

In this case the eccentricity of vertices u_{ij}, v_{ij} is the same as we discussed in case 3. Also, the eccentricity of the vertices x_{ij}, y_{ij}, $x_{(i+1)j}$, $y_{(i+1)j}$ is same as the eccentricity of the vertices $x_{(2n+3-i)j}$, $y_{(2n+3-i)j}$, $x_{(2n+2-i)j}$, $y_{(2n+2-i)j}$ where $i = 1,2,\dots,n/2$. The eccentricity of these vertices in i^{th} row is given by

$$\varepsilon(x_{ij}) = \varepsilon(y_{ij}) = 3p+2n+2-2i \quad \text{where } i = 1,2,\dots,n/2.$$

The eccentricity of the vertices x_{ij} and y_{ij} in the remaining 2 rows is $4p$.

Hence

$$\begin{aligned}
\xi^c(G) &= \sum_{p\in V_G} d_G(p)\cdot\varepsilon(p) \\
&= 2(2p)(2)(3p+2n+1)+2(2p)(4)(3p+2n+1) \\
&\quad +2(2p)(3)\sum_{i=2}^{n+1}(3p+2n+2-i)+2(2p)(5)\sum_{i=2}^{n+1}(3p+2n+2-i) \\
&\quad +4(2p)(2)\sum_{i=1}^{n/2}(3p+2n+2-2i)+2(2p)(2)(4p) \\
&= 120p^2n+60pn^2+72pn+104p^2+24p.
\end{aligned}$$

□

Theorem 6.4.3. *Consider $TiO_2[m,n]$ symbolize the six-layer titania nanotube, where $m = 2p$, then for p odd we have*

$$\xi^c(TiO_2[m,n]) =
\begin{cases}
160p^2n+128pn+192p^2+32p, & \text{when } p = 2n-1; \\
20p^3+80p^2n+80pn^2+96pn+80p^2+28p, & \text{when } \frac{p-1}{2} < n < p-1 \\
 & \text{and } p \neq 2n-1; \\
120p^2n+60pn^2+72pn+72p^2+28p, & \text{when } n > p-1 \text{ and } n \text{ is odd}; \\
120p^2n+60pn^2+80pn+96p^2+32p, & \text{when } n \geq p-1 \text{ and } n \text{ is even.}
\end{cases}$$

Proof. Consider $G = TiO_2[m,n]$. According to variation of eccentricity of vertices, we have the following cases.

Case 1. When $p = 2n-1$

In this case the eccentricity of vertices u_{ij}, v_{ij} is the same as the eccentricity of vertices $u_{(2n+3-i)j}$, $v_{(2n+3-i)j}$ where $1 = 1,2$. The eccentricity of these vertices in i^{th} row is given by

$$\varepsilon(u_{ij}) = \varepsilon(v_{ij}) = 3p + 2n + 2 - i \quad \text{where } i = 1,2$$

The eccentricity of vertices u_{ij}, v_{ij} in remaining $2n$ rows is $4p$.
Also, the eccentricity of the vertices x_{1j}, y_{1j} is the same as the eccentricity of vertices $x_{(2n+2)j}$, $y_{(2n+2)j}$. The eccentricity of the vertices x_{1j} and y_{1j} is given by

$$\varepsilon(x_{1j}) = \varepsilon(y_{1j}) = 3p + 2n + 1$$

The eccentricity of the vertices x_{ij}, y_{ij} in the remaining $2n$ rows is $4p$. The shortest paths having maximal length in $TiO_2[14,4]$ nanotube are shown in Figure 6.8. Hence

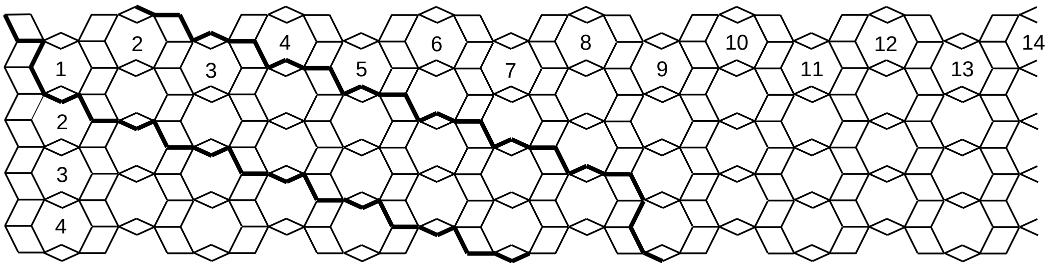

Figure 6.8: The shortest paths having maximal length in $TiO_2[14,4]$ nanotube.

$$\begin{aligned}
\xi^c(G) &= \sum_{p \in V_G} d_G(p) \cdot \varepsilon(p) \\
&= 2(2p)(2)(3p+2n+1) + 2(2p)(4)(3p+2n+1) + 2(2p)(3)(3p+2n) \\
&\quad +2(2p)(5)(3p+2n) + (2p)(2n)(3)(4p) + (2p)(2n)(5)(4p) \\
&\quad +2(2p)(2)(3p+2n+1) + (2p)(2n)(2)(4p) \\
&= 160p^2n + 128pn + 192p^2 + 32p.
\end{aligned}$$

Case 2. When $\frac{p-1}{2} < n < p-1$ and $p \neq 2n-1$

In this case the eccentricity of vertices u_{ij}, v_{ij} is the same as the eccentricity of vertices $u_{(2n+3-i)j}$, $v_{(2n+3-i)j}$ where $i = 1,2,\ldots,2n-p+1$. The eccentricity of these vertices in i^{th} row is given by

$$\varepsilon(u_{ij}) = \varepsilon(v_{ij}) = 3p+2n+2-i \quad \text{where } i = 1,2,\ldots,2n-p+1.$$

The eccentricity of vertices u_{ij}, v_{ij} in remaining $2p-2n$ rows is $4p$. The eccentricity of the vertices x_{1j}, y_{1j}, $x_{(2n+2)j}$, $y_{(2n+2)j}$ is the same as we discussed in Case 1. Also, the eccentricity of the vertices $x_{(i+1)j}$, $y_{(i+1)j}$, $x_{(i+2)j}$, $y_{(i+2)j}$ is the same as the eccentricity of the vertices $x_{(2n+2-i)j}$, $y_{(2n+2-i)j}$, $x_{(2n+1-i)j}$, $y_{(2n+1-i)j}$ where $i = 1,2,\ldots,(2n-p-1)/2$. The eccentricity of these vertices in $(i+1)^{\text{th}}$ row is given by

$$\varepsilon(x_{(i+1)j}) = \varepsilon(y_{(i+1)j}) = 3p+2n+1-2i \quad \text{where } i = 1,2,\ldots,(2n-p-1)/2.$$

The eccentricity of the vertices x_{ij} and y_{ij} in the remaining $(2p-2n+2)$ rows is $4p$. Hence

$$\begin{aligned}
\xi^c(G) &= \sum_{p\in V_G} d_G(p)\cdot\varepsilon(p) \\
&= 2(2p)(2)(3p+2n+1)+2(2p)(4)(3p+2n+1) \\
&\quad +2(2p)(3)\sum_{i=2}^{2n-p+1}(3p+2n+2-i)+2(2p)(5)\sum_{i=2}^{2n-p+1}(3p+2n+2-i) \\
&\quad +(2p)(2p-2n)(3)(4p)+(2p)(2p-2n)(5)(4p)+2(2p)(2)(3p+2n+1) \\
&\quad +4(2p)(2)\sum_{i=1}^{(2n-p-1)/2}(3p+2n+1-2i)+2p(2p-2n+2)(2)(4p) \\
&= 20p^3+80p^2n+80pn^2+96pn+80p^2+28p.
\end{aligned}$$

Case 3. When $n > p-1$ and n is odd

In this case the eccentricity of vertices u_{ij}, v_{ij} is the same as the eccentricity of vertices $u_{(2n+3-i)j}$, $v_{(2n+3-i)j}$ where $i = 1,2,\ldots,n+1$. The eccentricity of these vertices in i^{th} row is given by

$$\varepsilon(u_{ij}) = \varepsilon(v_{ij}) = 3p+2n+2-i \quad \text{where } i = 1,2,\ldots,n+1.$$

The eccentricity of the vertices x_{1j}, y_{1j}, $x_{(2n+2)j}$, $y_{(2n+2)j}$ is the same as we discussed in Case 1.

Also, the eccentricity of the vertices $x_{(i+1)j}$, $y_{(i+1)j}$, $x_{(i+2)j}$, $y_{(i+2)j}$ is the same as the eccentricity of the vertices $x_{(2n+2-i)j}$, $y_{(2n+2-i)j}$, $x_{(2n+1-i)j}$, $y_{(2n+1-i)j}$ where $i = 1,2,\ldots,(n-1)/2$. The eccentricity of theses vertices in $(i+1)^{\text{th}}$ row is given by

$$\varepsilon(x_{i+1}) = \varepsilon(y_{i+1}) = 3p+2n+1-2i \quad \text{where } i = 1,2,\ldots,(n-1)/2. \text{ Hence}$$

$$\begin{aligned}
\xi^c(G) &= \sum_{p \in V_G} d_G(p) \cdot \varepsilon(p) \\
&= 2(2p)(2)(3p+2n+1)+2(2p)(4)(3p+2n+1) \\
&\quad +2(2p)(3)\sum_{i=2}^{n+1}(3p+2n+2-i)+2(2p)(5)\sum_{i=2}^{n+1}(3m+2n+2-i) \\
&\quad +2(2p)(2)(3p+2n+1)+4(2p)(2)\sum_{i=1}^{(n-1)/2}(3p+2n+1-2i) \\
&= 120p^2n+60pn^2+72pn+72p^2+28p.
\end{aligned}$$

Case 4. When $n \geq p-1$ and n is even.

In this case the eccentricity of the vertices $x_{(i+1)j}$, $y_{(i+1)j}$, $x_{(i+2)}$, $y_{(i+2)j}$ is the same as the eccentricity of the vertices $x_{(2n+2-i)j}$, $y_{(2n+2-i)j}$, $x_{(2n+1-i)j}$, $y_{(2n+1-i)j}$ where $i = 1,2,\ldots,n/2$. The eccentricity of these vertices in $(i+1)^{\text{th}}$ row is given by

$$\varepsilon(x_{(i+1)j}) = \varepsilon(y_{(i+1)j}) = 3m+2n+1-2i \quad \text{where } i = 1,2,\ldots,n/2.$$

The eccentricity of the remaining vertices is the same as we discussed in case 3. Hence

$$\begin{aligned}
\xi^c(G) &= \sum_{p \in V_G} d_G(p) \cdot \varepsilon(p) \\
&= 2(2p)(2)(3p+2n+1)+2(2p)(4)(3p+2n+1) \\
&\quad +2(2p)(3)\sum_{i=2}^{n+1}(3p+2n+2-i)+2(2p)(5)\sum_{i=2}^{n+1}(3p+2n+2-i) \\
&\quad +2(2p)(2)(3p+2n+1)+4(2p)(2)\sum_{i=1}^{n/2}(3p+2n+1-2i) \\
&= 120p^2n+60pn^2+80pn+96p^2+32p.
\end{aligned}$$

□

6.4.2 Counting Polynomials of Six-layer Titania Nanostructures

In this part, we formulate the Omega, Sadhana and Theta polynomials of two-dimensional six-layer titania lattice and its corresponding six-layer titania nanotube.

Let $G = TiO_2[p,q]$ be the molecular graph of an infinite two-dimensional six-layer titania lattice, where p and q represent the number of octagons in a column and a row respectively. We denote the corresponding molecular graph of six-layer titania nanotube by $H = TiO_2[p,2q]$. Then $|V_G| = 6pq+6p+6q+6$, $|E_G| = 10pq+8p+8q+6$, $|V_H| = 6q(p+1)$ and $|E_H| = 20pq+16q$.

In the next Theorem, the Omega polynomial of two-dimensional six-layer titania lattice $TiO_2[p,q]$ is formulated.

Theorem 6.4.4. *Consider the two-dimensional six-layer titania lattice $TiO_2[p,q]$, then*

$$\begin{aligned}\Omega(TiO_2[p,q],x) &= 2(p+1)x+2(pq+q+1)x^2+(q+1)x^{2p+2}+2\sum_{i=2}^{\alpha}x^{2i}\\ &\quad +(|2p-q|+1)x^{2(\alpha+1)}\end{aligned}$$

where $\alpha = min\{2p,q\}$.

Proof. Consider $G = TiO_2[p,q]$. From Figure 2, we have five cases for distinct *qoc* strips in G. Suppose e_1, e_2, e_3, e_4 and e_5 are representative edges for these cases. Then $|C(e_1)| = 1$, $|C(e_2)| = 2$, $|C(e_3)| = 2p+2$, $|C(e_4)| = 2(\min\{2p,q\})$ and $|C(e_5)| = 2(\min\{2p,q\}+1)$. From Table 6.4, the Omega polynomial of G for α =min$\{2p,q\}$ is formulate as follows:

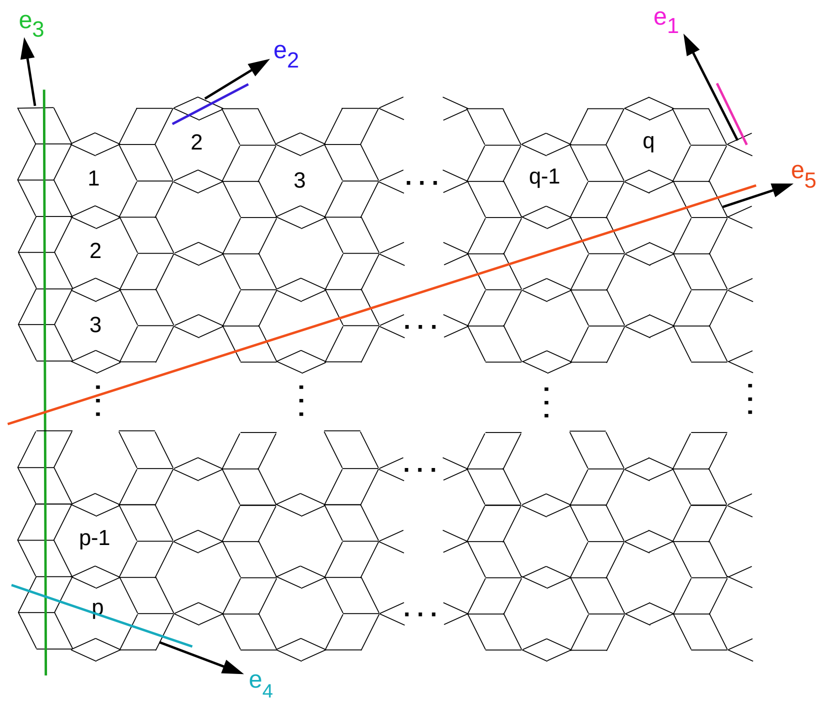

Figure 6.9: The *qoc* strips of two-dimensional six-layer TiO_2 lattice $G = TiO_2[p,q]$.

$$
\begin{aligned}
\Omega(G,x) &= 2(p+1)x+2q(p+1)x^2+(q+1)x^{2p+2}+2(x^2+x^4+\cdots+x^{2\alpha}) \\
&\quad +(|2p-q|+1)x^{2\alpha+2} \\
&= 2(p+1)x+2(pq+q+1)x^2+(q+1)x^{2p+2}+2\sum_{i=2}^{\alpha}x^{2i}+(|2p-q|+1)x^{2\alpha+2}.
\end{aligned}
$$

□

Table 6.4: The number of *qoc* strips of the two-dimensional six-layer lattice $TiO_2[p,q]$.

Categories of qoc's	Corresponding edges	Length of *qoc*	No. of *qoc*
C_1	e_1	1	$2(p+1)$
C_2	e_2	2	$2q(p+1)$
C_3	e_3	$2p+2$	$q+1$
C_4	e_4	$\begin{cases} 2 \\ 4 \\ \vdots \\ 2(min\{2p,q\}) \end{cases}$	$\begin{cases} 2 \\ 2 \\ \vdots \\ 2 \end{cases}$
C_5	e_5	$2(min\{2p,q\}+1)$	$\|2p-q\|+1$

By using Table 6.4, we present the expression of Sadhana polynomial for the two-dimensional six-layer titania lattice in the coming Corollary.

Corollary 6.4.5. *Consider the two-dimensional six-layer lattice $TiO_2[p,q]$, then*

$$
\begin{aligned}
Sd(TiO_2[p,q],x) &= 2(p+1)x^{\lambda+5}+2(pq+q+1)x^{\lambda+4}+(q+1)x^{\lambda-2p+4} \\
&\quad +2\sum_{i=2}^{\alpha}x^{\lambda+6-2i}+(|2p-q|+1)x^{\lambda+4-2\alpha}
\end{aligned}
$$

where $\lambda = 10pq+8p+8q$ and $\alpha = min\{2p,q\}$.

From Table 6.4, we formulate the Theta polynomial of the two-dimensional six-layer lattice in the coming Corollary.

Corollary 6.4.6. *Consider the two-dimensional six-layer lattice $TiO_2[p,q]$, then*

$$
\begin{aligned}
\Theta(TiO_2[p,q],x) &= 2(p+1)x+4(pq+q+1)x^2+2(q+1)(p+1)x^{2p+2}+4\sum_{i=2}^{\alpha}ix^{2i} \\
&\quad +2(q+1)(|2p-q|+1)x^{2\alpha+2}
\end{aligned}
$$

where $\alpha = min\{2p,q\}$.

In the coming Theorem, we present the expression of Omega polynomial for the six-layer titania nanotube.

Theorem 6.4.7. *Consider the six-layer titania nanotube $TiO_2[p,2q]$, then*

$$\Omega(TiO_2[p,2q],x) = 4q(p+1)x^2 + 2qx^{2p+2} + 2qx^{4p+2}.$$

Proof. Consider $H = TiO_2[p,2q]$. From Figure 6.10, we have three cases for distinct qoc strips in H. Suppose e_1, e_2 and e_3 are representative edges for these cases. Then

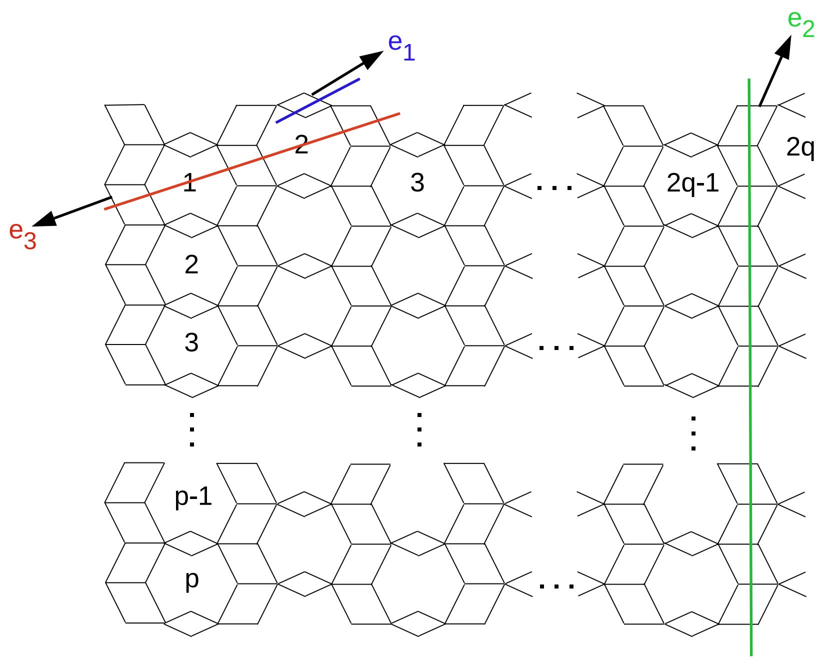

Figure 6.10: The qoc strips of six-layer titania nanotube $H = TiO_2[p,2q]$.

$|C(e_1)| = 2$, $|C(e_2)| = 2p+2$ and $|C(e_3)| = 4p+2$. Also, there are $4q(p+1)$, $2q$ and $2q$ edges similar to e_1, e_2 and e_3 respectively. Therefore

$$\Omega(H,x) = 4q(p+1)x^2 + 2qx^{2p+2} + 2qx^{4p+2}.$$

$\square$

By using the computations of Theorem 6.4.7, we present the Sadhana polynomial of the six-layer titania nanotube is in the coming Corollary.

Corollary 6.4.8. *Consider the six-layer titania nanotube $TiO_2[p,2q]$, then*

$$\begin{aligned} Sd(TiO_2[p,2q],x) &= 4q(p+1)x^{20pq+16q-2}+2qx^{20pq+16q-2p-2} \\ &\quad +2qx^{20pq+16q-4p-2}. \end{aligned}$$

Also, by using the computations of Theorem 6.4.7, we formulate the Theta polynomial of the six-layer titania nanotube in the following Corollary.

Corollary 6.4.9. *Consider the six-layer titania nanotube $TiO_2[p,2q]$, then*

$$\Theta(TiO_2[p,2q],x) = 8q(p+1)x^2+4q(p+1)x^{2p+2}+4q(2p+1)x^{4p+2}.$$

6.5 Eccentric Connectivity Index of *t*-Polyacenic Nanotubes

Polyacenes relate to a family of polycyclic aromatic hydrocarbon (PAH) compounds which are formed by the linearly fused benzene rings. Numerous molecules of this class have interesting optical, thermodynamic, electronic, Ferro-magnetic and photoconductive properties [5, 10, 13, 39]. In the first organic solid-state injection Laser, the lasing was discovered by using the single crystals of tetracene [78, 79]. They have application in rechargeable Li-ion batteries [97] and also have presence in various celestial objects like planetary nebulae [11]. In this sense, the polyacenes have received much attention. The molecular graphs of certain linear polyacene molecules are given in Figure 6.11. The generalized molecular graph of t- polyacenic nanotube $P^t[p,q]$ is

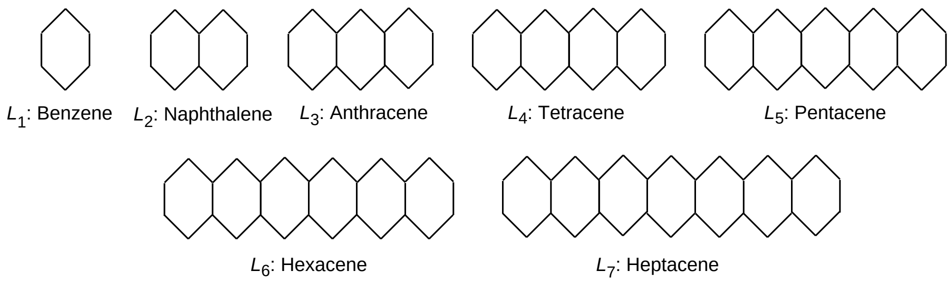

Figure 6.11: The polyacene molecules.

shown in Figure 6.12, where q counts the number of t hexagons in a row and p counts the number of alternative t hexagons in a column of the t- polyacenic nanotube. This molecular graph has $4p$ rows and q columns.

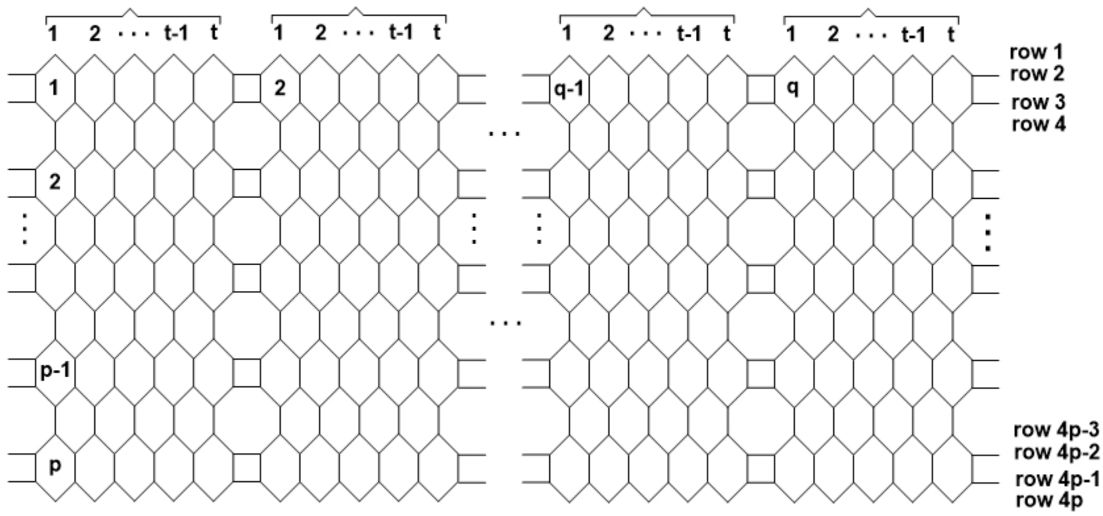

Figure 6.12: The generalized molecular graph of t-polyacenic nanotube $P^t[p,q]$.

For $1 \leq t \leq 6$, the t- polyacenic nanotube $P^t[p,q]$ are known as phenylenic, naphthalenic, anthacenic, tetracenic, pentacenic and hexacenic nanotubes respectively. The molecular graphs of these nanotubes are presented in Figure 6.13.

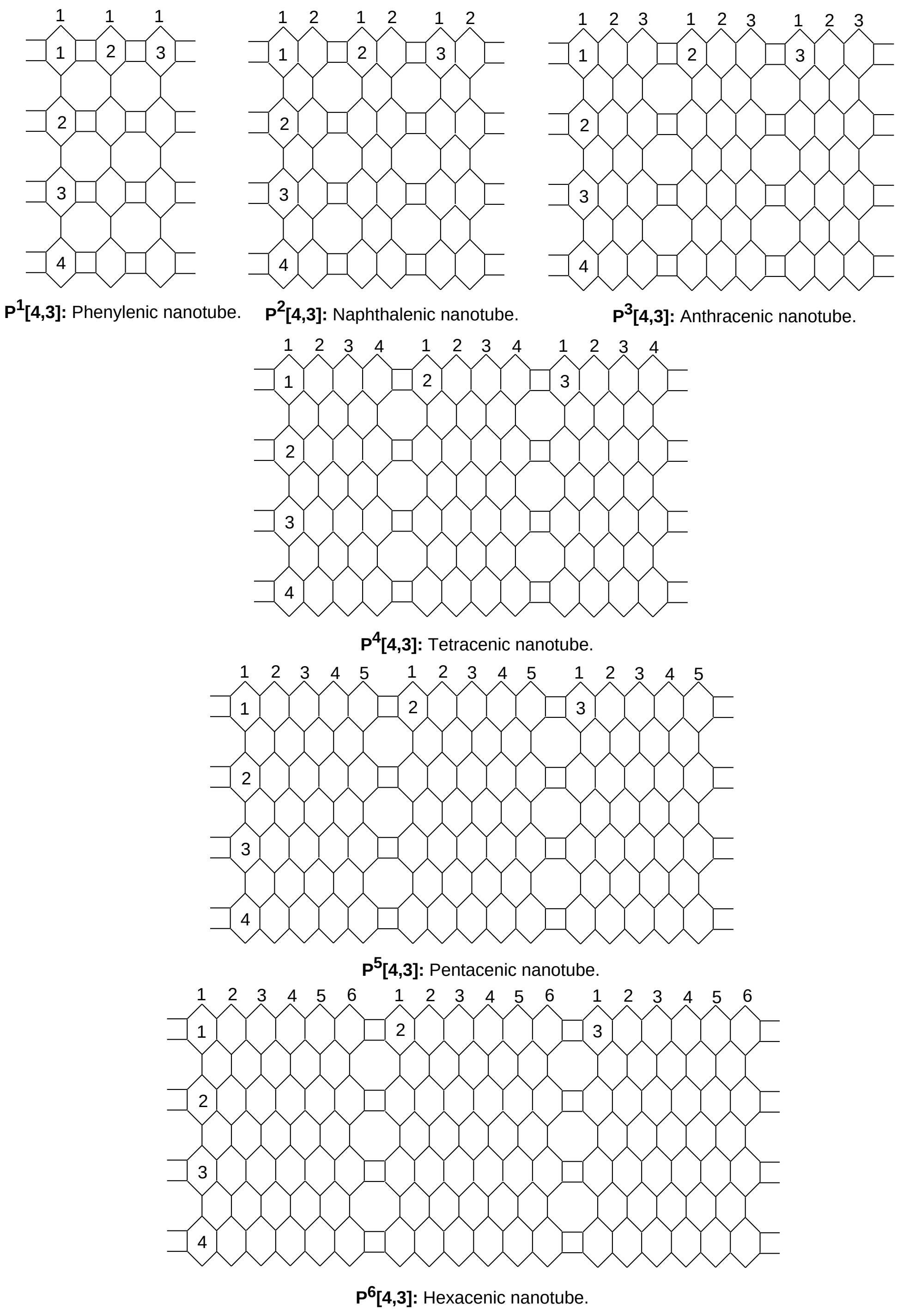

Figure 6.13: The molecular graphs of t- polyacenic nanotubes $P^t[p,q]$ for $1 \leq t \leq 6$.

Let G be a molecular graph of $P^t[p,q]$ nanotube, then we can observe that $2 \leq d_G(p) \leq 3$ for each $p \in V_G$. So, we have the vertex partitions as follows:

$$V_2 = \{p \in V_G | d_G(p) = 2\} \text{ and } V_3 = \{p \in V_G | d_G(p) = 3\}.$$

The vertex partitions of G along with their cardinalities corresponding to each row, are presented in Table 6.5.

Table 6.5: The vertex partitions of the $P^t[p,q]$ nanotube along with their cardinalities corresponding to each row.

Vertex partition	Rows	Cardinality for each row
V_2	$1, 4p$	tq
V_3	$2,3,6,7,\ldots,4p-2,4p-1$	$(t+1)q$
V_3	$4,5,8,9,\ldots,4p-4,4p-3$	tq

In the coming results, we formulate the eccentric connectivity index of $P^t[p,q]$ nanotubes for $t \geq 1$.

Theorem 6.5.1. *Consider the t-polyacenic nanotube $P^t[p,q]$, then for $t \geq 1$ and q even we have* $\xi^c(P^t[p,q]) =$

$$\begin{cases} (10t^2+11t+3)q^2+2(5t+3)q, & \text{if } p=1; \\ 9(2t+1)p^2q+3(4t^2+4t+1)pq^2-(10t+3)pq-t(2t+1)q^2 & \\ +2tq, & \text{if } 2 \leq p \leq \frac{tq}{2}; \\ 3t^2(2t+1)q^3+21(2t+1)p^2q-3(4t^2-1)pq^2-(14t+3)pq & \\ -tq^2+2tq, & \text{if } \frac{tq+2}{2} \leq p \leq tq-1; \\ 18(2t+1)p^2q+3(2t+1)pq^2-(14t+3)pq-tq^2+2tq, & \text{if } p \geq tq,\ p \text{ is even}; \\ 18(2t+1)p^2q+3(2t+1)pq^2-(14t+3)pq-tq^2+(2t-3)q, & \text{if } p \geq tq,\ p \text{ is odd}. \end{cases}$$

Proof. Consider $G = P^t[p,q]$. Let v_i represents the vertices in i^{th} row. With respect to $\varepsilon(v_i)$ or $d_G(v_i)$, we have the following cases.

Case 1. When $p=1$ and $t \geq 1$.

In this case, the eccentricity of each vertex in each row is $\frac{(2t+1)q+2}{2}$. Hence from Table 6.5 we have

$$\begin{aligned} \xi^c(G) &= \sum_{p \in V_G} d_G(p) \cdot \varepsilon(p) \\ &= 2(tq)(2)\left(\frac{(2t+1)q+2}{2}\right)+2(t+1)q(3)\left(\frac{(2t+1)q+2}{2}\right) \\ &= (10t^2+11t+3)q^2+2(5t+3)q. \end{aligned}$$

Case 2. when $2 \leq p \leq \frac{tq}{2}$ and $t \geq 1$.

In this case

$$\varepsilon(v_i) = \varepsilon(v_{i+1}) = \varepsilon(v_{4p+1-i}) = \varepsilon(v_{4p-i}) = \frac{4p+(2t+1)q}{2} - i \text{ where } i = 1,2,\ldots,p.$$

Hence from Table 6.5, we have

$$\begin{aligned}
\xi^c(G) &= \sum_{p \in V_G} d_G(p) \cdot \varepsilon(p) \\
&= 2\left[(tq)(2)+(tq+q)(3)\right]\left(\frac{4p+(2t+1)q}{2} - 1\right) \\
&\quad +2\left[(tq)(3)+(tq+q)(3)\right]\sum_{i=2}^{p}\left(\frac{4p+(2t+1)q}{2} - i\right) \\
&= 9(2t+1)p^2q + 3(4t^2+4t+1)pq^2 - (10t+3)pq - t(2t+1)q^2 + 2tq.
\end{aligned}$$

Case 3. When $\frac{tq+2}{2} \leq p \leq tq-1$ and $t \geq 1$.

In this case

$$\varepsilon(v_i) = \varepsilon(v_{4p+1-i}) = \frac{8p+q}{2} - i \text{ where } i = 1,2,\ldots,4\left(p - \frac{tq}{2}\right).$$

Also,

$$\varepsilon\left(v_{4(p-\frac{tq}{2})+i}\right) = \varepsilon\left(v_{4(p-\frac{tq}{2})+1+i}\right) = \varepsilon(v_{2tq+1-i}) = \varepsilon(v_{2tq-i}) = \frac{(4t+1)q}{2} - i,$$

where $i = 1,2,\ldots,tq-p$. Hence from Table 6.5 we have

$$\begin{aligned}
\xi^c(G) = &\sum_{p \in V_G} d_G(p) \cdot \varepsilon(p) \\
= \;& 2(tq)(2)\left(\frac{8p+q}{2} - 1\right) + 2(tq+q)(3)\left[2\left(p - \frac{tq}{2}\right)\frac{(8p+q)}{2} - \right. \\
& \left.\left[\left[2+6+\cdots+\left(4\left(p-\frac{tq}{2}\right)-2\right)\right] + \left[3+7+\cdots+\left(4\left(p-\frac{tq}{2}\right)-1\right)\right]\right]\right] \\
& +2(tq)(3)\left[\left(2\left(p-\frac{tq}{2}\right)-1\right)\frac{(8p+q)}{2} - \left[4+8+\cdots+4\left(p-\frac{tq}{2}\right)\right]\right] \\
& +2(tq)(3)\left[5+9+\cdots+\left(4\left(p-\frac{tq}{2}\right)-3\right)\right]
\end{aligned}$$

$$
\begin{aligned}
& +2\left[(tq)(3)+(tq+q)(3)\right]\sum_{i=1}^{tq-p}\left(\frac{(4t+1)q}{2}-i\right) \\
= \; & 3t^2(2t+1)q^3+21(2t+1)p^2q-3(4t^2-1)pq^2-(14t+3)pq-tq^2+2tq.
\end{aligned}
$$

Case 4. When $p \geq tq$, p even and $t \geq 1$.

In this case

$$\varepsilon(v_i)=\varepsilon(v_{4p+1-i})=\frac{8p+q}{2}-i \text{ where } i=1,2,\ldots,2p$$

Hence from Table 6.5 we have

$$
\begin{aligned}
\xi^c(G) &= \sum_{p\in V_G} d_G(p)\cdot\varepsilon(p) \\
&= 2(tq)(2)\left(\frac{8p+q}{2}-1\right)+2(tq+q)(3) \\
&\quad \left[\frac{p(8p+q)}{2}-((2+6+\cdots+2p-2)+(3+7+\cdots+2p-1))\right]+2(tq)(3) \\
&\quad \left[\frac{(p-1)(8p+q)}{2}-((4+8+\cdots+2p)+(5+9+\cdots+2p-3))\right] \\
&= 18(2t+1)p^2q+3(2t+1)pq^2-(14t+3)pq-tq^2+2tq.
\end{aligned}
$$

Case 5. When $p \geq tq$, p odd and $t \geq 1$.

In this case, the eccentricities of vertices of G are same as given in case 4. From Table 6.5 we have

$$
\begin{aligned}
\xi^c(G) &= \sum_{p\in V_G} d_G(p)\cdot\varepsilon(p) \\
&= 2(tq)(2)\left(\frac{8p+q}{2}-1\right)+2(tq+q)(3) \\
&\quad \left[\frac{p(8p+q)}{2}-((2+6+\cdots+2p)+(3+7+\cdots+2p-3))\right]+2(tq)(3) \\
&\quad \left[\frac{(p-1)(8p+q)}{2}-((4+8+\cdots+2p-2)+(5+9+\cdots+2p-1))\right] \\
&= 18(2t+1)p^2q+3(2t+1)pq^2-(14t+3)pq-tq^2+(2t-3)q.
\end{aligned}
$$

□

Theorem 6.5.2. *Consider the t- polyacenic nanotube $P^t[p,q]$, then for $t \geq 1$ and q odd we have*

$\xi^c(P^t[p,q]) =$

$$\begin{cases} 2(5t^2+8t+3), & \text{if } p=1,\ q=1 \text{ and } t \geq 2; \\ (10t^2+11t+3)q^2+(5t+3)q, & \text{if } p=1,\ q \geq 3 \text{ and } t \geq 1; \\ 9(2t+1)p^2q+3(4t^2+4t+1)pq^2-2(8t+3)pq & \\ -t(2t+1)q^2+3tq, & \text{if } 2 \leq p \leq \lfloor \frac{tq}{2} \rfloor \text{ and } tq \geq 4 \\ 3t^2(2t+1)q^3+21(2t+1)p^2q-3(4t^2-1)pq^2 & \\ -2(10t+3)pq-tq^2+3tq, & \text{if } \frac{tq+2}{2} \leq p \leq tq-1,\ t \text{ even}; \\ 3t(6t^2+5t+1)q^3-3(2t+1)p^2q-3(4t^2+4t+1)pq^2 & \\ +6(2t+1)pq+(t+1)(8t+3)q^2+(11t+9)q, & \text{if } p=\frac{tq+1}{2},\ t \text{ odd}; \\ 3t^3q^3+3(10t+3)p^2q+3(4t+1)pq^2+(8t+3)pq & \\ -t(9t+5)q^2-6(3t-2)q, & \text{if } \frac{tq+3}{2} \leq p \leq tq-2,\ t \text{ odd}; \\ 6(7t+3)p^2q+3(2t+1)pq^2-2(34t+15)pq & \\ +t(48t+23)q^2-3(9t+4)q, & \text{if } p=tq-1 \text{ and } t \text{ odd}; \\ 18(2t+1)p^2q+3(2t+1)pq^2-2(10t+3)pq-tq^2 & \\ +3tq, & \text{if } p \geq tq,\ p \text{ is even and } t \geq 1; \\ 18(2t+1)p^2q+3(2t+1)pq^2-2(10t+3)pq-tq^2 & \\ +3(t-1)q, & \text{if } p \geq tq,\ p \text{ is odd and } t \geq 1. \end{cases}$$

Proof. Consider $G = P^t[p,q]$. Let v_i represents the vertices in i^{th} row of G. With respect to $\varepsilon(v_i)$ or $d_G(v_i)$, we have the following cases.

Case 1. When $p = 1$, $q = 1$ and $t \geq 2$.

In this case, the eccentricity of each vertex in each row is $t+1$. Hence from Table 6.5 we have

$$\begin{aligned} \xi^c(G) &= \sum_{p \in V_G} d_G(p) \cdot \varepsilon(p) \\ &= 2(t)(2)(t+1)+2(t+1)(3)(t+1) \\ &= 2(5t^2+8t+3). \end{aligned}$$

Case 2. When $p = 1$, $q \geq 3$ and $t \geq 1$.

In this case, the eccentricity of each vertex in each row is $\frac{(2t+1)q+1}{2}$. Hence from Table 6.5 we have

$$\begin{aligned}
\xi^c(G) &= \sum_{p\in V_G} d_G(p)\cdot\varepsilon(p)\\
&= 2(tq)(2)\left(\frac{(2t+1)q+1}{2}\right)+2(tq+q)(3)\left(\frac{(2t+1)q+1}{2}\right)\\
&= (10t^2+11t+3)q^2+(5t+3)q.
\end{aligned}$$

Case 3. when $2\le p\le\lfloor\frac{tq}{2}\rfloor$ and $tq\ge 4$.
In this case

$$\varepsilon(v_i)=\varepsilon(v_{i+1})=\varepsilon(v_{4p+1-i})=\varepsilon(v_{4p-i})=\frac{4p+(2t+1)q-1}{2}-i,$$

where $i=1,2,\ldots,p$. Hence from Table 6.5 we have

$$\begin{aligned}
\xi^c(G) &= \sum_{p\in V_G} d_G(p)\cdot\varepsilon(p)\\
&= 2\left[(tq)(2)+(t+1)q(3)\right]\left(\frac{4p+(2t+1)q-1}{2}-1\right)\\
&\quad +2\left[(tq)(3)+(t+1)q(3)\right]\sum_{i=2}^{p}\left(\frac{4p+(2t+1)q-1}{2}-i\right)\\
&= 9(2t+1)p^2q+3(4t^2+4t+1)pq^2-2(8t+3)pq-t(2t+1)q^2+3tq.
\end{aligned}$$

Case 4. When $\frac{tq+2}{2}\le p\le tq-1$ and t even.
In this case

$$\varepsilon(v_i)=\varepsilon(v_{4p+1-i})=\frac{8p+q-1}{2}-i\ \text{ where } i=1,2,\ldots,4\left(p-\frac{tq}{2}\right).$$

Also,

$$\varepsilon\left(v_{4(p-\frac{tq}{2})+i}\right)=\varepsilon\left(v_{4(p-\frac{tq}{2})+1+i}\right)=\varepsilon(v_{2tq+1-i})=\varepsilon(v_{2tq-i})=\frac{(4t+1)q-1}{2}-i$$

where $i = 1, 2, \ldots, tq - p$. Hence from Table 6.5 we have

$$\begin{aligned}
\xi^c(G) = & \sum_{p \in V_G} d_G(p) \cdot \varepsilon(p) \\
= & \; 2(tq)(2)\left(\frac{8p+q-1}{2} - 1\right) + 2(tq+q)(3)\left[2\left(p - \frac{tq}{2}\right)\frac{(8p+q-1)}{2} - \right. \\
& \left[\left[2+6+\cdots+\left(4\left(p-\frac{tq}{2}\right)-2\right)\right] + \left[3+7+\cdots+\left(4\left(p-\frac{tq}{2}\right)-1\right)\right]\right]\Bigg] \\
& + 2(tq)(3)\left[\left(2\left(p-\frac{tq}{2}\right)-1\right)\frac{(8p+q-1)}{2} - \left[\left[4+8+\cdots+4\left(p-\frac{tq}{2}\right)\right]\right]\right] \\
& + 2(tq)(3)\left[5+9+\cdots+\left(4\left(p-\frac{tq}{2}\right)-3\right)\right] \\
& + 2\left[(tq)(3) + (t+1)q(3)\right]\sum_{i=1}^{tq-p}\left(\frac{(4t+1)q-1}{2} - i\right) \\
= & \; 3t^2(2t+1)q^3 + 21(2t+1)p^2q - 3(4t^2-1)pq^2 - 2(10t+3)pq - tq^2 + 3tq.
\end{aligned}$$

Case 5. When $p = \frac{tq+1}{2}$ and t odd.

In this case

$$\varepsilon(v_1) = \varepsilon(v_2) = \varepsilon(v_{4p}) = \varepsilon(v_{4p-1}) = \frac{4tq+q+1}{2}$$

and

$$\varepsilon(v_{i+2}) = \varepsilon(v_{4p-1-i}) = \varepsilon(v_{4p}) = \varepsilon(v_{4p-1}) = \frac{(4t+1)q+1}{2} - i \text{ where } i = 1, 2.$$

Also,

$$\varepsilon(v_{i+4}) = \varepsilon(v_{i+5}) = \varepsilon(v_{2tq-1-i}) = \varepsilon(v_{2tq-2-i}) = \frac{(4t+1)q-3}{2} - i$$

where $i = 1, 2, \ldots, tq - p - 1$. Hence from Table 6.5 we have

$$\begin{aligned}
\xi^c(G) &= \sum_{p \in V_G} d_G(p) \cdot \varepsilon(p) \\
&= 2\left[(tq)(2) + (tq+q)(3)\right]\left(\frac{(4t+1)q+1}{2}\right) \\
&\quad +2(tq+q)(3)\left(\frac{(4t+1)q+1}{2} - 1\right) + 2(tq)(3)\left(\frac{(4t+1)q+1}{2} - 2\right) \\
&\quad +2\left[(tq)(3) + (tq+q)(3)\right]\sum_{i=1}^{tq-p-1}\left(\frac{(4t+1)q-3}{2} - i\right)
\end{aligned}$$

$$= 3t(6t^2+5t+1)q^3-3(2t+1)p^2q-3(4t^2+4t+1)pq^2+6(2t+1)pq$$
$$+(t+1)(8t+3)q^2+(11t+9)q.$$

Case 6. When $\frac{tq+3}{2} \leq p \leq tq-2$ and t odd.
In this case

$$\varepsilon(v_i)=\varepsilon(v_{4p+1-i})=\frac{8p+q-1}{2}-i \text{ where } i=1,2,\ldots,4\left(p-\frac{tq+1}{2}\right),$$

$$\varepsilon\left(v_{4(p-\frac{tq+1}{2})+1}\right)=\varepsilon\left(v_{4(p-\frac{tq+1}{2})+2}\right)=\varepsilon(v_{2tq+2})=\varepsilon(v_{2tq+1})=\frac{(4t+1)q+1}{2}$$

and

$$\varepsilon\left(v_{4(p-\frac{tq+1}{2})+2+i}\right)=\varepsilon(v_{2tq+1-i})=\frac{(4t+1)q+1}{2}-i \text{ where } i=1,2.$$

Also,

$$\varepsilon\left(v_{4(p-\frac{tq+1}{2})+4+i}\right)=\varepsilon\left(v_{4(p-\frac{tq+1}{2})+5+i}\right)=\varepsilon(v_{2tq-1-i})=\varepsilon(v_{2tq-2-i})=\frac{(4t+1)q-3}{2}-i$$

where $i=1,2,\ldots,tq-p-1$. Hence from Table 6.5 we have

$$\xi^c(G)= \sum_{p\in V_G} d_G(p)\cdot\varepsilon(p)$$
$$= 2(tq)(2)\left(\frac{8p+q-1}{2}-1\right)+2(tq+q)(3)\left[2\left(p-\frac{tq+1}{2}\right)\frac{(8p+q-1)}{2}-\right.$$
$$\left.\left[\left[2+6+\cdots+\left(4\left(p-\frac{tq+1}{2}\right)-2\right)\right]\right]\right]+2(tq+q)(3)$$
$$\left[3+7+\cdots+\left(4\left(p-\frac{tq+1}{2}\right)-1\right)\right]+2(tq)(3)$$
$$\left[\left(2\left(p-\frac{tq+1}{2}\right)-1\right)\frac{(8p+q-1)}{2}-\left[\left[4+8+\cdots+4\left(p-\frac{tq+1}{2}\right)\right]\right]\right]$$
$$+2(tq)(3)\left[5+9+\cdots+\left(4\left(p-\frac{tq+1}{2}\right)-3\right)\right]$$
$$+2\left[(tq)(3)+(tq+q)(3)\right]\left(\frac{(4t+1)q+1}{2}\right)$$
$$+2(tq+q)(3)\left(\frac{(4t+1)q+1}{2}-1\right)+2(tq)(3)\left(\frac{(4t+1)q+1}{2}-2\right)$$

$$+2\left[(tq)(3)+(tq+q)(3)\right]\sum_{i=1}^{tq-p-1}\left(\frac{(4t+1)q-3}{2}-i\right)$$
$$= 3t^3q^3+3(10t+3)p^2q+3(4t+1)pq^2+(8t+3)pq-t(9t+5)q^2-6(3t-2)q.$$

Case 7. When $p = tq-1$ and t odd.

In this case

$$\varepsilon(v_i) = \varepsilon(v_{4p+1-i}) = \frac{8p+q-1}{2} - i \text{ where } i = 1,2,\ldots,2(p-2)$$

and

$$\varepsilon(v_{2p-3}) = \varepsilon(v_{2p-2}) = \varepsilon(v_{2p+3}) = \varepsilon(v_{2p+4}) = \frac{(4t+1)q+1}{2}.$$

Also,

$$\varepsilon(v_{2p-2+i}) = \varepsilon(v_{2p+3-i}) = \varepsilon(v_{2p+3}) = \varepsilon(v_{2p+4}) = \frac{(4t+1)q+1}{2} - i, \text{ where } i = 1,2.$$

Hence from Table 6.5 we have

$$\xi^c(G) = \sum_{p\in V_G} d_G(p)\cdot\varepsilon(p)$$

$$= 2(tq)(2)\left(\frac{8p+q-1}{2}-1\right)+2(tq+q)(3)\left[\frac{(p-2)(8p+q-1)}{2}-\right.$$
$$\left.((2+6+\cdots+2(p-2))+(3+7+\cdots+2(p-2)-1))\right]+2(tq)(3)$$
$$\left[\frac{(p-3)(8p+q-1)}{2}-((4+8+\cdots+2(p-2))+(5+9+\cdots+2(p-2)-3)\right]$$
$$+2\left[(tq)(3)+(tq+q)(3)\right]\left(\frac{(4t+1)q+1}{2}\right)+2(tq+q)(3)\left(\frac{(4t+1)q+1}{2}-1\right)$$
$$+2(tq)(3)\left(\frac{(4t+1)q+1}{2}-2\right)$$
$$= 6(7t+3)p^2q+3(2t+1)pq^2-2(34t+15)pq+t(48t+23)q^2-3(9t+4)q.$$

Case 8. When $p \geq tq$, p even and $t \geq 1$.

In this case

$$\varepsilon(v_i) = \varepsilon(v_{4p+1-i}) = \frac{8p+q-1}{2} - i, \text{ where } i = 1,2,\ldots,2p.$$

Hence from Table 6.5 we have

$$\begin{aligned}
\xi^c(G) = & \sum_{p \in V_G} d_G(p) \cdot \varepsilon(p) \\
= \;& 2(tq)(2)\left(\frac{8p+q-1}{2} - 1\right) + 2(tq+q)(3)\left[\frac{p(8p+q-1)}{2} - \right. \\
& \left. ((2+6+\cdots+2p-2)+(3+7+\cdots+2p-1))\right] + 2(tq)(3) \\
& \left[\frac{(p-1)(8p+q-1)}{2} - ((4+8+\cdots+2p)+(5+9+\cdots+2p-3))\right] \\
= \;& 18(2t+1)p^2q + 3(2t+1)pq^2 - 2(10t+3)pq - tq^2 + 3tq.
\end{aligned}$$

Case 9. When $p \geq tq$, p odd and $t \geq 1$.

In this case, we use the eccentricities of vertices as given in case 8. From Table 6.5 we have

$$\begin{aligned}
\xi^c(G) &= \sum_{p \in V_G} d_G(p) \cdot \varepsilon(p) \\
&= 2(tq)(2)\left(\frac{8p+q-1}{2} - 1\right) + 2(tq+q)(3) \\
& \quad \left[\frac{p(8p+q-1)}{2} - ((2+6+\cdots+2p)+(3+7+\cdots+2p-3))\right] + 2(tq)(3) \\
& \quad \left[\frac{(p-1)(8p+q-1)}{2} - ((4+8+\cdots+2p-2)+(5+9+\cdots+2p-1))\right] \\
&= 18(2t+1)p^2q + 3(2t+1)pq^2 - 2(10t+3)pq - tq^2 + 3(t-1)q.
\end{aligned}$$

□

Remark 6.5.1. The results presented by Rao and Lakhshmi in [77] become a special case of the results given in Theorem 6.5.1 and Theorem 6.5.2 for $t = 1$.

Chapter 7

Inequalities Between Degree- and Distance-based Graph Invariants

7.1 Introduction

Inequalities provide a way to study topological indices relatively. This relative study is being conducted in three directions. One direction is to study inequalities for a topological index; this includes upper/lower bounds of topological index and inequalities for topological index between a graph and its associated transformed graph. Ji et al. [54] characterized the bounds for the reformulated Zagreb index for trees and unicyclic graphs. Gao et al. [44] derived the sharp bounds for the hyper- Zagreb index for trees and bicyclic graphs. In [54, 44], they used the inequality relations between a graph and its associated transformed graphs for the said indices. Wang et al. [94] presented the inequalities for general sum-connectivity indices between a graph and its several graph transformations.

The second direction is to study inequality relations between two different topological indices which belong to the same class. Lokesha et al. [66] derived some inequality relations between Randić and GA indices. Ali et al. [4] studied the inequality relations between various degree-based indices. From the class of distance-based indices, Dankelmann et al. [18] presented the inequality relation between Wiener and eccentric connectivity indices. Das et al. [20] derived the inequality relation between eccentric connectivity and Szeged indices.

The third and most significant direction is to study inequalities between topological indices which belong to two different classes. Hua et al. [52] derived the inequality relations of eccentric connectivity with the Zagreb indices. Zhou et al. [102] presented the inequalities between Wiener, hyper-Wiener, and Zagreb indices. Das et al. [21] derived the inequality relations between different topological indices belonging to degree and distance-based classes.

In this chapter, we emphasize the relative study of topological indices belonging to two different classes. We establish inequality relations of Randić, GA, ABC, and harmonic indices with eccentric connectivity, connective eccentric, augmented eccentric connectivity, Wiener, and ABC_3 indices.

7.2 Randić and *GA* Indices in Relation with Distance-based Topological Indices

In the following Theorem, we derive inequalities between Randić connectivity index and certain distance-based topological indices such as eccentric connectivity, connective eccentric, augmented eccentric connectivity and Wiener indices.

Theorem 7.2.1. *Consider a connected (n,m)-graph G, then*

$$(a)\ R(G) > \frac{\xi^c(G)}{4m} + \sqrt{2} - 1, \tag{7.2.1}$$

$$(b)\ R(G) > \frac{m}{C^{\xi}(G)} + \sqrt{2} - 1, \tag{7.2.2}$$

$$(c)\ R(G) > \frac{n.\delta_G^{\delta_G}}{2\xi^{ac}(G)} + \sqrt{2} - 1, \tag{7.2.3}$$

$$(d)\ 8mnR(G) > 3W(G) + 8mn(\sqrt{2}-1) + 3(n-1)$$

where δ_G denotes the minimum degree of G.

Proof. By considering the functions $F(d_p,\varepsilon_p) = d_p.\varepsilon_p$, $F(d_p,\varepsilon_p) = d_p/\varepsilon_p$ and $F(M_p,\varepsilon_p) = M_p/\varepsilon_p$ in the general expressions for eccentricity related topological indices of any connected graph G as given in (3.3.3) and (3.3.4), we have eccentric connectivity, connective eccentric and augmented eccentric connectivity indices of G respectively as follows

$$\begin{aligned}
\xi^c(G) &= \sum_{p\in V_G} d_p.\varepsilon_p \\
C^{\xi}(G) &= \sum_{p\in V_G} d_p/\varepsilon_p \\
\xi^{ac}(G) &= \sum_{p\in V_G} M_p/\varepsilon_p.
\end{aligned}$$

From (4.2.3)-(4.2.5), we have the relations of these indices with the diameter of G as follows:

$$\frac{\xi^c(G)}{2m} \le d_G \tag{7.2.4}$$

$$\frac{2m}{C^{\xi}(G)} \leq d_G \tag{7.2.5}$$

and the equality holds in each of the inequalities (7.2.4)-(7.2.5) iff G is a self-centered graph. Also,

$$\frac{n.\delta_G^{\delta_G}}{\xi^{ac}(G)} \leq d_G \tag{7.2.6}$$

and the equality holds iff G is a regular self-centered graph.

Now, by considering the function $F(d_p, d_q) = 1/\sqrt{d_p.d_q}$ in the general expression of degree-based indices as given in (3.3.2), we have the Randić connectivity index of G as follows:

$$R(G) = \sum_{pq \in E_G} \frac{1}{\sqrt{d_p.d_q}}.$$

From (4.2.8), we have the relation of this index with the diameter of G as follows:

$$d_G \leq 2R(G) + 2 - 2\sqrt{2}. \tag{7.2.7}$$

and the equality holds iff $G \cong P_n$ for $n \geq 3$.

By combining the inequality (7.2.7) with the inequalities (7.2.4)-(7.2.6), we have

$$\frac{\xi^c(G)}{2m} < 2R(G) + 2 - 2\sqrt{2}$$
$$\frac{2m}{C^{\xi}(G)} < 2R(G) + 2 - 2\sqrt{2}$$
$$\frac{n.\delta_G^{\delta_G}}{\xi^{ac}(G)} < 2R(G) + 2 - 2\sqrt{2}.$$

The equality does not hold in each of these inequalities because if $G \cong P_n$ for $n \geq 3$, then G can not be a self-centered graph. After simplification, we get the required results (a), (b) and (c).

Also, from (4.2.7) we have the relation between Wiener and eccentric connectivity indices as follows

$$\xi^c(G) \geq \frac{3}{2n}(W(G) + n - 1) \tag{7.2.8}$$

and from result (a), we obtain

$$4mR(G)+4m-4\sqrt{2}m > \xi^c(G).$$

By combining this inequality with the inequality (7.2.8), we achieve the desired relation (d). $\square$

In the following corollary, we establish inequalities between *GA* index and certain distance-based topological indices such as eccentric connectivity, connective eccentric, augmented eccentric connectivity and Wiener indices.

Corollary 7.2.2. *Consider a connected (n,m)-graph G having order $n \geq 3$, then*

$$\begin{aligned}
&(a) \quad GA(G) > \frac{1}{\sqrt{12}}\frac{\xi^c(G)}{m}+2\sqrt{\frac{2}{3}}-\frac{2}{\sqrt{3}},\\
&(b) \quad GA(G) > \frac{2}{\sqrt{3}}\frac{m}{C^{\xi}(G)}+2\sqrt{\frac{2}{3}}-\frac{2}{\sqrt{3}},\\
&(c) \quad GA(G) > \frac{1}{\sqrt{3}}\frac{n.\delta_G^{\delta_G}}{\xi^{ac}(G)}+2\sqrt{\frac{2}{3}}-\frac{2}{\sqrt{3}},\\
&(d) \quad 4mnGA(G) > \sqrt{3}W(G)+\frac{8}{\sqrt{3}}mn(\sqrt{2}-1)+\sqrt{3}(n-1)
\end{aligned}$$

where δ_G denotes the minimum degree of G.

Proof. By considering the function $F(d_p,d_q)=2\sqrt{d_p.d_q}/(d_p+d_q)$ in the general expression of degree-based indices given in (3.3.2), we have the *GA* index of *G* as follows

$$GA(G)=\sum_{pq\in E_G}\frac{2\sqrt{d_p.d_q}}{d_p+d_q}.$$

From the compound inequality (4.2.11), we have the relation of this index with the Randić connectivity index as follows:

$$\sqrt{\frac{3}{4}}GA(G) \geq R(G).$$

With this inequality, Theorem 7.2.1 implies the required results. $\square$

In the coming Theorem, we derive an inequality between the Randić connectivity and ABC_3 indices.

Theorem 7.2.3. *Consider a connected (n,m)-graph G having diameter $d_G \geq 2$, then*

$$ABC_3(G) > \frac{m}{d_G}\sqrt{\frac{d_G^2}{R(G)+1-\sqrt{2}}-2}.$$

Proof. By considering the function $F(\varepsilon_p,\varepsilon_q) = \sqrt{(\varepsilon_p+\varepsilon_q-2)/\varepsilon_p.\varepsilon_q}$ in (3.3.6), we have the third *ABC* index as

$$ABC_3(G) = \sum_{pq\in E_G}\sqrt{\frac{\varepsilon_p+\varepsilon_q-2}{\varepsilon_p.\varepsilon_q}}.$$

From the lower bound of (4.2.6), we have the relation of this index with the diameter of G as follows:

$$\frac{2m^2}{d_G^2}(d_G-1) \leq (ABC_3(G))^2$$

where $d_G \geq r_G \geq 2$ and the equality holds iff G is a self-centered graph. It can be written as

$$\frac{1}{d_G}-\frac{1}{d_G^2} \leq \frac{(ABC_3(G))^2}{2m^2}. \tag{7.2.9}$$

Now, from the inequality (4.2.8) we have

$$\frac{1}{2R(G)+2-2\sqrt{2}} \leq \frac{1}{d_G}$$

and the equality holds iff $G \cong P_n$ for $n \geq 3$. From this inequality, we also have

$$\frac{1}{2R(G)+2-2\sqrt{2}}-\frac{1}{d_G^2} \leq \frac{1}{d_G}-\frac{1}{d_G^2}.$$

By combining it with inequality (7.2.9), we obtain

$$\frac{1}{2R(G)+2-2\sqrt{2}}-\frac{1}{d_G^2} < \frac{(ABC_3(G))^2}{2m^2}$$

where $d_G \geq 2$ and the equality does not hold because if $G \cong P_n$ for $n \geq 3$, then G can not be a self-centered graph. After simplification, we achieve the desired relation. $\square$

7.3 *ABC* Index in Relation with Distance-based Topological Indices

In the following Theorem, we derive inequalities between *ABC* index and certain distance-based indices such as eccentric connectivity, connective eccentric, augmented eccentric connectivity and Wiener indices.

Theorem 7.3.1. *Consider a connected (n,m)-graph G, then*

$$
\begin{aligned}
&(a) \quad ABC(G) > \frac{\xi^c(G)}{2m} + \frac{1}{\sqrt{2}}(n-1) - \left\lfloor \frac{n}{2} \right\rfloor, \\
&(b) \quad ABC(G) > \frac{2m}{C^{\xi}(G)} + \frac{1}{\sqrt{2}}(n-1) - \left\lfloor \frac{n}{2} \right\rfloor, \\
&(c) \quad ABC(G) > \frac{n.\delta_G^{\delta_G}}{\xi^{ac}(G)} + \frac{1}{\sqrt{2}}(n-1) - \left\lfloor \frac{n}{2} \right\rfloor, \\
&(d) \quad 4mnABC(G) > 3W(G) + 2\sqrt{2}mn(n-1) - 4mn\left\lfloor \frac{n}{2} \right\rfloor + 3(n-1)
\end{aligned}
$$

where δ_G represents the minimum degree of G.

Proof. By considering the function $F(d_p,d_q) = \sqrt{(d_p+d_q-2)/d_p.d_q}$ in the general expression (3.3.2) for degree-based indices of G, we have the *ABC* index of G as follows

$$ABC(G) = \sum_{pq \in E_G} \sqrt{\frac{d_p+d_q-2}{d_p.d_q}}.$$

From (4.2.2) we have $d_G \leq 2r_G$. Then from (4.2.9), we obtain the relation of this index with the diameter of G as follows

$$d_G \leq 2ABC(G) + 2\left\lfloor \frac{n}{2} \right\rfloor - \sqrt{2}(n-1) \tag{7.3.1}$$

and the equality holds iff $G \cong P_n$ for $n \geq 3$.

By combining the inequality (7.3.1) with the inequalities (7.2.4)-(7.2.6), we have

$$\frac{\xi^c(G)}{2m} < 2ABC(G) + 2\left\lfloor \frac{n}{2} \right\rfloor - \sqrt{2}(n-1)$$
$$\frac{2m}{C^{\xi}(G)} < 2ABC(G) + 2\left\lfloor \frac{n}{2} \right\rfloor - \sqrt{2}(n-1)$$
$$\frac{n\delta_G^{\delta_G}}{\xi^{ac}(G)} < 2ABC(G) + 2\left\lfloor \frac{n}{2} \right\rfloor - \sqrt{2}(n-1)$$

and the equality does not hold in each of these inequalities because if $G \cong P_n$ for $n \geq 3$, then G can not be a self-centered graph. After simplification, we get the required results (a), (b) and (c).

Also, from result (a) we have

$$2mABC(G) + 2m\left\lfloor \frac{n}{2} \right\rfloor - \sqrt{2}m(n-1) > \xi^c(G).$$

By combining this inequality with the inequality (7.2.8), we get the required result (d). □

In the coming Theorem, we derive an inequality between ABC and ABC_3 indices.

Theorem 7.3.2. *Consider a connected (n,m)-graph G having diameter $d_G \geq 2$, then*

$$ABC_3(G) > \frac{m}{d_G}\sqrt{\frac{d_G^2}{ABC(G) + \lfloor \frac{n}{2} \rfloor - \frac{1}{\sqrt{2}}(n-1)} - 2}.$$

Proof. From (7.3.1), we have

$$\frac{1}{2ABC(G) + 2\lfloor \frac{n}{2} \rfloor - \sqrt{2}(n-1)} \leq \frac{1}{d_G}$$

and the equality holds iff $G \cong P_n$ for $n \geq 3$.

From this inequality, we also have

$$\frac{1}{2ABC(G) + 2\lfloor \frac{n}{2} \rfloor - \sqrt{2}(n-1)} - \frac{1}{d_G^2} \leq \frac{1}{d_G} - \frac{1}{d_G^2}.$$

By combining it with the inequality (7.2.9), we obtain

$$\frac{1}{2ABC(G)+2\left\lfloor\frac{n}{2}\right\rfloor-\sqrt{2}(n-1)}-\frac{1}{d_G^2}<\frac{(ABC_3(G))^2}{2m^2}$$

where $d_G \geq 2$ and the equality does not hold because if $G \cong P_n$ for $n \geq 3$, then G can not be a self-centered graph. After simplification, we get the required result. □

7.4 Harmonic Index in Relation with Distance-based Topological Indices

In the following Theorem, we derive the inequalities between harmonic index and certain distance-based topological indices such as eccentric connectivity, connective eccentric, augmented eccentric connectivity and Wiener indices for any non self-centered graph.

Theorem 7.4.1. *Consider a non self-centered (n,m)-graph G, then*

$$(a)\ H(G)<\frac{\xi^c(G)}{m}+\frac{n}{2}-1, \tag{7.4.1}$$

$$(b)\ H(G)<\frac{4m}{C^{\xi}(G)}+\frac{n}{2}-1, \tag{7.4.2}$$

$$(c)\ H(G)<\frac{2n.\Delta_G^{\Delta_G}}{\xi^{ac}(G)}+\frac{n}{2}-1, \tag{7.4.3}$$

$$(d)\ mn(n-1)H(G)>\frac{\sqrt{3}}{4}W(G)+\frac{2}{\sqrt{3}}m(\sqrt{2}-1)+\frac{\sqrt{3}}{4}(n-1)$$

where Δ_G represents the maximum degree of G.

Proof. For a non self-centered graph G, from (4.2.2) we have $r_G < d_G \leq 2.r_G$. Then from the compound inequalities (4.2.3)-(4.2.5), we obtain the relation of diameter of G with the eccentric connectivity, connective eccentric and augmented eccentric connectivity indices as follows

$$d_G \leq \frac{\xi^c(G)}{m} \tag{7.4.4}$$

$$d_G \leq \frac{4m}{C^{\xi}(G)} \tag{7.4.5}$$

$$d_G \leq \frac{2n.\Delta^{\Delta}}{\xi^{ac}(G)}. \tag{7.4.6}$$

Now, by considering the function $F(d_p, d_q) = 2/(d_p + d_q)$ in the general expression of degree-based indices as given in (3.3.2), we have the harmonic index of G as follows

$$H(G) = \sum_{pq \in E_G} \frac{2}{d_p + d_q}.$$

From (4.2.10), we obtain the relation of this index with the diameter of G as follows

$$H(G) - \frac{n}{2} + 1 \leq d_G \tag{7.4.7}$$

and the equality holds iff $G \cong K_n$ for $n \geq 4$.

By combining the inequality (7.4.7) with the inequalities (7.4.4)-(7.4.6), we obtain

$$H(G) - \frac{n}{2} + 1 < \frac{\xi^c(G)}{m}$$
$$H(G) - \frac{n}{2} + 1 < \frac{4m}{C^{\xi}(G)}$$
$$H(G) - \frac{n}{2} + 1 < \frac{2n.\Delta_G^{\Delta_G}}{\xi^{ac}(G)}.$$

The equality does not exist in each of these inequalities because complete graph K_n is a self-centered graph. After simplification, we get the required results (a), (b) and (c).

Also, from the compound inequality (4.2.12), we obtain

$$(n-1)H(G) \geq GA(G) \tag{7.4.8}$$

and from the result (d) of Corollary 1, we have

$$GA(G) > \frac{\sqrt{3}}{4m}W(G) + \frac{2}{\sqrt{3}}(\sqrt{2}-1) + \frac{\sqrt{3}}{4m}(n-1).$$

By combining this inequality with inequality (7.4.8), we get the required result (d). $\square$

In the coming Theorem, we present the inequality relations of harmonic index with eccentric connectivity and connective eccentric indices for self-centered graphs.

Theorem 7.4.2. *Consider a self-centered (n,m)-graph G, then*

$$\begin{aligned} &(a) \quad H(G) \leq \frac{\xi^c(G)}{2m} + \frac{n}{2} - 1, \\ &(b) \quad H(G) \leq \frac{2m}{C^{\xi}(G)} + \frac{n}{2} - 1 \end{aligned}$$

and the equality holds iff $G \cong K_n$.

Proof. For a self-centered graph G, from (4.2.2) we have $d_G = r_G$. Then from the compound inequalities (4.2.3)-(4.2.4), we obtain the equality relation of diameter of G with the eccentric connectivity, connective eccentric and augmented eccentric connectivity indices as follows

$$\begin{aligned} d_G &= \frac{\xi^c(G)}{2m} \\ d_G &= \frac{2m}{C^{\xi}(G)}. \end{aligned}$$

By using these relations in the inequality (7.4.7), we achieve the desired relations. □

In the coming result, we establish an inequality between harmonic and augmented eccentric connectivity indices for regular self-centered graphs.

Theorem 7.4.3. *Consider a regular self-centered (n,m)-graph G of degree d having order $n \geq 4$, then*

$$H(G) \leq \frac{nd^d}{\xi^{ac}(G)} + \frac{n}{2} - 1$$

and the equality holds iff $G \cong K_n$.

Proof. For a self-centered graph G, from (4.2.2) we have $d_G = r_G$. Then from the compound inequality (4.2.5), we obtain the equality relation of diameter of G with the augmented eccentric connectivity indices as follows

$$d_G = \frac{nd^d}{\xi^{ac}(G)}.$$

By using this relation in the inequality (7.4.7), we achieve the desired relation. □

In the coming result, we derive an inequality relation between harmonic and ABC_3 indices for non self-centered graphs.

Theorem 7.4.4. *Consider a non self-centered (n,m)-graph G having order $n \geq 4$ and radius $r_G \geq 2$, then*

$$ABC_3(G) < \frac{m}{r_G}\sqrt{\frac{8r_G^2}{2H(G)-n+2}-2}.$$

Proof. For a non self-centered graph G, from (4.2.2) we have $r_G < d_G \leq 2r_G$. By using this relation, we obtain the inequality

$$\frac{1}{r_G}-\frac{1}{r_G^2} \leq \frac{2}{d_G}-\frac{1}{r_G^2}. \tag{7.4.9}$$

Now, from the compound inequality (4.2.6), we have

$$(ABC_3(G))^2 \leq \frac{2m^2}{r_G^2}(r_G-1).$$

It can be written as

$$\frac{1}{2m^2}(ABC_3(G))^2 \leq \frac{1}{r_G}-\frac{1}{r_G^2} \tag{7.4.10}$$

where $r_G \geq 2$ and the equality holds iff G is a self-centered graph.

By combining inequality (7.4.9) with the inequality (7.4.10), we have

$$\frac{1}{4m^2}(ABC_3(G))^2+\frac{1}{2r_G^2} < \frac{1}{d_G} \tag{7.4.11}$$

and the equality does not hold because G is a non self-centered graph.

Also, from (4.2.10) we have

$$\frac{1}{d_G} \leq \frac{1}{H(G)-\frac{n}{2}+1} \tag{7.4.12}$$

and the equality holds if and only if $G \cong K_n$ for $n \geq 4$.

By combining the inequality (7.4.12) with the inequality (7.4.11), we obtain

$$\frac{1}{4m^2}(ABC_3(G))^2+\frac{1}{2r_G^2} < \frac{1}{H(G)-\frac{n}{2}+1}.$$

After simplification, we achieve the desired relation. $\square$

In the coming Theorem, we derive an inequality between harmonic and ABC_3 indices for self-centered graphs.

Theorem 7.4.5. *Consider a self-centered (n,m)-graph G having order $n \geq 4$ and diameter $d_G \geq 2$, then*

$$ABC_3(G) < \frac{m}{d_G}\sqrt{\frac{4d_G^2}{2H(G)-n+2}-1}.$$

Proof. For a self-centered graph G, we have $d_G = r_G$. Then from the compound inequality (4.2.6), we have

$$\frac{1}{2m^2}(ABC_3(G))^2 = \frac{1}{d_G} - \frac{1}{d_G^2} \tag{7.4.13}$$

where $d_G \geq 2$.

Also, from the inequality (7.4.12) we have

$$\frac{1}{d_G} - \frac{1}{d_G^2} \leq \frac{1}{H(G)-\frac{n}{2}+1} - \frac{1}{d_G^2}$$

and the equality holds iff $G \cong K_n$ for $n \geq 4$.

By using (7.4.13), we obtain

$$\frac{1}{2m^2}(ABC_3(G))^2 < \frac{1}{H(G)-\frac{n}{2}+1} - \frac{1}{d_G^2}$$

where $d_G \geq 2$ and the equality does not hold because if $G \cong K_n$ for $n \geq 4$, then $d_G = 1$. And after simplification, we get the desired result. $\square$

Chapter 8

Topological Description of Para-line Transformation of Graphs

8.1 Introduction

Transformed graphs of the molecular graphs have significant chemical applications in chemical graph theory because some topological index of the transformed graph will capture other structural characteristics rather than the same topological index of the parent molecular graph. In this sense, a wide range of different properties of a chemical compound could be modeled by using some topological index. This idea has been applied in [50, 51].

The para-line transformed graphs have considerable chemical properties, see [59, 60]. Recently, various degree-based topological indices have been studied for the para-line transformation graphs of several molecular graphs. Nadeem et al. [70] presented the expressions of general Randić index, first general Zagreb index, general sum-connectivity index, ABC index, GA index, ABC_4 index and GA_5 index for the para-line transformed graphs of 2D-lattice, nanotube and nanotorus of $TUC4C8$. They also formulated the ABC_4 and GA_5 indices for the para-line transformed graphs of the ladder, wheel and tadpole graphs in [69]. Akhter et al. [2] calculated the general Randić index, first general Zagreb index, general sum-connectivity index, ABC index, GA index, ABC_4 index and GA_5 index for the para-line transformed graphs of hexagonal parallelogram nanotube, zigzag-edge coronoid fused nanotube and triangular benzenoids. In [3], they formulated the same indices for the para-line transformed graphs of honeycomb and graphene networks. These para-line transformed graphs have also been studied by Ahmad [1] for the Zagreb indices, Zagreb irregularity indices, AZI index, multiple Zagreb index and harmonic index. Gao et al. [43] formulated the general Randić index, first general Zagreb index, general sum-connectivity index, ABC index, GA index, ABC_4 index and GA_5 index for the para-line transformed graphs of V-Pantacenic nanotube, H-Pantacenic nanotube and V-Pantacenic nanotorus.

In this chapter we present the expressions of ABC, GA, harmonic, AZI, SDD, ISI, reformulated Zagreb, leap Zagreb, ABC_4, GA_5, and ABC_5 indices for the para-line transformed graph of any graph and thus generalized the existing results. We also formulate the Wiener index for the para-line transformed graph of any tree. In addition we present the bounds of various topological indices belonging to distance-based class for the para-line transformed graph.

8.2 General Expressions of Topological Indices for Para-line Transformed Graph

In this section, we achieve the general expressions of *ABC*, *GA*, harmonic, *AZI*, *SDD*, *ISI*, reformulated Zagreb, leap Zagreb, ABC_4, GA_5 and ABC_5 indices for the Para-line transformed graph. We also obtain the expression of Wiener index for the Para-line transformed graph of any tree by deriving a relation of this index between a tree and its Para-line transformed graph.

8.2.1 *ABC*, *GA*, Harmonic, *AZI*, *SDD* and *ISI* Indices of Para-line Transformed Graph

In this section, we obtain the expressions of *ABC*, *GA*, harmonic, *AZI*, *SDD* and *ISI* indices for the Para-line transformed graph of any graph.
In the following Lemma, we present a technique to construct the para-line transformed graph of any graph.

Lemma 8.2.1. *Consider a graph G, then its para-line transformed graph $PL(G)$ is constructed by replacing each vertex $p \in V_G$ with $C(p)$; the clique on $d_G(p)$ vertices having the same degree $d_G(p)$.*

Proof. Let $p \in V_G$ be any vertex having degree $d_G(p)$, then p is incident with the edges pq_i (say) where $1 \leq i \leq d_G(p)$. In the construction of subdivision graph $S(G)$, each of these edges is replaced by a path having length two $p \rightarrow r_i \rightarrow q_i$ (say). Then corresponding to the edges pr_i and r_iq_i, we have the adjacent vertices u_i and v_i in the para-line transformed graph $L(S(G)) \cong PL(G)$. Clearly all edges pr_i have the same end vertex p in $S(G)$, therefore all $d_G(p)$ corresponding vertices u_i in $PL(G)$ must be adjacent with each other along with the edges u_iv_i and hence have a clique $C(p)$ on $d_G(p)$ vertices having the same degree $d_G(p)$. □

A para-line transformed graph is shown in Figure 8.1 which is constructed from a graph G by the technique presenting in Lemma 8.2.1.

From Lemma 8.2.1, we can extract the following Observations.

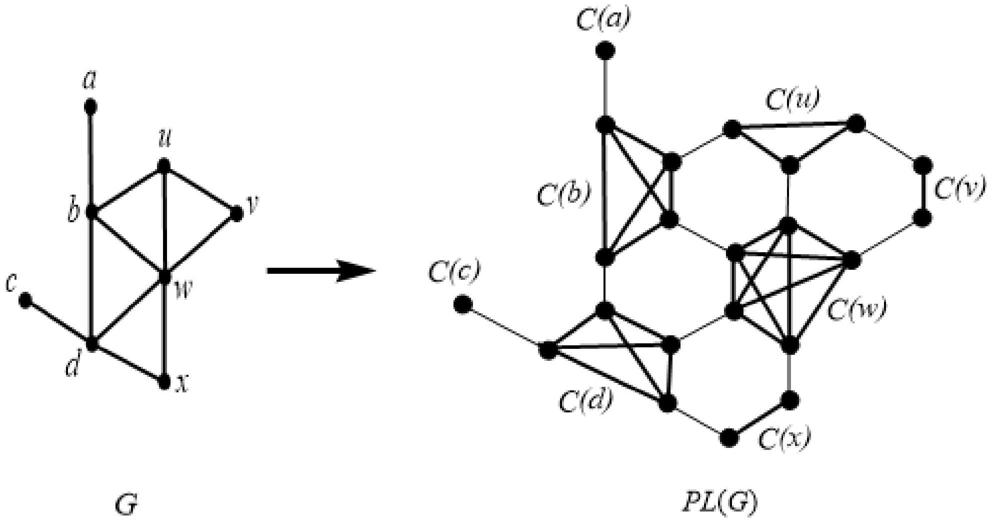

Figure 8.1: Para-line transformation of a graph G.

Observation 8.2.1. *Consider $PL(G)$ symbolize the para-line transformed graph of any graph G, then the edge set $E_{PL(G)}$ can be partitioned as follows:*
The edge set $E_{PL(G)}$ consists of two types of edges: the edges between any two cliques, called external edges, denoted by $E^{ext}_{PL(G)}$ and the edges within cliques, called the internal edges, denoted by $E^{int}_{PL(G)}$ i.e. $E_{PL(G)} = E^{ext}_{PL(G)} \cup E^{int}_{PL(G)}$ where

$$E^{ext}_{PL(G)} = \{e \in E_{PL(G)} : e \text{ joins } C(p) \text{ and } C(q) \text{ for some } p,q \in V_G\}$$
$$\text{and } E^{int}_{PL(G)} = \{e \in E_{PL(G)} : e \in E_{C(p)} \text{ for some } p \in V_G\}.$$

Observation 8.2.2. *There is an edge $e = uv \in E^{ext}_{PL(G)}$ between a vertex $u \in C(p)$ and a vertex $v \in C(q)$ for some vertices $p,q \in V_G$ if and only if there is an edge $f = pq \in E_G$.*

Observation 8.2.3. *Consider the para-line transformed graph $PL(G)$ of any (n,m)-graph G, then*

$$|E^{ext}_{PL(G)}| = |E_G| = m, \qquad |E^{int}_{PL(G)}| = \sum_{p \in V_G} |E_{C(p)}| = \sum_{p \in V_G} \binom{d_G(p)}{2}$$

$$\begin{aligned}
\text{and } |E_{PL(G)}| &= |E^{ext}_{PL(G)}| + |E^{int}_{PL(G)}| \\
&= m + \sum_{p \in V_G} \binom{d_G(p)}{2} \\
&= m + \frac{1}{2}\left[\sum_{p \in V_G} (d_G(p))^2 - \sum_{p \in V_G} (d_G(p))\right] \\
&= m + \frac{1}{2}[M_1(G) - 2m] \\
&= \frac{1}{2} M_1(G).
\end{aligned}$$

Observation 8.2.4. *If $e = uv \in E^{ext}_{PL(G)}$ is an edge between a vertex $u \in V_{C(p)}$ and a vertex $v \in V_{C(q)}$ for some vertices $p, q \in V_G$, then*

$$d_{PL(G)}(u) = d_G(p) \ \text{ and } \ d_{PL(G)}(v) = d_G(q).$$

Observation 8.2.5. *If $e = uv \in E^{int}_{PL(G)}$ is an edge between the vertices $u, v \in V_{C(p)}$ for some vertex $p \in V_G$, then*

$$d_{PL(G)}(u) = d_{PL(G)}(v) = d_G(p).$$

In the following Theorem, we formulate the *ABC* index for the para-line transformed graph of any graph.

Theorem 8.2.2. *Consider the para-line transformed graph $PL(G)$ of any (n, m)-graph G, then*

$$ABC(PL(G)) = ABC(G) + \frac{1}{\sqrt{2}} \sum_{p \in V_G} (d_G(p) - 1)^{3/2}.$$

Proof. From Observation 8.2.1, we can write

$$\begin{aligned}
ABC(PL(G)) &= \sum_{uv \in E^{ext}_{PL(G)}} \sqrt{\frac{d_{PL(G)}(u) + d_{PL(G)}(v) - 2}{d_{PL(G)}(u) d_{PL(G)}(v)}} \\
&\quad + \sum_{uv \in E^{\mathrm{int}}_{PL(G)}} \sqrt{\frac{d_{PL(G)}(u) + d_{PL(G)}(v) - 2}{d_{PL(G)}(u) d_{PL(G)}(v)}}.
\end{aligned}$$

From Observations 8.2.2 and 8.2.4, we have

$$ABC(PL(G)) = \sum_{pq\in E_G} \sqrt{\frac{d_G(p)+d_G(q)-2}{d_G(p)d_G(q)}} + \sum_{uv\in E_{C(p)}} \sum_{p\in V_G} \sqrt{\frac{d_{PL(G)}(u)+d_{PL(G)}(v)-2}{d_{PL(G)}(u)d_{PL(G)}(v)}}.$$

From Observation 8.2.5, we obtain

$$\begin{aligned} ABC(PL(G)) &= ABC(G) + \sum_{uv\in E_{C(p)}} \sum_{p\in V_G} \sqrt{\frac{d_G(p)+d_G(p)-2}{d_G(p)d_G(p)}} \\ &= ABC(G) + \sum_{uv\in E_{C(p)}} \sum_{p\in V_G} \frac{\sqrt{2d_G(p)-2}}{d_G(p)}. \end{aligned}$$

Now from Observation 8.2.3, we have

$$ABC(PL(G)) = ABC(G) + \sum_{p\in V_G} \binom{d_G(p)}{2} \frac{\sqrt{2d_G(p)-2}}{d_G(p)}.$$

After simplification, we get

$$ABC(PL(G)) = ABC(G) + \frac{1}{\sqrt{2}} \sum_{p\in V_G} (d_G(p)-1)^{3/2}.$$

□

In the coming Theorem, we present the expression of GA index for the para-line transformed graph of any graph.

Theorem 8.2.3. *Consider the para-line transformed graph $PL(G)$ of any (n,m)-graph G, then*

$$GA(PL(G)) = GA(G) + \frac{1}{2}M_1(G) - m.$$

Proof. From Observation 8.2.1, we can write

$$GA(PL(G)) = \sum_{uv\in E^{ext}_{PL(G)}} \frac{2\sqrt{d_{PL(G)}(u)d_{PL(G)}(v)}}{d_{PL(G)}(u)+d_{PL(G)}(v)} + \sum_{uv\in E^{int}_{PL(G)}} \frac{2\sqrt{d_{PL(G)}(u)d_{PL(G)}(v)}}{d_{PL(G)}(u)+d_{PL(G)}(v)}.$$

From Observations 8.2.2 and 8.2.4, we obtain

$$GA(PL(G)) = \sum_{pq\in E_G} \frac{2\sqrt{d_G(p)d_G(q)}}{d_G(p)+d_G(q)} + \sum_{uv\in E_{C(p)}} \sum_{p\in V_G} \frac{2\sqrt{d_{PL(G)}(u)d_{PL(G)}(v)}}{d_{PL(G)}(u)+d_{PL(G)}(v)}.$$

From Observation 8.2.5, we have

$$GA(PL(G)) = GA(G) + \sum_{uv\in E_{C(p)}} \sum_{p\in V_G} \frac{2\sqrt{d_G(p)d_G(p)}}{d_G(p)+d_G(p)}.$$

Now from Observation 8.2.3, we have

$$\begin{aligned} GA(PL(G)) &= GA(G) + \sum_{p\in V_G} \binom{d_G(p)}{2} \frac{2\sqrt{(d_G(p))^2}}{2d_G(p)} \\ &= GA(G) + \frac{1}{2}\left[\sum_{p\in V_G} (d_G(p))^2 - \sum_{p\in V_G} d_G(p)\right]. \end{aligned}$$

By using (4.2.1), we get

$$GA(PL(G)) = GA(G) + \frac{1}{2}M_1(G) - m.$$

□

In the coming Theorem, we present the expression of harmonic index for the para-line transformed graph of any graph.

Theorem 8.2.4. *Consider the para-line transformed graph $PL(G)$ of any (n,m)-graph G, then*

$$H(PL(G)) = H(G) + m - \frac{n}{2}. \tag{8.2.1}$$

Proof. From Observation 8.2.1, we can write

$$H(PL(G)) = \sum_{uv\in E^{ext}_{PL(G)}} \frac{2}{d_{PL(G)}(u)+d_{PL(G)}(v)} + \sum_{uv\in E^{int}_{PL(G)}} \frac{2}{d_{PL(G)}(u)+d_{PL(G)}(v)}.$$

From Observation 8.2.2 and 8.2.4, we have

$$H(PL(G)) = \sum_{pq\in E_G} \frac{2}{d_G(p)+d_G(q)} + \sum_{uv\in E_{C(p)}} \sum_{p\in V_G} \frac{2}{d_{PL(G)}(u)+d_{PL(G)}(v)}.$$

From Observation 8.2.5, we obtain

$$H(PL(G)) \;=\; H(G)+\sum_{uv\in E_{C(p)}}\sum_{p\in V_G}\frac{2}{d_G(p)+d_G(p)}.$$

Now from Observation 8.2.3, we have

$$\begin{aligned}
H(PL(G)) &= H(G)+\sum_{p\in V_G}\binom{d_G(p)}{2}\frac{1}{d_G(p)}\\
&= H(G)+\frac{1}{2}\sum_{p\in V_G}(d_G(p)-1)\\
&= H(G)+\frac{1}{2}\left[\sum_{p\in V_G}d_G(p)-\sum_{p\in V_G}(1)\right]\\
&= H(G)+\frac{1}{2}\left[\sum_{p\in V_G}d_G(p)-\sum_{p\in V_G}(1)\right].
\end{aligned}$$

By using (4.2.1), we get

$$H(PL(G)) \;=\; H(G)+m-\frac{n}{2}.$$

□

In the coming Theorem, we present the expression of *AZI* index for the para-line transformed graph of any graph.

Theorem 8.2.5. *Consider the para-line transformed graph $PL(G)$ of any (n,m)-graph G, then*

$$AZI(PL(G))=AZI(G)+\frac{1}{16}\sum_{p\in V_G}\frac{(d_G(p))^7}{(d_G(p)-1)^2}.$$

Proof. From Observation 8.2.1, we can write

$$\begin{aligned}
AZI(PL(G)) &= \sum_{uv\in E^{ext}_{PL(G)}}\left(\frac{d_{PL(G)}(u)d_{PL(G)}(v)}{d_{PL(G)}(u)+d_{PL(G)}(v)-2}\right)^3\\
&\quad+\sum_{uv\in E^{int}_{PL(G)}}\left(\frac{d_{PL(G)}(u)d_{PL(G)}(v)}{d_{PL(G)}(u)+d_{PL(G)}(v)-2}\right)^3.
\end{aligned}$$

From Observations 8.2.2 and 8.2.4, we have

$$\begin{aligned} AZI(PL(G)) &= \sum_{pq\in E_G}\left(\frac{d_G(p)d_G(q)}{d_G(p)+d_G(q)-2}\right)^3 \\ &\quad + \sum_{uv\in E_{C(p)}}\sum_{p\in V_G}\left(\frac{d_{PL(G)}(u)d_{PL(G)}(v)}{d_{PL(G)}(u)+d_{PL(G)}(v)-2}\right)^3. \end{aligned}$$

From Observation 8.2.5, we obtain

$$AZI(PL(G)) = AZI(G)+\sum_{uv\in E_{C(p)}}\sum_{p\in V_G}\left(\frac{d_G(p)d_G(p)}{d_G(p)+d_G(p)-2}\right)^3.$$

Now from Observation 8.2.3, we have

$$AZI(PL(G)) = AZI(G)+\sum_{p\in V_G}\binom{d_G(p)}{2}\left(\frac{(d_G(p))^2}{2d_G(p)-2}\right)^3.$$

After simplification, we get

$$AZI(PL(G)) = AZI(G)+\frac{1}{16}\sum_{p\in V_G}\frac{(d_G(p))^7}{(d_G(p)-1)^2}.$$

□

In the coming Theorem, we present the expression of *SDD* index for the para-line transformed graph of any graph.

Theorem 8.2.6. *Consider the para-line transformed graph $PL(G)$ of any (n,m)-graph G, then*

$$SDD(PL(G)) = SDD(G)+M_1(G)-2m.$$

Proof. From Observation 8.2.1, we can write

$$\begin{aligned} SDD(PL(G)) &= \sum_{uv\in E^{ext}_{PL(G)}}\left(\frac{d_{PL(G)}(u)}{d_{PL(G)}(v)}+\frac{d_{PL(G)}(v)}{d_{PL(G)}(u)}\right) \\ &\quad + \sum_{uv\in E^{int}_{PL(G)}}\left(\frac{d_{PL(G)}(u)}{d_{PL(G)}(v)}+\frac{d_{PL(G)}(u)}{d_{PL(G)}(v)}\right). \end{aligned}$$

From Observations 8.2.2 and 8.2.4, we obtain

$$SDD(PL(G)) = \sum_{pq\in E_G}\left(\frac{d_G(p)}{d_G(q)}+\frac{d_G(q)}{d_G(p)}\right)+\sum_{uv\in E_{C(p)}}\sum_{p\in V_G}\left(\frac{d_{PL(G)}(u)}{d_{PL(G)}(v)}+\frac{d_{PL(G)}(v)}{d_{PL(G)}(u)}\right).$$

From Observation 8.2.5, we have

$$SDD(PL(G)) = SDD(G)+\sum_{uv\in E_{C(p)}}\sum_{p\in V_G}\left(\frac{d_G(p)}{d_G(p)}+\frac{d_G(p)}{d_G(p)}\right).$$

Now from Observation 8.2.3, we have

$$\begin{aligned} SDD(PL(G)) &= SDD(G)+2\sum_{p\in V_G}\binom{d_G(p)}{2} \\ &= SDD(G)+\sum_{p\in V_G}\left[d_G(p)^2-d_G(p)\right]. \end{aligned}$$

By using (4.2.1), we get

$$SDD(PL(G)) = SDD(G)+M_1(G)-2m.$$

□

In the coming Theorem, we present the expression of *ISI* index for the para-line transformed graph of any graph.

Theorem 8.2.7. *Consider $PL(G)$ symbolize the para-line transformed graph of any (n,m)-graph G, then*

$$ISI(PL(G)) = ISI(G)+\frac{1}{4}\left[F(G)-M_1(G)\right].$$

Proof. From Observation 8.2.1, we can write

$$\begin{aligned} ISI(PL(G)) &= \sum_{uv\in E^{ext}_{PL(G)}}\left(\frac{d_{PL(G)}(u)d_{PL(G)}(v)}{d_{PL(G)}(u)+d_{PL(G)}(v)}\right) \\ &\quad + \sum_{uv\in E^{int}_{PL(G)}}\left(\frac{d_{PL(G)}(u)d_{PL(G)}(v)}{d_{PL(G)}(u)+d_{PL(G)}(v)}\right). \end{aligned}$$

From Observations 8.2.2 and 8.2.4, we obtain

$$ISI(PL(G)) = \sum_{pq\in E_G}\left(\frac{d_G(P)d_G(q)}{d_G(p)+d_G(q)}\right) + \sum_{uv\in E_{C(p)}}\sum_{p\in V_G}\left(\frac{d_{PL(G)}(u)d_{PL(G)}(v)}{d_{PL(G)}(u)+d_{PL(G)}(v)}\right).$$

From Observation 8.2.5, we have

$$ISI(PL(G)) = ISI(G) + \sum_{uv\in E_{C(p)}}\sum_{p\in V_G}\left(\frac{d_G(p)d_G(p)}{d_G(p)+d_G(p)}\right).$$

Now from Observation 8.2.3, we have

$$\begin{aligned} ISI(PL(G)) &= ISI(G) + \frac{1}{2}\sum_{p\in V_G}\binom{d_G(p)}{2} \\ &= ISI(G) + \frac{1}{4}\sum_{p\in V_G}\left[d_G(p)^3 - d_G(p)^2\right] \\ &= ISI(G) + \frac{1}{4}\left[F(G) - M_1(G)\right]. \end{aligned}$$

□

8.2.2 Reformulated Zagreb Indices of Para-line Transformed Graph

In this section, we obtain the expressions of first reformulated Zagreb and second reformulated Zagreb indices for the para-line transformed graph of any graph by deriving a relation between degree of each edge of the para-line transformed graph and degrees of some vertices of the parent graph.

By using the edge partition of $E_{PL(G)}$ defined in Observation 8.2.1, we have the following Lemma.

Lemma 8.2.8. *Consider the para-line transformed graph $PL(G)$ of any (n,m)-graph G and $e = uv \in E_{PL(G)}$ be any edge, then*
(a) If $e = uv \in E^{ext}_{PL(G)}$, then there is some edge $f = pq \in E_G$ such that

$$d_{PL(G)}(e) = d_G(f) = d_G(p) + d_G(q) - 2.$$

(b) If $e = uv \in E^{int}_{PL(G)}$*, then there is some vertex* $p \in V_G$ *such that*

$$d_{PL(G)}(e) = 2d_G(p) - 2.$$

Proof. Let $e = uv \in E_{PL(G)}$ be an edge. If $e = uv \in E^{ext}_{PL(G)}$, then from Observation 8.2.1, $u \in V_{C(p)}$ and $v \in V_{C(q)}$ for some vertices $p, q \in V_G$ and from Observation 8.2.2 there is some edge $f = pq \in E_G$. Moreover from Observation 8.2.4, we have $d_{PL(G)}(u) = d_G(p)$ and $d_{PL(G)}(v) = d_G(q)$. So we obtain

$$\begin{aligned} d_{PL(G)}(e) &= d_{PL(G)}(u) + d_{PL(G)}(v) - 2 \\ &= d_G(p) + d_G(q) - 2 = d_G(f). \end{aligned}$$

Also, if $e = uv \in E^{int}_{PL(G)}$, then from Observation 8.2.5, $e = uv \in E_{C(p)}$ for some vertex $p \in V_G$ and $d_{PL(G)}(u) = d_G(p)$. Thus we have

$$\begin{aligned} d_{PL(G)}(e) &= d_{PL(G)}(u) + d_{PL(G)}(v) - 2 \\ &= d_G(p) + d_G(p) - 2 = 2d_G(p) - 2. \end{aligned}$$

□

From the edge partition of $PL(G)$, defined in Observation 8.2.1, we can extract the following Observations.

Observation 8.2.6. *If* $e = uv \in E^{ext}_{PL(G)}$ *such that* $u \in V_{C(p)}$ *and* $v \in V_{C(q)}$ *for some* $p, q \in V_G$*, then e is adjacent to* $d_G(p) - 1$ *edges* $g = uz \in E_{C(p)} \subseteq E^{int}_{PL(G)}$ *and* $d_G(q) - 1$ *edges* $h = vw \in E_{C(q)} \subseteq E^{int}_{PL(G)}$.

Observation 8.2.7. *For each vertex* $p \in V_G$*, the number of adjacent pairs of edges of the corresponding clique* $C(p)$ *in* $PL(G)$ *are*

$$\frac{d_G(p)\,[d_G(p) - 1]\,[d_G(p) - 2]}{2}.$$

Theorem 8.2.9. *Consider* $PL(G)$ *symbolize the para-line transformed graph of any*

(n,m)*-graph G, then*

$$EM_1(PL(G)) = EM_1(G) + 2\left[M_1^4(G) - 3F(G) + 3M_1(G) - 2m\right].$$

Proof. From Observation 8.2.1, we can write

$$EM_1(PL(G)) = \sum_{e \in E^{ext}_{PL(G)}} d_{PL(G)}(e)^2 + \sum_{e \in E^{int}_{PL(G)}} d_{PL(G)}(e)^2.$$

By using Lemma 8.2.8 and from Observation 8.2.2, we have

$$EM_1(PL(G)) = \sum_{f \in E_G} d_G(f)^2 + \sum_{e \in E_{C(p)}} \sum_{p \in V_G} (2d_G(p) - 2)^2.$$

From Observation 8.2.3, we obtain

$$\begin{aligned} EM_1(PL(G)) &= EM_1(G) + \sum_{p \in V_G} \binom{d_G(p)}{2} (2d_G(p) - 2)^2 \\ &= EM_1(G) + 2\sum_{p \in V_G} d_G(p)(d_G(p) - 1)^3 \\ &= EM_1(G) + 2\sum_{p \in V_G} [d_G(p)^4 - 3d_G(p)^3 + 3d_G(p)^2 - d_G(p)] \\ &= EM_1(G) + 2\left[M_1^4(G) - 3F(G) + 3M_1(G) - 2m\right]. \end{aligned}$$

□

Theorem 8.2.10. *Consider the para-line transformed graph* $PL(G)$ *of any* (n,m)*-graph G, then*

$$EM_2(PL(G)) = 2\left[M_1^5(G) - 4M_1^4(G) + 5F(G) - M_1(G) - 4M_2(G) + ReZ_3(G)\right].$$

Proof. By using the edge partition of $PL(G)$ given in Observation 8.2.1, we can write

$$EM_2(PL(G)) = \sum_{\substack{e \sim f \\ e \in E^{ext}_{PL(G)}, \\ f \in E^{int}_{PL(G)}}} d_{PL(G)}(e) d_{PL(G)}(f) + \sum_{\substack{e \sim f \\ e,f \in E^{int}_{PL(G)}}} d_{PL(G)}(e) d_{PL(G)}(f).$$

From Observation 8.2.6, we have

$$\begin{aligned}
= & \sum_{\substack{e\sim g\\ e\in E^{ext}_{PL(G)},\\ g\in E_{C(p)}}} \sum_{p\in V_G} d_{PL(G)}(e)d_{PL(G)}(g) + \sum_{\substack{e\sim h\\ e\in E^{ext}_{PL(G)},\\ h\in E_{C(q)}}} \sum_{q\in V_G} d_{PL(G)}(e)d_{PL(G)}(h)\\
& + \sum_{\substack{e\sim f\\ e,f\in E_{C(p)}}} \sum_{p\in V_G} d_{PL(G)}(e)d_{PL(G)}(f).
\end{aligned}$$

By using Lemma 8.2.8 and from Observations 8.2.6-8.2.7, we obtain

$$\begin{aligned}
= & \sum_{pq\in E_G} [(d_G(p)-1)(d_G(p)+d_G(q)-2)(2d_G(p)-2)\\
& +(d_G(q)-1)(d_G(p)+d_G(q)-2)(2d_G(q)-2)]\\
& + \sum_{p\in V_G} \frac{d_G(p)(d_G(p)-1)(d_G(p)-2)}{2}(2d_G(p)-2)^2\\
= & \; 2\sum_{pq\in E_G} \left[(d_G(p)^3+d_G(q)^3)-4(d_G(p)^2+d_G(q)^2)\right]\\
& +2\sum_{pq\in E_G} [6(d_G(p)+d_G(q))-4d_G(p)d_G(q)-4]\\
& +2\sum_{pq\in E_G} d_G(p)d_G(q)\,[d_G(p)+d_G(q)]\\
& +2\sum_{p\in V_G} \left[d_G(p)^5-5d_G(p)^4+9d_G(p)^3-7d_G(p)^2+2d_G(p)\right]\\
= & \; 2\left[M_1^4(G)-4F(G)+6M_1(G)-4M_2(G)-4m\right]+2ReZ_3(G)\\
& +2\left[M_1^5(G)-5M_1^4(G)+9F(G)-7M_1(G)+4m\right]\\
= & \; 2\left[M_1^5(G)-4M_1^4(G)+5F(G)-M_1(G)-4M_2(G)+ReZ_3(G)\right].
\end{aligned}$$

□

8.2.3 Leap Zagreb Indices of Para-line Transformed Graph

In this section, we obtain the expressions of first leap Zagreb, second leap Zagreb and third leap Zagreb indices for the para-line transformed graph of any graph by deriving a relation between 2-distance degree of each vertex of the para-line transformed graph and degrees of some vertices of the parent graph.

Lemma 8.2.11. *Consider the para-line transformed graph $PL(G)$ of any graph G and $u \in V_{PL(G)}$ be any vertex such that $u \in V_{C(p)}$ for some $p \in V_G$, then there exits a vertex $v \in V_{C(q)}$ for some $q \in V_G$ such that $uv \in \overset{ext}{E}_{PL(G)}$ i.e. $v \in N_G(p)$ and*

$$d_2(u/PL(G)) = d_2(v/PL(G)) = d_G(p) + d_G(q) - 2.$$

Proof. Let $u \in V_{PL(G)}$, then there exists a vertex $p \in V_G$ such that $u \in V_{C(p)}$ and $d_{PL(G)}(u) = d_{C(p)}(u) = d_G(p)$. Also, clearly u is adjacent to $d_G(p) - 1$ vertices of $C(p)$ therefore there must be some vertex $v \in V_{C(q)}$ for some $q \in V_G$ such that $uv \in \overset{ext}{E}_{PL(G)}$ and we have the 2-distance neighborhood set of u as follows:

$$\begin{aligned} N_2(u/PL(G)) &= \{w \in V_{PL(G)} : d(u,w) = 2\} \\ &= X \cup Z \end{aligned}$$

where $X = \{x \in V_{PL(G)} : xy \in E_{PL(G)} \ \forall\, y \in V_{C(p)} - \{u\}\}$ and $Z = \{z \in V_{C(q)} : vz \in E_{C(q)}\}$. Then clearly $|X| = d_G(p) - 1$ and $|Z| = d_G(q) - 1$. Thus we obtain

$$\begin{aligned} d_2(u/PL(G)) &= |N_2(u/PL(G))| \\ &= |X| + |Z| \\ &= d_G(p) + d_G(q) - 2. \end{aligned}$$

Similarly, we get $d_2(v/PL(G)) = d_G(p) + d_G(q) - 2$. □

From Lemma 8.2.11, we can extract the following observation.

Observation 8.2.8. *If $e = uv \in \overset{int}{E}_{PL(G)}$ and $u, v \in V_{C(p)}$ for some $p \in V_G$, then there are some vertices $s, t \in N_G(p)$ such that*

$$d_2(u/PL(G)) = d_G(p) + d_G(s) - 2 \ \ \text{and} \ \ d_2(v/PL(G)) = d_G(p) + d_G(t) - 2.$$

Observation 8.2.9. *For any non-negative integer k, we have*

$$\sum_{p \in V_G} \sum_{q \in N_G(p)} d_G(q)^k = \sum_{p \in V_G} \sum_{q \in N_G(p)} d_G(p)^k = \sum_{p \in V_G} d_G(p)^{k+1}.$$

Observation 8.2.10. *For any function $f(d_G(p))$, we have*

$$\sum_{p\in V_G}\sum_{s,t\in N_G(p)} f(d_G(p)) = \sum_{p\in V_G}\binom{d_G(p)}{2} f(d_G(p)).$$

Observation 8.2.11. *From the definition of $M_2(G)$, we have*

$$M_2(G) = \frac{1}{2}\sum_{p\in V_G}\sum_{q\in N_G(p)} d_G(p)d_G(q).$$

Theorem 8.2.12. *Consider the para-line transformed graph $PL(G)$ of any (n,m)-graph G, then*

$$LM_1(PL(G)) = 4M_2(G) - 8M_1(G) + 2F(G) + 8m.$$

Proof. Let $u \in V_{PL(G)}$, then there exists some vertex $p \in V_G$ such that $u \in V_{C(p)}$ and we have

$$LM_1(PL(G)) = \sum_{u\in V_{C(p)}}\sum_{p\in V_G} d_2(u/PL(G))^2.$$

By using Lemma 8.2.11, we obtain

$$\begin{aligned}
LM_1(PL(G)) &= \sum_{p\in V_G}\sum_{q\in N_G(p)} (d_G(p)+d_G(q)-2)^2 \\
&= \sum_{p\in V_G}\sum_{q\in N_G(p)} \left[d_G^2(p) - 4d_G(p) + 4\right] + \sum_{p\in V_G}\sum_{q\in N_G(p)} \left[(d_G^2(q)) - 4d_G(q)\right] \\
&\quad +2\sum_{p\in V_G}\sum_{q\in N_G(p)} d_G(p)d_G(q).
\end{aligned}$$

From Observations 8.2.9 and 8.2.11, we get

$$\begin{aligned}
LM_1(PL(G)) &= \sum_{p\in V_G}\left[d_G(p)^3 - 4d_G(p)^2 + 4d_G(p)\right] + \sum_{p\in V_G}\left[(d_G(p)^3) - 4d_G(p)^2\right] \\
&\quad +4M_2(G) \\
&= F(G) - 4M_1(G) + 8m + F(G) - 4M_1(G) + 4M_2(G) \\
&= 4M_2(G) - 8M_1(G) + 2F(G) + 8m.
\end{aligned}$$

$\square$

Theorem 8.2.13. *Consider $PL(G)$ symbolize the para-line transformed graph of any (n,m)-graph G, then*

$$\begin{aligned} LM_2(PL(G)) &= 2M_2(G)+\frac{1}{2}M_1^4(G)-\frac{3}{2}F(G) \\ &\quad+\sum_{\substack{p\in V_G\\ s,t\in N_G(p)}}\left[(d_G(p)-2)(d_G(s)+d_G(t))+d_G(s)d_G(t)\right]. \end{aligned}$$

Proof. From the Observation 8.2.2, we can write

$$LM_2(PL(G))=\sum_{uv\in E^{ext}_{PL(G)}} d_2(u/PL(G))d_2(v/PL(G))+\sum_{uv\in E^{int}_{PL(G)}} d_2(u/PL(G))d_2(v/PL(G)).$$

By using Lemma 8.2.11 and Observation 8.2.8, we obtain

$$\begin{aligned} &= \sum_{pq\in E_G}(d_G(p)+d_G(q)-2)^2+\sum_{p\in V_G}\sum_{s,t\in N_G(p)}[d_G(p)+d_G(s)-2]\,[d_G(p)+d_G(t)-2] \\ &= \sum_{pq\in E_G}[d_G(p)^2+d_G(q)^2]-4\sum_{pq\in E_G}[d_G(p)+d_G(q)]+2\sum_{pq\in E_G}[d_G(p)d_G(q)+2] \\ &\quad+\sum_{p\in V_G}\sum_{s,t\in N_G(p)}[d_G(p)^2-4d_G(p)+4]+\sum_{p\in V_G}\sum_{s,t\in N_G(p)}d_G(p)\,[d_G(s)+d_G(t)] \\ &\quad-2\sum_{p\in V_G}\sum_{s,t\in N_G(p)}[d_G(s)+d_G(t)]+\sum_{p\in V_G}\sum_{s,t\in N_G(p)}d_G(s)d_G(t). \end{aligned}$$

From Observation 8.2.10, we have

$$\begin{aligned} &= F(G)-4M_1(G)+2M_2(G)+4m+\sum_{p\in V_G}\binom{d_G(p)}{2}\left[d_G(p)^2-4d_G(p)+4\right] \\ &\quad+\sum_{p\in V_G}\sum_{s,t\in N_G(p)}[d_G(p)-2][d_G(s)+d_G(t)]+\sum_{p\in V_G}\sum_{s,t\in N_G(p)}d_G(s)d_G(t) \\ &= F(G)-4M_1(G)+2M_2(G)+4m+\frac{1}{2}\sum_{p\in V_G}\left[d_G(p)^4-d_G(p)^3\right] \\ &\quad-2\sum_{p\in V_G}\left[d_G(p)^3-d_G(p)^2\right]+2\sum_{p\in V_G}\left[d_G(p)^2-d_G(p)\right] \\ &\quad+\sum_{p\in V_G}\sum_{s,t\in N_G(p)}[d_G(p)-2]\,[d_G(s)+d_G(t)]+\sum_{p\in V_G}\sum_{s,t\in N_G(p)}d_G(s)d_G(t) \\ &= F(G)-4M_1(G)+2M_2(G)+4m+\frac{1}{2}M_1^4(G)-\frac{1}{2}F(G)-2F(G)+2M_1(G) \end{aligned}$$

$$
\begin{aligned}
& +2M_1(G)-4m+\sum_{p\in V_G}\sum_{s,t\in N_G(p)}[d_G(p)-2][d_G(s)+d_G(t)] \\
& +\sum_{p\in V_G}\sum_{s,t\in N_G(p)} d_G(s)d_G(t) \\
= \; & 2M_2(G)+\frac{1}{2}M_1^4(G)-\frac{3}{2}F(G) \\
& +\sum_{\substack{p\in V_G \\ s,t\in N_G(p)}}[(d_G(p)-2)(d_G(s)+d_G(t))+d_G(s)d_G(t)].
\end{aligned}
$$

□

Theorem 8.2.14. *Consider the para-line transformed graph $PL(G)$ of any (n,m)-graph G, then*

$$LM_3(PL(G)) = F(G)-2M_1(G)+2M_2(G).$$

Proof. Let $u \in V_{PL(G)}$, then there exists some vertex $p \in V_G$ such that $u \in V_{C(p)}$ and we have

$$LM_3(PL(G)) = \sum_{u\in V_{C(p)}}\sum_{p\in V_{(G)}} d_{C(p)}(u)d_2(u/PL(G)).$$

By using Lemma 8.2.11, we obtain

$$
\begin{aligned}
LM_3(PL(G)) &= \sum_{p\in V_G}\sum_{q\in N_G(p)} d_G(p)[d_G(p)+d_G(q)-2] \\
&= \sum_{p\in V_G}\sum_{q\in N_G(p)}[d_G(p)^2-2d_G(p)]+\sum_{p\in V_G}\sum_{q\in N_G(p)} d_G(p)d_G(q).
\end{aligned}
$$

From Observations 8.2.9 and 8.2.11, we have

$$
\begin{aligned}
LM_3(PL(G)) &= \sum_{p\in V_G}[d_G(p)^3-2d_G(p)^2]+2M_2(G) \\
&= F(G)-2M_1(G)+2M_2(G).
\end{aligned}
$$

□

8.2.4 ABC_4, GA_5 and ABC_5 Indices of Para-line Transformed Graph

In this section, the expressions of Consider $PL(G)$ symbolize the para-line transformed graph of any (n,m)-graph G, "ABC_4 and GA_5" indices for the Para-line transformed graph of any graph are achieved.

Lemma 8.2.15. *Consider the para-line transformed graph $PL(G)$ of any graph G, then for any edge $e = uv \in E^{ext}_{PL(G)}$ there exist some vertices $p, q \in V_G$ such that*

$$\begin{aligned}
(a) \quad & \delta_{PL(G)}(u) = d_G(p)\,[d_G(p) - 1] + d_G(q) \\
& \text{and } \delta_{PL(G)}(v) = d_G(q)\,[d_G(q) - 1] + d_G(p) \\
(b) \quad & M_{PL(G)}(u) = d_G(q) \cdot (d_G(p))^{d_G(p)-1} \\
& \text{and } M_{PL(G)}(v) = d_G(p) \cdot (d_G(q))^{d_G(q)-1}.
\end{aligned}$$

Proof. Let $e = uv \in E^{ext}_{PL(G)}$ be any edge, then from Observation 8.2.1 there exist some vertices $p, q \in V_G$ such that $u \in V_{C(p)}$ and $v \in V_{C(q)}$. Thus, we have the neighborhood set of vertex u as follows:

$$\begin{aligned}
N_{PL(G)}(u) &= \{w \in V_{PL(G)} : uw \in E_{PL(G)}\} \\
&= \{z \in V_{C(p)} : uz \in E_{C(p)}\} \cup \{v\}
\end{aligned}$$

and

$$\begin{aligned}
\delta_{PL(G)}(u) &= \sum_{uw \in E_{PL(G)}} d_{PL(G)}(w) \\
&= \sum_{uz \in E_{C(p)}} d_{C(p)}(z) + d_{C(q)}(v) \\
&= d_{C(p)}(z)\left[d_{C(p)}(z) - 1\right] + d_{C(q)}(v) \\
&= d_G(p)\,[d_G(p) - 1] + d_G(q).
\end{aligned}$$

Similarly, we have

$$\delta_{PL(G)}(v) = d_G(q)\,[d_G(q) - 1] + d_G(p).$$

Also,

$$\begin{aligned} M_{PL(G)}(u) &= \prod_{w\in N_{PL(G)}(u)} d_{PL(G)}(w) \\ &= \prod_{uw\in E_{PL(G)}} d_{PL(G)}(w) \\ &= \prod_{uz\in E_{C(p)}} d_{C(p)}(z)\cdot d_{C(q)}(v) \\ &= (d_{C(p)}(z))^{d_{C(p)}(z)-1}\cdot d_{C(q)}(v) \\ &= d_G(q)\cdot (d_G(p))^{d_G(p)-1}. \end{aligned}$$

Similarly, we obtain

$$M_{PL(G)}(v) = d_G(p)\cdot (d_G(q))^{d_G(q)-1}.$$

□

Lemma 8.2.16. *Consider the para-line transformed graph $PL(G)$ of any graph G, then for any edge $e = uv \in E^{int}_{PL(G)}$ there exist a vertex $p \in V_G$ and for vertex p there exist vertices $s,t \in N_G(p)$ such that*

$$\begin{aligned} &(a)\quad \delta_{PL(G)}(u) = d_G(p)\,[d_G(p)-1]+d_G(s) \\ &\qquad \textit{and } \delta_{PL(G)}(v) = d_G(p)\,[d_G(p)-1]+d_G(t) \\ &(b)\quad M_{PL(G)}(u) = d_G(s)\cdot (d_G(p))^{d_G(p)-1} \\ &\qquad \textit{and } M_{PL(G)}(v) = d_G(t)\cdot (d_G(p))^{d_G(p)-1}. \end{aligned}$$

Proof. Let $e = uv \in E^{int}_{PL(G)}$ be any edge, then from Observation 8.2.2 there exist a vertex $p \in V_G$ such that $u,v \in V_{C(p)}$ and $d_{C(p)}(u) = d_{C(p)}(v) = d_G(p)$. Also, clearly u is adjacent to all $d_G(p)-1$ vertices of $C(p)$. Therefore there exist a vertex $x \in V_{C(s)}$ that is adjacent to u for some vertex $s \in N_G(p)$ and we have the neighborhood set of vertex u as follows:

$$\begin{aligned} N_{PL(G)}(u) &= \{w \in V_{PL(G)} : uw \in E_{PL(G)}\} \\ &= \{z \in V_{C(p)} : uz \in E_{C(p)}\} \cup \{x\} \end{aligned}$$

and

$$\begin{aligned}
\delta_{PL(G)}(u) &= \sum_{uw \in E_{PL(G)}} d_{PL(G)}(w) \\
&= \sum_{uz \in E_{C(p)}} d_{C(p)}(z) + d_{C(s)}(x) \\
&= d_{C(p)}(z)\left[d_{C(p)}(z) - 1\right] + d_{C(s)}(x) \\
&= d_G(p)\left[d_G(p) - 1\right] + d_G(s).
\end{aligned}$$

Similarly, for vertex $p \in V_G$ there also exist a vertex $t \in N_G(p)$ such that

$$\delta_{PL(G)}(v) = d_G(p)\left[d_G(p) - 1\right] + d_G(t).$$

Also,

$$\begin{aligned}
M_{PL(G)}(u) &= \prod_{w \in N_{PL(G)}(u)} d_{PL(G)}(w) \\
&= \prod_{uw \in E_{PL(G)}} d_{PL(G)}(w) \\
&= \prod_{uz \in E_{C(p)}} d_{C(p)}(z) \cdot d_{C(s)}(x) \\
&= (d_{C(p)}(z))^{d_{C(p)}(z)-1} \cdot d_G(s) \\
&= d_G(s) \cdot (d_G(p))^{d_G(p)-1}.
\end{aligned}$$

Similarly, for some vertex $t \in N_G(p)$ we obtain

$$M_{PL(G)}(v) = d_G(t) \cdot (d_G(p))^{d_G(p)-1}.$$

□

In the coming Theorem, we present the expression of ABC_4 index for the para-line transformed graph of any graph.

Theorem 8.2.17. *Consider $PL(G)$ symbolize the para-line transformed graph of any*

(n,m)-graph G, then

$$ABC_4(PL(G)) = \sum_{pq\in E_G}\sqrt{\frac{(d_G(p))^2+(d_G(q))^2-2}{[(d_G(p))^2-d_G(p)+d_G(q)]\,[(d_G(q))^2-d_G(q)+d_G(p)]}}$$
$$+\sum_{\substack{p\in V_G\\ s,t\in N_G(p)}}\sqrt{\frac{2d_G(p)(d_G(p)-1)+d_G(s)+d_G(t)-2}{[(d_G(p))^2-d_G(p)+d_G(s)]\,[(d_G(p))^2-d_G(p)+d_G(t)]}}.$$

Proof. From Observation 8.2.1, we can write

$$\begin{aligned} ABC_4(PL(G)) &= \sum_{uv\in E^{ext}_{PL(G)}}\sqrt{\frac{\delta_{PL(G)}(u)+\delta_{PL(G)}(v)-2}{\delta_{PL(G)}(u)\cdot\delta_{PL(G)}(v)}} \\ &+ \sum_{uv\in E^{int}_{PL(G)}}\sqrt{\frac{\delta_{PL(G)}(u)+\delta_{PL(G)}(v)-2}{\delta_{PL(G)}(u)\cdot\delta_{PL(G)}(v)}}. \end{aligned}$$

By using Lemma 8.2.15 (a), Lemma 8.2.16 (a) and Observation 8.2.2, we obtain

$$= \sum_{pq\in E_G}\sqrt{\frac{d_G(p)(d_G(p)-1)+d_G(q)+d_G(q)(d_G(q)-1)+d_G(p)-2}{[d_G(p)(d_G(p)-1)+d_G(q)]\,[d_G(q)(d_G(q)-1)+d_G(p)]}}$$
$$+ \sum_{p\in V_G}\sum_{s,t\in N_G(p)}\sqrt{\frac{d_G(p)(d_G(p)-1)+d_G(s)+d_G(p)(d_G(p)-1)+d_G(t)-2}{[d_G(p)(d_G(p)-1)+d_G(s)]\,[d_G(p)(d_G(p)-1)+d_G(t)]}}.$$

After simplification, we have

$$\begin{aligned} ABC_4(PL(G)) &= \sum_{pq\in E_G}\sqrt{\frac{(d_G(p))^2+(d_G(q))^2-2}{[(d_G(p))^2-d_G(p)+d_G(q)]\,[(d_G(q))^2-d_G(q)+d_G(p)]}} \\ &+ \sum_{\substack{p\in V_G\\ s,t\in N_G(p)}}\sqrt{\frac{2d_G(p)(d_G(p)-1)+d_G(s)+d_G(t)-2}{[(d_G(p))^2-d_G(p)+d_G(s)]\,[(d_G(p))^2-d_G(p)+d_G(t)]}}. \end{aligned}$$

□

In the coming Theorem, we present the expression of GA_5 index for the para-line transformed graph of any graph.

Theorem 8.2.18. *Consider the para-line transformed graph $PL(G)$ of any (n,m)-graph G, then*

$$GA_5(PL(G)) = \sum_{pq\in E_G} \frac{2\sqrt{[(d_G(p))^2 - d_G(p) + d_G(q)][(d_G(q))^2 - d_G(q) + d_G(p)]}}{(d_G(p))^2 + (d_G(q))^2} + \sum_{\substack{p\in V_G \\ s,t\in N_G(p)}} \frac{2\sqrt{[(d_G(p))^2 - d_G(p) + d_G(s)][(d_G(q))^2 - d_G(q) + d_G(t)]}}{2d_G(p)(d_G(p)-1) + d_G(s) + d_G(t)}.$$

Proof. From Observation 8.2.1, we can write

$$GA_5(PL(G)) = \sum_{uv\in E^{ext}_{PL(G)}} \frac{2\sqrt{\delta_{PL(G)}(u)\cdot\delta_{PL(G)}(v)}}{\delta_{PL(G)}(u)+\delta_{PL(G)}(v)} + \sum_{uv\in E^{int}_{PL(G)}} \frac{2\sqrt{\delta_{PL(G)}(u)\cdot\delta_{PL(G)}(v)}}{\delta_{PL(G)}(u)+\delta_{PL(G)}(v)}.$$

By using Lemma 8.2.15 (a), Lemma 8.2.16 (a) and Observation 8.2.2, we obtain

$$\begin{aligned} &= \sum_{pq\in E_G} \frac{2\sqrt{[d_G(p)(d_G(p)-1)+d_G(q)][d_G(q)(d_G(q)-1)+d_G(p)]}}{d_G(p)(d_G(p)-1)+d_G(q)+d_G(q)(d_G(q)-1)+d_G(p)} \\ &+ \sum_{p\in V_G}\sum_{s,t\in N_G(p)} \frac{2\sqrt{[d_G(p)(d_G(p)-1)+d_G(s)][d_G(p)(d_G(p)-1)+d_G(t)]}}{d_G(p)(d_G(p)-1)+d_G(s)+d_G(p)(d_G(p)-1)+d_G(t)}. \end{aligned}$$

After simplification, we get

$$\begin{aligned} GA_5(PL(G)) &= \sum_{pq\in E_G} \frac{2\sqrt{[(d_G(p))^2 - d_G(p) + d_G(q)][(d_G(q))^2 - d_G(q) + d_G(p)]}}{(d_G(p))^2 + (d_G(q))^2} \\ &+ \sum_{\substack{p\in V_G \\ s,t\in N_G(p)}} \frac{2\sqrt{[(d_G(p))^2 - d_G(p) + d_G(s)][(d_G(p))^2 - d_G(p) + d_G(t)]}}{2d_G(p)(d_G(p)-1) + d_G(s) + d_G(t)}. \end{aligned}$$

□

In the coming Theorem, we present the expression of ABC_5 index for the para-line transformed graph of any graph.

Theorem 8.2.19. *Consider the para-line transformed graph $PL(G)$ of any (n,m)-graph*

G, then

$$ABC_5(PL(G)) = \sum_{pq \in E_G} \sqrt{\frac{d_G(q)\cdot(d_G(p))^{d_G(p)-1} + d_G(p)\cdot(d_G(q))^{d_G(q)-1} - 2}{(d_G(p))^{d_G(p)}\cdot(d_G(q))^{d_G(q)}}} + \sum_{\substack{p \in V_G \\ s,t \in N_G(p)}} \sqrt{\frac{(d_G(s)+d_G(t))\cdot(d_G(p))^{d_G(p)-1} - 2}{d_G(s)\cdot d_G(t)\cdot(d_G(p))^{2d_G(p)-2}}}.$$

Proof. From Observation 8.2.1, we can write

$$\begin{aligned} ABC_5(PL(G)) &= \sum_{uv \in E^{ext}_{PL(G)}} \sqrt{\frac{M_{PL(G)}(u)+M_{PL(G)}(v)-2}{M_{PL(G)}(u)\cdot M_{PL(G)}(v)}} \\ &+ \sum_{uv \in E^{int}_{PL(G)}} \sqrt{\frac{M_{PL(G)}(u)+M_{PL(G)}(v)-2}{M_{PL(G)}(u)\cdot M_{PL(G)}(v)}}. \end{aligned}$$

By using Lemma 8.2.15 (b), Lemma 8.2.16 (b) and Observation 8.2.2, we obtain

$$\begin{aligned} &= \sum_{pq \in E_G} \sqrt{\frac{d_G(q)\cdot(d_G(p))^{d_G(p)-1} + d_G(p)\cdot(d_G(q))^{d_G(q)-1} - 2}{d_G(q)\cdot(d_G(p))^{d_G(p)-1}\cdot d_G(p)\cdot(d_G(q))^{d_G(q)-1}}} \\ &+ \sum_{p \in V_G}\sum_{s,t \in N_G(p)} \sqrt{\frac{d_G(s)\cdot(d_G(p))^{d_G(p)-1} + d_G(t)\cdot(d_G(p))^{d_G(p)-1} - 2}{d_G(s)\cdot(d_G(p))^{d_G(p)-1}\cdot d_G(t)\cdot(d_G(p))^{d_G(p)-1}}}. \end{aligned}$$

After simplification, we get

$$\begin{aligned} ABC_5(PL(G)) &= \sum_{pq \in E_G} \sqrt{\frac{d_G(q)\cdot(d_G(p))^{d_G(p)-1} + d_G(p)\cdot(d_G(q))^{d_G(q)-1} - 2}{(d_G(p))^{d_G(p)}\cdot(d_G(q))^{d_G(q)}}} \\ &+ \sum_{\substack{p \in V_G \\ s,t \in N_G(p)}} \sqrt{\frac{(d_G(s)+d_G(t))\cdot(d_G(p))^{d_G(p)-1} - 2}{d_G(s)\cdot d_G(t)\cdot(d_G(p))^{2d_G(p)-2}}}. \end{aligned}$$

□

8.2.5 Wiener Index of Para-line Transformed Graph of Tree

In this section, we derive a connection of the Wiener index between a tree and its para-line transformed graph. By using this connection, we formulate the Wiener index for the para-line transformed graph of any tree.

In the coming result, we present a connection of the Wiener index between any tree and its para-line transformed graph.

Theorem 8.2.20. *Consider $PL(T)$ symbolize the para-line transformed graph of any $(n,n-1)$-tree T, then*

$$W(PL(T)) = 8W(T) - 4n^2 + 5n - 1. \tag{8.2.2}$$

Proof. Consider a $(n,n-1)$-tree T, then from (4.2.14) we obtain the relation of the Wiener index of T and its line graph $L(T)$ as follows:

$$W(L(T)) = W(T) - \binom{n}{2}.$$

The subdivision graph $S(T)$ of a tree T is also a tree. Therefore, by replacing the tree T in this relation with the $(2n-1,2n-2)$-tree $S(T)$ we obtain

$$W(PL(T)) = W(L(S(T))) = W(S(T)) - \binom{2n-1}{2}. \tag{8.2.3}$$

By taking $k = 1$ in (4.2.15), we have

$$W(S(T)) = 8W(T) - \binom{2n}{3} - 8\binom{n+1}{3}.$$

After simplification, we get

$$W(S(T)) = 8W(T) - 2n(n-1). \tag{8.2.4}$$

Now, by using (8.2.4) in (8.2.3), we obtain

$$W(PL(T)) = 8W(T) - 2n(n-1) - \binom{2n-1}{2}.$$

After simplification, we obtain the desired relation. $\square$

In the coming Corollary, we present the expression of Wiener index for the para-line transformed graph of any tree.

Corollary 8.2.21. *Consider the para-line transformed graph $PL(T)$ of any $(n,n-1)$-tree T, then*

$$W(PL(T)) = 2\sum_{p\in V_T} d_T(p)\cdot d(p|T) - 2n^2 + 3n - 1.$$

Proof. By using (4.2.13) in (8.2.2), we have

$$W(PL(T)) = 2\left[n(n-1) + \sum_{p\in V_T} d_T(p)\cdot d(p|T)\right] - 4n^2 + 5n - 1.$$

After simplification, we obtain the desired expression. □

8.3 Topological Indices/Coindices of Iterated Para-line Graphs

In this part, we formulate the first general Zagreb index, first Zagreb Coindex, F-coindex for the iterated para-line transformed graphs. We also formulate the first Zagreb index, F-index and F-coindex for the complements of iterated para-line transformed graphs.

In the coming result, we present the first general Zagreb index for the k-th iterated para-line graphs of any graph.

Theorem 8.3.1. *Consider the k-th iterated para-line graph $PL^k(G)$ of any graph G, then for $k \geq 1$ we have*

$$M_1^{\alpha}(PL^k(G)) = \sum_{p\in V_G} t\cdot (d_G(p))^{k+\alpha} \tag{8.3.1}$$

where t is the number of vertices having degree $d_G(p)$ in G and α is an arbitrary real number except 0 and 1.

We prove this Theorem by using the following lemma.

Lemma 8.3.2. *Let $d_G(p)$ be the degree of a vertex $p \in V_G$, then corresponding to t vertices having degree $d_G(p)$ of graph G, there are $t\cdot (d_G(p))^k$ vertices having degree $d_G(p)$ of the k-th iterated para-line graph $PL^k(G)$.*

Proof. Let $PL^k(G)$ be the k-th iterated para-line graph of a graph G. To prove this result, we apply induction on k. Let p be a vertex having degree $d_G(p)$ of G, then p is incident with the edges say pq_i $(1 \leq i \leq d_G(p))$. By the construction of subdivision graph S_G, each of these edges is replaced by a path of length two say $p \to w_i \to q_i$. Then we have the vertices u_i and v_i (say) of $PL(G)$ corresponding to the edges pw_i and w_iq_i respectively. Since all the edges pw_i are adjacent by the vertex p of S_G. Therefore we have a complete graph $K_{d_G(p)}$ in $PL(G)$ having vertices u_i together with edges u_iv_i. Then clearly all the vertices u_i of $PL(G)$ have the same degree $d_G(p)$. Thus corresponding to t vertices of G having degree $d_G(p)$, we have $t \cdot d_G(p)$ vertices of PL_G having degree $d_G(p)$. We suppose that there are $t \cdot (d_G(p))^r$ vertices of r-th para-line graph PL_G^r having degree $d_G(p)$. Now we construct $(r+1)$-th para-line graph of graph G as $PL^{r+1}(G) = PL(PL^r(G))$. We take a vertex x of $PL^r(G)$ such that $d_{PL^r(G)}(x) = d_G(p)$. Then the vertex x is incident with the edges say xy_i $(1 \leq i \leq d_G(p))$. As we discussed above, in constructing the para-line graph of PL_G^r the vertex x in $PL^r(G)$ is replaced by a complete graph $K_{d_{PL^r(G)}(x)} = K_{d_G(p)}$ in $PL^{r+1}(G)$ having vertices say h_i $(1 \leq i \leq d_G(p))$ together with edges h_iy_i. Thus, corresponding to one vertex x of degree $d_G(p)$ of graph $PL^r(G)$ we have $d_G(p)$ vertices of $PL^{r+1}(G)$ having the same degree $d_G(p)$. Because there are $t \cdot (d_G(p))^r$ vertices of $PL^r(G)$ having degree $d_G(p)$ (by our supposition), so we have total $t \cdot (d_G(p))^r \cdot (d_G(p)) = t \cdot (d_G(p))^{r+1}$ number of vertices of $PL^{r+1}(G)$ having the same degree $d_G(p)$. □

Now, we present the proof of Theorem 8.3.1 as follows:

Proof. For each k, the first general Zagreb index of k-th iterated para-line graph $PL^k(G)$ is computed by using lemma 8.3.2 as follows

$$M_1^{\alpha}(PL_G^k) = \sum_{x \in V_{PL^k(G)}} \left(d_{PL^k(G)}(x)\right)^{\alpha} = \sum_{p \in V_G} t \cdot (d_G(p))^k \cdot (d_G(p))^{\alpha} = \sum_{p \in V_G} t \cdot (d_G(p))^{k+\alpha}.$$

□

Theorem 8.3.3. *Consider the k-th iterated para-line graph $PL^k(G)$ of any graph G, then for $k \geq 1$ we have*

$$(a)\ n_k = |V_{PL^k(G)}| = \sum_{p\in V_G} t.(d_G(P))^k, \tag{8.3.2}$$

and

$$(b)\ m_k = |E_{PL^k(G)}| = \frac{1}{2}\sum_{p\in V_G} t\cdot(d_G(p))^{k+1} \tag{8.3.3}$$

where t is the number of vertices of G having degree $d_G(p)$.

Proof. For each k, the cardinality of the vertex set $V_{PL^k(G)}$ is directly followed by lemma 8.3.2. In order to find the cardinality of the edge set $E_{PL^k_G}$ for each k, we use the hand-shaking lemma as follows

$$\sum_{p\in V_{PL^k(G)}} d_{PL^k(G)}(p) = 2|E_{PL^k(G)}|.$$

Now by lemma 8.3.2, we get the required result as follows

$$\sum_{p\in V_G} t\cdot(d_G(p))^k\cdot(d_G(p)) = \sum_{p\in V_G} t\cdot(d_G(p))^{k+1} = 2|E_{PL^k(G)}|.$$

□

In the coming Theorem, we present the first Zagreb coindex of $PL^k(G)$ and the first Zagreb index of its complement.

Theorem 8.3.4. *Consider the k-th iterated para-line graph $PL^k(G)$ of any graph G, then for $k\geq 1$ we have*

$$(a)\ \overline{M_1}(PL^k(G)) = \sum_{p\in V_G} t\cdot(d_G(p))^{k+1}\left(\sum_{p\in V_G} t\cdot(d_G(p))^k - 1\right) - \sum_{p\in V_G} t\cdot(d_G(p))^{k+2}. \tag{8.3.4}$$

$$\begin{aligned}(b)\ M_1(\overline{PL^k(G)}) \quad = \quad & \sum_{p\in V_G} t\cdot(d_G(p))^{k+2} + \sum_{p\in V_G} t\cdot(d_G(p))^k\left(\sum_{p\in V_G} t\cdot(d_G(p))^k - 1\right)^2 \\ & -2\sum_{p\in V_G} t\cdot(d_G(p))^{k+1}\left(\sum_{p\in V_G} t\cdot(d_G(p))^k - 1\right)\end{aligned}$$

where t is the number of vertices having degree $d_G(p)$ in G.

Proof. By taking $\alpha = 2$ in (8.3.1), we have the first Zagreb index of k-th iterated para-line graph $PL^k(G)$ as follows

$$M_1(PL^k(G)) = \sum_{p \in V_G} t \cdot (d_G(p))^{k+2}. \tag{8.3.5}$$

Now, by replacing the (n,m)-graph G in (4.2.16) and (4.2.17) by its k-th para-line (n_k, m_k)-graph $PL^k(G)$ for each k we have

$$M_1(\overline{PL^k(G)}) = M_1(PL^k(G)) + 2(n_k - 1)\left(\frac{n_k(n_k-1)}{2} - 2m_k\right) \tag{8.3.6}$$

and

$$\overline{M_1}(PL^k(G)) = 2m_k(n_k - 1) - M_1(PL^k(G)). \tag{8.3.7}$$

By using (8.3.2), (8.3.3) and (8.3.5) in (8.3.6) and (8.3.7), we achieve the required results. $\square$

In coming Theorem, we present the F-coindex of $PL^k(G)$ and of its complement, and F-index of $\overline{PL^k(G)}$.

Theorem 8.3.5. *Consider the k-th iterated para-line graph $PL^k(G)$ of any graph G, then for $k \geq 1$ we have*

$$(a)\ \overline{F}(PL^k(G)) = \sum_{p \in V_G} t \cdot (d_G(p))^{k+2}\left(\sum_{p \in V_G} t \cdot (d_G(p))^k - 1\right) - \sum_{p \in V_G} t \cdot (d_G(p))^{k+3}, \tag{8.3.8}$$

$$\begin{aligned}
(b)\ F(\overline{PL^k(G)}) &= \sum_{p \in V_G} t \cdot (d_G(p))^k \left(\sum_{p \in V_G} t \cdot (d_G(p))^k - 1\right)^3 \\
&\quad -3\sum_{p \in V_G} t \cdot (d_G(p))^{k+1} \left(\sum_{p \in V_G} t \cdot (d_G(p))^k - 1\right)^2 \\
&\quad +3\sum_{p \in V_G} t \cdot (d_G(p))^{k+2} \left(\sum_{p \in V_G} t \cdot (d_G(p))^k - 1\right) - \sum_{p \in V_G} t \cdot (d_G(p))^{k+3}, \\
(c)\ \overline{F}(\overline{PL^k(G)}) &= \sum_{p \in V_G} t \cdot (d_G(p))^{k+1} \left(\sum_{p \in V_G} t \cdot (d_G(p))^k - 1\right)^2 \\
&\quad -2\sum_{p \in V_G} t \cdot (d_G(p))^{k+2} \left(\sum_{p \in V_G} t \cdot (d_G(p))^k - 1\right) + \sum_{p \in V_G} t \cdot (d_G(p))^{k+3}
\end{aligned}$$

where t is the number of vertices of G having degree $d_G(p)$.

Proof. By taking $\alpha = 3$ in (8.3.1), we have the F-index of k-th para-line (n_k, m_k)-graph $PL^k(G)$ for each k as follows

$$F(PL^k(G)) = \sum_{p \in V_G} \left(d_G^p\right)^{k+3}. \tag{8.3.9}$$

Now, by replacing the (n,m)-graph G in (4.2.18), (4.2.19) and (4.2.20) by its k-th para-line (n_k, m_k)-graph $PL^k(G)$ for each k we have

$$\overline{F}(PL^k(G)) = (n_k - 1)M_1(PL^k(G)) - F(PL^k(G)), \tag{8.3.10}$$

$$F(\overline{PL^k(G)}) = n_k(n_k-1)^3 - 6m_k(n_k-1)^2 + 3(n_k-1)M_1(PL^k(G)) - F(PL^k(G)) \tag{8.3.11}$$

and

$$\overline{F}(\overline{PL^k(G)}) = 2m_k(n_k-1)^2 - 2(n_k-1)M_1(PL^k(G)) + F(PL^k(G)). \tag{8.3.12}$$

By using (8.3.2), (8.3.3), (8.3.5) and (8.3.9) in (8.3.10), (8.3.11) and (8.3.12), we get the desired results. □

8.4 Bounds for Distance-based Topological Indices of Para-line Transformed Graph

In this part, we obtain the lower and upper bounds for the eccentric-connectivity, connective eccentric, augmented eccentric connectivity, ABC_3 and Wiener indices of the para-line transformed graph in terms of different degree-based topological indices of the corresponding parent graph.

In the coming Theorem, we present that there are the same types of degrees in the para-line transformed graph as in the parent graph.

Theorem 8.4.1. *Consider a simple graph G and $v \in V_G$ be any vertex having degree $d_G(v)$, then there are $d_G(v)$ number of vertices having degree $d_G(v)$ in its para-line* *transformed graph $PL(G)$.*

Proof. Let v be any vertex of a graph G having degree $d_G(v)$, then v is incident with the edges vw_i (say) where $1 \leq i \leq d_G(v)$. In the construction of subdivision graph $S(G)$, each of these edges is replaced by a path having length two $v \to u_i \to w_i$ (say). Then corresponding to the edges vu_i and u_iw_i, we have the vertices p_i and q_i in the para-line transformed graph $L(S(G)) \cong PL(G)$. Clearly all edges vu_i have the same end vertex as v in $S(G)$, therefore we have a clique $C(v)$ in $PL(G)$ having the vertices p_i along with edges p_iq_i. So all vertices p_i $(1 \leq i \leq d_G(v))$ have the same degree as $d_G(v)$ in $PL(G)$. $\square$

The minimum and maximum degrees of a para-line transformed graph are presented in the following corollary which directly follows from Theorem 8.4.1

Corollary 8.4.2. *Consider a simple graph G having minimum degree δ_G and maximum degree Δ_G, then the minimum degree $\delta_{PL(G)}$ and maximum degree $\Delta_{PL(G)}$ of its para-line transformed graph are given by*

$$(a)\ \delta_{PL(G)} = \delta_G \tag{8.4.1}$$

$$(b)\ \Delta_{PL(G)} = \Delta_G. \tag{8.4.2}$$

In the coming result, the order and size of para-line transformed graph is obtained in terms of its parent graph parameters.

Corollary 8.4.3. *Consider a para-line transformed (n',m')-graph $PL(G)$ of simple (n,m)-graph G, then*

$$(a)\ n' = 2m \tag{8.4.3}$$

$$(b)\ m' = \frac{1}{2}M_1(G). \tag{8.4.4}$$

Proof. Consider a para-line transformed (n',m')-graph $PL(G)$ of simple (n,m)-graph G, then from Theorem 8.4.1 for each vertex $v \in V_G$ there exists $d_G(v)$ number of vertices in $PL(G)$ having the same degree $d_G(v)$. Thus we have

$$n' = |V_{PL(G)}| = \sum_{v \in V_G} d_G(v).$$

By using handshaking lemma, we get the result (a).

Also by using handshaking lemma, we have

$$\sum_{v\in V_{PL(G)}} d_{PL(G)}(v) = 2m'.$$

Again from Theorem 8.4.1, we can write

$$\sum_{v\in V_G} d_G(v)\cdot d_G(v) = 2m'.$$

After simplification, we achieve the desired result (b). $\square$

8.4.1 Bounds for Eccentric Connectivity Index of Para-line Transformed Graph

In the next result, we achieve the upper bound of the eccentric connectivity index for the para-line transformed graph in terms of Randić connectivity and first Zagreb indices of the corresponding parent graph.

Theorem 8.4.4. *Consider a para-line transformed (n',m')-graph $PL(G)$ of any connected (n,m)-graph G, where $n'\geq 3$, then*

$$\xi^c(PL(G)) < M_1(G)\left[2R(G)+2m-n+2-2\sqrt{2}\right]. \tag{8.4.5}$$

Proof. By choosing the functions $F(d_G(v),d_G(w)) = 1/\sqrt{d_G(v)\cdot d_G(w)}$ and $F(d_G(v),\varepsilon_v) = d_G(v)\cdot\varepsilon_v$ in the general expressions as presented in (3.3.2) and (3.3.3), we have respectively the Randić connectivity and eccentric connectivity indices of a graph G as follows:

$$\begin{aligned} R(G) &= \sum_{vw\in E_G} \frac{1}{\sqrt{d_G(v)\cdot d_G(w)}} \\ \xi^c(G) &= \sum_{v\in V_G} d_G(v)\cdot\varepsilon_v. \end{aligned}$$

From (7.2.1), we have the relation between these indices for a connected (n,m)-graph

G where $n \geq 3$ as follows:

$$\xi^c(G) < 4m\left[R(G) + 1 - \sqrt{2}\right]. \tag{8.4.6}$$

Now, by replacing the graph G in (8.4.6) with its para-line transformed (n', m')-graph $PL(G)$ where $n' \geq 3$, we have

$$\xi^c(PL(G)) < 4m'\left[R(PL(G)) + 1 - \sqrt{2}\right]. \tag{8.4.7}$$

By taking $\alpha = -1/2$ in (4.2.22), we have

$$R(PL(G)) = R_{-1/2}(PL(G)) = R_{-1/2}(G) + \frac{1}{2}\sum_{v \in V_G}\left[d_G(v) - 1\right]$$

and by using hand-shaking lemma (4.2.1), we get

$$R(PL(G)) = R(G) + m - \frac{n}{2}. \tag{8.4.8}$$

By using (8.4.4) and (8.4.8) in (8.4.7), we achieve the desired result. $\square$

In the coming result, we achieve the lower bound of the eccentric connectivity index for the para-line transformed graph in terms of first Zagreb and harmonic indices of the corresponding parent graph.

Theorem 8.4.5. *Consider a non-self-centered para-line transformed (n', m')-graph $PL(G)$ of any connected (n, m)-graph G, then*

$$\xi^c(PL(G)) > \frac{1}{4}M_1(G)\left[2H(G) - n + 2\right].$$

Proof. By taking the function $F(d_G(v), d_G(w)) = 2/(d_G(v) + d_G(w))$ in the general expression presented in (3.3.2), we formulate the harmonic index of a graph G as follows:

$$H(G) = \sum_{vw \in E_G} \frac{2}{d_G(v) + d_G(w)}.$$

From (7.4.1), we obtain a relation between this index and eccentric connectivity index for any non-self-centered (n,m)-graph G as follows:

$$H(G) < \frac{n}{2} + \frac{\xi^c(G)}{m} - 1.$$

By replacing the (n,m)-graph G with its non-self-centered para-line transformed (n',m')-graph $PL(G)$, we have

$$H(PL(G)) < \frac{n'}{2} + \frac{\xi^c(PL(G))}{m'} - 1. \tag{8.4.9}$$

Now, by using (8.2.1), (8.4.3), and (8.4.4) in (8.4.9), we obtain

$$H(G) + m - \frac{n}{2} < m + \frac{2\xi^c(PL(G))}{M_1(G)} - 1.$$

After simplification, we achieved the desired result. □

8.4.2 Bounds for Connective Eccentric Index of Para-line Transformed Graph

In the next result, we achieve the lower bound of the connective eccentric index for the para-line transformed graph in terms of the Randić connectivity and first Zagreb index of the corresponding parent graph.

Theorem 8.4.6. *Consider a para-line transformed (n',m')-graph $PL(G)$ of any connected (n,m)-graph G, where $n' \geq 3$, then*

$$C^{\xi}(PL(G)) > \frac{M_1(G)}{2R(G) + 2m - n + 2 - 2\sqrt{2}}.$$

Proof. By taking the function $F(d_G(v), \varepsilon_v) = d_G(v)/\varepsilon_v$ in the general expression presented in (3.3.3) we have the connective eccentric index of a graph G as follows:

$$C^{\xi}(G) \quad = \quad \sum_{v \in V_G} \frac{d_G(v)}{\varepsilon_v}.$$

From (7.2.2), we get the relation between this index and the Randić connectivity index for a connected (n,m)-graph G where $n \geq 3$ as follows:

$$C^{\xi}(G) > \frac{m}{R(G)+1-\sqrt{2}}.$$

Now, by replacing the graph G with its para-line transformed (n',m')-graph $PL(G)$ where $n' \geq 3$, we have

$$C^{\xi}(PL(G)) > \frac{m'}{R(PL(G))+1-\sqrt{2}}. \tag{8.4.10}$$

By using (8.4.4) and (8.4.8) in (8.4.10), we achieve the desired result. □

In the coming Theorem, we present the upper bound for the connective eccentric index of para-line transformed graph in terms of first Zagreb and harmonic indices of the corresponding parent graph.

Theorem 8.4.7. *Consider a non-self-centered para-line transformed (n',m')-graph $PL(G)$ of any connected (n,m)-graph G, then*

$$C^{\xi}(PL(G)) < \frac{4M_1(G)}{2H(G)-n+2}.$$

Proof. From (7.4.2), we have the relation between connective eccentric and harmonic index for a connected non-self-centered (n,m)-graph G as follows:

$$H(G) < \frac{n}{2} + \frac{4m}{C^{\xi}(G)} - 1.$$

By replacing the (n,m)-graph G with its non-self-centered para-line transformed (n',m')-graph $PL(G)$, we have

$$H(PL(G)) < \frac{n'}{2} + \frac{4m'}{C^{\xi}(PL(G))} - 1.$$

Now, by using (8.2.1), (8.4.3), and (8.4.4), we obtain

$$H(G) + m - \frac{n}{2} < m + \frac{2M_1(G)}{C^{\xi}(PL(G))} - 1.$$

After simplification, we achieved the required result. □

8.4.3 Bounds for Augmented Eccentric Connectivity Index of Para-line Transformed Graph

In the coming result, we achieve the lower bound of the augmented eccentric connectivity index for the para-line transformed graph in terms of Randić connectivity index of the corresponding parent graph.

Theorem 8.4.8. *Consider a para-line transformed (n',m')-graph $PL(G)$ of any connected (n,m)-graph G, where $n' \geq 3$, then*

$$\xi^{ac}(PL(G)) > \frac{2m \cdot (\delta_G)^{\delta_G}}{2R(G) + 2m - n + 2 - 2\sqrt{2}}.$$

Proof. By choosing the function $F(M_G(v), \varepsilon_v) = M_G(v)/\varepsilon_v$ in the general expression presented in (3.3.4), we have the augmented eccentric connectivity index of a connected graph G as follows:

$$\xi^{ac}(G) \quad = \quad \sum_{v \in V_G} \frac{M_G(v)}{\varepsilon_v}.$$

From (7.2.3), we obtain a connection between this index and the Randić connectivity index for a connected (n,m)-graph G where $n \geq 3$ as follows:

$$\xi^{ac}(G) > \frac{n \cdot (\delta_G)^{\delta_G}}{2R(G) + 2 - 2\sqrt{2}}.$$

By replacing the graph G with its para-line transformed (n',m')-graph $PL(G)$ where $n' \geq 3$, we obtain

$$\xi^{ac}(PL(G)) > \frac{n' \cdot (\delta_{PL(G)})^{\delta_{PL(G)}}}{2R(PL(G)) + 2 - 2\sqrt{2}}. \tag{8.4.11}$$

By using the results (8.4.1), (8.4.3), and (8.4.8) in (8.4.11), we achieve the desired result. □

In the coming Theorem, we achieve the upper bound for the augmented eccentric connectivity index of para-line transformed graph in terms of harmonic index of the corresponding parent graph.

Theorem 8.4.9. *Consider a non-self-centered para-line transformed (n',m')-graph $PL(G)$*

of any connected (n,m)*-graph G, then*

$$\xi^{ac}(PL(G)) < \frac{8m\cdot(\Delta_G)^{\Delta_G}}{2H(G)-n+2}.$$

Proof. From (7.4.3), we have the connection between augmented eccentric connectivity index and harmonic index for a connected (n,m)-graph G as follows:

$$H(G) < \frac{n}{2} + \frac{2n\cdot(\Delta_G)^{\Delta_G}}{\xi^{ac}(G)} - 1.$$

By replacing the (n,m)-graph G with its non-self-centered para-line transformed (n',m')-graph $PL(G)$, we have

$$H(PL(G)) < \frac{n'}{2} + \frac{2n'\cdot(\Delta_{PL(G)})^{\Delta_{PL(G)}}}{\xi^{ac}(PL(G))} - 1. \tag{8.4.12}$$

By using (8.2.1), (8.4.2), (8.4.3), and (8.4.4) in (8.4.12), we obtain

$$H(G)+m-\frac{n}{2} < m + \frac{4m\cdot(\Delta_G)^{\Delta_G}}{\xi^{ac}(PL(G))} - 1.$$

After simplification, we get the desired result. □

8.4.4 Bounds for ABC_3 Index of Para-line Transformed Graph

In the next result, we achieve the upper bound of the third ABC index for the para-line transformed graph in terms of F-index and first Zagreb index of the corresponding parent graph.

Theorem 8.4.10. *Consider a para-line transformed graph* $PL(G)$ *of any connected* (n,m)*-graph G, then*

$$ABC_3(PL(G)) \leq \frac{\sqrt{(2m-1)(M_1(G))^2 - M_1(G)\cdot F(G)}}{2}.$$

Proof. From the general expression presented in (3.3.6), we obtain the third ABC index by taking the function $F(\varepsilon_v, \varepsilon_w) = \sqrt{(\varepsilon_v + \varepsilon_w - 2)/\varepsilon_v \cdot \varepsilon_w}$ as follows:

$$ABC_3(G) = \sum_{vw \in E_G} \sqrt{\frac{\varepsilon_v + \varepsilon_w - 2}{\varepsilon_v \cdot \varepsilon_w}}.$$

From (4.2.23), we obtain the upper bound of this index in terms of first Zagreb index for a connected (n,m)-graph G as follows:

$$2(ABC_3(G))^2 \leq 2nm^2 - mM_1(G) - 2m^2.$$

Now, we replace the graph G with its para-line transformed (n', m')-graph $PL(G)$, we obtain

$$2(ABC_3(PL(G)))^2 \leq 2n'(m')^2 - m'M_1(PL(G)) - 2(m')^2. \tag{8.4.13}$$

By taking $\alpha = 2$ in (4.2.21) we have

$$M_1(PL(G)) = M_1^2(PL(G)) = \sum_{v \in V_G} (d_v)^3 = F(G). \tag{8.4.14}$$

Now, by using (8.4.3), (8.4.4) and (8.4.14) in (8.4.13), we obtain

$$2(ABC_3(PL(G)))^2 \leq \left(m - \frac{1}{2}\right)(M_1(G))^2 - \frac{1}{2}M_1(G).F(G).$$

After simplification, we achieve the desired result. □

In the coming result, we achieve the lower bound of the third ABC index for the para-line transformed graphs in terms of F-index and Zagreb indices of the corresponding parent graphs.

Theorem 8.4.11. *Consider a para-line transformed graph $PL(G)$ of any connected (n,m)-graph G, then*

$$ABC_3(PL(G)) \geq \frac{\sqrt{2}}{\sqrt{4m^2M_1(G) - (4m+1)F(G) + 2M_2(G) + M_1^4(G)}}.$$

Proof. From (4.2.23), we obtain the lower bound of third ABC index in terms of Zagreb indices for a connected (n,m)-graph as follows:

$$(ABC_3(G))^2 \geq \frac{1}{n^2m - nM_1(G) + M_2(G)}.$$

Now, by replacing the graph G with its para-line transformed (n',m')-graph $PL(G)$, we obtain

$$(ABC_3(PL(G)))^2 \geq \frac{1}{(n')^2m' - n'M_1(PL(G)) + M_2(PL(G))}. \tag{8.4.15}$$

By taking $\alpha = 1$ in (4.2.22), we obtain

$$M_2(PL(G)) = M_2(G) + \frac{1}{2}\sum_{v \in V_G}\left[(d_v)^3(d_v - 1)\right]. \tag{8.4.16}$$

After simplification, we get

$$M_2(PL(G)) = M_2(G) + \frac{1}{2}M_1^4(G) - \frac{1}{2}F(G). \tag{8.4.17}$$

By using (8.4.3), (8.4.4), (8.4.14) and (8.4.17) in (8.4.15), we have

$$(ABC_3(PL(G)))^2 \geq \frac{1}{2m^2M_1(G) - \left(2m + \frac{1}{2}\right)F(G) + M_2(G) + \frac{1}{2}M_1^4(G)}.$$

After simplification, we get the desired result. □

8.4.5 Bounds for Wiener Index of Para-line Transformed Graph

In the next result, we achieve the upper bound of the Wiener index for the para-line transformed graphs in terms of first Zagreb and Randić connectivity indices of the corresponding parent graphs.

Theorem 8.4.12. *Consider a para-line transformed (n',m')-graph $PL(G)$ of any connected (n,m)-graph G, where $n' \geq 3$, then*

$$W(PL(G)) < \frac{4}{3}mM_1(G)\left[2R(G) + 2m - n + 2 - 2\sqrt{2}\right] - 2m + 1.$$

Proof. From (4.2.7), we have the connection between eccentric connectivity and Wiener indices for a connected (n,m)-graph G where $n \geq 3$ as follows:

$$\xi^c(G) \geq \frac{3}{2n}\left[n + W(G) - 1\right].$$

Now, by replacing the graph G with its para-line transformed (n',m')-graph $PL(G)$ where $n' \geq 3$, we have

$$\xi^c(PL(G)) \geq \frac{3}{2n'}\left[n' + W(PL(G)) - 1\right].$$

By using (8.4.3), we obtain

$$\xi^c(PL(G)) \geq \frac{3}{4m}\left[2m + W(PL(G)) - 1\right].$$

Now, by combing this inequality with the inequality (8.4.5), we get

$$\frac{3}{4m}\left[W(PL(G)) + 2m - 1\right] < M_1(G)\left[2R(G) + 2m - n + 2 - 2\sqrt{2}\right].$$

After simplification, we achieve the desired result. □

In the coming result, we achieve the lower bound of Wiener index for the para-line transformed graph which are independent of 3- and 4-cycles in terms of F-index and first Zagreb index of the corresponding parent graph.

Theorem 8.4.13. *Consider a para-line transformed graph $PL(G)$ independent of 3- and 4-cycles of any connected (n,m)-graph G, then*

$$W(PL(G)) \geq \frac{1}{2}\left[6m(2m-1) - M_1(G) - F(G)\right].$$

Proof. From (4.2.24), we have a lower bound of the Wiener index for a connected (n,m)-graph G which is independent of 3- and 4-cycles.

By replacing the graph G in (4.2.24) with its para-line transformed (n',m')-graph $PL(G)$

which is independent of 3- and 4-cycles, we have

$$W(PL(G)) \geq \frac{3n'(n'-1)}{2} - \frac{1}{2}M_1(PL(G)) - m'. \tag{8.4.18}$$

Now, by using (8.4.3), (8.4.4) and (8.4.14) in (8.4.18), we achieve the required result.

$\square$

Chapter 9

Conclusions

9.1 Conclusions

In this thesis, we discuss different degree-based topological indices such as *ABC*, *GA*, ABC_4 and GA_5 indices for the boron triangular nanotube, boron-α nanotube, boron tri-hexagonal nanotube, boron-α nanotorus, and boron tri-hexagonal nanotorus by using the edge-partition technique. We also study the *ECI* for molecular graphs of three- and six-layer titania nanotubes and whole class of polyacene nanotubes by using the symmetries of these nanostructures. In addition, we formulate certain variants of *ECI* such as connective eccentric index, reverse eccentric connectivity index and modified eccentric connectivity index for the three-layer titania nanotube. In this study, we formulate different counting polynomials such as Omega, Sadhana and Theta polynomials for the molecular graphs of $2D$ six-layer titania lattice and six-layer titania nanotube.

We also present the comparative study between two topological indices belonging to degree- and distance-based topological indices. We derived the relations of Randić connectivity, *GA*, *ABC*, and harmonic indices with eccentric connectivity, connective eccentric, augmented eccentric connectivity, Wiener, and third *ABC* indices.

The applicability of topological indices of molecular graphs is evidently increased by using some of their transformed graphs in the sense that a topological index of the transformed graph necessarily reflects other structural features than the same topological index of the parent molecular graph. In this thesis, we studied certain degree-based indices for the para-line transformed graphs of V-phenylenic nanostructures. We obtained the general expressions of *ABC* index, *GA* index, harmonic index, *AZI* index, *SDD* index, *ISI* index, reformulated Zagreb indices, leap Zagreb indices, fourth version of *ABC* index (ABC_4), fifth version of *ABC* index (ABC_5) and fifth version of *GA* index (GA_5) for the para-line transformation of graphs. We also achieved the expression of the Wiener index for the para-line transformed graph of any tree. In addition, we achieved the lower and upper bounds of the eccentric connectivity index, connective eccentric index, augmented eccentric connectivity index, ABC_3 index and Wiener index for the para-line transformation of graphs.

9.2 Open Problems

The work in this thesis can be extended in the following directions.

- We studied different degree-based topological indices for boron nanotubes and boron nanotori. These degree-based topological indices can also be studied for dendrimers, nanobelts, nanoribbons, nonocages and fullerenes.

- We formulated the eccentric connectivity index for certain titania and polyacene nanostructures. This topological index can also be studied for the boron containing nanostructures.

- The formulation of counting polynomials for t-polyacenic nanotubes, remains an open problem.

- We presented the comparative study between certain degree- and distance-based topological indices. It would be interesting to obtain the equality relations between these topological indices.

- We achieved the general expressions of different topological indices for the para-line transformation of graphs. It would be worthwhile to obtain the general expressions of these indices for some other graph transformations such as line transformation and Harary transformation.

- We obtained the general expression of the Wiener index for the para-line transformation of tree. It would be interesting to obtain the general expression of the Wiener index and other distance-based topological indices for the para-line transformation of any cyclic connected graph.

- We achieved the lower and upper bounds of certain distance-based topological indices for the para-line transformation of graphs. It would be interesting to achieve the sharpness of these lower and upper bounds.

Chapter 10

References

[1] Ahmad, A. (2017) Computation of certain topological properties of para-line graph of honeycomb networks and graphene, *Discrete Math. Algorithm. Appl.* 9, 1750064.

[2] Akhter, S. & Imran, M. (2016) On molecular topological properties of benzenoid structures, *Can. J. of Chem.* 94, 687 – 698.

[3] Akhter, S., Imran, M., Gao, W. & Farahani, M. R. (2018) On topological indices of honeycomb networks and graphene networks, *Hacettepe J. of Math. Stat.* 47, 19 – 35.

[4] Ali, A., Bhatti, A. A. & Raza, Z. (2017) Further inequalities between vertex-degree-based topological indices, *Int. J. Appl. Comput. Math.* 3, 1921 – 1930.

[5] Anthony, J. E. (2006) Functionalized acenes and heteroacenes for organic electronics, *Chem. Rev.* 106, 5028 – 5048.

[6] Ashrafi, A. R., Ghorbani, M. (2010) A study of fullerenes by MEC polynomials, *Electro. Mater. Lett.* 6, 87 – 90.

[7] Ashrafi, A. R., Došlić, T. & Hamzeh, A. (2010) The Zagreb coindices of graph operations, *Discrete Appl. Math.* 158, 1571 – 1578.

[8] Battersby, S. (2008) Boron Nanotubes Could Outperform Carbon, New Scientist, London, UK, http://www. newscientist.com.

[9] Bavykin, D. V., Friedrich, J. M. & Walsh, F. C. (2006) Protonated titanates and TiO_2 nanostructured materials: synthesis, properties, and applications, *Adv. Mater.* 18(21), 2807 – 2824.

[10] Bendikov, M., Wudl, F. & Perepichka, D. F. (2004) Tetrathiafulvalenes, oligoacenenes, and their buckminsterfullerene derivatives: the brick and mortar of organic electronics, *Chem. Rev.* 104, 4891 – 4946.

[11] Biennier, L., Alsayed-Ali, M., Foutel-Richard, A., Novotny, O., Carles, S., Rebrion-Rowe, C. & Rowe, B. (2006) Laboratory measurements of the recombination of PAH ions with electrons: implications for the PAH charge state in interstellar clouds, *Faraday Discuss.* 133, 289 – 301.

[12] Bollabás, B., Erdös, P. (1998) Graphs of extremal weights, *Ars Combin.* 50, 225 – 233.

[13] Brédas, J. L., Calbert, J. P. & Cornil, J. (2002) Organic semiconductors: A theoretical characterization of the basic parameters governing charge transport, *Proc. Natl. Acad. Sci. USA* 99, 5804 – 5809.

[14] Buckley, F. (1981) Mean distance in line graphs, *Congr. Numer.* 32, 153 – 162.

[15] Calimli, M. H. (2011) The fifth version of atom bond connectivity index (ABC_5) of an infinite class of dendrimers, *Optoelectron. Adv. Mater. Rapid Commun.* 5, 1091 – 1092.

[16] Chartrand, G., Zhang, P. (2006) Introduction to Graph Theory, McGraw-Hill, New York.

[17] Chen, Y. (2007) Nanotechnology in space, Nanowerk. http://www.nanowerk.com.

[18] Dankelmann, P., Morgan, M. J., Mukwembi, S., Swart, H. C. (2014) On the eccentric connectivity index and Wiener index of a graph, Quaestiones Mathematicae, 37, 39 – 47.

[19] Das, K. C. & Gutman, I. (2004) Some properties of the second Zagreb index, *MATCH Commun. Math. Comput. Chem.* 52, 103 – 112.

[20] Das, K. C. & Nadjafi-Arani, M. J. (2015) Comparison between the Szeged index and the eccentric connectivity index. *Discrete Appl. Math.* 186, 74 – 86.

[21] Das, K. C., Gutman, I. & Nadjafi-Arani, M. J. (2015) Relations between distance-based and degree-based topological indices, *App. Math. and Comput.* 270, 142 – 147.

[22] De, N. (2012) Bounds for the connective eccentric index, *Int. J. Contemp. Math. Sci.* 7, 2161 – 2166.

[23] De, N. (2013) Relationship between augmented eccentric connectivity index and some other graph invariants, *Int. J. of Adv. Math. Sci.* 1, 26 – 32.

[24] Diudea, M. V. (2006) Omega polynomial, *Carpath. J. Math.* 22, 43 – 47.

[25] Diudea, M. V., Vizitiu, A. E., Janežič D. (2007) Cluj and related polynomials applied in correlating studies, *J. Chem. Inf. Model.* 47, 864 – 874.

[26] Diudea, M. V., Cigher S. & John, P. E. (2008) Omega and Related Counting Polynomials, *MATCH Commun. Math. Comput. Chem.* 60, 237 – 250.

[27] Diudea, M. V. (2009) Omega polynomial in twisted/chiral polyhex tori. *J. Math. Chem.* 45, 309 – 315.

[28] Dobrynin, A. A. & Gutman, I. (1994) On a graph invariant related to the sum of all distances in a graph, *Publ. Inst. Math. (Beograd)* 56, 18 – 22.

[29] Dobrynin, A. A. & Gutman, I. (1998) The Wiener index for trees and graphs of hexagonal systems, *Diskret. Anal. Issled. Oper.* 5, 34 – 60.

[30] Dobrynin, A., Entringer, R. & Gutman, I. (2001) Wiener index of trees: theory and applications, *Acta Appl. Math.* 66, 211 – 249.

[31] Došlić, T. (2008) Vertex-Weighted Wiener polynomials for composite graphs, *Ars Math. Contemp.* 1, 66 – 80.

[32] Du, Z. (2015) On the atom-bond connectivity index and radius of connected graphs, *J. Inequal. Appl.* 188, 1 – 8.

[33] Dureja, H., Madan, A. K. (2007) Superaugmented eccentric connectivity indices: new generation highly discriminating topological descriptors for QSAR/QSPR modeling, *Med. Chem. Res.* 16, 331 – 341.

[34] Ediz, S. (2012) Reverse eccentric connectivity index, *Optoelectron Adv. Mater. Rapid. Comm.* 6, 664 – 667.

[35] Enyashin, A. N. & Seifert, G. (2005) Structure, stability and electronic properties of TiO_2 nanostructures, *Phys. Stat. Sol.* 242, 1361 – 1370.

[36] Estrada, E., Torres, L., Rodriguez, L. & Gutman, I. (1998) An atom-bond connectivity index: modelling the enthalpy of formation of alkane, *Indian J. Chem.* 37A, 849 – 855.

[37] Evarestov, R. A., Zhukovskii, Y. F., Bandura, A. V. & Piskunov, S. (2011) Symmetry and models of single-walled TiO_2 nanotubes with rectangular morphology, *Cent. Eur. J. Phys.* 9, 492 – 501.

[38] Fajtlowicz, S. (1987) On conjectures of Graffiti-II, Congr. Numer. 60, 187 – 197.

[39] Firouzi, R. & Zahedi, M. (2008) Polyacenes electronic properties and their dependence on molecular size, *Journal of Molecular Structure: THEOCHEM* 862, 7 – 15.

[40] Furtula, B., Graovac, A. & Vukičević, D. (2010) Augmented Zagreb index, *J. Math. Chem.* 48, 370 – 380.

[41] Furtula, B. & Gutman, I. (2015) A forgotten topological index, *J. Math. Chem.* 53, 1184 – 1190.

[42] Furtula, B., Gutman, I., Vukićević, Ž. K., Lekishvili, G., & Popivoda, G. (2015) On an old/new degree-based topological index, *Bull. Cl. Sci. Math. Nat. Sci. Math.* 40, 19 – 31.

[43] Gao, W., Nadeem, M. F., Zafar, S., Zahid, Z. & Farhani, M. R. (2017) On the para-line graphs of certain nanostructures based on topological indices, *U.P.B. Sci. Bull., Series B* 79, 93 – 104.

[44] Gao, W., Jamil, M. K., Javed, A., Farahani, M. R., Wang, S. & Liu, J.-B. (2017) Sharp bounds of the hyper-Zagreb index on acyclic, unicylic, and bicyclic Graphs, *Discrete Dyn. Nat. Soc.*, 6079450.

[45] Ghorbani, M. & Hosseinzadeh, M. A. (2010) Computing ABC_4 index of nanostar dendrimers, *Optoelectron. Adv. Mater. Rapid Commun.* 4, 1419 – 1422.

[46] Graovac, A., Ghorbani, M. & Hosseinzadeh, M. A. (2011) Computing fifth geometric-arithmetic index for nanostar dendrimers, *J. Math. Nanosci.* 1, 33 – 42.

[47] Gupta, S., Singh, M., Madan, A. K. (2000) Connective eccentricity Index: A novel topological descriptor for predicting biological activity, *J. Mol. Graph. Model.* 18, 18 – 25.

[48] Gutman, I. & Trinajstić, N. (1992) Graph theory and molecular orbitals, total π-electron energy of alternant hydrocarbons, *Chem. Phys. Lett.* 17, 535 – 538.

[49] Gutman, I. & Potgieter, J. J. (1997) Wiener index and intermolecular forces. *J. Serb. Chem. Soc.* 62, 185 – 192.

[50] Gutman, I. & Tomović, Ž. (2000) On the application of line graphs in quantitative structure-property studies, *J. Serb. Chem. Soc.* 65, 577 – 580.

[51] Gutman, I., Tomović, Ž. Mishra, B. K. & Kuanar, M. (2001) On the use of iterated line graphs in quantitative structure-property studies, *Indian J. Chem.* 40A, 4 – 11.

[52] Hua, H. & Das, K. C. (2013) The relationship between the eccentric connectivity index and Zagreb indices. *Discrete Appl. Math.* 161, 2480 – 2491.

[53] Ivanovskaya, V. V., Enyashin, A. N. & Ivanovskii, A. L. (2004) Nanotubes and Fullerene-Like Molecules Based on TiO_2 and Zrs_2: Electronic Structure and Chemical Bond, *Russ. J. Inorg. Chem.* 49, 244 – 251.

[54] Ji, S., Li, X. & Huo, B. (2014) On reformulated Zagreb indices with respect to acyclic, unicyclic and bicyclic graphs, *MATCH Commun. Math. Comput. Chem.* 72, 723 – 732.

[55] Khadikar, P. V., Karmarkar, S., Varma, R. G. (2002) On the estimation of PI index of polyacenes, *Acta Chim. Slov.* 49, 755 – 771.

[56] Khadikar, P. V., Singh, J. & Ingle, M. (2010) Topological Estimation of Aromatic Stabilities of Polycenes and Helicenes, *J. Math. Chem.* 42, 433 – 446.

[57] Khadikar, P. V., Ashrafi, A. R., Diudea, M. V., Aziz, S., Pandit, S., Achrya, H., Shaik, B. & Agrawal, V. K. (2012) Sadhana index in nanotechnology, *J. Comput. Theor. Nano. Sci.* 10, 181 – 188.

[58] Klein, D. J., Lukovits, I. & Gutman, I. (1995) On the definition of the hyper-Wiener index for cycle-containing structures, *J. Chem. Inf. Comput. Sci.* 35, 50 – 52.

[59] Klein, D. J. & Yi, E. (2012) A Comparison on Metric Dimension of Graphs, Line Graphs, and Line Graphs of the Subdivision Graphs, *Euro. J. Pure and Appli. Math.* 5, 302 – 316.

[60] Klein, D. J. & Larson, C. E. (2013) Eigenvalues of saturated hydrocarbons, *J. Math. Chem.* 51, 1608 – 1618.

[61] Kunstmann, J. & Quandt, A. (2006) Broad boron sheets and boron nanotubes: An ab initio study of structural, electronic and mechanical properties. *Phys. Rev. B.* 74, 354 – 362.

[62] Lee R. K. F., Cox, B. J., Hill, J. M. (2009) Ideal polyhedral model for boron nanotubes with distinct bond lengths. *J. Phys. Chem. C.* 113, 19794 – 19805.

[63] Lee, D.-W. (2016) Some lower and upper bounds on the third *ABC* index, *AKCE Int. J. Graphs Comb.* 13, 11 – 15.

[64] Li, X. & Zhao, H. (2004) Trees with the first three smallest and largest generalized topological indices, *MATCH Commun. Math. Comput. Chem.* 50, 57 – 62.

[65] Liu, J. (2013) On harmonic index and diameter of graphs, *J. of Appl. Math. and Phy.* 1, 5 – 6.

[66] Lokesha, V., Shetty, B. S., Ranjini, P. S., Cangul, I. N. & Cevik, A. S. (2013) New bounds for Randić and *GA* indices, *J. Inequal. Appl.* 180, 1 – 7.

[67] Miličević, A., Nikolić, S., Trinajstić, N. (2004) On reformulated Zagreb indices, *Mol. Divers.* 8, 393 – 399.

[68] Miller, M. (2008) Boron Nanotubes Beat Carbon at Its Own Game, Engadget, San Francisco, CA, USA, http://www. engadget.com.

[69] Nadeem, M. F., Zafar, S. & Zahid, Z. (2015) On certain topological indices of the line graph of subdivision graphs, *Appl. Math. Comput.* 271, 790 – 794.

[70] Nadeem, M. F., Zafar, S. & Zahid, Z. (2016) On topological properties of the line graphs of subdivision graphs of certain nanostructures, *Appl. Math. Comput.* 273, 125 – 130.

[71] Naji, A. M., Soner, N. D., Gutman, I. (2017) On leap Zagreb indices of graphs, *Commun. Comb. Optim.* 2, 99 – 117.

[72] Pham, H. T., Duong, L. V., Tam, N. M., Pham-Ho, M. P. & Nguyen, M. T. (2014) The boron conundrum: bonding in the bowl B^{30} and B^{36}, fullerene B^{40} and triple ring B^{42} clusters, *Chemical Physics Letters*, 608, 295 – 302.

[73] Quandt, A. & Kunstmann, J. (2006) Broad boron sheets and boron nanotubes: An ab initio study of structural, electronic, and mechanical properties, *Phys. Rev.* 74, 1 – 14.

[74] Ramane, H. S., Manjalapur, V. V. & Gutman, I. (2017) General sum-connectivity index, general product-connectivity index, general Zagreb index and coindices of line graph of subdivision graphs, *AKCE Int. J. Graphs Comb.* 14, 92 – 100.

[75] Randić, M. (1975) On characterization of molecular branching, *J. Am. Chem. Soc.* 97, 6609 – 6615.

[76] Ranjini, P. S., Lokesha, V., Usha, A. (2013) Relation between phenylene and hexagonal squeeze using harmonic index, *Int. J. Appl. Graph Theory* 1, 116 – 121.

[77] Rao, N. P. & Lakshmi, K. L. (2010) Eccentric connectivity index of V-Phenylenic nanotubes, *Digest J. of Nano. and Bio.* 6, 81 – 87.

[78] Schön, J. H., Kloc, C., Dodabalapur, A. & Batlogg, B. (2000) An organic solid state injection laser, *Science* 289, 599 – 601.

[79] Schön, J. H., Kloc, C. & Batlogg, B. (2000) Superconductivity inmolecular crystals induced by charge injection, *Nature* 406, 702 – 704.

[80] Sharma, V., Goswami, R., Madan, A. K. (1997) Eccentric connectivity index: A novel highly discriminating topological descriptor for structure-property and structure-activity studies, *J. Chem. Inf. Comput. Sci.* 37, 273 – 282.

[81] Singh A. K., Sadrzadeh A. & Yakobson B. I. (2008) Probing properties of boron α-tubes by ab initio calculations *Nano Lett.* 8, 1314 – 1317.

[82] Slanina, Z., Sun, M.-L. & Lee, S.-L. (1997) Computations of boron and boron-nitrogen cages, *Nanostructured Materials*, 8, 623 – 635.

[83] Sun, M.-L., Slanina, Z. & Lee, S.-L. (1995) Square/hexagon route towards the boron-nitrogen clusters, *Chemical Physics Letters*, 233, 279 – 283.

[84] Tang, H. & Ismail-Beigi S. (2007) Novel precursors for boron nanotubes: the competition of two-center and three-center bonding in boron sheets, *Phys. Rev. Lett.* 99, 115501 – 115504.

[85] Tiwari, J. N., Tiwari, R. N. & Kim, K. S. (2012) Zero-dimensional, one-dimensional, two-dimensional and three-dimensional nanostructured materials for advanced electrochemical energy devices, *Progr. in Mater. Sci.* 57, 724 – 803.

[86] Todeschini, R. Consonni, V., Mannhold, R., Kubinyi, H. & Timmerman, H. (2008) Handbook of Molecular Descriptors. Methods and Principles in Medicinal Chemistry. Wiley-VCH.

[87] Vizitiu, A. E. & Diudea, M. V. (2009) Cluj polynomial description of TiO_2 nanostructures, *Studia Univ. Babes- Bolyai* 54, 173 – 180.

[88] Vukicevic, D. & Furtula, B. (2009) Topological index based on the ratios of geometrical and arithmetical means of end-vertex degrees of edges. *J. Math. Chem.* 46, 1369 – 1376.

[89] Vukičević, D., Gašperov, M. (2010) Bond Additive Modeling 1: Adriatic Indices, *Croat. Chem. Acta.* 83, 243 – 260.

[90] Wang, Y. Q., Hu, G. Q., Duan, X. F., Sun, H. L. & Xue, Q. K. (2002) Microstructure and formation mechanism of titanium dioxide nanotubes, *Chem. Phys. Lett.* 365, 427 – 431.

[91] Wang, W., Varghese, O. K., Paulose, M. & Grimes, C. A. (2004) Study on the growth and structure of titania nanotubes, *J. Mater. Res.* 19, 417 – 422.

[92] Wang, J., Liu, Y., You-Cheng, P., Prof, L. (2009) A New Class of Boron Nanotube, *ChemPhysChem.* 10, 3119 – 3121.

[93] Wang, S., Farhani, M. R. & Baig, A. Q. (2016) The Sadhana polynomial and Sadhana index of polycyclic aromatic hydrocarbon PAH_k, *Journal of Chemical and Pharmaceutical Research*, 8, 526 – 531.

[94] Wang, H., Liu, J.-B., Wang, S., Gao, W., Akhter, S., Imran, M., Farahani, M. R. (2017) Sharp bounds for the general sum-connectivity indices of transformation graphs, *Discrete Dyn. Nat. Soc.*, 2941615.

[95] Wiener, H. (1947) Structural determination of the paraffin boiling points, *J. Am. Chem. Soc.* 69, 17 – 20.

[96] Yang, X., Ding, Y. & Ni J. (2008) Ab initio prediction of stable boron sheets and boron nanotubes: Structure, stability and electronic properties, *Phys. Rev. B.* 77, 041402(R).

[97] Yamabe, T., Yata, S. & Wang, S. (2003) The Structures and Properties of Conjugated Hydrocarbons such as Polyacenic Materials and Polycyclic Aromatic Hydrocarbons (PAHs) Doped with Lithium, *Syn. Met.* 137, 949 – 951.

[98] Yang, Y. & Lu, L. (2011) The Randic index and the diameter of graphs, *Discr. Math.* 311, 1333 – 1343.

[99] Zhao, J., Wang, X., Sun, T. & Li, L. (2005) Insitu templated synthesis of anatase single-crystal nanotube arrays, *Nanotechnology*, 16, 2450 – 2454.

[100] Zhou, B. & Gutman, I. (2004) Relations between Wiener, hyper-Wiener and Zagreb indices, *Chem. Phy. Lett.* 394, 93 – 95.

[101] Zhou, B. & Trinajstić, N. (2010) On general sum-connectivity index, *J. Math. Chem.* 47, 210 – 218.

[102] Zhou, B. & Du, Z. (2010) On eccentric connectivity index, *MATCH Commun. Math. Comput. Chem.* 63, 181 – 198.

[103] Zhu, Y., Li, H., Koltypin, Y., Hacohen, Y. R. & Gedanken, A. (2001) Sonochemical synthesis of titania whiskers and nanotubes, *Chem. Commun.* 24, 2616 – 2617.